



UNIVERSIDAD
DE MÁLAGA

TESIS DOCTORAL

Nitrogen Metabolism in Plants: New insights into nitrogen uptake and assimilation in conifers.

PROGRAMA DE DOCTORADO EN BIOLOGÍA CELULAR Y MOLECULAR

DEPARTAMENTO DE BIOLOGÍA MOLECULAR Y BIOQUÍMICA
FACULTAD DE CIENCIAS
UNIVERSIDAD DE MÁLAGA

Director: Francisco Miguel Cánovas Ramos
Director: Rafael Antonio Cañas Pendón


José Miguel Valderrama Martín
2023





UNIVERSIDAD
DE MÁLAGA

AUTOR: José Miguel Valderrama Martín

 <https://orcid.org/0000-0003-1350-899X>

EDITA: Publicaciones y Divulgación Científica. Universidad de Málaga



Esta obra está bajo una licencia de Creative Commons Reconocimiento-NoComercial-SinObraDerivada 4.0 Internacional:

<http://creativecommons.org/licenses/by-nc-nd/4.0/legalcode>

Cualquier parte de esta obra se puede reproducir sin autorización pero con el reconocimiento y atribución de los autores.

No se puede hacer uso comercial de la obra y no se puede alterar, transformar o hacer obras derivadas.

Esta Tesis Doctoral está depositada en el Repositorio Institucional de la Universidad de Málaga (RIUMA): riuma.uma.es



DEPARTAMENTO DE BIOLOGÍA MOLECULAR Y BIOQUÍMICA

FACULTAD DE CIENCIAS

El Dr. Francisco Miguel Cánovas Ramos, catedrático del departamento de Biología Molecular y Bioquímica de la Facultad de Ciencias de la Universidad de Málaga, y el Dr. Rafael Antonio Cañas Pendón, profesor titular del departamento de Biología Molecular y Bioquímica de la Facultad de Ciencias de la Universidad de Málaga, CERTIFICAN:

Que D. José Miguel Valderrama Martín ha realizado bajo nuestra dirección, en el departamento de Biología Molecular y Bioquímica de la Facultad de Ciencias de la Universidad de Málaga, el trabajo de investigación recogido en esta memoria de tesis doctoral, con el título original "Nitrogen Metabolism in Plants: New insights into nitrogen uptake and assimilation in conifers".

Tras la revisión de la presente memoria, se ha estimado oportuna su presentación ante la Comisión de Evaluación correspondiente, por lo que autorizamos su exposición y defensa para optar al grado de Doctor en Biología.

Para que así conste, firmamos el presente certificado en Málaga a 30 de noviembre de 2022

Dr. Francisco Miguel Cánovas Ramos

Dr. Rafael Antonio Cañas Pendón

--	--

**DECLARACIÓN DE AUTORÍA Y ORIGINALIDAD DE LA TESIS PRESENTADA
PARA OBTENER EL TÍTULO DE DOCTOR**

D./Dña JOSÉ MIGUEL VALDERRAMA MARTÍN

Estudiante del programa de doctorado en **BIOLOGÍA CELULAR Y MOLECULAR** de la Universidad de Málaga, autor/a de la tesis, presentada para obtención del título de doctor por la Universidad de Málaga, titulada:



Realizada bajo la co-dirección de **FRANCISCO MIGUEL CÁNOVAS RAMOS** y **RAFAEL ANTONIO CAÑAS PENDÓN**.

DECLARO QUE:

La tesis presentada es una obra original que no infringe los derechos de propiedad intelectual ni los derechos de propiedad industrial u otros, conforme al ordenamiento jurídico vigente (Real Decreto Legislativo 1/1996, de 12 de abril, por el que se aprueba el texto refundido de la Ley de Propiedad Intelectual, regularizando, aclarando y armonizando las disposiciones legales vigentes sobre la materia), modificado por la Ley 2/2019, de 1 de marzo.

Igualmente asumo ante la Universidad de Málaga y ante cualquier otra instancia, la responsabilidad que pudiera derivarse en caso de plagio de contenidos en la tesis presentada, conforme al ordenamiento jurídico vigente.

En Málaga, a 30 de noviembre de 2022

 Doctorando/a	Fdo.: FRANCISCO MIGUEL CÁNOVAS RAMOS Tutor/a
 Fdo.: FRANCISCO MIGUEL CÁNOVAS RAMOS Y RAFAEL ANTONIO CAÑAS Director/es de tesis	

AUTOR: José Miguel Valderrama-Martín (JMVM)



<https://orcid.org/0000-0003-1350-899X>

EDITA: Publicaciones y Divulgación Científica. Universidad de Málaga.

Cualquier parte de esta obra se puede reproducir sin autorización, pero con el reconocimiento y atribución de los autores.

No se puede hacer uso comercial de la obra y no se puede alterar, transformar o hacer obras derivadas.

Esta Tesis Doctoral está depositada en el Repositorio Institucional de la Universidad de Málaga (RIUMA): riuma.uma.es

Este trabajo de Tesis Doctoral ha sido financiado por los proyectos BIO2015-73512-JIN MINECO/AEI/FEDER, UE, BIO2015-69285-R, RTI2018-094041-B-I00/MICINN y TRI2018-094041-B-I00; y por la Junta de Andalucía con el proyecto P20_00036 PAIDI 2020/FEDER, UE. JMVM ha sido financiado por una beca de Formación de Profesorado Universitario (FPU), referencia FPU17/03517.

ARTÍCULOS DERIVADOS DE ESTA TESIS DOCTORAL:

- **Valderrama-Martín et al.** 2022. A revised view on the evolution of glutamine synthetase isoenzymes in plants. *The Plant Journal*. 110: 946-960.
- **Valderrama-Martín et al.** 2022. A new gene encoding a cytosolic glutamine synthetase in pine is linked to developmental tissues. Sometido a publicación.
- **Valderrama-Martín et al.** 2022. Transcriptome dynamics of maritime pine in response to nitrate nutrition (en preparación)

A mi familia

Agradecimientos

Bueno, quien me iba a decir a mi que después de escribir una tesis doctoral la parte más difícil vendría con este apartado.

Esta tesis doctoral no habría sido posible de no ser por el profesor Francisco Cánovas. Gracias por abrirme las puertas a tu laboratorio permitiéndome realizar mi trabajo de Fin de Máster. Gracias además por tu guía, por tus consejos y por la oportunidad de realizar la tesis doctoral que hoy nos traen a este punto. También, agradecer a Concepción Ávila su ayuda y su inmensa paciencia conmigo. Afortunadamente la tasa de consumo de *Evagreen* decaerá tras mi partida.

Por supuesto, agradecer a mi otro director y supervisor en esta tesis, Rafael Cañas. Quien me iba a decir que aquel profesor de cuarto de carrera iba a acabar siendo uno de los directores de mi tesis doctoral (me sigues debiendo una foto tuya firmada por haber ganado el Kahoot). Cinco años han pasado ya desde que comencé el máster, cinco años de risas y penurias, pero cinco buenos años, al fin y al cabo. Se que echarás de menos alguien que te de tanta conversación como yo, aunque te quejes de que no te dejo trabajar. Gracias por tus enseñanzas a lo largo del camino, siempre serás un referente y un amigo.

Me gustaría también agradecer a todas aquellos compañeros y compañeras de laboratorio, que me han acompañado durante esta travesía. Al profesor Francisco Cantón por su consejo y sus anécdotas con las que me he reído a niveles insospechados. La convivencia ha sido corta, pero intensa. A los profesores Fernando de la Torre y Belén Pascual por toda su ayuda y por las risas. A Jorge, fiel compañero que, además de echarme una mano cuando lo necesitaba, siempre se apuntaba a todos mis planes, aunque alguna vez se nos haya ido de las manos teniendo que coger el coche un viernes a las 9 de la noche para personarnos en los carnavales de Cádiz. Grata aventura, no obstante. A Paco, Paquito, mi primer amigo en el laboratorio y la primera persona que me enseñó a como desenvolverme y trabajar en el mismo. Atrás quedan los fines de semana en el laboratorio, los trasplantes de pinos en invernaderos cuasidesmantelados y los viajes al PTA. Te estaré eternamente agradecido. También quiero mencionar a nuestro más reciente doctor, Alberto, una gran persona, compañero y amigo con el que siempre se puede contar y con el que puedes hablar desde ciencia hasta el mal gusto de Cañas eligiendo videoconsolas, por no hablar de nuestra invención, el iPachuelo, donde yo puse la torpeza y tú el ingenio. Tampoco hay que olvidarse de nuestro sevillano particular, César, que, aunque ahora este por tierras norteñas siempre lo recordaré por sus chistes, por ser poseedor del vehículo más accidentado de la historia y

por ser uno de los maquinadores de aquella comida en buffet que casi acaba conmigo. También agradecer Mayte y Vanessa, compañeras que ahora quedan a cargo del laboratorio y a las que les deseo la mejor de las suertes. No quisiera acabar este párrafo sin mencionar a algunos alumnos que pasaron por el laboratorio y con los que también he compartido buenos momentos: Juan Antonio, Cristina, María Rosa, David, Marina. Muchas gracias a todos/as, espero que hayáis podido aprender tanto de mi como yo de ustedes.

No puedo olvidar tampoco a mis maravillosos micros, con los que siempre me lo he pasado genial: Alvaro, Virginia, Laura, Yandira, Irene, Lola, Alba, Isa, Nisrine, Jesús... De los que estábamos en lo que yo llamo “el comienzo de los tiempos”, pocos quedamos ya (y en la torre menos), pero siempre recordaré todas las cervecitas y salidas juntos que tanto echo de menos, como buen nostálgico que soy. A los más recientes, quiero decirlos que, aunque me da pena no haber coincidido más tiempo con ustedes, me lo he pasado muy bien, espero que sigáis el legado (y si no ya me aseguro yo cuando vuelva por vacaciones).

Por supuesto, también he de agradecer el apoyo que he recibido fuera del ámbito laboral. Mis amigos y amigas, aquellas personas que siempre han estado a mi lado apoyándome y a los que les debo tanto. También a aquellos que considero como una segunda familia, que me han acogido como uno más y a los que les tengo mucho aprecio: Paco, Mar, Pepa, Carlos, Eva, Joaquin. Gracias a todos, esta tesis también es vuestra.

En este punto quisiera hacer especial mención a mi familia, a los que les dedico esta tesis y a los que les debo tanto. A mi hermano, por ser una pieza clave en mi mundo. A mis padres, que me dieron alas para volar y a los que me gustaría dedicarle unas palabras: Papá, Mamá, si a alguien le tengo que agradecer que haya llegado hasta aquí, es a vosotros dos. Os debo todo lo que soy y todo lo que he conseguido. Si no fuese por vuestro trabajo duro, vuestra constancia y vuestra educación, hoy no podría estar aquí agradeciendóos todo lo que me habéis dado. Muchas gracias, os quiero.

Por último, pero no menos importante (aunque si muy pequeña), a ti. Podría escribir varios libros solo rememorando los buenos momentos que hemos pasado juntos. Podría aprender cada uno de los idiomas de este planeta y todavía no encontraría palabras que describan todo lo que siento por ti y todo lo que significas para mi. Gracias por ser un pilar en mi vida, gracias por ser mi luz. Eres todo lo que pudiera desear como compañera de vida. Te amo, Alejandra. Esta tesis también va por ti y por todos esos momentos que nos quedan por vivir junto a los tequeños.

Table of contents

Resumen.....	1
Introduction.....	16
1. Importance of nitrogen metabolism in plants	17
2. Nitrate as nitrogen source for plants.....	18
3. Nitrogen assimilation in plants.....	25
Objectives.....	32
Chapter 1. A revised view on the evolution of glutamine synthetase isoenzymes in plants	34
1. Introduction.....	35
2. Results.....	37
3. Discussion.....	45
Chapter 2. A new gene encoding a cytosolic glutamine synthetase in pine is linked to developmental tissues.	51
1. Introduction.....	52
2. Results.....	54
3. Discussion.....	67
Chapter 3. Transcriptome dynamics of maritime pine in response to nitrate nutrition	71
1. Introduction.....	72
2. Results.....	73
3. Discussion.....	82

General discussion.....	87
General conclusions	94
Material and methods	96
1. Glutamine synthetase sequence retrieve and phylogenetic analyses	97
2. Promoter analysis.....	98
3. Protein structure prediction and modeling.....	99
4. Plant material.....	99
5. Total RNA extraction.....	101
6. Reverse transcription quantitative polymerase chain reaction (RT-qPCR) ...	103
7. Statistics	106
8. Direct RNA sequencing	106
9. Functional annotation and enrichment analyses	107
10. Cloning	107
11. Site-directed mutagenesis	108
12. Bacteria transformation	109
13. Recombinant expression of proteins	110
14. Protein purification.....	110
15. SDS-page and western-blot analysis	110
16. GS physicochemical assays.....	113
17. GS kinetic assays.....	113
References.....	114
Appendix.....	148

Abbreviations

ABA: Abscisic acid

ACC: 1-aminocyclopropane-1-carboxylate

ACS: 1-aminocyclopropane-1-carboxylate synthase

ACO: 1-aminocyclopropane-1-carboxylate oxidase

ADP: Adenosine diphosphate

ATP: Adenosine triphosphate

bZIP: basic-leucine zipper transcription factor

C: Carbon

CDS: Coding DNA sequence

CPM: counts per million

CK: Cytokinin

DRS: RNA direct sequencing

Ea: Activation energy

EC50: The concentration of substrate that produces a half-maximal enzyme velocity

FD: Ferredoxin

FDH: Formate dehydrogenase

FNR: Fd-NADP-reductase

GA: Gibberellic acid/ Gibberellin

GAST/GASA: Gibberellic acid stimulated transcript/Arabidopsis

GA3OX1: Gibberellin 3-beta-dioxygenase 1

GOGAT: Glutamate synthase

GS: Glutamine synthetase

GSIIb: eubacterial origin GSII

GSIIe: eukaryotic origin GSII

HGT: Horizontal gene transfer

IPT: Isopentenyl transferase

Ki: Dissociation constant for substrate binding

Km: Michaelis-Menten constant

L/D: Light/dark

LAX: LIKE-AUXIN RESISTANT

LCM: Laser capture microdissection

Mya: Million years ago

N: Nitrogen

NADH: Nicotinamide adenine dinucleotide

NADPH: Nicotinamide adenine dinucleotide phosphate

NGS: Next-generation sequencing

nH: Hill slope

NiR: Nitrite reductase

NLP: NIN LIKE PROTEIN

NPF: Nitrate transporter1/ peptide transporter family

NR: Nitrate reductase

NRT2: Nitrate transporter 2 family

NRT3: Nitrate transporter 3 family

NUE: Nitrogen use efficiency

NUPE: Nitrogen uptake efficiency

NUtE: Nitrogen utilization efficiency

ONT: Oxford Nanopore Technologies

PG: Phosphoglycolate

PGA: Phosphoglycerate

PIN: PIN-FORMED

PLC: Phospholipase C

PNR: Primary nitrate response

RT-qPCR: reverse transcription- quantitative PCR

SAUR: Small auxin upregulated RNA

TGA: TGACG MOTIF-BINDING FACTOR

TF: Transcription factor

TM: Transmembrane

V_{max}: Maximum enzyme velocity

WT: Wild type

ΔG^\ddagger : Gibbs free activation energy

Resumen

RESUMEN

El nitrógeno (N) es un elemento esencial y constituyente de biomoléculas de gran importancia tales como ácidos nucleicos y proteínas, además de metabolitos primarios y secundarios (Kishorekumar et al., 2020). Además, en ambientes naturales el N es el principal limitante para el crecimiento de las plantas lo cual tiene consecuencias directas sobre la producción de los cultivos (Hirel y Krapp, 2021). A pesar de ser el principal componente de la atmósfera terrestre, solo los microorganismos diazotrofos, ya sean libres en el medio o en simbiosis con algunas plantas, son capaces de fijar directamente el N atmosférico (N_2) (Sharma et al., 2021). Por ello, la mayoría de las plantas toman el nitrógeno que necesitan del propio suelo (Shafreen et al., 2021) donde debido a la competencia por el N orgánico, usado mayormente por microorganismos, se encuentra mayormente en forma inorgánica (Näsholm et al., 2009; Franklin et al., 2017). No obstante, la abundancia relativa de las formas inorgánicas en el suelo depende de numerosos factores tales como las condiciones ambientales o la naturaleza química del suelo (Esteban et al., 2016).

La importancia del N en la producción de los cultivos condujo al proceso conocido como “Revolución verde” tras la Segunda Guerra Mundial. Consistió en un aumento considerable del uso de fertilizantes en la agricultura con el objetivo de mantener una producción de alimentos que pudiera sostener el crecimiento constante de la población global (Galloway et al., 2013; Nacry et al., 2013). Sin embargo, el proceso de síntesis de estos fertilizantes mediante el método Haber-Bosch es bastante costoso y supone hasta el 50% de los costes de producción de ciertos cultivos (Hirel et al., 2011). Además, la mayor parte del nitrógeno aportado a estos cultivos no es utilizado por la plantas y se pierde por lixiviación en los suelos o se libera como N gaseoso a la atmósfera (Britto y Kronzucker, 2002; Hirel et al., 2011; Cameron et al., 2013) provocando grandes problemas medioambientales (Diaz y Rosenberg, 2008; Canfield et al., 2010; Hirel et al., 2011; Gutiérrez et al., 2012)

Por todo esto, los estudios sobre la eficiencia en el uso del nitrógeno (NUE), la eficiencia en la toma del nitrógeno (NUpE) y la eficiencia en la utilización del nitrógeno (NUE) han cobrado gran importancia en las últimas décadas (Hirel y Krapp, 2021) con el objetivo de mejorar la producción de cultivos y reducir el impacto medioambiental provocado por las actividades agrícolas.

En los suelos, las formas predominantes de N inorgánico son el amonio y el nitrato (Bernard y Habash, 2009). De estas dos moléculas, el nitrato es la más abundante en condiciones aeróbicas debido al proceso de nitrificación llevado a cabo por microorganismos que utilizan amonio para la producción de nitrato (Huérfano et al., 2015; Wang et al., 2018). Además, debido a las características del nitrato y a la toxicidad provocada por el amonio en

plantas, el nitrato se ha convertido en el recurso preferente para la mayoría de plantas que han evolucionado, o han sido seleccionadas, en base a una nutrición con nitrato (Cassman et al., 2002; Miller y Cramer, 2005; Esteban et al., 2016). Este hecho ha conducido a que el nitrato, junto con la urea, sea uno de los fertilizantes más usados en la agricultura en la actualidad (Fax et al., 2017). Además, esta molécula tiene una gran capacidad señalizadora regulando multitud de procesos en las plantas (O'Brien et al., 2016).

En las plantas, la toma y transporte del nitrato se realiza mediante un simporte acoplado a protones que recae principalmente sobre 3 familias de transportadores: *nitrate transporter1/peptide transporter family* (NPF), *nitrate transporter 2 family* (NRT2), *nitrate transporter 3 family* (NRT3) (Wang et al., 2020). Estas familias de proteínas han sido muy estudiadas en diferentes especies de plantas angiospermas de gran interés agronómico.

La familia de transportadores NPF es extensa y está formada por un número variable de transportadores según la especie que se distribuyen entre 8 y 10 subfamilias (Léran et al., 2014). Los transportadores NPF tienen diferentes sustratos, aquellos que son capaces de transportar nitrato son en su totalidad transportadores de baja afinidad a excepción del transportador NPF6.3 de *Arabidopsis thaliana*, NPF6.5 de *Oryza sativa* y NPF6.8 de *Medicago truncatula*, que han sido descritos como transportadores de doble afinidad regulados por fosforilación (Liu et al., 1999; Liu et al., 2003, Wang et al., 2018). Estos transportadores se expresan en diferentes órganos, tejidos y tipos celulares desempeñando una gran diversidad de funciones (Wang et al., 2018). Los miembros de esta familia se encargan principalmente de la removilización del nitrato, aunque también intervienen en procesos como la toma del nitrato en raíces, desarrollo vascular, acumulación de nitrato en las semillas o incluso la respuesta inducida por estrés abiótico o biótico (Almagro et al., 2008; Hsu et al., 2013; Lia et al., 2015; O'Brien et al., 2016). Curiosamente, un gran número de trabajos han indicado la capacidad de estas proteínas de membrana para transportar otras moléculas aparte del nitrato. Entre los diferentes sustratos que pueden ser usados por estos transportadores caben mencionar algunas de gran importancia para las plantas como las fitohormonas (Wang et al., 2018)

Por otro lado, la familia NRT2 está constituida en su totalidad por transportadores de alta afinidad con capacidad de transportar nitrato únicamente. A pesar de que el número de transportadores que pertenecen a esta familia puede variar entre especie, este es bastante más reducido en comparación con el de la familia NPF (O'Brien et al., 2016), encontrando 7 miembros de esta familia en *A. thaliana* y 4 en *O. sativa*, por ejemplo (Wang et al., 2018). Esta familia se encuentra asociada principalmente a la toma de nitrato en raíces (Wang et al.,

2018), aunque también se han propuesto otras funciones como la interacción planta-patógeno, el desarrollo de raíces laterales o la carga de nitrato en semillas (Little et al., 2005; Remans et al., 2006b; Chopin et al., 2007; Wang et al., 2018).

Finalmente, la familia NRT3 ha sido descrita como el segundo componente del sistema de transporte de alta afinidad (Zoghbi-Rodríguez et al., 2021). Aunque los mecanismos moleculares subyacentes son aún desconocidos, estos transportadores parecen jugar un papel regulador de la toma de nitrato y ser necesarios para estabilizar las proteínas NRT2 y dirigirlas a la membrana plasmática (Wang et al., 2018). De hecho, la interacción entre transportadores de la familia NRT2 y NRT3 ya ha sido confirmada y la coexpresión de ambas proteínas en oocitos de *Xenopus laevis* parece mejorar la captación de nitrato por parte de los transportadores NRT2 (Feng et al., 2011; Kiba et al., 2012; Kotur et al., 2012)

En el caso de gimnospermas, son ya varios los estudios que han recalado una preferencia por el amonio sobre el nitrato en algunos grupos como las coníferas (McFee y Stone, 1968; Van den Driessche, 1971; Kronzucker et al., 1997; Marschner et al., 1991; Lavoie et al., 1992; Warren et al., 2002; Boczulak et al., 2014). De hecho, esta hipótesis está también sustentada por la distribución de estas especies en zonas boreales donde la temperatura impide procesos de nitrificación en el suelo (Sponsler et al., 2016). Sin embargo, estudios recientes muestran que las concentraciones de ambas formas de N inorgánico (amonio y nitrato) parece igualarse en el suelo a unos pocos centímetros de profundidad (Zhou et al., 2021). De hecho, algunas especies de coníferas habitan en zonas más templadas donde puede darse el proceso de nitrificación. Este es el caso del pino marítimo (*Pinus pinaster*) una especie autóctona del mediterráneo occidental y modelo para el estudio de coníferas en la cual se han identificado previamente los miembros de las familias NRT y NPF (Castro-Rodríguez et al., 2017). Experimentos llevados a cabo por Ortigosa et al. (2020) probaron que el pino marítimo es capaz de usar nitrato además de amonio, al igual que se ha demostrado con posterioridad en otras especies de coníferas (Zhou et al., 2021). No obstante, la toma de nitrato en *P. pinaster* se encuentra estrictamente regulada y la acumulación de biomasa fue mas elevada en plántulas tratadas con amonio(Ortigosa et al., 2020).

Como se ha expuesto anteriormente, el nitrato es una molécula con un gran potencial señalizador siendo capaz de disparar y regular una respuesta transcripcional que afecta a una gran cantidad de genes y es conocida como la respuesta primaria a nitrato (PNR según sus siglas en inglés). Esta respuesta transcripcional desencadenada por el nitrato también puede implicar la acción de segundos mensajeros como el calcio y de numerosos factores de transcripción (Riveras et al., 2015; O'Brien et al., 2016). Además, el nitrato también es

RESUMEN

capaz de modular diferentes procesos de la planta mediante la regulación del transporte y del metabolismo de diferentes hormonas como auxina, citoquininas (CKs), etileno o ácido abscísico (ABA) (Wang et al., 2004; Gutiérrez et al., 2007; Hu et al., 2009; Tian et al., 2009; Medici y Krouk, 2014; O'Brien et al., 2016; Wang et al., 2018)

Una vez que esta molécula se incorpora a las plantas es asimilada metabólicamente en un proceso que incluye la reducción del nitrato a nitrito por la nitrato reductasa en el citosol (NR, EC 1.7.1.1), la reducción del nitrito a amonio por la nitrito reductasa en el cloroplasto (NiR, EC 1.7.2.1) y la asimilación de amonio a glutamato a través del ciclo glutamina sintetasa (GS, EC 6.3.1.2) / glutamato sintasa (NADH-GOGAT, EC 1.4.1.14; Fd-GOGAT, EC 1.4.7.1). En el ciclo GS/GOGAT el amonio es primero asimilado por la GS en glutamina con gasto de ATP y posteriormente, la glutamina, junto con 2-oxoglutarato y poder reductor, produce 2-moléculas de glutamato por acción catalítica de la GOGAT. Una de las moléculas de glutamato producidas se utiliza para realimentar el ciclo y la otra es el producto neto del mismo (Heldty Piechulla, 2011). Se considera que este ciclo es la mayor ruta de asimilación de N inorgánico en moléculas orgánicas utilizando como esqueleto carbonado el 2-oxoglutarato derivado del ciclo de Krebs. Este ciclo GS/GOGAT es además uno de los mayores nexos de unión entre el metabolismo del N y el metabolismo del carbono (C) pues emplea 2-oxoglutarato, proporcionado directamente por el ciclo de Krebs, como esqueleto carbonado para la asimilación del N. (Hirel y Krapp, 2021).

Los aminoácidos glutamina y el glutamato producidos en el ciclo GS/GOGAT se usan como donadores de nitrógeno para la biosíntesis de todas las moléculas nitrogenadas de la planta, posicionando a estas proteínas como enzimas clave para la NUE (Chardon et al., 2012). Concretamente, el papel de la GS en procesos tan importantes como la removilización del N, la producción de grano y el crecimiento de las plantas ha provocado que esta enzima haya sido una de las más estudiadas en términos de mejora de la NUE (Hirel y Krapp, 2021).

La importancia de la GS queda reflejada en su amplia distribución en todos los organismos, en los que se pueden encontrar hasta 3 superfamilias de GS conocidas como GSI, GSII y GSIII, cada una de ellas caracterizadas por su distribución entre los diferentes reinos, tamaño molecular y número de subunidades (Goshroy et al., 2010). Mientras que la presencia de GSI se da principalmente en procariotas y la de GSIII principalmente en bacterias, incluyendo cianobacterias, la familia GSII se da principalmente en eucariotas (Mathis et al., 2000; Nogueira et al., 2005; Kumar et al., 2017; James et al., 2018).

RESUMEN

En las plantas, la actividad GS es realizada por miembros de la superfamilia GSII para las que se han descrito estructuras tridimensionales octaméricas y decaméricas (Eisenberg et al., 2000; Llorca et al., 2006; Unno et al., 2006; Krajewski et al., 2008; He et al., 2009). Dentro de esta superfamilia GSII se pueden distinguir dos clados: GSII de origen eucariota (GSIIe) y GSII de origen eubacteriano, el cual se cree que apareció como resultado de una transferencia génica horizontal (HGT según sus siglas en inglés) que tuvo lugar después de la divergencia entre eucariotas y procariotas (Tateno et al., 1994, Ghoshroy et al., 2010).

Tradicionalmente, se han descrito dos grupos de genes GSIIe en las plantas angiospermas: uno que codifica para proteínas citosólicas (GS1) y un segundo que codifica para proteínas plastidiales (GS2), cada uno desempeñando papeles funcionales no redundantes en la planta (Ghoshroy et al., 2010; Hirel y Krapp, 2021). Generalmente, el grupo GS1 está compuesto por una pequeña familia génica codifica para varias isoformas citosólicas mientras el grupo GS2 suele estar compuesto por un único gen que codifica una enzima plastidial (James et al., 2018). Los análisis filogenéticos previos han sugerido que el gen GS2 pudo aparecer originalmente como el resultado de una duplicación génica de un gen GS1 (Biesiadka y Legocki, 1997) antes de la divergencia entre monocotiledóneas y cotiledóneas (Bernard y Habash, 2009). Hasta el momento se desconoce la presencia de GS2 en coníferas en la que podemos encontrar dos grupos de proteínas citosólicas: GS1a y GS1b, cada una codificada por un único gen y con diferentes características moleculares y cinéticas (Ávila-Sáez et al., 2000; de la Torre et al., 2002).

Tanto en angiospermas como en gimnospermas, la síntesis y la actividad relativa de cada isoforma de GS es específica de cada especie y su expresión se encuentra además regulada acorde al estado nutricional, el tejido, el estado de desarrollo y las condiciones ambientales (Cánovas et al., 2007; Bernard y Habash, 2009; Mondal et al., 2021), tarea en la que los factores de transcripción desempeñan un papel clave (Thomsen et al., 2014). Como reflejo de la importancia de esta enzima, cabe destacar que se encuentra regulada a todos los niveles: a nivel transcripcional, control del procesamiento, estabilidad y acumulación de RNA mensajero (mRNA según sus siglas en inglés), control de la traducción, así como modificaciones post-traduccionales (Sakakibara et al., 1997; Watanabe et al., 1997; Cantón et al., 1999; Oliveira y Coruzzi, 1999; Finnemann y Schjoerring, 2000; Ortega et al., 2001; Gómez-Maldonado et al., 2004a; Masclaux-Daubresse et al., 2005; Lima et al., 2006a; Lima et al., 2006b; Ortega et al., 2006; Simon y Sengupta-Gopalan, 2010; Melo et al., 2011; Lozano-Juste et al., 2011; Ortega et al. 2012)

RESUMEN

La GS2 se expresa principalmente en tejido fotosintético asociada al parénquima clorofílico (Blackwell et al., 1987), lo cual encaja perfectamente con su papel en la asimilación de amonio liberado en la fotorrespiración o producido en la reducción del nitrato (Wallsgrave et al., 1987; Blackwell et al., 1987; Tegeder y Masclaux-Daubresse, 2017). Por otro lado, los miembros de la familia GS1 se encuentran asociados principalmente a tejido vascular y la expresión de las diferentes isoenzimas cubre la totalidad de la planta (Lea y Miflin, 2018). Estas enzimas se encargan principalmente de la asimilación primaria de N en raíces, así como de la removilización y reciclado del N, jugando un papel importante en procesos como la senescencia o la respuesta a estrés biótico y abiótico (Bernard y Habash, 2009; Thomsen et al., 2014). Además, se ha visto que miembros de esta familia están implicados en diferentes procesos de desarrollo como la producción de grano en diferentes especies (Habash et al., 2001; Tabuchi et al., 2005; Martin et al., 2006; Funayama et al., 2013; Lothier et al., 2011; Goodall et al., 2013; Bao et al., 2014; Guan et al., 2015; Urriola y Rathore, 2015; Gao et al., 2019; Ji et al., 2019; Wei et al., 2021; Fujita et al., 2022)

En gimnospermas, el gen *GS1a* presenta un patrón de expresión similar al de *GS2* en angiospermas, asociado también al parénquima clorofílico de órganos fotosintéticos y, al igual que *GS2*, este gen se induce en respuesta a la luz (Cantón et al., 1999; Ávila et al., 2001; Gómez-Maldonado et al., 2004a). Por ello, se ha propuesto que el gen *GS1a* tenga funciones similares en gimnospermas a las de *GS2* en plantas angiospermas (Cantón et al., 1999). En lo referente al gen *GS1b* de gimnospermas, se encuentra filogenéticamente más relacionado con la familia GS1 de angiospermas que con el gen *GS1a*, y presenta funciones similares a las de la familia GS1 de angiospermas con implicaciones en desarrollo, así como en asimilación, reasimilación y removilización de N (Ávila et al., 2001, Suárez et al., 2002, Cantón et al., 2005; Pérez-Rodríguez et al., 2005).

En base a estos conocimientos previos, esta tesis doctoral presenta como objetivo general ahondar en aspectos claves de la nutrición nitrogenada de las plantas de interés forestal y específicamente de las coníferas. Con este fin, proponemos estudios más profundos de las familias génicas de GS en plantas aprovechando la disponibilidad y mejora en los recursos transcriptómicos y genómicos de gimnospermas. Por otro lado, también proponemos el estudio de la toma y transporte de nitrato, así como de la respuesta transcriptómica provocada por esta molécula, utilizando como modelo experimental la conífera *P. pinaster*. Estos estudios permitirán alcanzar una mejor comprensión de la nutrición nitrogenada basada en nitrato en esta especie de conífera y de la evolución de las familias de transportadores de nitrato en plantas. >

Tres objetivos específicos se han propuesto para cumplir con el objetivo general de esta tesis:

1. Entender las relaciones filogenéticas y evolutivas de los genes codificantes de GS en plantas con semillas aprovechando los nuevos recursos genómicos y transcriptómicos disponibles.
2. Determinar el juego completo de genes codificantes para GS en coníferas en base a los nuevos datos genómicos y transcriptómicos disponibles.
3. Caracterizar la expresión de la familia de los transportadores de nitrato en pino, así como la respuesta transcriptómica general en raíces, en respuesta a una nutrición con nitrato.

Con respecto al primer objetivo, se han realizado estudios filogenéticos usando un total de 168 secuencias de proteínas y de ácidos nucleicos de diferentes especies pertenecientes al grupo *Viridiplantae*. Estos estudios concuerdan con hipótesis previas que apoyan un evento de transferencia génica horizontal y por tanto la presencia de dos clados de GS dentro de la superfamilia GSII de plantas: GSIIb y GSIIe (Tateno et al., 1994; Goshroy et al., 2010). En este trabajo a las secuencias del grupo GSIIb se las ha denominado como GLN2 mientras que a las del grupo GSIIe se las ha llamado GLN1/GS siguiendo la nomenclatura de los genes de *Chlamydomonas reinhardtii*. En las secuencias GLN2 se ha podido detectar la presencia de un péptido señal para dirigir a estas proteínas a plastos o mitocondrias. No obstante, esta familia de genes se ha perdido en plantas vasculares, esto podría estar relacionado con el desarrollo de las estructuras vasculares asociadas al proceso de colonización del medio terrestre. De hecho, este mismo evento pudo ser el causante de la selección de los genes GLN1/GS en las plantas vasculares más ancestrales lo que apoyaría la relación de estos genes con la síntesis y transporte de glutamina y amino ácidos derivados (Bernard y Habash, 2009) y la producción de monolignoles usados como precursores en la biosíntesis de lignina (El-Azaz et al., 2022). Además, los resultados obtenidos durante los análisis filogenéticos sugieren que el grupo de genes de GLN1 podría considerarse como el punto de partida de las secuencias codificantes para GS en plantas semillas. Por otro lado, la filogenia en clados de *Embryophyta*, donde se han encontrado secuencias de GLN1/GS y GLN2, sugiere que los grupos de GS pertenecientes a las plantas con semillas (*Spermatophyta*) no se originaron en los grupos más antiguos de plantas terrestres no vasculares (*Embryophyta*). Viendo la concurrencia de los genes GLN1/GS y GLN2 en *Embryophyta*, las diferencias entre los árboles filogenéticos de proteínas y ácidos nucleicos de los grupos *Lycopodiopsida* y *Polypodiopsida* quizás puedan deberse a un proceso de adaptación debido

a la pérdida del gen GLN2 unido a cambios en las condiciones ambientales como un aumento de relación O₂/CO₂ (Renault et al., 2019) durante la evolución de estos grupos de plantas. De hecho, esto explicaría la presencia de péptidos de tránsito plastidial en algunas GS de estos grupos que sugieren que la aparición de una GS plástidica podría ser beneficiosa debido al enriquecimiento en oxígeno de la atmósfera.

Estos análisis filogenéticos también han permitido la reclasificación de las GS en plantas con semillas (*Spermatophyta*) en 3 grupos: GS1a, GS1b y GS2. El grupo de GS1a incluye todas aquellos genes que codifican para GS1a en gimnospermas pero también se ha podido comprobar que esta subfamilia se encuentra en ginkgo, angiospermas basales y algunas especies de Magnoliidae. A su vez, el grupo GS1b está constituido por los genes que codifican para GS1b en gimnospermas, así como por el resto de genes codificantes de isoformas citosólicas de angiospermas. Finalmente, el grupo GS2 está compuesto por los genes que codifican para GS de localización cloroplastídica, incluyendo por primera vez genes de GS2 en el grupo de *Cycadopsida*. La identificación y clonación de genes codificantes para GS2 en *Cycadopsida* apoyan la teoría de que este clado forma un grupo monofilético junto con las ginkopsidas (Wu et al., 2013; Li et al., 2017; One Thousand Plant Transcriptomes Initiative, 2019), donde previamente se habían identificado genes de GS2.

En base a los resultados obtenidos, dos hipótesis se han propuesto con respecto a la aparición de los genes codificantes de GS2:

1. La GS2 pudo originarse en un ancestro común de gimnospermas y angiospermas, posiblemente en *Polypodiopsida*, cuyas secuencias GS1 están filogenéticamente más relacionadas a secuencias GS2, y en el que donde un proceso de especialización pudo conducir a la adición de un péptido de tránsito plastidial. Esto conllevaría un segundo evento evolutivo que implicaría la pérdida de GS2 en un ancestro común de *Coniferopsida* y *Gnetopsida*.
2. La GS2 pudo originarse en un ancestro común de los grupos *Cycadopsida*/*Ginkgoopsida* y angiospermas lo que explicaría la ausencia de estos genes en los clados de *Coniferopsida* y *Gnetopsida* implicando un solo evento evolutivo. Esta hipótesis implicaría que el clado monofilético conformado por *Cycadopsida*/*Ginkgoopsida* (One Thousand Plant Transcriptomes Initiative, 2019) estaría más relacionado filogenéticamente con angiospermas de lo que se había considerado en un primer momento.

Esta segunda hipótesis además se vería apoyada por la presencia de GS1a en especies de ginkgo, angiospermas basales y Magnoliidae, resultados que no se habían descrito hasta el momento. De acuerdo con esta hipótesis, GS1a y GS2 tendrían por tanto papeles redundantes en tejidos fotosintéticos como ya se ha propuesto con anterioridad (Cantón et al., 1999; Ávila et al., 2001; Gómez-Maldonado et al., 2004a). Este papel redundante de ambas isoformas además se ve apoyado por la presencia de un residuo de cisteína, descrito como importante para la modulación redox de la actividad GS2, en todas las secuencias de GS1a analizadas, así como en las secuencias GS1 de *Polypodiopsida*, algunas especies de *Lycopodiopsida* y secuencias GLN1. Curiosamente, este residuo no se ha detectado en ninguna de las GS1b analizadas. Adicionalmente, los análisis de expresión realizados en este trabajo demuestran que la luz es capaz de controlar de forma similar la expresión de GS1a y GS2, y que además se expresan en los mismos tejidos, apoyando esto también un papel redundante de ambas enzimas. Este papel redundante explicaría la desaparición de GS1a en las angiospermas más recientes.

Atendiendo a estos resultados se podría asumir que GS2 apareció como resultado de una duplicación génica y especialización de GS1a en Cycadopsida/Ginkgoopsida, grupo que apareció hace 270 millones de años (Wu et al., 2013; Li et al., 2017; One Thousand Plant Transcriptomes Initiative, 2019) durante el permo-carbonífero, período donde los niveles atmosféricos de oxígeno incrementaron de un 21 a un 35%. En consecuencia, la tasa de fotorrespiración se vería incrementada lo cual conduciría a su vez a un aumento en los niveles de amonio. Paralelamente, este aumento en los niveles de oxígeno conllevaría un aumento en los niveles de nitrificación en la rizosfera y por tanto en los niveles de nitrato. El uso de nitrato como principal fuente de nitrógeno también contribuiría a un aumento en los niveles de amonio en el cloroplasto ya que el nitrito derivado del nitrato es reducido, en última instancia, a amonio en el cloroplasto por la NiR. Todo esto generaría una presión evolutiva sobre la selección de una GS cloroplastídica que pudiera asimilar el amonio procedente de ambos procesos.

Con respecto al objetivo 2, la mejora de los recursos transcriptómicos y genómicos ha permitido la identificación en primer lugar de un nuevo gen de GS en la conífera *P. pinaster* (Cañas et al., 2017). Aunque esta nueva GS presenta alta homología de secuencias (nucleotídica y aminoacídica) con la ya conocida GS1b de coníferas, los promotores de ambos genes presentan diferencias considerables. Atendiendo a la clasificación de este gen dentro de la familia GS1b en los análisis filogenéticos llevados a cabo en este trabajo, este isogen se ha denominado *PpGS1b.2*, posiblemente originado mediante una duuplicación

génica del gen ahora denominado *PpGS1b.1*. Además, este fenómeno de duplicación génica parece ser relativamente reciente pues en este trabajo se ha podido detectar la presencia de ortólogos en miembros de los géneros *Pinus* y *Picea* pero no en el resto de coníferas incluidas en los análisis.

Para explorar la posibilidad de un evento de duplicación génica y neofuncionalización, se ha analizado los patrones de expresión de los diferentes genes de GS en pino marítimo. Al contrario que *PpGS1b.1*, cuya expresión ha mostrado ser alta en todos los tejidos analizados, *PpGS1b.2* presenta una expresión muy localizada y asociada a órganos y tejidos en desarrollo, además de poseer una expresión estrechamente regulada a lo largo del desarrollo embrionario. Estos resultados podrían indicar una especialización de esta nueva isoforma que pasaría a estar asociada a procesos de desarrollo en la planta de manera similar a otros isógenos de la familia GS1b en angiospermas (Habash *et al.*, 2001; Tabuchi *et al.*, 2005; Martin *et al.*, 2006; Lothier *et al.*, 2011; Funayama *et al.*, 2013; Goodall *et al.*, 2013; Bao *et al.*, 2014; Guan *et al.*, 2015; Urriola y Rathore, 2015; Gao *et al.*, 2019; Ji *et al.*, 2019; Wei *et al.*, 2021; Fujita *et al.*, 2022), lo que sugiere un proceso de convergencia evolutiva. Atendiendo a los datos de expresión, se pueden plantear dos hipótesis diferentes: a) GS1b.2 puede apoyar la actividad de GS1b.1 en tejidos en desarrollo con una alta demanda de glutamina o de asimilados de N; b) GS1b.2 puede jugar un papel específico en ciertos tejidos en desarrollo.

En base a estas dos hipótesis se procedió al análisis de la estructura y de las características cinéticas y fisicoquímicas de ambas enzimas. Acorde a sus secuencias aminoacídicas, ambas proteínas parecen presentar pequeñas diferencias en su estructura cuaternaria y terciaria, aunque esto podría indicar grandes cambios en sus propiedades cinéticas y fisicoquímicas. De hecho, a pesar de que ambas isoformas presentan una temperatura óptima de 42 °C, GS1b.1 es termodinámicamente más estable que GS1b.2 y el pH óptimo para ambas enzimas ha resultado ser de 6.5 y 6, respectivamente.

Los análisis cinéticos llevados a cabo en este trabajo han mostrado que ambas enzimas también presentan diferencias en su comportamiento hacia los diferentes sustratos que emplean. Por ejemplo, la enzima GS1b.1 se inhibe por altas concentraciones de glutamato y ATP, lo cual podría suponer un mecanismo homeostático asociado a su papel en la asimilación primaria. Por otro lado, GS1b.2 presenta cooperatividad positiva para el glutamato e inhibición por exceso de sustrato en el caso del amonio. La cooperatividad positiva podría permitir que esta nueva isoforma respondiera rápidamente ante cambios en la disponibilidad de glutamato (Levitzki y Koshland, 1976). La inhibición por exceso de

amonio podría suponerse un mecanismo para controlar los niveles de este sustrato y de glutamato, producto final del ciclo GS/GOGAT, ya que ambas moléculas se han visto asociadas con procesos de desarrollo en plantas (Qiu X.M. et al., 2020; Ortigosa et al., 2022).

Atendiendo a la similitud en la secuencia aminoacídica de ambas proteínas y con el objetivo de desentrañar una posible implicación de ciertos aminoácidos en la estructura y actividad de estas enzimas, se ha procedido a realizar mutagénesis puntuales dirigidas y a la caracterización estructural, fisicoquímica y cinética de los mutantes. Los mutantes han consistido en el intercambio de los residuos aminoacídicos en posición 264 y 267 entre ambas isoformas, en las diferentes combinaciones posibles. Ninguna de las mutaciones realizadas tuvo grandes efectos sobre la estructura de GS1b.1 y GS1b.2, lo cual explicaría que ninguna de estas isoenzimas haya visto comprometida su estabilidad termodinámica. Al mismo tiempo, a pesar de que los niveles de actividad se vieron afectados en todos los mutantes, solo GS1b.1K264E,K267H y GS1b.2E264K sufrieron variaciones en su pH óptimo y solo GS1b.2E264K presentó una variación de su temperatura óptima. Curiosamente estas mutaciones produjeron grandes cambios en las propiedades cinéticas de ambas enzimas sugiriendo una implicación de los aminoácidos mutados en la afinidad por el amonio. A su vez, estos resultados apoyarían la hipótesis propuesta por Castro-Rodríguez et al. (2015) que sugiere que los aminoácidos esenciales para la afinidad de la GS por el amonio pueden variar entre las diferentes especies de plantas. Por otro lado, a pesar de que también se han producido numerosos cambios en el comportamiento de estas enzimas para los diferentes sustratos, solo se ha conseguido una inversión en los dobles mutantes con respecto a su comportamiento para el ATP.

Todo esto sugiere que las diferencias en las propiedades de ambas enzimas podrían deberse al esfuerzo conjunto de diferentes residuos aminoacídicos, posiblemente aquellos que difieren en la secuencia de ambas isoformas. En este contexto, GS1b.1 y GS1b.2 podrían haber sufrido un proceso de selección evolutiva para satisfacer diferentes necesidades de la planta con solo pequeños cambios en sus secuencias de aminoácidos. Esta hipótesis se ve además apoyada por las diferencias en la estabilidad de la estructura de ambas proteínas. Esto queda reflejado en el análisis de sustitución de residuos *in silico* en el que determinados aminoácidos en ciertas posiciones de ambas secuencias primarias producían grandes cambios en una isoforma, pero no en la otra.

En lo concerniente al objetivo 3, en primer lugar se han realizado estudios filogenéticos con 56 secuencias proteicas de NRT3 para intentar tener una mejor perspectiva de la evolución de esta familia de transportadores en plantas. Sobre la evolución de esta familia génica en

plantas se puede inferir que los NRT3 de angiospermas y gimnospermas parecen estar bien diferenciados. Estos resultados también indican un proceso de expansión génica de esta familia en algunas especies de gimnospermas.

Por otro lado, los análisis de expresión mediante *reverse transcription-quantitative PCR* (RT-qPCR) y secuenciación directa de ARN (DRS según sus siglas en inglés) con la tecnología de Oxford Nanopore (ONT según sus siglas en inglés) han permitido caracterizar la respuesta génica en respuesta a la nutrición basada en nitrato de los diferentes transportadores de nitrato en pino. Los resultados obtenidos mediante RT-qPCR muestran una respuesta limitada de la mayoría de los transportadores ante una nutrición con 1 y 10 mM de nitrato tanto a 2 horas como a 24 horas respectivamente. Resultados similares se obtuvieron en los análisis de DRS donde se utilizaron raíces plantas tratadas con 10 mM de nitrato y recolectadas a las 2 h. Solo unos cuantos transportadores vieron su expresión regulada positivamente en respuesta a nitrato, perteneciendo gran parte de estos genes a la familia NRT3. En lo correspondiente a la familia NRT2, solo NRT2.1 fue significativamente sobreexpresado en los análisis con DRS, pero no se observó un resultado similar en el análisis mediante RT-qPCR. Acorde a estudios previos, la toma de nitrato en pino marítimo se ve estrictamente regulada, cayendo por completo a los 15 minutos en presencia de nitrato (Ortigosa et al., 2020). Esto podría indicar que estos transportadores se ven altamente regulados a nivel post-transcripcional, posiblemente mediante su interacción con miembros de la familia NRT3.

En lo correspondiente a la familia NPF, solo ciertos transportadores se vieron sobreexpresados de forma estadísticamente significativa. No obstante, la expresión de varios transportadores NPF se reprimió de forma estadísticamente significativa, indicando que el nitrato juega un papel importante en la regulación de la expresión de ciertos miembros de la familia NPF. Como se ha explicado anteriormente, estos transportadores juegan un papel en el transporte de numerosas otras moléculas además del nitrato. De hecho, en *A. thaliana*, planta modelo en la que la toma y transporte de nitrato ha sido enormemente estudiada, no todos los miembros de esta familia se han descrito capaces de transportar nitrato (Corratgé-Faillie y Lacombe, 2017). Además, estos transportadores están implicados en la removilización de nitrato en la planta, lo cual puede ocurrir de forma independiente a la presencia de nitrato. Es por ello, que la falta de respuesta por parte de numerosos transportadores de esta familia podría explicarse por su expresión constitutiva en la planta como es el caso de *AtNPF2.3* (Wang et al., 2018). El nitrato, molécula de gran capacidad señalizadora (O'Brien et al., 2016), podría además controlar la expresión de

ciertos NPF para regular el transporte de nitrato y de otras moléculas a través de estos transportadores. Adicionalmente, estos transportadores podrían verse regulados a nivel post-traducciona l en respuesta a nitrato, ya sea mediante fosforilación, como ya se ha demostrado para *AtNPF6.3* (Wang et al., 2018), o mediante la familia NRT3, cuya expansión génica puede haber conducido a un proceso de neofuncionalización permitiendo la regulación de los transportadores NPF a través de esta familia. Sin embargo, no hay que descartar la posibilidad de que la respuesta a nitrato se vea fuertemente regulada y no sea posible detectar estos cambios tras dos horas en presencia de este nutriente.

Los análisis de DRS han mostrado que el nitrato es capaz de alterar la expresión de numerosos genes. No obstante, no se ha podido detectar la presencia de ciertos factores de transcripción previamente relacionados a la nutrición con nitrato (Obertello et al., 2010; Para et al., 2014; O'Brien et al., 2016). Esto podría explicarse por un efecto de dilución donde la poca expresión de estos genes no haya permitido su detección mediante el uso de esta técnica. Otra posibilidad podría ser su incorrecta anotación o a la ausencia de cambios significativos en la expresión de estos factores de transcripción transcurridas dos horas en presencia de nitrato

Los resultados obtenidos reflejan que el nitrato es capaz de alterar numerosos procesos en la planta. Entre los procesos biológicos que se encuentran sobrepresados se pueden destacar aquellos relacionados con el balance del poder reductor. A pesar de que la asimilación de nitrato está estrechamente relacionada con la fotosíntesis en tejidos fotosintéticos debido a la gran cantidad de poder reductor requerido en la reducción de nitrato, la asimilación de esta molécula también se ha indicado que puede ocurrir en raíces gracias a rutas metabólicas que permiten producir ferredoxina reducida en los plastos de las raíces (Yoneyama y Suzuki, 2019).

Entre estos procesos alterados en respuesta a nitrato cabe destacar aquellos relacionados con ciertas hormonas. En este estudio, la nutrición con nitrato parece afectar al transporte de auxinas y a ciertos factores de respuesta a esta hormona. Contrariamente, la última enzima de su ruta de síntesis del etileno parece verse reprimida, lo cual resulta curioso teniendo en cuenta que la síntesis de etileno se ve estimulada en raíces de pinos tratadas con amonio (Ortigosa et al., 2022). Sin embargo, esta represión en la síntesis del etileno podría ser acorde con la ausencia de regulación del metabolismo de las citoquininas (CKs), que se han descrito capaces de estimular la síntesis de etileno (Chae et al., 2003). En estudios anteriores, se ha demostrado la capacidad del nitrato para alterar la arquitectura de la raíz estimulando el crecimiento en longitud de la raíz principal, aunque sin estimular

RESUMEN

la formación y crecimiento de raíces laterales (Ortigosa et al., 2022). En conjunto, estos resultados sugieren que el nitrato podría producir este efecto mediante la modulación del transporte y el metabolismo de estas hormonas. Las diferencias en esta modulación por parte del amonio y del nitrato podrían explicar la capacidad del amonio de promover además la formación y crecimiento de raíces laterales al contrario que el nitrato (Ortigosa et al., 2022).

Introduction

1. Importance of nitrogen metabolism in plants

Nitrogen (N) is an essential element and as a constituent of the main biomolecules of paramount importance for life such as nucleic acids and proteins as well as primary and secondary metabolites (Kishorekumar et al., 2020). In natural environments, N is one of the main limiting factors for plant growth determining, in consequence, raw material production and crop yield (Hirel and Krapp, 2021). Moreover, N is also involved in plant architecture and resistance against stresses (Kishorekumar et al., 2020). Although N is the most abundant element in the atmosphere, only diazotrophic microorganisms, either free-living or associated with plants such as leguminous, can fix atmospheric dinitrogen (N₂) (Sharma et al., 2021). In this sense, plants acquired N from the soil in huge amounts (Shafreen et al., 2021), where a substantial part of the available N is indeed provided by microorganisms (Courty et al., 2015; Verzeaux et al., 2017; Rosenblueth et al., 2018).

In soils, N can be found in both organic and inorganic forms. Plants have evolved N uptake and assimilation mechanisms in order to reach adaptation for their own environments, thus allowing the incorporation of a wide range of N forms such as peptides, amino acids and inorganic N compounds such as nitrate or ammonium (Bernard and Habash, 2009; Näsholm et al., 2009; Gutiérrez et al., 2012; Krapp et al., 2015; Castro-Rodríguez et al., 2017; Bajgain et al., 2018). Furthermore, some of these mechanisms also allow plants to uptake N from soils that are poor in nitrogenous compounds (Jackson and Cadwell., 1993), and others protect them from toxicity due to eventual high concentration on some nitrogenous compounds (Clement et al., 1978; Forde and Clarkson, 1999; von Wiren et al., 2000; Britto and Kronzucker, 2001; Britto and Kronzucker, 2002; Glass et al., 2002; Xu et al., 2012; Nacry et al., 2013). Several works have shown that, especially under low inorganic N conditions, a wide range of plant species can uptake organic N such as amino acids or peptides (Moran-Zuloaga et al., 2015). Indeed, production rates of organic N compounds have been found to be higher than rates from N mineralization in some ecosystems (Näsholm et al., 2009). Nevertheless, the high competition for these organic N forms, mostly used by microorganism, together with adsorption process by the soil, do not allow plants to fulfill their requirements, even though those compounds are a great source of N for different plant species in several ecosystems (Näsholm et al., 2009; Franklin et al., 2017).

Nitrate and ammonium are the two main forms of inorganic N in soils, mostly produced by microbial mineralization of organic compounds (Bernard and Habash, 2009). The relative abundance of these substrates in soil depends on several factors such as environmental

conditions or the chemical nature of the soil (Esteban et al., 2016), thus producing a concentration range that goes from micromolar to molar (Britto and Kronzucker, 2006).

The importance of N in crop production led to the “Green Revolution” after the Second World War through the use of N fertilizers in agriculture suffered a huge increase in order to keep an enough food incoming for a constantly growing population (Galloway et al., 2013; Nacry et al., 2013). Nevertheless, almost the 50% of the production costs of some crops come from the synthesis of those fertilizers (Hirel et al., 2011). In addition, the massive use of fertilizers has a negative impact on the biosphere and environment. Over the 50% up to the 75% of the N supplied by fertilizers is lost by leaching into the soil or released as N gases to the atmosphere (Britto and Kronzucker, 2002; Hirel et al., 2011; Cameron et al., 2013). Excess of N can also lead to eutrophication of aquatic and terrestrial systems (Gutiérrez et al., 2012), increase of N reactive species input into the environment (Diaz and Rosenberg, 2008; Canfield et al., 2010) and other environmental problems (Hirel et al., 2011), which have repercussion in the biodiversity of the ecosystems (de Graaf et al., 1998). Since the world population is estimated to be 9 billion people by 2050, the agriculture production should increase 70-100% (McKenzie and Williams, 2015) along with the use of fertilizers, (Hirel and Krapp, 2021) which would lead to environmental crisis.

Therefore, the study of the mechanisms involved in plant N use efficiency (NUE), and its components, N uptake efficiency (NUpE) and N utilization efficiency (NUE) (Hirel and Krapp, 2021), has gained increased importance in the scientific field in last decades, particularly those focusing on crop yield improvement, as well as the attenuation of the environmental impact due to extensive agricultural activities. For this purpose, biotechnological advances, together with crop and forest management strategies, are required.

2. Nitrate as nitrogen source for plants

Nitrate is one of the two main forms of inorganic N in soils and the most predominant under aerobic conditions (Wang et al., 2018), since most of the ammonium is normally used by microorganisms in the nitrification process (Figure I.1) (Huérffano et al., 2015). Furthermore, ammonium shows a tendency to bound clay particles due to its positive charge (Figure I.1), thus making it difficult for the plant to uptake it (Miller and Cramer, 2005). In contrast, the high particle mobility of nitrate allows it to be easily uptaken by plants (Miller and Cramer, 2005). Ammonium is also found to be toxic to most plants

INTRODUCTION

(Esteban et al., 2016), meanwhile, high amounts of nitrate can be stored into vacuoles from where it could be retrieved in response to N requirements (Wang et al., 2018). Indeed, once nitrate is incorporated from the soil, it can be either assimilated or remobilized to shoots, which differ between species and depend on environmental conditions (Wang et al., 2018).

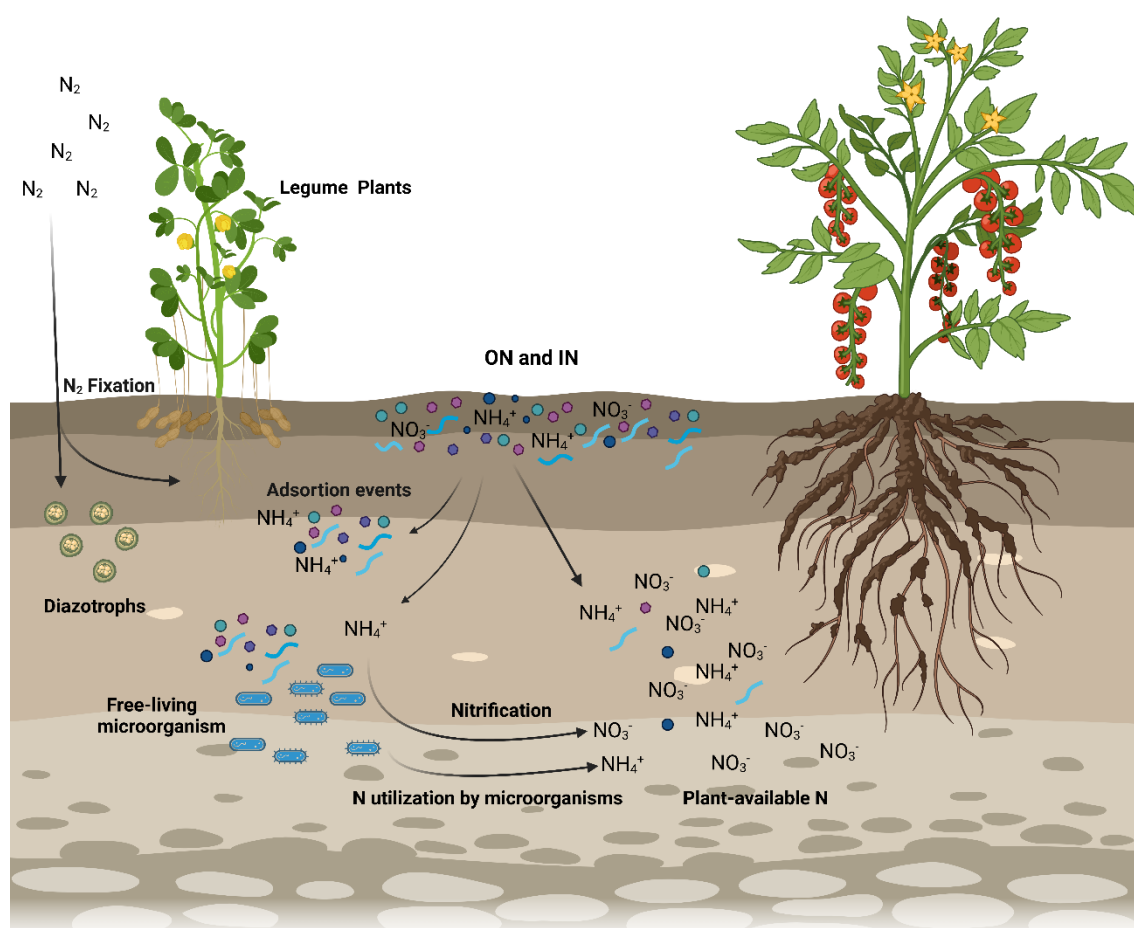


Figure I.1. Plant-available N sources. ON, organic nitrogen; IN, inorganic nitrogen. This figure has been designed with BioRender.

Based on these characteristics, nitrate is one of the main N sources used in agriculture (Hirel and Krapp, 2021). Thus, many plants have developed a preference for nitrate over ammonium, especially crop plants, which have been selected upon nitrate-based fertilization in temperate regions (Cassman et al., 2002).

Besides of being a great N source for several plant species, nitrate is also a signaling molecule that modulates a great number of processes which include flowering, seed dormancy and germination, shoot development, plant growth, root architecture and leaf development (Nacry et al., 2013; O'Brien et al., 2016; Lin et al., 2017). For plants, a complex

system is required to integrate all the information implying nitrogen requirement, nitrate perception, uptake, transport, assimilation, allocation and signaling (Wang et al., 2018).

2.1 Nitrate uptake in plants

Nitrate uptake is a proton-coupled symport mechanism (Figure I.2), the molecular basis of which, as well as its role in signaling, has been extensively studied (Wang et al., 2012; Medici and Krouk, 2014; Krapp et al., 2015; O'Brien et al., 2016; Fan et al., 2017; Li et al., 2017; Undurraga et al., 2017; Xuan et al., 2017; Tegeder and Masclaux-Daubresse, 2017; Wang et al., 2018). Nitrate uptake and transport in plants is the result of the collaborative effort of high-affinity and low-affinity transporters (O'Brien et al., 2016). These two systems may have arisen due to the urgency of dealing with different concentrations of nitrate in natural environments forming several families of nitrate transporters (O'Brien et al., 2016): nitrate transporter 1/ peptide transporter family (NPF), nitrate transporter 2 family (NRT2), and nitrate transporter 3 family (NRT3) (Wang et al., 2020).

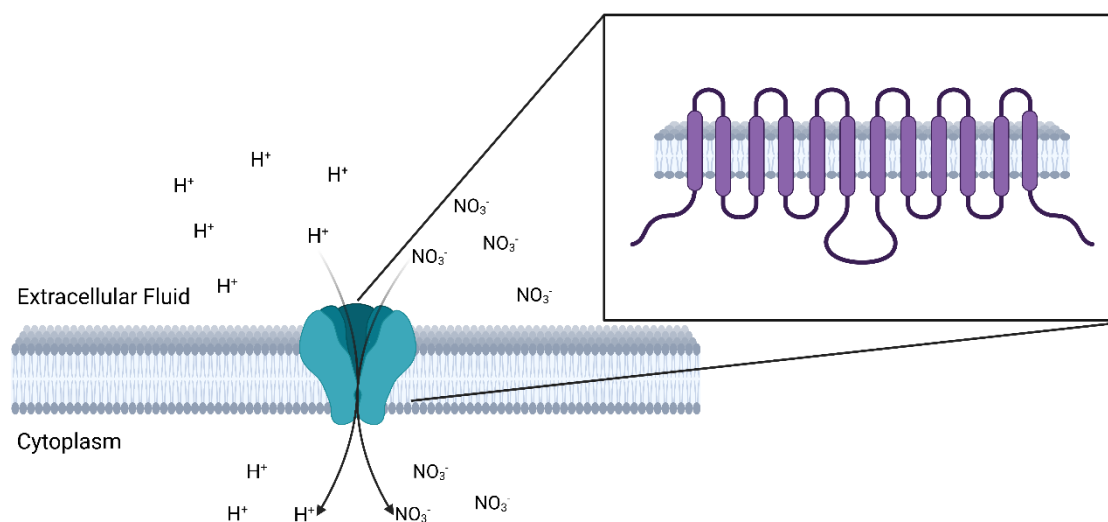


Figure I.2. Nitrate transport mechanism and scheme of the transmembrane domain organization proposed for some NPF and NRT2 transporters. This figure has been designed with BioRender.

Transporters belonging to the NPF family have been proposed to display a conserved structure of 12 transmembrane (TM) domains connected by short peptide loops (Figure I.2) (Léran et al., 2014), nevertheless, *OsNPF8.9b* has been described to possess only 6 TM domains (Fan et al., 2016). The NPF is a complex family of transporters with different number of members depending on the plant species and forming a total of 8-10 subfamilies (Léran et al., 2014). In *Arabidopsis thaliana*, 53 NPF transporters have been identified and

INTRODUCTION

36 of them have been characterized (Hirel and Krapp, 2021). This family is mainly conformed, by low-affinity transporters except for *A. thaliana* NPF6.3, *Oryza sativa* NPF6.5 and *Medicago truncatula* NPF6.8, which act as dual affinity nitrate transporters regulated by phosphorylation of one of their residues (Thr101 in *AtNPF6.3*) depending on nitrate level on the medium (Liu et al., 1999; Liu and Tsay, 2003, Wang et al., 2018).

NPF transporters are expressed in different organs, tissues, and cell types of the plant (Wang et al., 2018), most of them located in the plasma membrane except for 3 members of the NPF5 subfamily of transporters which are located in the tonoplast (Figure I.3) (He et al., 2017). Within the NPF family, a great versatility of functions can be highlighted (Figure I.3) (Wang et al., 2018). In *Arabidopsis*, only NPF6.3, NPF4.6, and NPF2.7 seem to play a role in nitrate uptake in roots, meanwhile, the rest of the NPF transporter mediate nitrate transport within the plant (O'Brien et al., 2016). In this sense, some NPF transporters have been described to be responsible for the remobilization of nitrate from mature leaves to developing tissues (Hsu et al., 2013), root-to-shoot nitrate transport and vascular development (Li et al., 2015), and nitrate accumulation in seeds, which is crucial for early embryo development (Almagro et al., 2008). The expression of some transporters is also induced by biotic and abiotic stresses, thus controlling nitrate accumulation in processes such as response to cadmium stress, N starvation conditions, and regulation of the stress-initiated nitrate allocation to roots (Fan et al., 2009; Gojon and Gaymard, 2010; Li et al., 2010; Zhang et al., 2014; Taochy et al., 2015). On its part, NPF6.3 is additionally involved in both nitrate sensing (acting as a transceptor) (Rentsch et al., 1995; Muños et al., 2004; Remans et al., 2006a; Ho et al., 2009) and stomatal opening (Guo et al., 2003).

Within the NPF family, specificity for a single substrate is not conserved, since there are NPF transporter with the capacity to transport molecules other than nitrate (O'Brien et al., 2016). Among the different compounds than can be transported by the NPF family, hormones are the most prominent ones. In *Arabidopsis*, NPF6.3 also mediated auxin transport, which has been described to be modulated by nitrate in order to promote lateral root elongation by auxin accumulation in the tips (Krouk et al., 2010a; Bouguyon et al., 2016). Abscisic acid (ABA) has been shown to be transported by members of the NPF family, concretely, *AtNPF4.1*, *AtNPF4.2*, *AtNPF4.5* and *AtNPF4.6* (Kanno et al., 2012; Kanno et al., 2013). On the other hand, *AtNPF3.1* transports gibberellin (GA) modulating its accumulation into the root endodermis (Tal et al., 2016). Several works have also shown the capacity of some members of the NPF family to transport glucosinolates, jasmonic acid/

INTRODUCTION

jasmonic acid -Ile, monoterpene indole alkaloids or dipeptides (Song et al., 1997; Dietrich et al., 2004; Komarova et al., 2008; Wang et al., 2018).

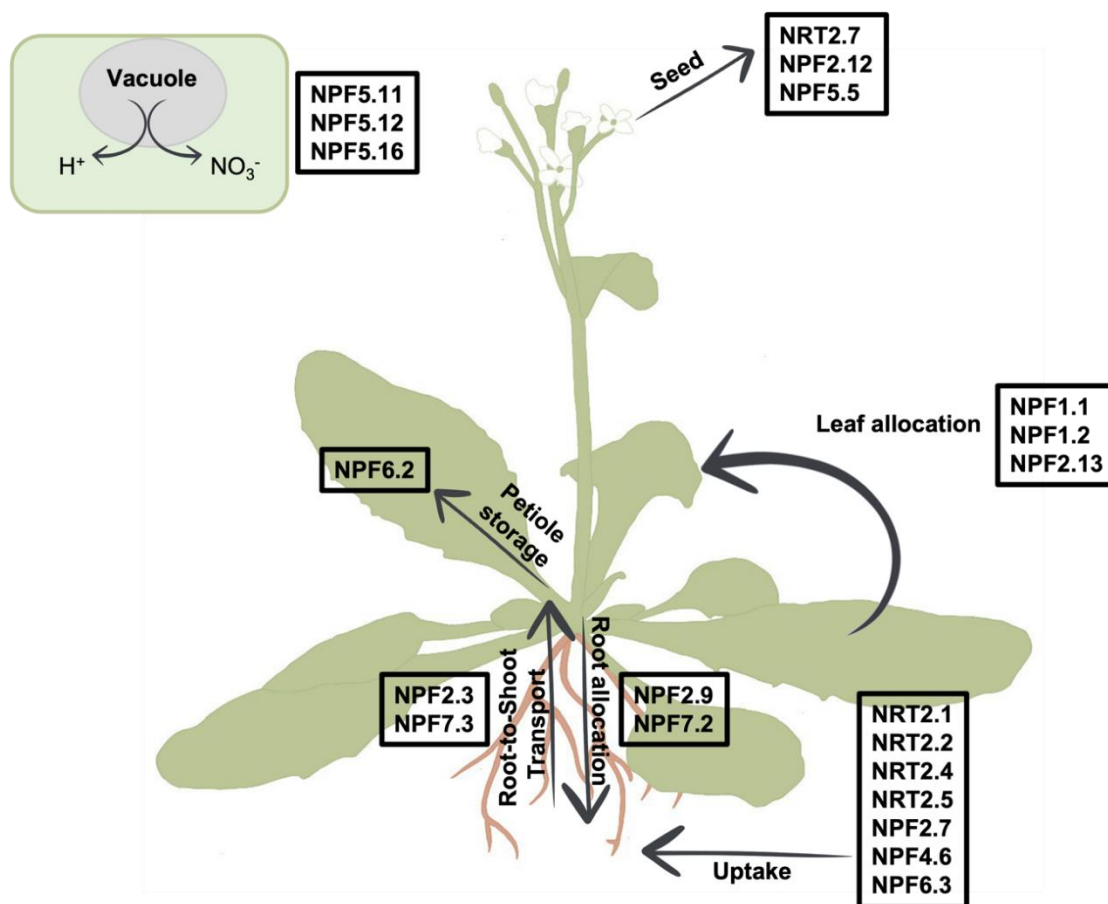


Figure I.3. Physiological function described for different transporters of the NPF and NRT2 families in *Arabidopsis thaliana*. NPF, nitrate transporter 1 (NRT1)/peptide transporter (PTR) family (NPF); NRT, nitrate transporter. Figure modified from Wang et al., 2018.

The NRT2 family is conformed by high affinity nitrate transporters that, despite not having a high sequence homology with NPF transporters, have been proposed to present 12 TM domains and a proton-driven symport mechanism as well (Figure I.2) (von Wittgenstein et al., 2014). However, this number of TM domains have been found to be different in some NRT2 transporters (Castro-Rodríguez et al., 2017) and, unlike NPF, NRT2 family only transport nitrate. The number of NRT2 transporters that can be found also differs between plant species, and it is much lower than those from the NPF family (O'Brien et al., 2016). For example, seven NRT2 transporters have been identified in *Arabidopsis* and only 4 in rice (Wang et al., 2018). NRT2 subfamily is mainly involved in nitrate acquisition but also in other processes (Figure I.3) (Wang et al., 2018). In *Arabidopsis*, it is well known that NRT2.1 and NRT2.2 directly participate in high affinity nitrate uptake (Cerezo et al., 2001; Filleur et

INTRODUCTION

al., 2001). Nevertheless, *AtNRT2.4* and *AtNRT2.5* has been observed to contribute to this purpose only under N starvation (Kiba et al., 2012; Lezhneva et al., 2014). Although the mechanisms are yet to be determined, there are evidences suggesting a role of *AtNRT2.1*, *AtNRT2.2* and *AtNRT2.6* in plant-microbe interaction (Wang et al., 2018) and a role of *AtNRT2.1* in lateral root development (Little et al., 2005; Remans et al., 2006b). *AtNRT2.7* is specifically located in the tonoplast of the seed cells where it is involved in the nitrate loading into the vacuoles (Chopin et al., 2007).

NRT3 transporters, specifically NRT3.1 (NAR2.1), are closely associated with NRT2 transporters constituting one of the two components of the high affinity transport system (Zoghbi-Rodríguez et al., 2021). Although the exact molecular mechanisms remain unknown, NRT3 transporters appear to play a regulatory role in nitrate transport and are necessary for NRT2 protein stability and targeting to the plasma membrane (Wang et al., 2018). The interaction between *AtNRT3.1* and the NRT2 transporters of *Arabidopsis* have been confirmed except for *AtNRT2.7* (Kotur et al., 2012). Furthermore, the activity of *AtNRT2.1*, *AtNRT2.2*, *AtNRT2.5*, *OsNRT2.1* and *OsNRT2.3a* were enhanced when coexpressed together with *AtNRT3.1* and *OsNRT3s*, respectively, in *Xenopus* oocytes (Feng et al., 2011; Kotur et al., 2012), whereas neither *AtNRT2.4*, nor *OsNRT2.3b* activity required or was affected by its coexpression with members of the NRT3 family in *Xenopus* oocytes (Feng et al., 2011; Kiba et al., 2012).

In gymnosperms, numerous studies have shown that some species, such as conifers, seems to present a preference for ammonium over nitrate as N source (McFee and Stone, 1968; Van den Driessche, 1971; Marschner et al., 1991; Lavoie et al., 1992; Kronzucker et al., 1997; Warren and Adams, 2002; Boczulak et al., 2014). This hypothesis has been supported by conifers distribution in boreal ecosystem where nitrification happens at lower rates due to low temperatures (Sponseller et al., 2016).

However, nitrate and ammonium concentrations seem to equalize from 10 cm depth in some cold climate soils (Zhou et al., 2021). In addition, some conifers are native to ecosystems of temperate climates that allows nitrification to happen. That is the case of maritime pine (*Pinus pinaster*), a conifer with a great ecological and economical importance (De Seoane et al., 2007; Aranda et al., 2010), which is autochthonous from the Western Mediterranean region. This pine has become a model for the study of gymnosperms in recent years and the improvement in its genomic and transcriptomic resources (Cañas et al., 2017) allowed a first identification of the NRT and NPF gene families members (Castro-

Rodríguez et al., 2017). A nutritional study in *P. pinaster* seems to indicate that this pine can use nitrate as well as ammonium with a strict regulation over nitrate uptake, although the biomass production was better under ammonium nutrition (Ortigosa et al., 2020). Moreover, a recent work over mature trees of 4 different conifer species has shown efficient assimilation of nitrate when irrigated with $^{15}\text{NH}_4\text{NO}_3$ and $\text{NH}_4^{15}\text{NO}_3$ in their natural environment (Zhou et al., 2021). This demonstrates the lack of knowledge about nitrate uptake and utilization in gymnosperms

2.2 Nitrate as signaling molecule.

Nitrate triggers and regulates a transcriptional response named as primary nitrate response (PNR) (O'Brien et al., 2016). Genes induced during PNR include those with a role in nitrate uptake and transport, such as the nitrate transporters, nitrate assimilation, such as nitrate and nitrite reductase (NR, EC 1.7.1.1, and NiR, EC 1.7.7.1, respectively), and several other genes related to different metabolic pathways.

Recently, studies in *Arabidopsis* have shown that *AtNPF6.3* is probably implicated in the increase of cytoplasmic calcium, a second messenger in several plants, through phospholipase C (PLC, EC 3.1.4.3) activity (Riveras et al., 2015), thus modulating several processes. Transcription factors (TFs) are another key component of the nitrate signaling system and, although the number of TFs associated with nitrate response is still growing, some of them have been already identified such as NIN LIKE PROTEIN 7 (NLP7), TGACG MOTIF-BINDING FACTOR 1 (TGA1), TGA4, or TCP20 among others (O'Brien et al., 2016). Within the plant, these transcription factors allow nitrate to modulate processes such as hormone metabolism and transport, the PNR or even the root architecture (Ruffel et al., 2011; Marchive et al., 2013, Alvarez et al., 2014; O'Brien et al., 2016; Ruffel et al., 2016)

Phytohormones are molecules with a key role in plant growth and development all over their life cycle. As mentioned above, hormone metabolism and transport, and thus their signaling, are closely linked to nitrate signaling. Previous works have demonstrated that nitrate is able to enhance cytokinin (CK) biosynthesis by transcriptionally activating isopentenyl transferase (IPT) genes that are involved in the limiting step of CK production (Wang et al., 2004). Interestingly, this regulation has been demonstrated to be dependent on NPF6.3 nitrate transceptor activity (Wang et al., 2004; Hu et al., 2009; Medici and Krouk, 2014). This nutrient is also connected to ethylene biosynthesis by upregulating 1-

aminocyclopropane-1-carboxylate (ACC) synthase (ACS, EC 4.4.1.14) and ACC oxidase (ACO, EC 1.14.17.4) at the transcriptional level (Tian et al., 2009). On the other hand, ABA synthesis seems to be repressed in response to nitrate thus alleviating seed dormancy (Matakiadis et al., 2009), nevertheless, little else is known about the effect of nitrate over this hormone (O'Brien et al., 2016). Some antecedents show a direct correlation between auxins levels and nitrate supply (Avery et al., 1937; Avey and Pottorf, 1945), even though actors of N-controlled shoot auxin synthesis are still elusive (O'Brien et al., 2016). However, a family of auxin transporters, PIN-FORMED (PIN), has been reported to respond to the provision of N (Gutiérrez et al., 2007).

3. Nitrogen assimilation in plants

In plants, any form of inorganic N is first reduced to ammonium and then assimilated into organic molecules through the glutamine synthetase (GS, EC 6.3.1.2) / glutamate synthase (GOGAT) cycle. Nitrate is first reduced to nitrite in the cytosol by the NR which use nicotinamide adenine dinucleotide (NADH) in this reaction. Afterward, nitrite is reduced to ammonium by the NiR a plastid located enzyme (Hirel and Krapp, 2021). As nitrite and ammonium are toxic molecules for the plant, their assimilation must be well coordinated in response to nitrogen demand and supply (Wang et al., 2018). Ammonium is then used by GS to produce glutamine in an adenosine triphosphate (ATP)-dependent reaction (Heldt and Piechulla, 2011). In a final instance, GOGAT use glutamine, along with 2-oxoglutarate and redox power, ferredoxin (Fd) or nicotinamide adenine dinucleotide (NADH), to produce two molecules of glutamate. One of these two molecules will be used as substrate of the GS/GOGAT cycle and the other one is the net product resultant of the reactions of these two enzymes during assimilation of N (Figure I.4) (Bernard and Habash, 2009).

The GS/GOGAT cycle is the major pathway for incorporation of inorganic N into organic N (Hirel and Krapp, 2021). Some studies using ¹⁵N and mutants deficient in GS and GOGAT have shown that the 95% of ammonium in plants is assimilated via GS (Lea and Ireland, 1999). This cycle is also one of the main links between carbon (C) and N metabolism, as it allows the assimilation of N into C skeletons by using 2-oxoglutarate provided directly through the Krebs Cycle (Hirel and Krapp, 2021). Glutamine and glutamate are used as precursors for the rest of all the N-containing molecules on the plant such as amino acids, proteins, chlorophyll, secondary metabolites, or nucleic acids (Forde and Lea, 2007; Bernard and Habash, 2009). These amino acids are also used to transport organic N to developing and storage organs (Tegeeder and Masclaux-Daubresse, 2017). Therefore,

INTRODUCTION

GS/GOGAT cycle has a main role in NUE [Chardon et al., 2012] emphasizing GS activity whose complex regulation and importance in N remobilization, yield, grain production and growth rate has been reiterated by some studies focusing on quantitative trait loci and by using different types of crop plants exhibiting contrasts in NUE (Hirel et al., 2001, Obara et al., 2001; Gallais and hirel, 2004; Obara et al., 2004; Habash et al., 2007; Fontaine et al., 2009; Kaminski et al., 2015). Consequently, GS probably remains as the most studied enzyme in terms of NUE enhancement in monocot and dicot plants (Hirel and Krapp, 2021).

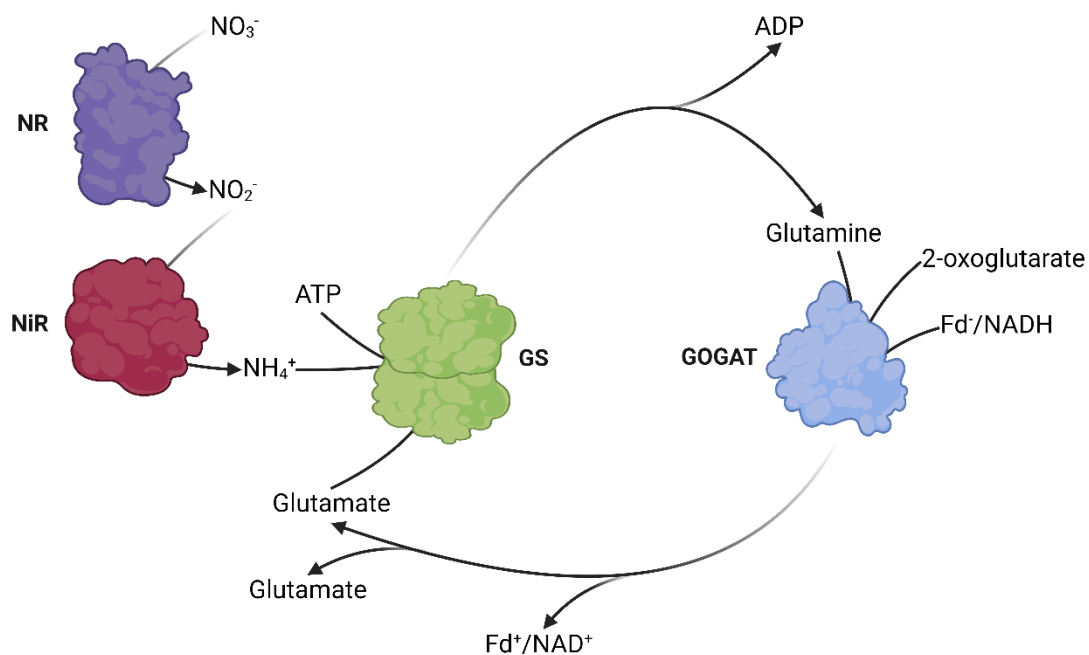


Figure I.4. Scheme of the nitrate reduction and ammonium assimilation by the Glutamine synthetase/Glutamate synthase cycle. NR, nitrate reductase; NiR, nitrite reductase; GS, glutamine synthetase; GOGAT, glutamate synthase. This figure has been designed with BioRender.

In plants, there are different isoforms of both enzymes. Regarding GOGAT, two different plastid located isoenzymes can be found, one using NADH as reducing power (NADH-GOGAT, EC 1.4.1.14), and the other one that use Fd (Fd-GOGAT, EC 1.4.7.1). Both isoforms playing a key role in primary N assimilation and recycling, Fd-GOGAT mainly acting in photosynthetic tissues whereas NADH-GOGAT in non-photosynthetic tissues (Bernard and Habash, 2009).

3.1 Glutamine synthetase: a key enzyme in plants nitrogen metabolism

Studies over the past two decades have provided a very deep understanding over GS phylogeny. Three GS superfamilies have been identified so far, namely, GSI, GSII and GSIII, all of them differentiated by the number of subunits, molecular size, and kingdom distribution (Ghoshroy et al., 2010). GSI superfamily is predominantly present in prokaryotes, although its presence in mammals and plants has also been reported (Mathis et al., 2000; Nogueira et al., 2005; Kumar et al., 2017). GSII superfamily was described as a characteristic group of *Eukarya* and some *Bacteria* such as *Proteobacteria* and *Actinobacteria* (James et al., 2018). However, this superfamily appears to be also present in *Euryarchaeota*, a phylum of *Archea* domain, in the public sequence databases. Finally, GSIII superfamily has been found and described in bacteria, including cyanobacteria (James et al., 2018), and some eukaryotes as diatoms and other heterokonts, thus suggesting the presence of GSIII in the nucleus of early eukaryotes (Robertson et al., 2006). Different works support that these gene superfamilies appeared prior to the divergence of eukaryotes and prokaryotes (Robertson et al., 2006)

In plants, GS activity is carried out by members of the GSII superfamily (James et al., 2018), which have been described to present an octameric and decameric tridimensional structures in different organisms (Eisenberg et al., 2000; Llorca et al., 2006; Unno et al., 2006; Krajewski et al., 2008; He et al., 2009). Two main GSII clades have been identified in the *Viridiplantae* group: eukaryotic origin GSII (GSIIe) and eubacterial origin GSII (GSIIb). It has been hypothesized that GSIIb arose as a result of a horizontal gene transfer (HGT) that took place after the prokaryote and eukaryote divergence, which indeed constitutes a sister group with GSII from γ -proteobacteria (Tateno et al., 1994; Ghoshroy et al., 2010). Regarding GSIIe, its importance in plant growth and development has led to extensive studies of these enzymes in vascular plants, particularly in crops. (Plett et al., 2017; Mondal et al., 2021).

It is generally indicated that angiosperms present two groups of nuclear *GSIIe* genes, one coding for cytosolic proteins (GS1) and a second coding for a plastidic GS (GS2), each playing non redundant physiological roles within the plant (Ghoshroy et al., 2010; Hirel and Krapp, 2021). Usually, there are different cytosolic isoforms codified by a small multigene family while only one nuclear gene codifies for a plastid isoform (James et al., 2018) with some exceptions such as wheat (*Triticum aestivum*), *M. truncatula* and poplar (*Populus*

INTRODUCTION

trichocarpa) where multiple *GS2* genes have been detected (Bernard et al., 2008; Seabra et al., 2010; Castro-Rodríguez et al., 2011).

Phylogenetic analyses suggest that *GS2* may have arisen as a result of a *GS1* gene duplication (Biesiadka and Legocki, 1997) 300 million years ago (Mya), before the divergence between monocots and dicots (Bernard and Habash, 2009). Interestingly, the presence of a *GS2* have been reported in the gymnosperm *Ginkgo biloba*, but no biochemical, molecular or microscopic analysis has allowed the detection of a plastid isoforms in conifers (Cánovas et al., 2007) and no *GS2* have been reported in fully sequenced genomes from different gymnosperms (Biol et al., 2013; Nystedt et al., 2013; Neale et al., 2014; Zimin et al., 2014; Stevens et al., 2016; Neale et al., 2017; Wan et al., 2018; Kuzmin et al., 2019; Mosca et al., 2019; Scott et al., 2020). Instead, conifers present two well differentiated families of cytosolic GS isoforms: *GS1a* and *GS1b*, each encoded by only one gene and with different molecular and kinetic properties (Ávila-Sáez et al., 2000; de la Torre et al., 2002).

In gymnosperms and angiosperms, both the synthesis and relative activity of each GS isoenzyme are species-specific, but its expression is also regulated according to nutritional status, tissue, developmental stages, and environmental conditions (Cánovas et al., 2007; Bernard and Habash, 2009; Mondal et al., 2021) where TFs plays a key role (Figure I.5)(Thomsen et al., 2014). In addition, a wide variety of other regulatory mechanisms have been observed on GS at all levels (Figure I.5), thus showing the precise regulation to which this enzyme is subjected. At the transcriptional level, the transcription rate of *GS* isogenes from different plants has showed to be affected by light (Cantón et al., 1999; Oliveira and Coruzzi, 1999; Gómez-Maldonado et al., 2004a) and C levels (Oliveira and Coruzzi, 1999). N metabolites have been also described to regulate GS expression. For instance, glutamate can directly upregulate *GS1* gene expression (Masclaux-Daubresse et al., 2005) and the cellular ratio of glutamine to glutamate is also a possible regulation parameter of *GS1* expression (Watanabe et al., 1997). Furthermore, nitrate positively regulates *GS2* expression in leaves of maize (*Zea mays*) and alfalfa (*Medicago sativa*) (Sakakibara et al., 1997; Ortega et al., 2001) and ammonium has been previously reported to upregulate *GS1* expression in roots of *P. pinaster* (Ortigosa et al., 2022). At the same time, nitrate seems to reduce the accumulation of *GS1* transcripts in leaves at the post-transcriptional level (Ortega et al., 2001). Indeed, *GS1* transcript accumulation in *M. sativa* has been shown to be mediated by nitrate and C:N ratios within the cell through the 3'UTR of these transcripts (Ortega et al., 2006; Simon and Sengupta-Gopalan, 2010).

INTRODUCTION

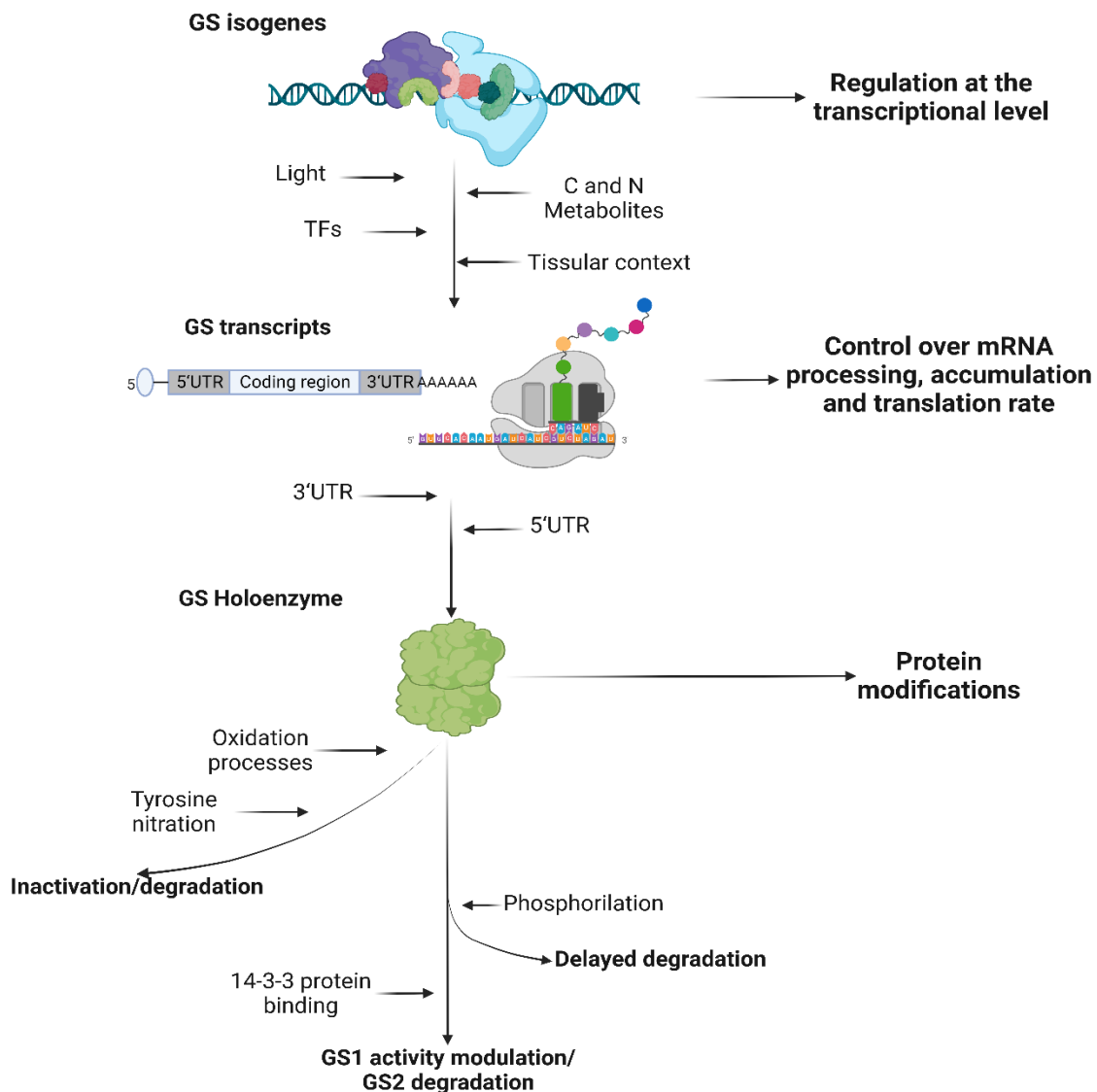


Figure I.5. GS regulatory mechanism. Factors such as light, metabolites or even the cellular type or the tissue could determine which GS is going to be transcribed and the rate of transcription (A). The 3'UTR is also responsible for the regulation of this enzyme at the post-transcriptional level (B). The 5'UTR of the mRNA acts as a translation enhancer, thereby promoting protein accumulation. (C). Post-translational protein modifications such as phosphorylation of serine residues, nitration of cysteine residues or nitration of tyrosine residues, determines the activity of the different isoforms or mark them for degradation (D). C, carbon; GS, glutamine synthetase; N, nitrogen; TFs, transcription factors. This figure has been designed with BioRender.

However, studies suggest that it is probably not nitrate the one who mediated this 3'UTR-turnover but glutamine or a product of glutamine metabolism (Simon and Sengupta-Gopalan, 2010). On its part, the 5'UTR acts as a translation enhancer, and although the molecular mechanisms remain elusive, it is thought to require the interaction with specific plant's factors such as proteins (Ortega et al., 2012). Besides regulation at the transcriptional

INTRODUCTION

level, GS has also been reported to be regulated by different proteins modifications such as oxidation (Ortega et al., 1999), phosphorylation and binding to 14-3-3 proteins (Finnemann and Schjoerring, 2000; Lima et al., 2006a; Lima et al., 2006b), and tyrosine nitration (Melo et al., 2011; Lozano-Juste et al., 2011), those producing different effects over GS isoenzymes (Figure I.5)

GS2 gene codifies for a 44-45 kDa protein, which is indeed larger than *GS1* proteins (38-40 kDa), mainly due to the presence of the plastidic signaling peptide in the N-terminal and a C-terminal extension of approximately 16 amino acids. The function of this C-terminal extension remains unknown, but it has been described to be important for *GS2*-glutamate interaction in *M. truncatula* (Ferreira et al. 2017). This isoform is mainly expressed in photosynthetic tissues associated to the chlorophyllous parenchyma (Blackwell et al., 1987). This expression pattern suits its role in the assimilation of ammonium from photorespiration and nitrate reduction (Wallsgrave et al., 1987; Blackwell et al., 1987; Tegeder and Masclaux-Daubresse, 2017).

On the other hand, although expression of *GS1* isoforms is mainly related to vascular tissues, the expression pattern of the different *GS1* isoenzymes cover the entire plant (Lea and Miflin, 2018). *GS1* isoforms are predominantly implied on primary N assimilation in roots, remobilization, and recycling (Thomsen et al., 2014). These isoforms have been also described as a key component of plant NUE with roles in processes such as senescence (Thomsen et al., 2014), amino acid catabolism and different stress responses (Bernard and Habash, 2009). Moreover, the direct implication of some *GS1* isoenzymes in developmental processes such as grain production has been demonstrated in *A. thaliana*, *Oriza sativa*, *Hordeum vulgare*, *Sorghum bicolor*, *Z. mays*, *Phaseolus vulgaris* and *Triticum aestivum* (Figure I.6) (Habash et al., 2001; Tabuchi et al., 2005; Martin et al., 2006; Lothier et al., 2011; Funayama et al., 2013; Goodall et al., 2013; Bao et al., 2014; Guan et al., 2015; Urriola and Rathore, 2015; Gao et al., 2019; Ji et al., 2019; Wei et al., 2021; Fujita et al., 2022).

Previous works over *GS1a* in conifers have determined a similar expression pattern of this gene to that showed by *GS2*. This cytosolic enzyme has been found to be also associated to the chlorophyllous parenchyma of photosynthetic organs (Ávila et al., 2001) and, as well as *GS2* from angiosperms, its expression is upregulated by light (Cantón et al., 1999; Gómez-Maldonado et al., 2004a). In this sense, *GS1a* has been proposed to fulfill the role of *GS2* in gymnosperms (Cantón et al., 1999).

INTRODUCTION

On its part, *GS1b* in conifers is phylogenetically more related to cytosolic isoforms from angiosperms than to conifers *GS1a* (Ávila et al., 2000). This isoform is ubiquitously expressed in the plant and its expression is also related to vascular tissues (Ávila et al., 2001). *GS1b* has been proposed to play a role in N remobilization between source and sinks organs during active growth period (Suárez et al., 2002). Furthermore, studies in pine suggest a role of *GS1b* in the canalization of ammonium to glutamine during seed germination and early developmental stages of seedlings (Ávila et al., 2001), hypothesis which is supported by its expression patterns in different developmental stages of zygotic and somatic pine embryos (Pérez-Rodríguez et al., 2005). The upregulated expression of this gene in reaction wood, together with its association to vascular tissues, seems to indicate that this gene is also involved in ammonium reassimilation during lignin biosynthesis (Cantón et al., 2005).

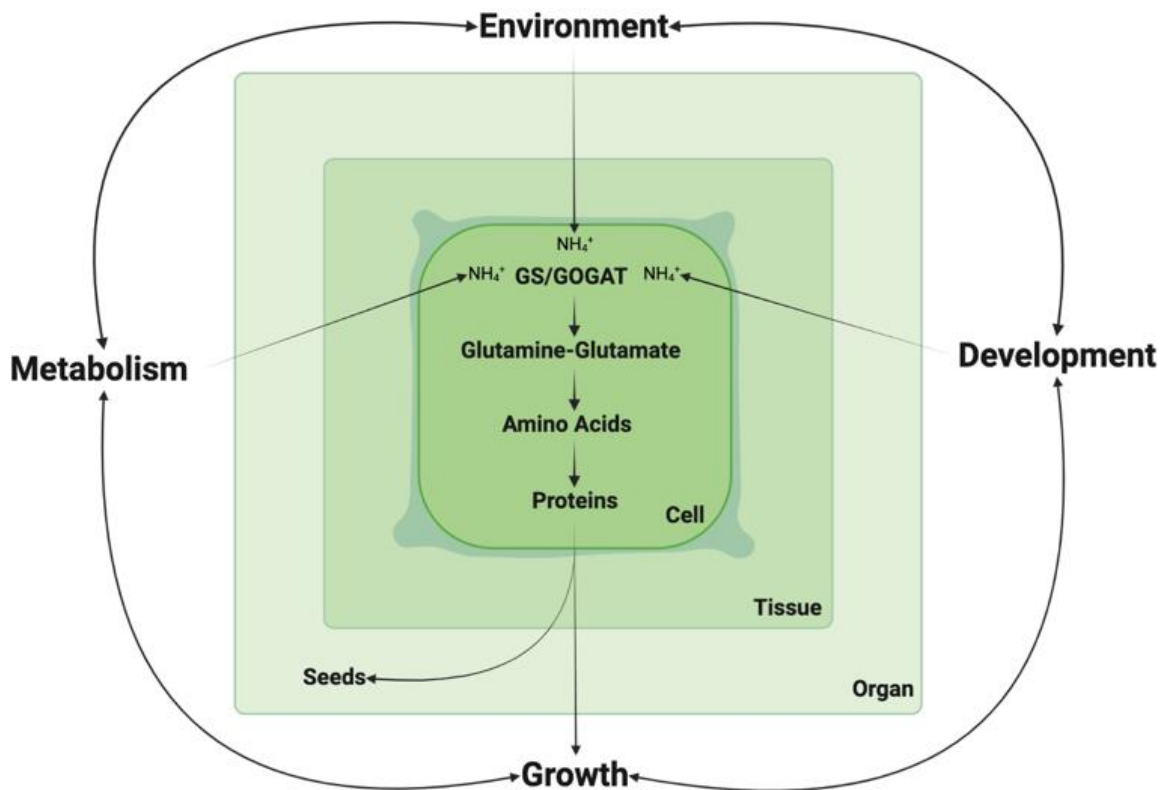


Figure I.6. Involvement of glutamine synthetase in different functional process of the plant. GS, glutamine synthetase; GOGAT, glutamate synthase. Figure adapted from Bernard and Habash (2009).

Objectives

OBJECTIVES

The general aim of this PhD thesis work is to increase the understanding of key aspects of N nutrition in plants. To this end, we propose to take advantage of the improved genome and transcriptome data available for gymnosperms to perform more in-depth studies on plant GS gene families. On the other hand, we also propose to study nitrate uptake, transport and signaling in the conifer *P. pinaster* to gain a better understanding of nitrate nutrition in pines and evolutionary relationships of N nutrition regulation in plants.

Three specific objectives proposed to fulfill the general objective of this PhD Thesis:

- 1. To understand the phylogenetic and evolutionary relationships of GS gene in seed plants by taking advantage of newly available transcriptome and genome data resources.**
- 2. To determine of the complete set of GS genes in conifers based on newly available genomic and transcriptomic data.**
- 3. To characterize the expression of pine nitrate transporter families as well as the global transcriptome response in roots in response to nitrate-based nutrition**

Chapter 1

A revised view on the evolution of glutamine synthetase isoenzymes in plants.

1. Introduction

GS catalyzes the incorporation of ammonium into glutamate using ATP to produce glutamine while releasing Pi and adenosine diphosphate (ADP) (Heldt and Piechulla, 2011). GS is an enzyme of major importance, as it represents the main, if not the only, mechanism incorporating inorganic N into organic molecules in virtually all living organisms (Shatters and Kahn, 1989). It has been suggested that the genes encoding GS are not only some of the oldest genes in evolutionary history (Kumada et al., 1993) but also represent an excellent 'molecular clock' that can be used to perform phylogenetic studies (Pesole et al., 1991).

Three GS superfamilies have been identified, namely GSI, GSII and GSIII, with the corresponding proteins characterized by different molecular masses, different numbers of subunits and their occurrence in the three different domains of life (Archaea, Bacteria and Eukarya) (Ghoshroy et al., 2010). The GSI superfamily was first found in prokaryotes, although its presence in mammals and plants has also been reported (Mathis et al., 2000; Nogueira et al., 2005; Kumar et al., 2017). The GSII superfamily was described as a group characteristic of Eukarya and some Bacteria, such as Proteobacteria and Actinobacteria (James et al., 2018). However, the nucleotide sequences deposited in public databases indicate that this GS superfamily is also present in Euryarchaeota, a phylum of the Archaea domain. Finally, the GSIII superfamily is characteristic of bacteria, including cyanobacteria (James et al., 2018), and some eukaryotes, such as diatoms and other heterokonts, suggesting that GSIII is present in the nuclear genome of early eukaryotes (Robertson and Tartar, 2006). The hypothesis that these three gene superfamilies appeared prior to the divergence of eukaryotes and prokaryotes has been proposed in several studies (Robertson and Tartar, 2006).

In plants, glutamine synthesis is catalyzed by enzymatic proteins belonging to the GSII superfamily. Two main groups of GSII have been shown to occur in the Viridiplantae group, one of eukaryotic origin, GSII (GSIIe), and the other of eubacterial origin, GSII (GSIIb). GSIIb genes are the result of HGT following the divergence of prokaryotes and eukaryotes, which in turn represent a sister group of γ -proteobacteria GSII (Tateno, 1994; Ghoshroy et al., 2010). As N is one of the main limiting nutrients for plant growth and development, the functions and characteristics of GS have been studied extensively in a large number of vascular plant species, and particularly in crops (Plett et al., 2017; Mondal et al., 2021). It is generally indicated that angiosperms contain two groups of nuclear genes encoding GSIIe, represented by cytosolic GS (GS1) and plastidic GS (GS2), each playing distinct physiological roles (Ghoshroy et al., 2010; Hirel and Krapp, 2021). GS2 is generally

CHAPTER 1

encoded by a single gene, whereas GS1 is encoded by a small multigene family (Cánovas et al., 2007; James et al., 2018). Phylogenetic analyses suggest that GS2 probably evolved from GS1 gene duplication (Biesiadka and Legocki, 1997) that diverged from a common ancestor 300 Mya. Therefore, this gene duplication probably occurred before the divergence of monocotyledons and dicotyledons (Bernard and Habash, 2009). Interestingly, the gene encoding GS2 is present in the gymnosperm *G. biloba* (García-Gutiérrez et al., 1998; Guan et al., 2016). This gene is absent in all the other gymnosperms examined thus far, including conifers (Coniferopsida) and the Gnetales (Gnetopsida), in which the gene encoding GS2 has not been found in their genomes (Birol et al., 2013; Nystedt et al., 2013; Neale et al., 2014; Zimin et al., 2014; Stevens et al., 2016; Neale et al., 2017; Wan et al., 2018; Kuzmin et al., 2019; Mosca et al., 2019; Scott et al., 2020). Furthermore, this gene also seems to be absent in cycads (Cycadopsida), as the GS2 protein was not detected in Western blot analyses (Miyazawa et al., 2018).

In both angiosperm and gymnosperm plants, the synthesis and relative activity of the different GS isoforms are regulated in a species-specific manner, but also according to plant developmental stages, tissue, N nutritional status and environmental conditions (Cánovas et al., 2007; Bernard and Habash, 2009; Mondal et al., 2021). Consequently, each GS isoform plays a different role during N assimilation and N remobilization throughout the life cycle of a plant (Thomsen et al., 2014; Hirel and Krapp, 2021). GS2 predominates in photosynthetic tissues, such as leaf mesophyll cells, in order to assimilate the ammonium generated from nitrate reduction and released during photorespiration (Blackwell et al., 1987; Wallsgrove et al., 1987; Tegeder and Masclaux-Daubresse, 2017). In contrast, GS1 is present in almost all plant organs and tissues (Lea and Miflin, 2018). Cytosolic GS isoforms are mostly involved in primary N assimilation in roots and N remobilization and translocation in shoots (Thomsen et al., 2014). As such, it has been shown that they play a key role during plant growth and development, notably for biomass and storage organ production (Xu et al., 2012; Krapp, 2015; Havé et al., 2017; Amiour et al., 2021). In conifers, as a result of the absence of GS2, studies have focused on GS1a and GS1b, which are each encoded by a single gene. These two cytosolic isoforms of GS also exhibit distinct molecular and kinetic properties (Ávila-Sáez et al., 2000; de la Torre et al., 2002). GS1a has been proposed to fulfill the same function as GS2 in angiosperms because of its close relationship with chloroplast development and the presence of ammonium arising from photorespiration. This hypothesis was also supported by the fact that the gene encoding GS1a is expressed in photosynthetic organs, notably in chlorophyllous parenchyma cells (Ávila et al., 2001), and that its expression is also upregulated in the presence of light

CHAPTER 1

(Cantón et al., 1999; Gómez-Maldonado et al., 2004a). Moreover, GS1b is phylogenetically and functionally more closely related to the cytosolic isoforms of GS in angiosperms than to those of GS1a in conifers (Ávila-Sáez et al., 2000; Cánovas et al., 2007).

In this work, the increasing number of plant genome sequences made available in public databases were gathered to perform a deep phylogenetic analysis of the GSII family. The present study includes representative GS sequences from the entire plant evolutionary spectra, including those from monocot and dicot angiosperms and a number of model species that were representative of other taxa. This new phylogenetic study allowed us to propose a revised classification and nomenclature for the different GS isoforms in seed plants. In addition, GS gene expression experiments were conducted in *G. biloba*, *Magnolia grandiflora* and *P. pinaster* in order to strengthen the results obtained in the GS1a phylogeny.

2. Results

2.1 Phylogenetic analyses

A total of 168 nucleotide sequences from the coding DNA sequences (CDSs) and the corresponding protein sequences of the genes encoding GSII from 45 different Viridiplantae species were retrieved from different public databases or assembled using next-generation sequencing (NGS) data from the Sequence Read Archive (SRA) database (Table S1). Additionally, *Escherichia coli* glnA (GSI) was used as an external group. The sequences and species analyzed cover the evolutionary history of Viridiplantae and included members of the main Viridiplantae clades, unless the sequences were not available in the public databases. These sequences were used to perform phylogenetic analyses to assess GSII evolution in Viridiplantae. The final names of the sequences were assigned depending on phylogenetic analyses (Figures 1.1, 1.2; Table S1.1). The GSIIb sequences were named GLN2 following the nomenclature of *GLN2*, the gene encoding GS in *Chlamydomonas reinhardtii*. The GSIIe group, which corresponds to species older than the Embryophyta, was named GLN1. The sequences from Embryophyta species were named GS1, except those included in the group of the Spermatophyta GS2 sequences.

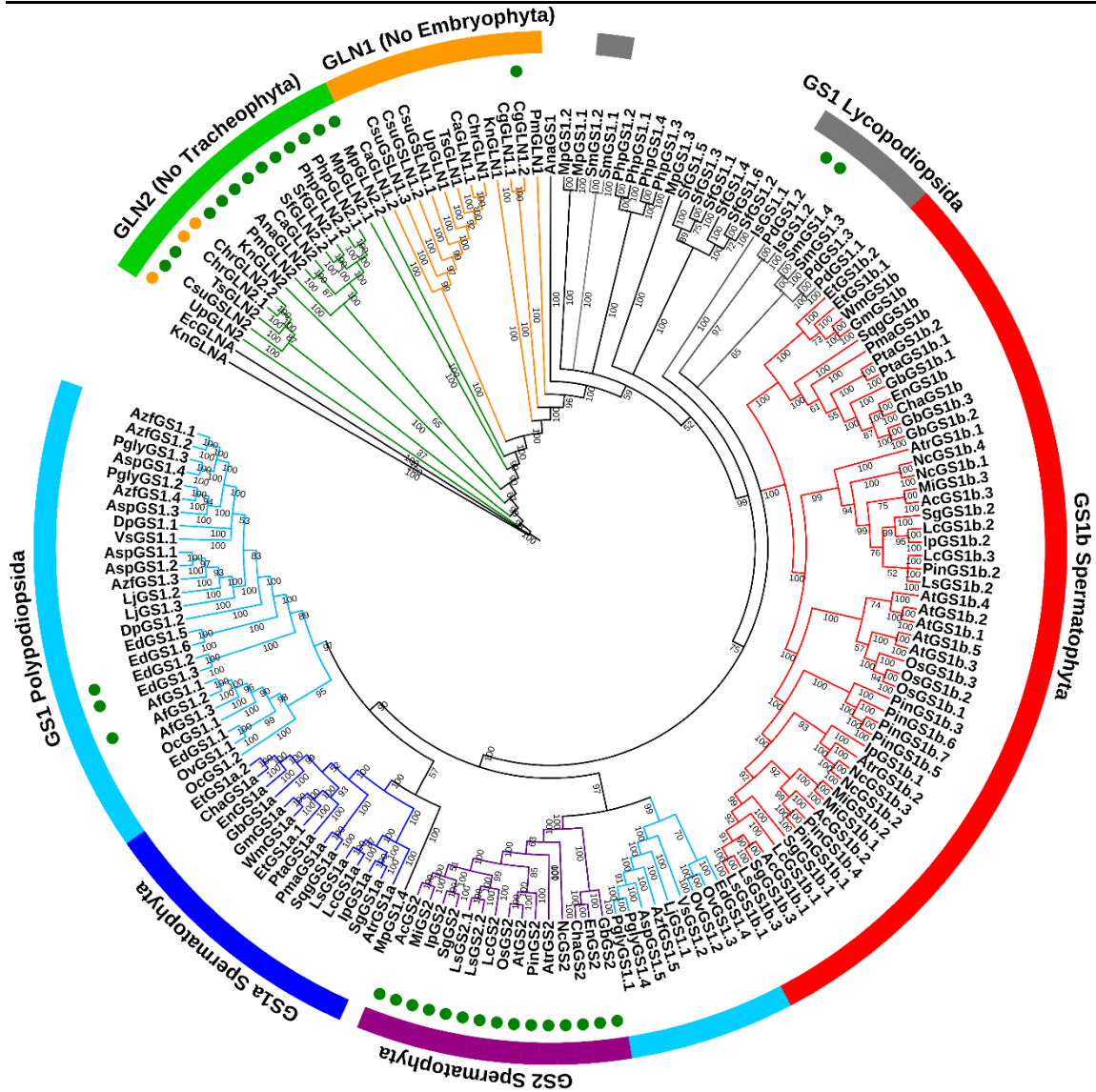


Figure 1.1 Phylogenetic tree of plant glutamine synthetase (GS) nucleotide sequences obtained following a Bayesian analysis. The first two letters of the sequence names correspond to the genera and species listed in Table MS1. Green circles highlight the sequences exhibiting a predicted plastidic localization. Orange circles highlight the sequences exhibiting a predicted mitochondrial localization. Branch lengths are not presented.

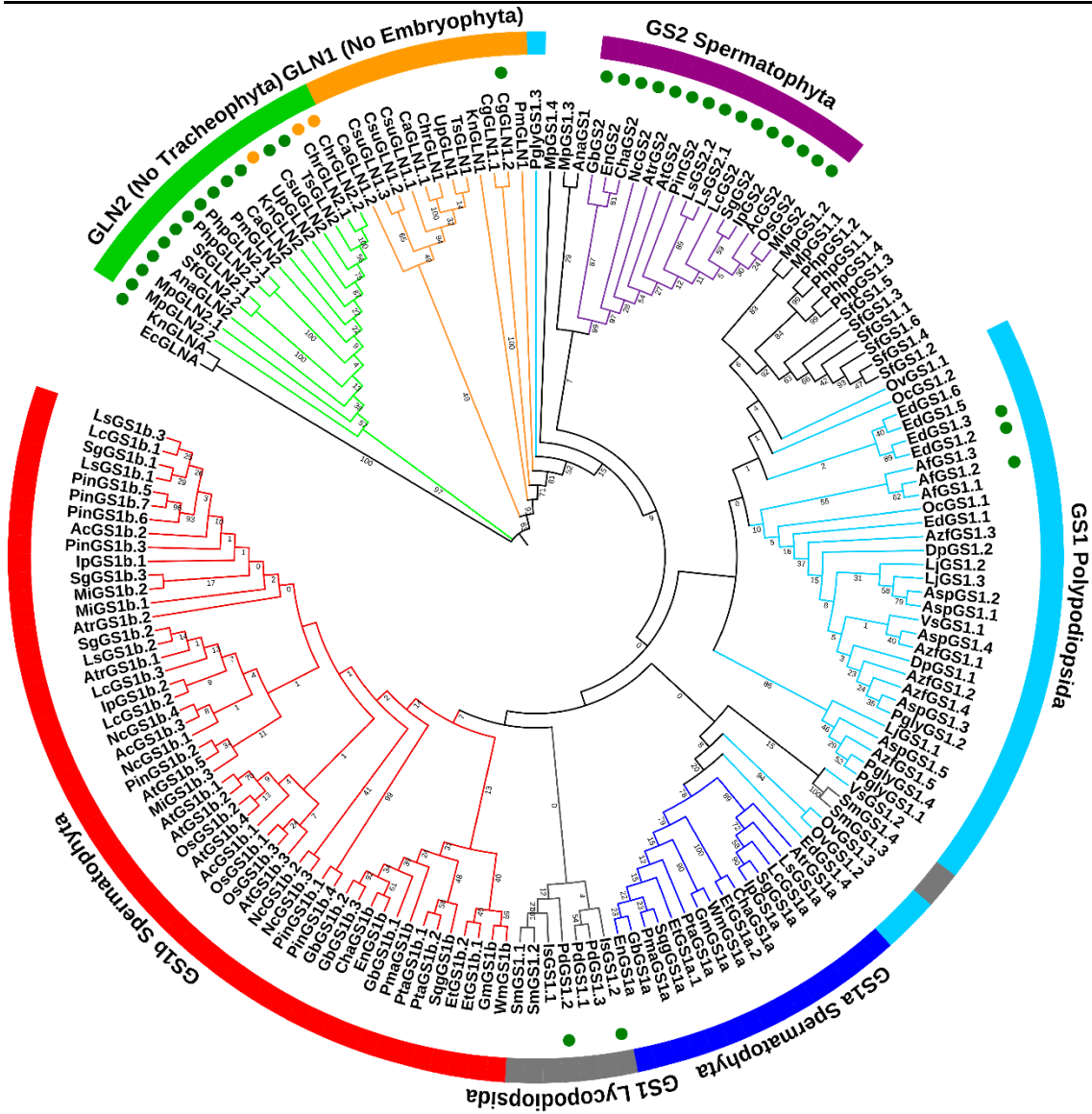


Figure 1.2. Protein phylogenetic tree of plant glutamine synthetase (GS) protein sequences following a maximum-likelihood analysis. The first two letters of the sequence names correspond to the genera and species listed in Table MS1. Green circles highlight the sequences with a predicted chloroplastic localization. Orange circles highlight the sequences with a predicted mitochondrial localization. Branch lengths are not presented.

The phylogenetic studies were conducted with nucleotide sequences using Bayesian analyses (Figure 1.1; Table S1.1). For the protein sequences, a maximum-likelihood approach was used (Figure 1.2; Table S1.2). The results were similar for the main GS groups whether the nucleotide or the protein sequences were analyzed. The *KnGLNA* sequence of *Klebsormidium nitens*, a charophyte green algae, was the most divergent GS close to the outer sequence *EcGLNA* (GSI) of *E. coli* (Figures S1.1 and S1.2). Both sequences were very distant from the other plant GS genes (mean length 2.0756), with a node/branch probability of 1 in the Bayesian analysis.

CHAPTER 1

The first cluster contained all GLN2 (GSIIb) sequences. Notably, no GLN2 sequence was identified in vascular plants (Tracheophyta). In the protein sequence analyses, we observed that the GLN2 cluster shared a common origin. In addition, different subgroups for GLN2 were identified in the nucleotide sequence clustering analyses. These GLN2 subgroups were distant from the other plant GS sequences (GSIIe; mean length 0.7142) (Figures S1.1 and S1.2). For both the GLN2 nucleotide and protein sequences, the node/branch probability/bootstrap was high (>0.65). In all GLN2 sequences, we found a predicted localization in the chloroplast using targetp, except for UpGLN2, ChrGLN2.1 and ChrGLN2.2, for which mitochondrial localization (Figures 1.1 and 1.2; Table S1.1).

The most ancient GSIIe plant sequences were named GLN1, and in both analyses, they were distributed in a main group containing four non-clustered sequences, including *KnGLN1* (Klebsormidiophyceae class), *CgGLN1.1* and *CgGLN1.2* (Coleochaetophyceae class), and *PmGLN1* (Zygnemophyceae class). These four sequences were in an intermediary position between the main GLN1 cluster and the other GS sequences from land plants. A predicted chloroplast localization was only found for *CgGLN1.2* (Figures 1.1 and 1.2).

Three clusters were identified in seed plants (Spermatophyta), including plastidic GS2 and gymnosperm GS1a-like and GS1b-like sequences (Figures 1.1 and 1.2). Interestingly, within the GS2 group, three sequences from gymnosperms were identified (*GbGS2*, *ChaGS2* and *EnGS2*). They corresponded to a ginkgo sequence and two Cycadopsida sequences. The GS1a-like group contained known GS1a sequences from gymnosperms and GS1 from basal angiosperms and from some Magnoliidae, except Ranunculales, Proteales, Liliopsida and Eudycotyledon species. However, an ortholog of the GS1a gene was not identified in the genome of *Piper nigrum*, a Magnoliidae species from the Piperales order (Hu et al., 2019). Finally, the GS1b-like cluster contained GS1b found in gymnosperms and the GS1 enzymes previously characterized in angiosperms.

The phylogeny of GS from Anthocerotophyta, Bryophyta, Lycopodiopsida, Marchantiophyta and Polypodiopsida was more complex than that of Spermatophyta, especially when the protein sequences were analyzed (Figures 1.1 and 1.2). However, with the cognate gene sequences, Anthocerotophyta, Bryophyta, Lycopodiopsida and Marchantiophyta were in a basal position compared with the other Embryophyta species. Such a distribution corresponded to the expected evolutionary relationships between plant species, except for the outlier sequence *MpGS1.4* that was found in the GS1a-like cluster (Figure 1.1). Fern (Polypodiopsida) GS genes were grouped into two clusters. The first one contained most of

CHAPTER 1

the nucleotide sequences linked to the GS1a-like sequences, and the second was grouped with GS2 and was composed of *AspGS1.5*, *AzfGS1.5*, *EdGS1.4*, *LjGS1.1*, *OvGS1.2*, *OvGS1.3*, *PglyGS1.1*, *PglyGS1.4* and *VsGS1.1*. For these two clusters, the mean probabilities were very high (0.9 and 0.97, respectively) when Bayesian analysis was used (Figures 1.1 and S1.1).

In contrast, the phylogenetic relationships with the protein sequences were unclear because of a different cluster distribution and the occurrence of outlier sequences such as *PglyGS1.3* and *MpGS1.4* (Figure 1.2). Most of the Marchantiophyta and Bryophyta GS enzymes were grouped with most of the Polypodiopsida sequences, although *MpGS1.3* and *AnaGS1* clustered with the GS2 from Spermatophyta. This group of GS proteins was closer to that of the Spermatophyta GS1 compared with GS2, even though the node/branch bootstraps were very low (<1). The Lycopodiopsida GS enzymes were grouped together with GS1b-like protein sequences even though the node/branch bootstrap was also very low (<1). Nevertheless, two sequences (*SmGS1.3* and *SmGS1.4*) were grouped with the Spermatophyta GS1a cluster together with four Polypodiopsida sequences (*EdGS1.4*, *OvGS1.2*, *OvGS1.3* and *VsGS1.2*) (Figure 1.2).

As expected, for all members of GS2, the presence of a signal peptide that allows the targeting of the protein to the chloroplast was predicted (Figures 1.1 and 1.2; Table S1.1). Only five of the remaining Embryophyta proteins were predicted to be localized in the chloroplast, including *IsGS1.2* and *PdGS1.2* from Lycopodiopsida species and *EdGS1.2*, *EdGS1.3* and *AfGS1.2* from Polypodiopsida species. Moreover, one could observe that these five GS enzymes did not belong to the GS2 cluster (Figures 1.1, 1.2; Table S1.1).

2.2 Spermatophyta GS gene expression

To further decipher the role of GS1a in ginkgo and in angiosperms, the level of expression of different GS genes was quantified in *G. biloba*, *M. grandiflora* and *P. pinaster*. Maritime pine (*P. pinaster*) was included in the study because the role and gene expression pattern of GS1a is well established in this gymnosperm, characterized by the absence of a gene encoding GS2 (Cánovas et al., 2007). The gymnosperm *G. biloba* and the angiosperm *M. grandiflora* were also studied because they possess GS genes corresponding to the three main Spermatophyta GS groups (GS1a, GS1b and GS2).

In maritime pine seedlings, the profiles of *PpGS1a* and *PpGS1b* gene expression were analyzed under different light/dark regimes (Figure 1.3): germination with a light/dark (L/D) cycle (16 h of light/8 h of darkness), continuous darkness and two opposite

nychthemeral regimes (from light to dark and from dark to light). *PpGS1a* was mainly expressed in the needles, irrespective of the light/dark regime, and in the stem only during the L/D cycle. In roots, the *PpGS1a* expression level was at the limit of detection under the four different light/dark conditions. In the needles, *PpGS1a* reached the highest level of expression in the dark–light transition, even though it was slightly lower under the L/D cycle. Compared with these two conditions, the *PpGS1a* expression level in the needles was at least five times lower when the plants were placed under continuous darkness and approximately two times lower following a light–dark transition. In contrast, *PpGS1b* was expressed in all three organs. In the needles and in the roots, the expression level of *PpGS1b* was significantly higher only during the light–dark transition. In the stem, the expression level of *PpGS1b* was highest when the seedlings were grown under the L/D cycle.

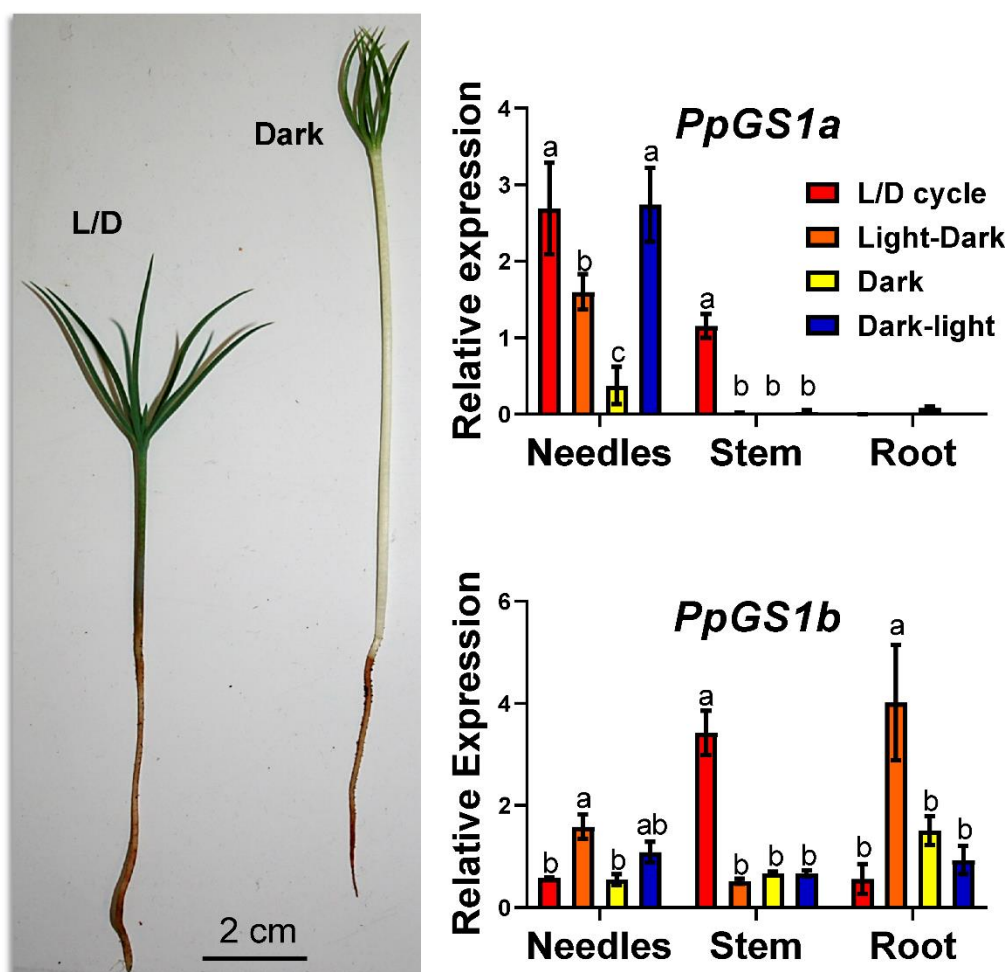


Figure 1.3. *PpGS1a* and *PpGS1b* gene expression in *Pinus pinaster* seedlings grown under different light regimes. L/D cycle (16-h light /8-h dark photoperiod, red bars), transition from light photoperiod to continuous darkness (orange bars), continuous darkness (yellow bars) and transition from complete darkness to light photoperiod (blue bars). Significant differences were determined using two-way analysis of variance (ANOVA) that compares the mean for each condition with the mean of the other condition in

CHAPTER 1

the same organ. Letters above the columns indicate significant differences on a Tukey's post hoc test ($p < 0.05$).

In *G. biloba* seedlings, the expression levels of *GbGS1a*, *GbGS2* and *GbGS1b* (1–3) were quantified during the L/D cycle and when plants were placed into continuous darkness (Figure 1.4a). The absence of leaves in *G. biloba* seedlings germinated under continuous darkness did not allow us to quantify the level of GS gene expression in this organ (García-Gutiérrez et al., 1998). Therefore, light/dark transition experiments were carried out using the leaves of 1-year-old *G. biloba* plants (Figure 1.4b). The level of *GbGS2* transcripts was very low both in the stems and the roots when the seedlings were grown under L/D or continuous darkness conditions. In contrast, the expression level of *GbGS2* was at least 20-fold higher in leaves grown under L/D conditions. Although the level of *GbGS1a* transcripts was higher in the leaves than in the other organs, it was four times lower than that of *GbGS2*. The three genes encoding *GbGS1b* were expressed at a higher level in the stems and in the roots than in the leaves. Two significant correlations were found: between the expression levels of *GbGS1a* and *GbGS2* (0.9) and between the expression levels of *GbGS1b.1* and *GbGS1b.2* (0.89). When fully expanded leaves were used, *GbGS1a* exhibited the highest level of expression compared with all the other GS genes during the L/D cycle. The pattern of *GbGS2* gene expression was similar to that of *GbGS1a*, although the transcript accumulation was three times lower. Transcripts for *GbGS1b.3* were not detected, irrespective of the light/dark regime (Figure 1.4b).

M. grandiflora seedlings were also exposed to different light treatments to study the GS gene expression pattern in this species (Figure 1.5). The transcripts of *MgGS1a* and *MgGS2* were more abundant in the leaves than in the stems and roots, and their levels were similar for *MgGS1a* in the L/D cycle and light–dark treatments. A very low level of expression was obtained for *MgGS1a* when seedlings were placed under continuous darkness.

Its level of expression was approximately fourfold lower than that of the L/D and light/dark treatments following a dark–light transition. *MgGS2* and *MgGS1a* exhibited a similar pattern of transcript accumulation, except that for *MgGS2* there was a significant decrease in the light–dark treatment and an increase during the transfer from dark to light. *MgGS1b.1* was the gene exhibiting the highest level of expression compared with all the other genes encoding GS. Its pattern of expression in the different organs was similar to that of *MgGS2*. However, the levels of *MgGS1b.1* transcripts were much higher in the stems, notably in L/D conditions, and in the

CHAPTER 1

roots. *MgGS1b.2* expression levels were similar in the three organs. No marked differences between the light and dark treatments were observed for this gene. *MgGS1b.3* transcript accumulation was similar irrespective of the organ and light/dark regimes, except in the stem, in which it was much higher during the L/D cycle. As shown in Figure 1.5, only four significant correlations were found between the expression level of the gene encoding GS in magnolia, where the highest correlation was between *MgGS1a* and *MgGS2* (0.92).

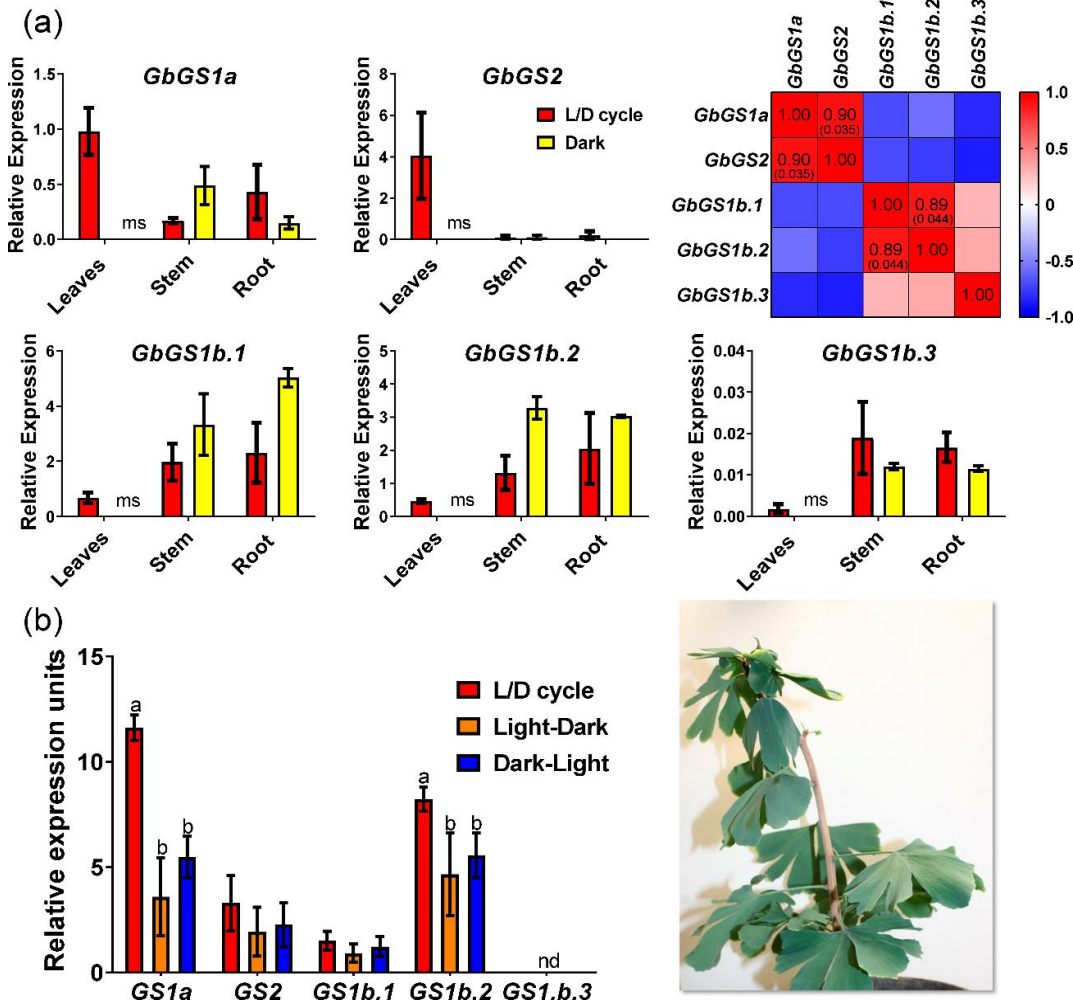


Figure 1.4. Glutamine synthetase (GS) gene expression in *Ginkgo biloba* seedlings grown under different light regimes. (a) One-month-old seedlings grown under the L/D cycle (16-h light/8-h dark photoperiod, red bars) and under continuous darkness (yellow bars). A Pearson correlation test was applied to the expression level of the different GS genes to quantify their relationship, indicated in the red squares. The significant p values (<0.05) for the Pearson coefficient are indicated in brackets. (b) One-year-old seedlings grown under the L/D cycle (16-h light/8-h dark photoperiod, red bars), under transition from the light photoperiod to continuous darkness (orange bars) and under transition from complete darkness to light photoperiod (blue bars). Significant differences were determined using a two-way analysis of variance (ANOVA) to compare the mean for each growth condition with the mean of the other conditions in the

CHAPTER 1

same organ. Letters above the columns indicate significant differences based on a Tukey's post hoc test ($p < 0.05$); nd, not detected; ms, missing sample.

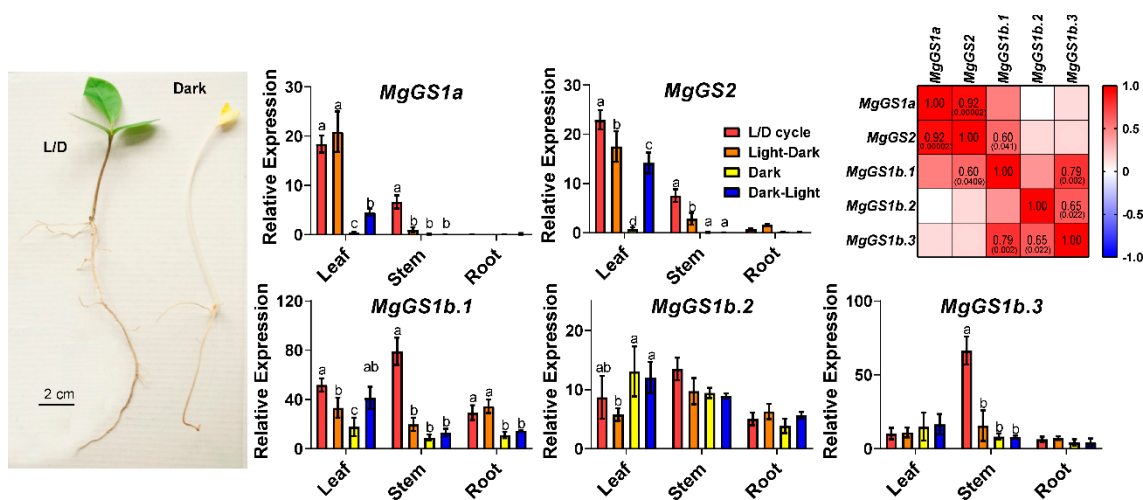


Figure 1.5. Glutamine synthetase (GS) gene expression in *Magnolia grandiflora* seedlings grown under different light regimes: L/D cycle (16-h light/8-h dark photoperiod, red bars); transition from light photoperiod to continuous darkness (orange bars); continuous darkness (yellow bars); and transition from complete darkness to light photoperiod (blue bars). Significant differences were determined using a two-way analysis of variance (ANOVA) that compares the mean for each condition with the mean of the other condition for the same organ. Letters above the columns indicate significant differences on a Tukey's post hoc test ($p < 0.05$). Pearson's correlation test was used to test for correlations between the expression levels of the different genes expressed in *M. grandiflora*. The significant p values (< 0.05) are indicated in brackets.

3. Discussion

In all plant species, each GS isoenzyme plays a key role, either in primary N assimilation or N recycling, as most of the N-containing molecules required for growth and development are derived from glutamine, the product of the reaction catalyzed by this enzyme. Throughout evolution, such important metabolic functions are subject to high selective pressure, which made GS particularly suitable for plant phylogenetic analyses. However, our knowledge of the phylogeny of the GS isoenzymes gathered in the evolutionary group called GSII remains limited. The aim of the present study was thus to improve our knowledge on the classification and phylogeny of the Viridiplantae GSII. This study was performed using the corresponding gene sequences belonging to the main clades that are representative of plant evolution and covering a large portfolio of species, not limited to the model and crop angiosperms.

In the present investigation, the resulting phylogenetic analysis agreed with previous studies in which two main groups of plant GSII encoded by nuclear genes were identified, namely GSIIb (GLN2) and GSIIe (GLN1/GS) (Figures 1.1 and 1.2). An HGT event from

CHAPTER 1

eubacteria was previously proposed as the more parsimonious process for the emergence of the GLN2 group (Tateno, 1994; Ghoshroy et al., 2010). This hypothesis is further supported by the fact that we identified a signal peptide in all members of GLN2 that allows the targeting of the proteins to organelles such as plastids and mitochondria (Table S1.1). Interestingly, genes encoding GLN2 were not identified in vascular plant (tracheophyte) species. Therefore, GLN2 seemed to be lost, coinciding with the final adaptation of plants to land habitats. Such an adaptive mechanism notably included the development of vascular structures for assimilate transport and the presence of lignin involved in plant stature (Raven, 2018; Renault et al., 2019). In fact, the massive production of lignin, a metabolic feature of vascular plants, was enabled by a deregulation of phenylalanine biosynthesis that occurred at some point during the evolution of non-vascular plants and tracheophytes (El-Azaz et al., 2022). These developmental and regulatory processes could also be related to the selection of the GLN1/GS genes in the most ancient vascular plants. Thus, it was hypothesized that GLN1/GS isoenzymes are involved: (i) in the synthesis of the transport of glutamine and derived amino acids (Bernard and Habash, 2009); and (ii) in the production of monolignols used as precursors for lignin biosynthesis. As lignin represents one of the main sinks for the photosynthetic C assimilated by the plant, high levels of GS activity are thus required to assimilate the large quantities of ammonium released during the reaction catalyzed by the enzyme phenylalanine ammonia lyase (Pascual et al., 2016). The phylogenetic analyses performed in the present study suggest that the group represented by GLN1 isoenzymes can be considered the starting point for the evolution of the most recent genes encoding GS in plants.

The phylogeny of the ancient Embryophyta clades (Anthocerotophyta, Bryophyta and Marchantiophyta) suggests that the current GS subgroups in Spermatophyta clades were not established in non-vascular land plants (Figures 1.1 and 1.2). Curiously, GLN2 was also found in these three clades, which could be the result of a stable situation related to the interaction of genotypic and environmental conditions during the expansion of this group of plants. However, a different clustering of GS in Lycopodiopsida and Polypodiopsida was observed between gene and protein phylogenetic trees, resulting in an unclear phylogenetic relationship (Figures 1.1 and 1.2). This finding suggests that during plant evolution there was an active adaptation process that resulted from changes in environmental conditions, such as an increase in the O₂/CO₂ ratio (Renault et al., 2019), and the loss of the GLN2 gene. According to this hypothesis, several Lycopodiopsida and Polypodiopsida GS protein sequences contain a predicted transit peptide allowing its import into plastids (Table S1.1).

CHAPTER 1

Therefore, under an oxygen-enriched atmosphere, the occurrence of plastidic GS seems to be beneficial for the plant, in turn leading to positive selection.

We also refined the classification of GS in seed plants (Spermatophyta), leading to the identification of three distinct clusters. One was the well-known group of genes from angiosperms encoding plastidic GS (GS2) (for a review, see Hirel and Krapp, 2021). The two other clusters contained the genes encoding cytosolic GS (GS1). One of the clusters included all the GS1 isoenzymes classically found in angiosperms and the GS1b from gymnosperms (Cánovas et al., 2007; Bernard and Habash, 2009). The third group included the GS1a sequences from gymnosperms, including ginkgo (Cantón et al., 1993; Ávila-Sáez et al., 2000), and different GS1 sequences from basal angiosperms and some Magnoliidae species. We thus propose to modify the nomenclature of GS genes from spermatophyte species into three subsets, namely GS1a, GS1b and GS2. Consequently, GSIIe can be used as a good phylogenetic marker in seed plants, as the presence or absence of the different GS gene groups is characteristic of the main taxa.

Surprisingly, searches for GS sequences in the NGS data from public databases allowed us to identify genes encoding GS2 in Cycadopsida species, contrary to previous findings (Miyazawa et al., 2018). Such a finding was experimentally confirmed by cloning a cDNA encoding GS2 from *Cycas revoluta* (MZ073670). The obtained sequence of the cloned *GS2* cDNA from *C. revoluta* validated the assembly of the *Cycas hainanensis* sequence using public NGS data (Figures S1.3 and S1.4). Consequently, this result demonstrated that there are more plant clades that possess GS2, which forms a new perspective on the evolution of GS2. In line with such a finding, recent phylogenomic studies showed that Cycadopsida and Ginkgoopsida formed a monophyletic group (Wu et al., 2013; Li et al., 2017; One Thousand Plant Transcriptomes Initiative, 2019). The presence of the genes encoding GS2 in both clades and its absence in the other gymnosperm clades (Coniferopsida and Gnetopsida) supports this taxonomic classification.

Based on our phylogenetic analysis, two hypotheses can be proposed concerning GS2 emergence and evolution.

1. A two-event evolutionary process, in which the gene encoding GS2 arose from a common ancestor of gymnosperms and angiosperms (Figure 1.6a). GS1 from Polypodiopsida, which is more closely related to GS2, could have been the origin of the plastid isoform following a specialization process that included the addition of a sequence that allowed the protein to be imported into the plastids. This hypothesis implies that there was a second genetic event

CHAPTER 1

consisting of the loss of GS2 in the common ancestor of Coniferopsida and Gnetopsida plants.

2. A single event during which GS2 sequences emerged from a common ancestor of Cycadopsida/Ginkgoopsida and angiosperm clades, leaving Coniferopsida and Gnetopsida without this gene (Figure 1.6b). Although gymnosperms are considered a monophyletic clade that is sister to angiosperms (One Thousand Plant Transcriptomes Initiative, 2019), the single-event hypothesis for GS2 evolution is more parsimonious and suggests a revision of the phylogenetic relationships of the Cycadopsida/Ginkgoopsida clade with angiosperms.

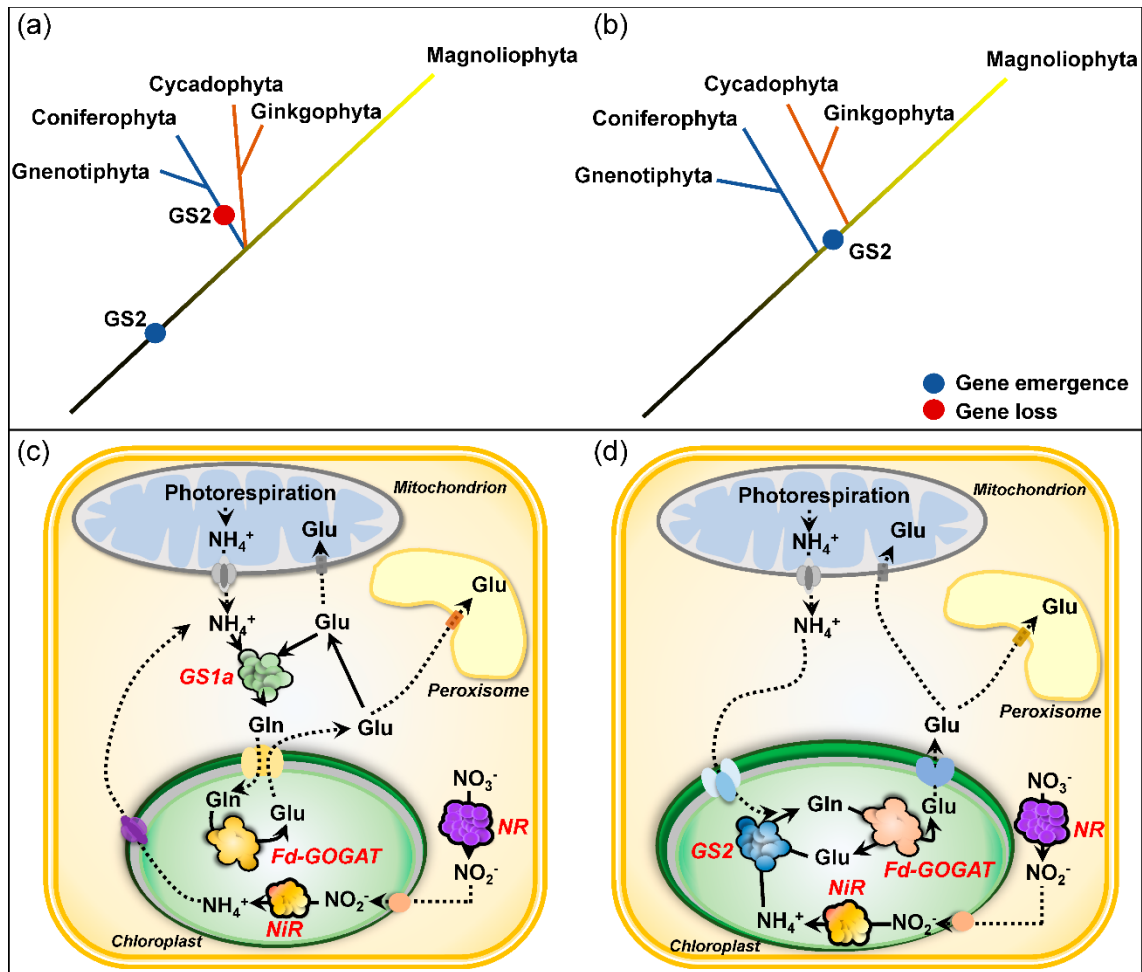


Figure 1.6. Schematic representation of GS2 emergence hypotheses: (a) two-event hypothesis; (b) single-event hypothesis. (c) Simplified metabolic pathways in a photosynthetic cell in which ammonium assimilation is catalyzed by GS1a. (d) Metabolic pathway of a photosynthetic cell in which ammonium assimilation is catalyzed by GS2. GS, glutamine synthetase; Fd-GOGAT, ferredoxin-dependent glutamate synthase; NR, nitrate reductase; NiR, nitrite reductase.

The occurrence of a gene encoding GS1a has never been previously described in ginkgo, basal angiosperms and Magnoliidae species. The physiological function of GS1a was extensively studied in conifers because it compensates for the lack of GS2. Although GS1a is

CHAPTER 1

a cytosolic form of the enzyme, its light-dependent expression level is also associated with chloroplast development, photorespiration, and N assimilation and recycling in photosynthetic tissues (Cánovas et al., 2007). One can hypothesize that, even though they are in different cellular compartments, GS1a and GS2 play redundant roles in photosynthetic cells, which could explain the disappearance of GS1a in the most recent angiosperm species. The light dependence and organ gene expression of GS1a and GS2 in *P. pinaster* (Figure 1.3), *G. biloba* (Figure 1.4) and *M. grandiflora* (Figure 1.5) strengthened the previous hypothesis that GS1a might fulfill the function of GS2 (Cantón et al., 1999; Ávila et al., 2001; Gómez-Maldonado et al., 2004a). Interestingly, one of the two Cys residues involved in the redox modulation of GS2 activity (e.g. C306 in *Arabidopsis*) was conserved in all of the GS1a proteins (Cantón et al., 1993; Choi et al., 1999; Miyazawa et al., 2018). We also observed that this residue was conserved in all the GS1a and GS2 protein sequences analyzed in this study, and in sequences from Polypodiopsida (ancient Embryophyta clades), several Lycopodiopsida species and GLN1 sequences (Figure S1.5). Remarkably, this Cys residue is absent in all GS1b sequences, suggesting a specific role of this residue in the function of GS2 and GS1a. In angiosperms, a second Cys residue is present in GS2 (e.g. C371 in *Arabidopsis*) and in several GLN1 proteins. Moreover, this second Cys residue is not present in ginkgo or Cycadopsida GS2, which suggests that it was acquired by angiosperms during plant evolution (Figure S1.5).

When the single-event hypothesis is considered, the emergence of GS2 sequences following the loss of GS1a sequences in recent angiosperms indicates that they probably have redundant physiological functions. The Cycadopsida/Ginkgoopsida group emerged at least 270 Mya (Wu et al., 2013; Li et al., 2017; One Thousand Plant Transcriptomes Initiative, 2019) during the Permo-Carboniferous period, when the atmospheric oxygen level rose from 21 to 35%. Such an elevation in oxygen level led to a drastic increase in the oxygenase activity of the photosynthetic enzyme Rubisco, leading to increased photorespiration (Berling and Bermer, 2000). The series of events that occurred during the Permo-Carboniferous period could result in the appearance of a plastidic GS isoenzyme (GS2) through a positive selection process, allowing for a more efficient reassimilation of ammonium that is released during photorespiration. The mutation of GS2 in several species induced lethality under photorespiratory conditions (Blackwell et al., 1987; Wallsgrove et al., 1987; Pérez-Delgado et al., 2015), which is not the case in *Arabidopsis*, as it can cope with the toxicity of ammonium released from the photorespiratory pathway (Ferreira et al., 2019; Hachiya et al., 2021). Conifers, which are C3 species possessing only cytosolic GS isoenzymes (Figure 1.6c), are also able to reassimilate the ammonium released during

CHAPTER 1

photorespiration. However, the increase in the level of atmospheric oxygen during the Permo-Carboniferous period would imply an increase in nitrification rates, as oxygen is a substrate for nitrification (Ward, 2008), thus leading to an increase in nitrate availability in the rhizosphere. One can therefore hypothesize that such an increase in nitrate availability induced additional evolutionary pressure towards the selection of plastidic GS (GS2), which, in addition to photorespiratory ammonium reassimilation, is also responsible for the assimilation of ammonium in plastids derived from nitrate reduction (Figure 1.6d) (Hirel and Krapp, 2021). Consistent with this hypothesis, it is known that most conifers prefer or tolerate ammonium as an inorganic N source, which can be readily assimilated by cytosolic GS in the absence of GS2.

Concerning the process of GS2 selection, the most likely hypothesis is the duplication of genes encoding cytosolic GS, leading to functional specialization through changes such as those in the gene promoter and the addition of a sequence encoding a signal peptide used to import the protein into the chloroplasts (Biesiadka and Legocki, 1997; Ávila-Sáez et al., 2000). Gene expression patterns, specific Cys residue conservation and nucleotide sequence-based GS phylogeny suggest that GS1a could be at the origin of GS2 (Figures 1.1 and 1.3-1.5).

Finally, we were able to conclude that the group represented by GS1b evolved in a different way than the groups represented by GS1a and GS2. In ginkgo and angiosperms, GS1b is generally represented by a small multigene family, with each member playing distinct roles either in N assimilation or N recycling, depending on the organ examined (Thomsen et al., 2014). In contrast, there is usually only one gene of GS1a or GS2, strongly suggesting that GS1b genes play non-redundant roles compared with GS1a and GS2 (Ghoshroy et al., 2010; Hirel and Krapp, 2021). Related to their different roles, the comparison between the GS1a and GS1b proteins in pine showed distinctive characteristics, such as a higher thermal stability of GS1b (de la Torre et al., 2002).

Chapter 2

**A gene encoding a cytosolic glutamine synthetase in pine is linked
to developing tissues**

1. Introduction

N is an essential element, a constituent of the main biomolecules and a limiting factor for plant growth (Hirel and Krapp, 2021). N is assimilated from ammonium into organic molecules by the GS/GOGAT cycle. Ammonium is first incorporated into glutamate to form glutamine in an ATP-dependent reaction catalyzed by the GS enzyme (Heldt and Piechulla, 2011), and then this glutamine together with 2-oxoglutarate is used to produce two glutamate molecules by the GOGAT enzyme (Bernard and Habash, 2009). Studies have shown that up to 95% of ammonium is assimilated via the GS/GOGAT cycle (Lea et al., 1999) for the formation of glutamine and glutamate, which, in turn, will be used to produce all N-containing biomolecules in the plant (Forde and Lea, 2007; Bernard and Habash, 2009).

The GS enzyme has been widely studied in plants since it is directly responsible for the incorporation of inorganic N into organic molecules. Recently, three different lineages of *GS* genes have been identified in seed plants: *GS1a* and *GS1b* encode cytosolic enzymes, and *GS2* encodes a plastid-located enzyme (Valderrama-Martín et al., 2022). The three *GS* gene lineages are present in cycads and *G. biloba*, as well as basal angiosperms. Nevertheless, no *GS2* genes have been found in other gymnosperms, such as conifers and gnetales, and no *GS1a* genes have been found in modern angiosperms, including monocot and eudicotyledon species (Valderrama-Martín et al., 2022). In general, *GS1b* is encoded by a small multigene family, while *GS1a* and *GS2* are usually encoded by a single nuclear gene (James et al., 2018; Valderrama-Martín et al., 2022).

GS2 and *GS1a* are associated with photosynthetic organs (Blackwell et al., 1987; Ávila et al., 2001), and their expression is regulated by light conditions (Cantón et al., 1999; Gómez-Maldonado et al., 2004a; Valderrama-Martín et al., 2022). Indeed, *GS2* and *GS1a* are considered to play a fundamental role in the assimilation of the ammonium released during photorespiration and nitrate photoassimilation processes (Wallsgrave et al., 1987; Blackwell et al., 1987; Cantón et al., 1999; Tegeder and Masclaux-Daubresse, 2017). In this sense, new evidence suggests that the *GS2* gene may have arisen through a gene duplication from a *GS1a* gene in a common ancestor of cycads, ginkgo, and angiosperms (Valderrama-Martín et al., 2022).

GS1b corresponds to the *GS1* isoenzyme traditionally studied in model angiosperms. Although this lineage is represented by a unique gene in most of the gymnosperms, in ginkgo and angiosperms, *GS1b* is represented by a small multigenic family. These genes have different expression patterns depending on the organ and physiological conditions

accounting for their different functions (Hirel and Krapp, 2021). These enzymes have been described as a key components of plant nitrogen use efficiency, with essential roles in processes such as senescence (Thomsen et al., 2014), amino acid catabolism, primary assimilation, and different stress responses (Bernard and Habash, 2009). The different genes of this lineage are differentially regulated by developmental state, tissue, nutritional status, and external stimuli (Thomsen et al. 2014; Hirel and Krapp, 2021). Finally, several studies have focused on the enzymatic characterization of GS from angiosperms and gymnosperms (Sakakibara et al., 1996; de la Torre et al., 2002; Ishiyama et al., 2004a; Ishiyama et al., 2004b; Ishiyama et al., 2006; Yadav, 2009; Zhao et al., 2014; Castro-Rodríguez et al., 2015) to define a more accurate role landscape for the different GS isoforms.

Some GS1b isoforms are directly related to developmental processes and have been associated with plant productivity. *AtGS1.1* and *AtGS1.2* from *A. thaliana* are involved in seed production and germination (Guan et al., 2015). *AtGS1.1* has also been described to be involved in root development during seed germination and *AtGS1.2* plays a role in rosette development (Lothier et al., 2011; Guan et al., 2015). Indeed, a recent study over of *AtGS1.1*, *AtGS1.2* and *AtGS1.3 Arabidopsis* mutants suggested synergistic roles for these genes in plant growth and development (Ji et al., 2019). In cereals, enzymes of this GS lineage are involved in seed yield and plant development, such as *GS1;3* from *Oryza sativa* and *Hordeum vulgare*, which play roles in seed maturation and germination (Goodall et al., 2013; Fujita et al., 2022). Thus, overexpressing lines of *HvGS1.1* showed an improvement in grain yield (Gao et al., 2019). Rice mutants lacking the *OsGS1;1* gene presented reduced grain filling and growth (Tabuchi et al., 2005), although the same phenotype was present in rice lines overexpressing *OsGS1;1* (Bao et al., 2014). In addition, rice lines grown in culture chambers and overexpressing *OsGS1;1* presented an increase in spikelet yield. Rice mutants for *OsGS1b;2* also presented a depletion in the number of tillers (Funayama et al., 2013), and *Sorghum bicolor* lines overexpressing *GS1* genes exhibited the opposite phenotype (Urriola and Rathore, 2015). Studies in *Z. mays* using mutant lines for *ZmGS1b.3* and *ZmGS1b.4* have shown the roles of these genes in kernel number and size, respectively (Martin et al., 2006). Transgenic lines of *P. vulgaris* overexpressing GS1 also showed earlier flower and seed development, while overexpressing GS1 lines of wheat showed an increase in grain weight (Habash et al., 2001). Moreover, a recent study on wheat indicated that *TaGS1.1* and *TaGS1.3* are mainly expressed in embryos and grain transport tissues, where these isoforms synergistically carry out ammonium assimilation (Wei et al., 2021).

In conifers, only one isoform of the GS1b family has been identified to date. The unique GS1b identified in conifers has been suggested to play an essential role in N remobilization to developing organs (Suárez et al., 2002). Previous works in pine have shown that GS1b is involved in the canalization of ammonium into glutamine during seed germination and the early developmental stages of seedlings (Ávila et al., 2001), which could be important for the loss of seed dormancy (Schneider and Gifford, 1994). Indeed, the roles of GS1b in seed development and germination are also supported by its expression patterns associated with the vascular system of zygotic and somatic pine embryos at different developmental stages and by its expression in procambium cells of pine zygotic embryos (Pérez-Rodríguez et al., 2005). Moreover, the expression of this isoenzyme has been suggested to be controlled by GA, a phytohormone involved in many aspects of plant growth and development (Gómez-Maldonado et al., 2004b).

In this work, a gene encoding a cytosolic GS (*PpGS1b.2*) was identified in maritime pine (*P. pinaster*). This gene was discovered through sequence searches in transcriptomic data from isolated tissues through laser capture microdissection (Cañas et al., 2017). Orthologs of this gene have also been identified in the genomes of other conifers, and phylogenetic analysis has revealed that *PpGS1b.2* belongs to the *GS1b* lineage. Although this *GS1* gene presents a high sequence homology to the already known *PpGS1b*, hereafter *PpGS1b.1*, *PpGS1b.2* showed low expression levels with characteristic and localized tissue expression. The expression patterns suggest that this gene could play a specific role during plant development, mainly during embryo development, as has been shown for other *GS1b* genes in angiosperms. Furthermore, a detailed comparative analysis of the kinetic properties of the isoenzymes GS1b.1 and GS1b.2 and single/double-point mutants of both isoforms support distinct functions for these enzymes in pine.

2. Results

2.1 Sequence and phylogenetic analyses

An unknown cytosolic *GS* gene was identified in a transcriptomic analysis of tissues isolated using laser capture microdissection (Cañas et al., 2017). At the amino acid sequence level, the GS presents 80.85% and 92.68% identity with *PpGS1a* and *PpGS1b*, respectively (Figure 2.1A). Despite the high identity between the coding sequences of this gene and *PpGS1b*, the promoter regions of both genes are very distinct (Figure S2.2A). The lengths of the three pine GS proteins are very similar, with 357 residues for *PpGS1a*, 355 for *PpGS1b* and 357 for the enzyme identified in the present study (Figure 2.1A). However, the calculated

isoelectric points were more different between the pine GS proteins, being 6.21 in the case of *PpGS1a*, 5.73 for *PpGS1b* and 5.36 for the presented protein.

A phylogenetic analysis confirmed the classification of the GS from seed plants into three main groups, GS2, GS1a and GS1b, in line with previously reported results (Valderrama-Martín et al., 2022) (Figure 2.1B). As expected, no GS2 sequence was detected in conifers, but only those of GS1a and GS1b (Figure 2.1B). The identified GS isoform was grouped within the conifer GS1b sequences; thus, the gene coding this GS1b isoenzyme has been named *PpGS1b.2*. Orthologs of *PpGS1b.2* have also been detected in other members of the *Pinaceae* family of the genera *Pinus* and *Picea* but not in the rest of the conifers included in this analysis (Figure 2.1B).

CHAPTER 2

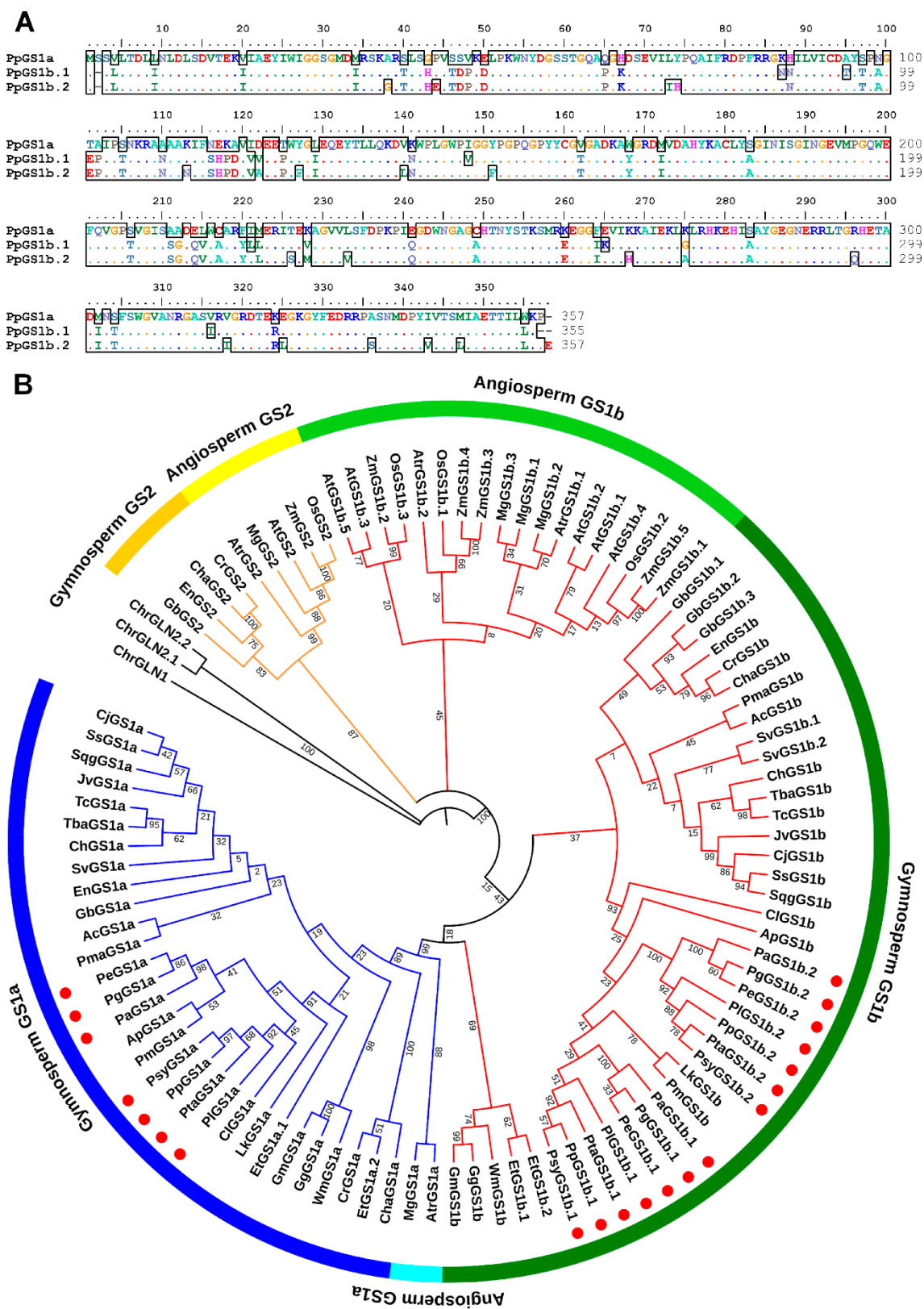


Figure 2.1. Protein alignment and evolutionary analysis by Maximum Likelihood method. A. Protein alignment of maritime pine GSs. PpGS1a sequence is showed as reference, dots highlight conserved residues in the three sequences. **B.** The evolutionary history was inferred by using the Maximum Likelihood method and JTT matrix-based model (Jones et al., 1992). The tree with the highest log likelihood (-12198.89) is shown. The

percentage of trees in which the associated taxa clustered together is shown next to the branches. Initial tree(s) for the heuristic search were obtained automatically by applying Neighbor-Join and BioNJ algorithms to a matrix of pairwise distances estimated using the JTT model, and then selecting the topology with superior log likelihood value. The tree is drawn to scale, with branch lengths measured in the number of substitutions per site. This analysis involved 96 amino acid sequences. All positions containing gaps and missing data were eliminated (complete deletion option). There was a total of 348 positions in the final dataset. Evolutionary analyses were conducted in MEGA11 (Tamura et al, 2021). Numbers close to the branches shown bootstrap values. The first two letters of the sequence names correspond to the genera and species listed in Table MS1. Golden tree branches correspond to GS2 sequences; blue branches to GS1a sequences; and red branches to GS1b sequences. Discontinuous lines in GS1b branches highlight the new sequences found in *Pinus* and *Picea* genera. Red dots shown the sequences from *Pinus* and *Picea* genera.

2.2 Gene expression analyses

The expression of *GS* genes in *P. pinaster* has been analyzed in different tissues and conditions to establish a framework that allows us to unravel the potential role of *PpGS1b.2* by comparing its expression pattern to other *GS* genes in maritime pine.

The expression profiles were analyzed in embryos and seedlings during the initial developmental stages (Figure 2.2A). *PpGS1a* expression was high in cotyledons and needles, lower in hypocotyls and nearly undetectable in roots and embryos except for germinated embryos. *PpGS1b.1* and *PpGS1b.2* expression patterns in embryos were very similar, with a peak of expression in germinated embryos. In seedlings, the expression was ubiquitous in all organs for both genes, although *PpGS1b.2* expression levels were lower than those of *PpGS1b.1*, between 5- and 10-fold. This expression pattern was different when isolated tissues were considered (Figure 2.2B). *PpGS1b.1* was expressed at high levels throughout the plant, especially in the root cortex, where the expression was 40 times that shown by this gene in the other samples. However, *PpGS1b.2* expression was very localized, mainly in the shoot apical meristem, emerging needles, developing root vascularization and root meristem. Expression was almost undetectable in the rest of the tissues analyzed. Finally, the expression of *PpGS1a* was detected only in the three photosynthetic tissues: the mesophyll of young needles, the mesophyll of cotyledons and the hypocotyl cortex.

The seasonal expression of the three *GS* genes has also been quantified in needles from adult trees (Figure 2.3A). *PpGS1a* showed the highest expression, followed by *PpGS1b.1*, which was expressed between 10 and 30 times less than *PpGS1a*. The expression patterns of the three genes in different whorls were as before, with higher levels in the first months of the year and lower levels at the end of the year. There was a remarkable exception for whorl 0 in May, the first harvesting month for the needles that emerged during the sampling year.

PpGS1b.2 exhibited an expression peak in whorl 0 in May. In contrast, *PpGS1a* had its lowest expression, and *PpGS1b.1* was expressed at similar levels to the other whorls.

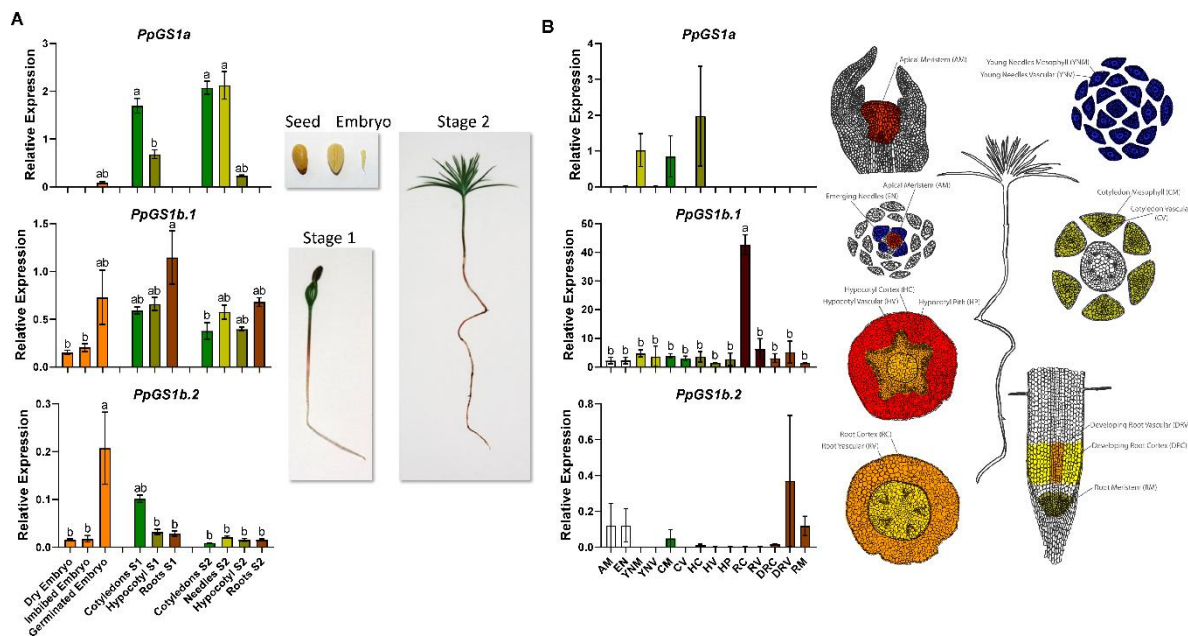


Figure 2.2. GS gene expression in maritime pine seedlings. **A.** Expression levels of GS genes of maritime pine during germination and initial seedling development. Stage 1 (S1) corresponds to seedlings with active mobilization of reserves from megagametophyte to the seedling (one-week-old from emergence). Stage 2 (S2) corresponds to seedlings without megagametophyte and developing the first new needles (one-month-old from emergence). **B.** Gene expression levels of GS in tissues from one-month-old seedlings (Cañas et al., 2017). AM, shoot apical meristem; EN, emerging needles; YNM, young needles mesophyll tissue; YNV, young needles vascular tissue; CM, cotyledon mesophyll tissue; CV, cotyledon vascular tissue; HC, hypocotyl cortex; HV, hypocotyl vascular tissue; HP, hypocotyl pith; RC, root cortex; RV, root vascular tissue; DRC, root developing cortex; DRV, root developing vascular tissue; RM, root apical meristem. Letters above the columns highlight the statistical significance ($p < 0.05$) in a Tukey post-hoc test after an ANOVA analysis. Error bars show SE with $n = 3$.

The relative abundance of *PpGS1b.2* transcripts was still one and two orders of magnitude lower than those of *PpGS1b.1* and *PpGS1a*, respectively. According to these results, the expression levels of the three genes were also analyzed in buds and emerging needles (Figure 2.3B-D). The expression of *PpGS1a* was almost undetectable in buds, but its expression rapidly increased in nascent needles by the end of the month. *PpGS1b.1* expression remained almost invariable in both organs with a similar expression pattern. The levels of *PpGS1b.2* were higher in the buds and decreased from Day 14 to 28 when the expression was similar in buds and emerging needles. The relative abundance of *PpGS1b.1* transcripts was still higher than that of *PpGS1b.2*.

GS gene expression has also been analyzed at different developmental stages, including juvenile and mature xylem and phloem, as well as the male and female reproductive structures, different root zones and different stages of zygotic embryo development (Figure 2.4).

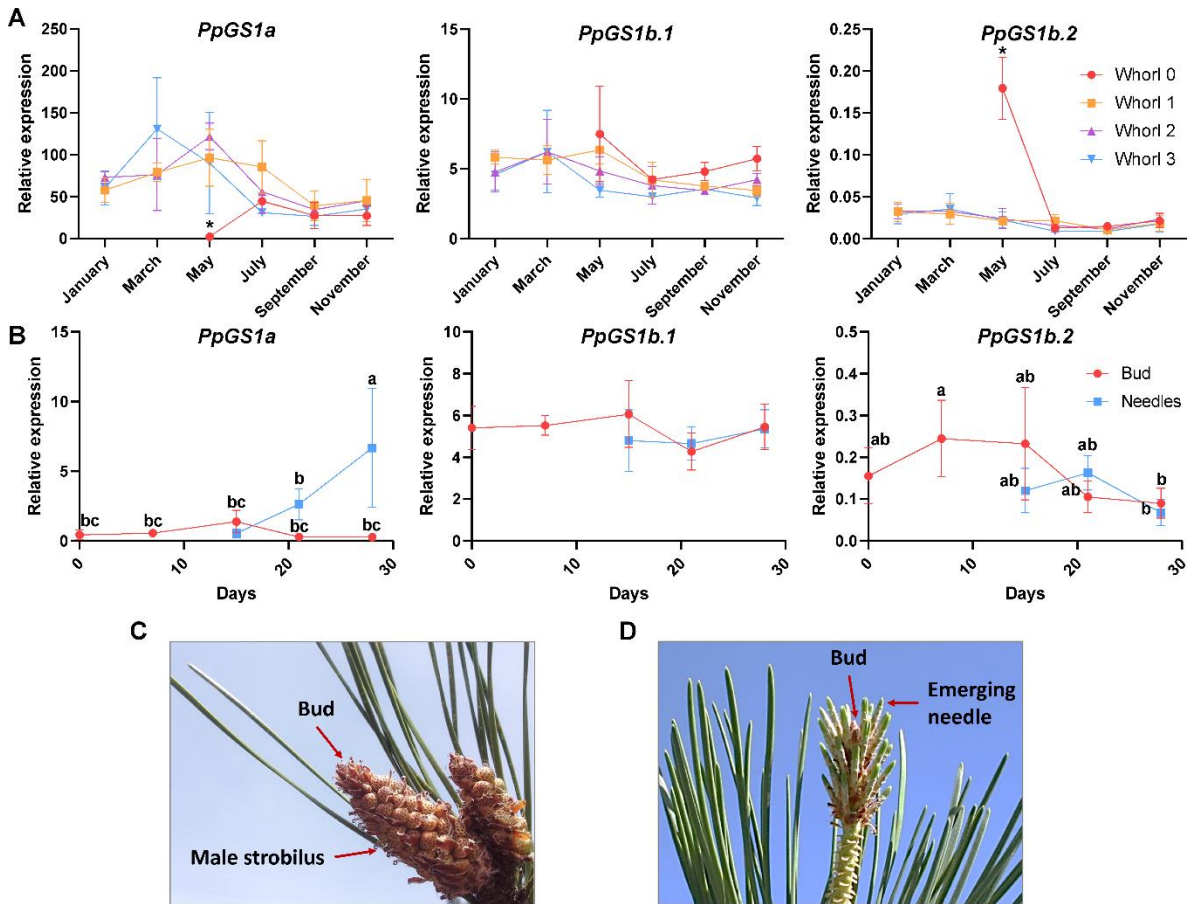


Figure 2.3. Seasonal *GS* expression profiles in pine needles from adult trees. **A.** Expression levels of *GS* genes were determined in needles from maritime pine along a year. Each needle whorl corresponds to the annual growth of a single year, the whorls were named by numbers, from 0 to 3 being this the oldest whorl. The whorl 0 corresponds to needles emerged in the same year of harvesting. For supplementary information see Cañas et al. (2015). **B.** Expression levels of *GS* genes in buds and developing needles during the first 21 days of emergence. **C.** Picture of buds and male strobilus in April during the first harvesting time. **D.** Picture of buds and emerging needles in May at four harvesting point (21 days). Letters above the columns highlight the statistical significance ($p < 0.05$) in a Tukey post-hoc test after an ANOVA analysis. Error bars show SE with $n=3$.

In all those samples, *PpGS1a* expression was barely detectable. An example of *PpGS1a* expression is shown for phloem, xylem, and male and female strobili, with very low levels (< 0.04), even in female strobilus with an expression peak (< 0.08) (Figure 2.4A). *PpGS1b.1* expression was the highest observed thus far among the *GS* genes analyzed in vascular tissues and strobili (Figure 2.4A). Interestingly, *PpGS1b.2* expression was almost

undetectable in vascular tissues, but its levels peaked in the male strobilus (approximately 0.28), opposite to what occurred with *PpGS1b.1* in that organ. In root samples, *PpGS1b.1* and *PpGS1b.2* presented a similar expression pattern, with increased expression in lateral roots and root tips, although the expression levels for *PpGS1b.1* were approximately 80-fold higher than that shown by *PpGS1b.2* (Figure 2.4B). Finally, in zygotic embryos, the expression levels of both genes were significantly higher in the precotyledonary and early cotyledonary stages, where *PpGS1b.2* levels were higher than those shown by *PpGS1b.1* (Figure 2.4C). However, this ratio of the expression of both genes was reversed in the later stages of development in cotyledonary and mature embryos. Nevertheless, the differences in expression between the two genes were not statistically significant in either case.

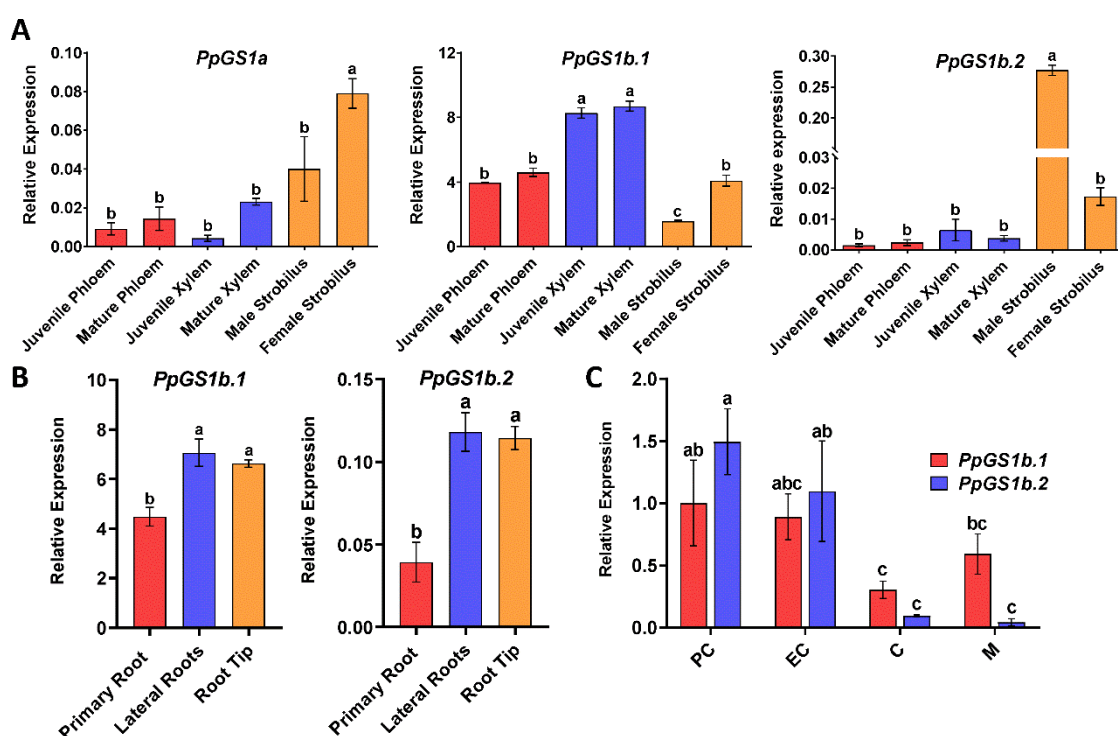


Figure 2.4. GS expression levels in different developing tissues. **A.** Gene expression levels of *PpGS1a*, *PpGS1b.1* and *PpGS1b.2* in different tissues of adult trees: juvenile and mature phloem; juvenile and mature xylem; and male and female strobili. **B.** Gene expression of *PpGS1b.1* and *PpGS1b.2* in different parts of the root from one-month-old seedlings: primary root, lateral roots, and root tip. **C.** Genes expression of *PpGS1b.1* and *PpGS1b.2* in different developmental stages of zygotic embryos: PC (pre-cotyledonary stage); EC (early cotyledonary stage), C (cotyledonary stage) and M (mature embryo). Letters above the columns highlight the statistical significance ($p < 0.05$) in a Tukey post-hoc test after an ANOVA analysis. Error bars show SE with $n=3$.

2.3 Protein structure prediction, physicochemical and kinetic properties

Very few differences were observed between the GS1b.1 and GS1b.2 subunit structures due to the similarity of their amino acid sequences (Figure 2.5A,B). Both proteins presented a

predicted decameric structure formed by two pentameric rings with small differences in structure and the disposition of the subunits in the quaternary structure (Figure S2.3A,B). However, the thermodynamic stability of GS1b.1 monomers was three times higher than that of GS1b.2 monomers (Table 2.1). The *in silico* replacement of residues of the GS1b.1 and GS1b.2 amino acid sequences displayed some differences in the structural stability of both enzymes (Figure S2.4). Some of the amino acids used for this analysis did not cause any notable effects on the structure or destabilized both proteins equally. However, several amino acids gave rise to large differences in the free energy of folding. Specifically, the inclusion of arginine or glutamate around position 280 produced a great destabilization of the structure of GS1b.2 but not of GS1b.1. Some of these amino acids also caused great destabilization of GS1b.2 when substituted at position 148 but did not have the same effect in GS1b.1. In fact, only isoleucine and arginine produced marked effects on the structural stability of GS1b.1. As small differences in the structure suggested that there might be changes in the physicochemical and kinetic properties of both enzymes, a functional comparison of the recombinant isoforms of GS1b.1 and GS1b.2 was performed (Figure 2.5, S2.4; Tables 2.1, 2.2).

Both isoforms were tested over a wide pH range; GS1b.1 maximum activity was reached at pH 6.5 while that of GS1b.2 maximum activity was reached at pH 6 (Figure 2.5C). The activity of both enzymes increased with the reaction temperature, reaching the maximum activity at 42 °C (Figure 2.5D). These data have allowed the calculation of the activation energy (E_a) for each enzyme (Table 2.1). The E_a was different for both enzymes: the E_a of GS1b.1 was 39.9 kJ/mol, and the E_a values of GS1b.2 for its elemental reaction steps were 46.1 kJ/mol and 18.7 kJ/mol, with a break point at 24 °C. Regarding the thermal stability, GS1b.1 was very stable, only decreasing its activity at 60 °C after 5 minutes of preincubation, although it never completely lost its activity, even after 20 min at 60 °C (Figure 2.5E). However, GS1b.2 showed a decreased activity even after 5 minutes of preincubation at 45 °C with almost a total loss of activity after 5 minutes at 60 °C (Figure 2.5E).

GS1b.1 and GS1b.2 showed distinctive behaviors for ammonium and glutamate (Figure 2.5F,G). GS1b.2 exhibited substrate inhibition for ammonium (K_i 22.57 mM). The affinities of both enzymes for ammonium were high (GS1b.1 K_m 0.12 mM and GS1b.2 K_m 0.21 mM). However, the V_{max} was 5.88 times higher for GS1b.1 (Table 2.2). Regarding to glutamate, GS1b.1 showed substrate inhibition at high concentrations (K_i 84.51 mM), while GS1b.2 presented positive cooperativity. In both cases, the affinity was very low (GS1b.1 K_m 64.15 mM and GS1b.2 EC_{50} 48.63 mM), with large differences in the V_{max} values of both enzymes

(GS1b.1 101.6 nkat/mg protein and GS1b.2 7.66 nkat/mg protein) (Table 2.2). GS1b.1 and GS1b.2 showed equal behavior for Mg_2^+ , with positive cooperativity and similar affinity (EC50 values of 14.49 and 10.87 mM, respectively) but different V_{max} values (71.32 and 5.64 nkat/mg protein, respectively) (Figure S2.5, Table 2.2). Finally, the affinities for ATP were high and similar for both enzymes (K_m of 0.18 and 0.29 mM for GS1b.1 and GS1b.2, respectively), with a higher V_{max} for GS1b.1 (24.96 nkat/mg protein) than for GS1b.2 (7.39 nkat/mg protein). However, there was substrate inhibition for GS1b.1 at moderate levels of ATP (K_i 5.88 mM).

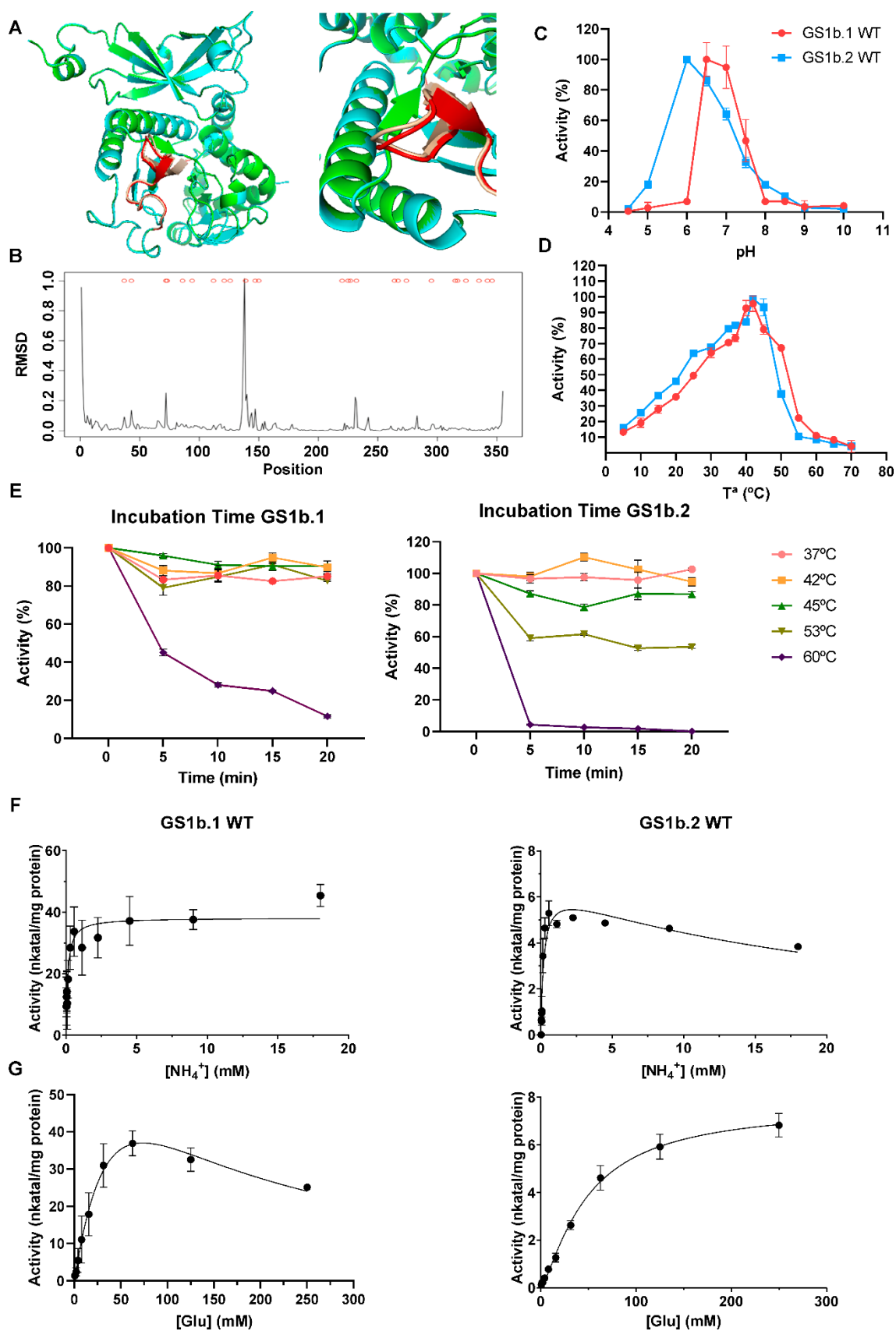


Figure 2.5. Enzymatic characterization of recombinant GS1b.1 and GS1b.2 isoforms. A. Comparison of GS1b.1 and GS1b.2 subunit structure GSb1.1 is represented in green and GS1b.2 in cyan. The region that

presented most differences between GS1b.1 and GS1b.2 (amino acids from 125 to 150) are represented in red and pink respectively. **B** Root mean square deviation (RMSD) values between GS1b.1 and GS1b.2 monomers structure. **C**. Enzyme activity at different assay pH (from 4.5 to 10) for GS1b.1 (red line) and GS1b.2 (blue line). **D**. Enzyme activity at different assay temperature (from 5 to 70°C) for GS1b.1 (red line) and GS1b.2 (blue line). **E**. Thermal stability of GS1b.1 and GS1b.2 at different temperatures (37, 42, 45, 53 and 60°C) after different preincubation times (from 0 to 20 min). **F**. Kinetics of GS1b.1 and GS1b.2 for ammonium. **G**. Kinetics of GS1b.1 and GS1b.2 for glutamate. Error bars show the SD. Mean values are composed with at least three independent determinations.

2.4 Analysis of mutant proteins

To determine the roles that certain residues could play in GS activity, mutants of GS1b.1 and GS1b.2 were obtained by exchanging amino acids at positions 264 and 267. These residues belong to a region that accumulates a significant number of differences between the two isoforms and is important for stability, as shown by the *in silico* substitution analysis (Figure S2.4). Additionally, these residues have been selected based on their charge and structural differences between both GSs. The amino acid swapping at positions 264 and 267 seemed to produce only slight changes in the subunit arrangement, even in the double mutant. Calculation of hydrogen bonds revealed interactions between residues 264 and 267 with those present at positions 261, 263, 265 and 268. These residues were analyzed in detail, and only small differences in their arrangements could be observed (Figure 2.6A-G, S2.5). The quaternary structures of the mutants also showed no significant differences when compared (Fig. S7) and the thermodynamic stability of the monomers was similar to that of the wild type (WT) (Table 2.1).

Compared to WT, none of the optimal pH values were affected in any of the mutants tested, except for GS1b.2E264K, where the optimum was reached at pH 7 (Figure S2.8A), and the double mutants, where the optimum pH was 6 for both enzymes (Figure 2.6H, S2.9).

A slight increase in the optimal temperature (45 °C) was detected in all mutants except for GS1b.2E264K, which experienced a large change in its optimal temperature (30 °C) (Figure 2.6I, S2.7B). Although the activity patterns in response to reaction temperature were similar in the mutants with respect to the WT enzymes, the activity was slightly higher at all temperatures in the GS1b.1K267H single and GS1b.2 double mutants. In the case of GS1b.1 K264E and GS1b.2 H267K, the activity was higher at temperatures above the optimum (45 °C). Finally, the GS1b.1 double mutant retains considerable activity levels (>40%) even at very low reaction temperatures, such as 4 °C (Figure 2.6I, S2.7B). E_a was barely affected (Table 2.1) in GS1b.1K264E (34.8 kJ/mol). In contrast, the GS1b.1 double mutant E_a was strongly affected (15.2 kJ/mol), and GS1b.1 K267H showed different E_a values for its

elemental reaction steps (35.2 kJ/mol and 6.7 kJ/mol), similar to GS1b.2 WT. However, GS1b.2 E264K presented a unique E_a for its reaction (39.9 kJ/mol), and different E_a values were detected for the elemental reaction steps of GS1b.2 H267K (33.7 kJ/mol and 10.3 kJ/mol) and the GS1b.2 double mutant (28.4 kJ/mol and 6.7 kJ/mol). Interestingly, all GS1b.1 mutants experienced decreases in their thermostability compared to that of the WT, and only GS1b.2H267K showed an increased thermostability compared to GS1b.2 WT (Figure 2.6J, S2.7C).

GS1b.1 behavior regarding ammonium was only modified in the GS1b.1K267H mutant, which showed substrate inhibition for ammonium (K_i 13.14 mM). Furthermore, the affinity was increased in this mutant, GS1b.2H267K, and both double mutants (K_m between 0.02 and 0.09 mM). Meanwhile, all the GS1b.2 mutants lost substrate inhibition by ammonium, and all exhibited normal hyperbolic saturation (Figure 2.6K, S2.8, Table 2.2). Regarding glutamate, GS1b.1K264E lost substrate inhibition, now presenting normal hyperbolic saturation with an increase in its affinity (K_m 2.2 mM) accompanied by a reduction in V_{max} (16.82 nkat/mg protein). Additionally, none of the mutants in 267 and double mutants reached saturation and seemed to have lost affinity for this substrate, as occurred with Mg_2^+ in all the mutants except for GS1b.2E264K (Figure S2.10, S2.11, Table 2.2). GS1b.1 mutants exhibited substrate inhibition by ATP, but only the double mutants of GS1b.1 lost substrate inhibition by ATP and presented a normal hyperbolic saturation for this substrate (Figure S2.12, Table 2.2). Interestingly, all GS1b.2 mutants presented inhibition by ATP (K_i ranging from 5.06 to 8.76 mM), in contrast to the hyperbolic Michaelis-Menten saturation exhibited by the WT (Figure S2.12, Table 2.2).

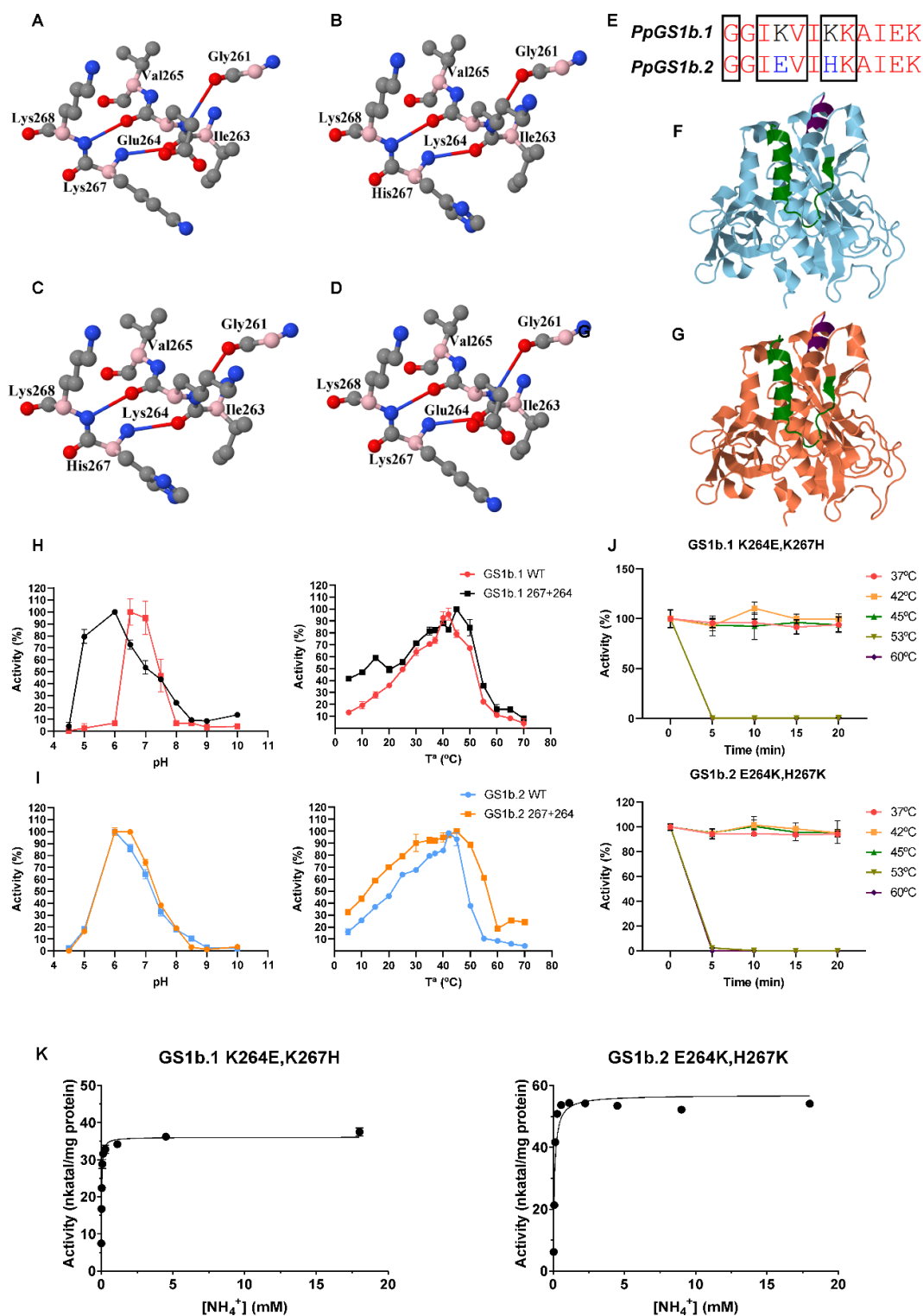


Figure 2.6. Characterization of mutated GS1b.1 and GS1b.2 proteins. Disposition of the amino acids, either those that have been exchanged and those associated with them by hydrogen bonds in the GS1b.1 K264E (A), GS1b.2 E264K (B), GS1b.1 K267H (C) and GS1b.2 H267K (D) mutants. Alpha carbons of the amino acids are represented in pink. E. Amino acid region affected by mutations. Subunit structure of the GS1b.1 (F) and GS1b.2 (G) double mutant. Amino acids exchanged and amino acids associated with them by hydrogen bonds are represented in dark magenta. Amino acids from 330 to the end of the protein are represented in green. H. Comparison of the physicochemical properties of the GS1b.1 wild type (WT) and its double mutant. I

Comparison of the physicochemical properties of the GS1b.2 WT and its double mutant. **J.** Thermal stability of the double mutants at different temperatures (37, 42, 45, 53 and 60°C) after different preincubation times (from 0 to 20 min). **K.** Kinetics of GS1b.1 and GS1b.2 double mutants for ammonium. Error bars show the SD. Mean values are composed with at least three independent determinations.

3. Discussion

The phylogenetic analysis carried out in this work (Figure 2.1) grouped the identified GS isoform (GS1b.2) within the conifer GS1b.1 group. Furthermore, the identification of *GS1b.2* in the genome, its different promoter sequences, including different TF binding sites (Figure S2.2B), and its different gene expression patterns rule out the possibility that it is an allelic variant of *PpGS1b.1* (HF548531.1), suggesting that *PpGS1b.2* (KU641799.1; KU641800.1) is likely the result of a gene duplication. The presence of *GS1b.2* in members of the genera *Pinus* and *Picea* indicates (Figure 2.1), that this gene duplication should have taken place in a common ancestor of these two groups but not of the entire *Pinaceae* family since orthologs of *GS1b.2* have not been identified in other conifers. Gene duplication is very common in plants (De Smet and Van de Peer, 2012), and it could lead to the acquisition of new functions (neofunctionalization) or simply to redundant activity to maintain the correct metabolic flux, as occurs with GS in *Populus* and rice (Yamaya and Kusano, 2014; Castro-Rodríguez et al., 2015), contributing to metabolic homeostasis (Moreira et al., 2022). In fact, the GS1b family in angiosperms has been extended by gene duplication so that different isoenzymes can play nonredundant or synergistic roles within the plant, as proposed for *Arabidopsis* GS1 genes (Ji et al., 2019).

To explore the possible neofunctionalization of this GS isoform after gene duplication, the expression patterns of the maritime pine GS genes were analyzed in different organs and tissues (Figure 2.2-2.4). *PpGS1b.2* appears to be expressed primarily in developing organs and tissues and is tightly regulated throughout embryonic development. This contrasts with *PpGS1b.1* expression, which was high in all analyzed samples. This could indicate a strong regulation of *PpGS1b.2* at both the localization and expression levels, suggesting a specialized function. The expression of *PpGS1b.2* is consistent with the association of some GS1b isogenes with plant developmental processes in angiosperms (Habash et al., 2001; Tabuchi et al., 2005; Martin et al., 2006; Lothier et al., 2011; Funayama et al., 2013; Goodall et al., 2013; Bao et al., 2014; Guan et al., 2015; Urriola and Rathore, 2015; Gao et al., 2019; Ji et al., 2019; Wei et al., 2021; Fujita et al., 2022). These data suggest an evolutionary convergence that has led to the emergence of GS1b isoforms with similar roles in different plant species. The expansion of the GS1b family in certain conifers supports that GS1b diversification in angiosperms responds to different plant needs associated with N

assimilation (Hirel and Krapp, 2021). In pine, *GS1b.1* has also been associated with this function due to its expression during zygotic and somatic embryo development (Pérez-Rodríguez *et al.*, 2005). All these expression data pose different hypotheses about the role of this isoenzyme: a) *GS1b.2* could support *GS1b.1* activity in developing tissues with a high demand for glutamine or assimilated N; and b) *GS1b.2* could play a specific role in certain developing tissues. In this sense, *GS1b.2* could play a role similar to that of certain angiosperm GSs that have been described as being involved in developmental processes. At this respect, the enzymatic characteristics of *PpGS1b.2* could be more accurate to the needs of developing tissues than *PpGS1b.1* ones, an enzyme clearly related to global ammonium (nitrogen) assimilation in the plant. This could provide an evolutionary advantage.

To explore the differential roles of *GS1b.1* and *GS1b.2* in maritime pine, the structure, as well as the physicochemical and kinetic properties of both enzymes, were analyzed. Modeling of both maritime pine *GS1b* isoforms reports small differences between *GS1b.1* and *GS1b.2* when their tertiary and quaternary structures were compared (Figure 2.5A,B; S2.2). However, any minor difference in subunit arrangements could be of great importance since the GS active site is formed by the N- and C-terminal domains of adjacent subunits (Llorca *et al.*, 2006).

Although *GS1b.1* and *GS1b.2* are very similar in their primary sequences and structures, quite a few differences have been found in their properties. The thermodynamic stability of *GS1b.1* was three times higher than that shown by *GS1b.2* (Table 2.1) Both isoenzymes present similar values (approximately 63 kJ/mol) for the change in Gibbs free activation energy (ΔG^\ddagger), but their kinetic response to temperature changes below and above 24°C may be very different (Table 2.1). For *GS1b.2*, ΔG^\ddagger and the rate-limiting step are dominated by different activation parameters at different operating temperatures: ΔH^\ddagger for temperatures below 24°C and $T \Delta S^\ddagger$ for temperatures above 24°C. In contrast, *GS1b.1* showed a nonvariable activation energy throughout the whole range of temperatures assayed (Table 2.1). These differences in dominant activation parameters could reflect functional differences between the two active sites, as has been previously suggested for glutamine synthetase isoforms from other sources (Wedler and Horn, 1976).

The optimum pH levels for *GS1b.1* and *GS1b.2* are 6.5 and 6, respectively (Table 2.1; Figure 2.5C), similar to those of *GS1b.2* and *GS1b.3* from poplar (Castro-Rodríguez *et al.*, 2015). Interestingly, these optimal pH values are lower than the cytosolic pH (7.1-7.5) (Zhou *et al.*, 2021), which could be a mechanism to avoid enzyme inhibition by the acidification process associated with GS activity and ammonium (Hachiya *et al.*, 2021). The optimum temperature for

both enzymes (42°C) (Table 2.1; Figure 2.5D) is very similar to that shown by GS1b isoenzymes in other plants (Zhao et al., 2014, Castro-Rodríguez et al., 2015). However, both GS1b enzymes had exceptional thermostability compared to other GS1b enzymes of plants (Figure 2.5E) (Sakakibara et al., 1996; Zhao et al., 2014; Castro-Rodríguez et al., 2015). Concerning glutamate and ATP, GS1b.1 exhibited substrate inhibition behavior, as previously observed for *Arabidopsis* GLN1;3 (Table 2.2; Figure 2.5G) (Ishiyama et al., 2004b). These inhibitions are consistent with the role of GS1b.1 in primary nitrogen assimilation in pine and its high expression since high levels of glutamate and ATP, outside of their homeostatic ranges, could indicate metabolic and energetic problems in the cell that may result in unnecessary or detrimental large-scale nitrogen assimilation. Interestingly, GS1b.2 exhibited positive cooperativity for glutamate (Table 2.2; Figure 2.5G) and showed substrate inhibition for ammonium (Table 2.2; Figure 2.5F). The positive cooperativity mechanism provides high sensitivity to fluctuating substrate concentrations (Levitzki and Koshland, 1976), enabling GS1b.2 to respond rapidly to changes in glutamate availability. In this case, the inhibition of GS1b.2 by ammonium could lead to control of the levels of the final product or to a specific function on the signaling pathway of one of its substrates. This is because both the end product and the substrate of the GS/GOGAT cycle, glutamate and ammonium, have been reported to play roles in plant growth and development (Qiu et al., 2020; Ortigosa et al., 2021), where GS could act as an integrating link for both signaling pathways. Interestingly, glutamate has been described to play important roles in seed germination (Kong et al., 2015), root architecture (Forde, 2014; López-Bucio et al., 2019) and pollen germination and pollen tube growth (Michard et al., 2011; Wudick et al., 2018), among other functions (Qiu et al., 2020). Ammonium has been shown recently to modulate plant root architecture in pine seedlings (Ortigosa et al., 2022). Therefore, based on the *PpGS1b.2* expression patterns, the kinetic characteristics toward glutamate, and previous works, this enzyme could be involved in developmental processes. Furthermore, this could also be a mechanism to avoid high GS activity levels when ammonium is in excess, which could lead to excessive cytosol acidification (Hachiya et al., 2021) of sensitive cells in developing tissues.

The structural, physicochemical, and kinetic analysis carried out in this work on the mutant enzymes showed some differences from the WT isoforms, but almost none of them achieved a complete exchange of the properties between GS1b.1 and GS1b.2. The mutations tested in this work did not greatly affect the protein structure, either in the surroundings of the exchanged amino acids and the subunit structure (Figure 2.6A-G), or in the quaternary structure (Figure S2.7) which could explain why the thermodynamic stability of the mutants was not compromised in any case (Table 2.1). Although all the mutants presented alterations in the activity levels at the different pH values and temperatures analyzed in comparison with the WT, only GS1b.1K264E,K267H and GS1b.2E264K produced variations

in the optimal pH, and only GS1b.2E264K presented a considerable variation in its optimum temperature (Figure S2.8B) and E_a (Table 2.1). In fact, among all the mutants, GS1b.2E264K presented the greatest number of changes in physicochemical properties. In fact, this could indicate that none of these amino acids have strong involvement in these enzyme properties or, perhaps, that the changes that can produce these mutations are being buffered by other residues.

Interestingly, these mutations had large effects on the kinetic properties (Table 2.2; Figure 2.6K; S2.9-S2.12). The results suggest that these residues are involved in affinity toward ammonium. Although it has been described that the presence of glutamine and serine at positions 49 and 174, respectively, is essential for the high affinity for ammonium in *Arabidopsis* GS (Ishiyama et al., 2006), these residues are not present in either GS1b.1 or GSb1.2 of *P. pinaster*. Previous kinetic studies have shown the presence of high-affinity GS isoforms that either do not have this combination of amino acids or have none of them (Sakakibara et al., 1996; de la Torre et al., 2002; Yadav, 2009; Zhao et al., 2014; Castro-Rodríguez et al., 2015). These previous works and the current results support the hypothesis proposed by Castro-Rodríguez et al. (2015), indicating that key residues determining GS behavior for ammonium may vary between plant species.

Mutations have produced a great number of changes in the behavior of these enzymes against their substrates and in their kinetic parameters. However, a reversal has only been achieved for ATP in double mutants, suggesting that the differences in these properties are due to the collaborative efforts of several residues, probably those that differ between the two enzymes. This may indicate that GS1b.1 and GS1b.2 have undergone evolutionary selection so that the two enzymes satisfy different plant needs, with only minor changes in their amino acid sequences. This hypothesis is also supported by the differences between the two enzymes at the structural stability level (Figure S2.4). When introduced at certain positions, some amino acids had a large effect on the protein stability of one isoform but not the other. The region between amino acids 260-300 of GS1b.2 was particularly affected by the introduction of some amino acids, but none of these substitutions appear to produce similar effects on GS1b.1. In fact, these data suggest that the two enzymes are probably undergoing different evolutionary paths although further experiments will be required to confirm this hypothesis.

Chapter 3

Transcriptome dynamics of maritime pine in response to nitrate nutrition.



1. Introduction

In recent years, the limitation of plant growth and development in relation to N sources has led to an excessive use of fertilizers in agriculture (Hirel and Krapp, 2021). Many plants have evolved or have been selected upon nitrate-based nutrition based on its characteristics and high availability in soils (Cassman et al., 2002), making nitrate one of the most widely used fertilizers alongside urea (Hirel and Krapp, 2021).

In plants, it is generally indicated that three families of transporters are involved in the uptake and transport of nitrate: NPF, NRT2, NRT3 (Wang et al., 2020). In angiosperms, between 51 and 139 members belonging to the NPF family have been described, all of them grouped in 8-10 subfamilies that also depend on the plant species (Léran et al., 2014). This family consists mainly of low affinity transporters, except for *A. thaliana* NPF6.3/NRT1.1, *Oryza sativa* NPF6.5 and *M. truncatula* NRT1.3, which have been shown to exhibit dual-affinity transport under a phosphorylation regulatory mechanism (Liu et al, 1999; Liu et al., 2003; Wang et al., 2018). NPF transporters can be mainly found in the plasma membrane (He et al., 2017) of almost all plant tissues and organs and has been described to transport other molecules besides nitrate, and displaying a great variety of functions such as stomatal regulation or seed development (Wang et al., 2018).

On the other hand, the NRT2 family consists entirely of high affinity-transporters that are only able to transport nitrate. The number of nitrate transporters belonging to this family also depends on the plant species, but only a few NRT2 transporters have been identified compared to the NPF transporters (O'Brien et al., 2016). Although these proteins are mainly related to nitrate acquisition in roots, differences on their spatial expression have been presented (Kiba et al., 2012; Lezhneva et al., 2014). Indeed, members of the NRT2 family from *Arabidopsis* have been described to play a specific role in the nitrate loading into the seed vacuoles (Chopin et al., 2007), plant-microbe interaction (Wang et al., 2018) and lateral root development (Little et al., 2005; Remans et al., 2006b). Finally, NRT3 transporter family is closely linked to NRT2 as it has been described as the second component of the high affinity transporter (Kotur et al., 2012). NRT3 has been proposed to be involved in NRT2 protein stability and targeting to the plasma membrane (Wang et al., 2018) and its interactions with members of the NRT2 family have been confirmed (Kotur et al., 2012). Moreover, some studies have also shown an increase in the activity of some NRT2 from *Arabidopsis* and rice when co-expressed with NRT3 in *X. laevis* oocytes (Feng et al., 2011; Kotur et al., 2012).

Nitrate is also a molecule with a great signaling potential which control and modulate several processes within the plant such as plant growth, and seed germination and dormancy (O'Brien et al., 2016). The transcriptional response triggered by nitrate includes the transcriptional regulation of genes related to nitrate uptake, transport, and assimilation such as NR and NiR (Wang et al., 2018). The crosstalk between nitrate and various hormones also allows this nitrogen molecule to modulate plant growth and architecture by controlling hormone signaling (O'Brien et al., 2016). Nitrate uptake and transport system have been extensively studied in angiosperms, but much remains to be done in gymnosperms. Although several works have pointed out a preferential use of ammonium over nitrate in conifers (McFee and Stone, 1968; Van den Driessche, 1971; Kronzucker et al., 1997; Marschner et al., 1991; Lavoie et al., 1992; Warren et al., 2002; Boczulak et al., 2014), recent studies seems to indicate that conifers are also able to use nitrate as efficiently as ammonium (Zhou et al., 2021), with a strict regulation over nitrate uptake in the case of *P. pinaster* seedlings (Ortigosa et al., 2020).

In the present work, the response of maritime pine seedlings to different nitrate concentrations over time have been characterized. Expression analyses by *reverse transcription-quantitative PCR* (RT-qPCR) have shown a limited effect of nitrate nutrition over the expression of NPF family at 2 hours and 24 hours. This suggests tight regulation of the expression of these transporters at an early point of nitrate acquisition, or regulation of these transporters at the post-transcriptional level. Nevertheless, two members of the NRT3 family have been significantly affected in response to nitrate at 2 hours, which is interesting since only the expression of NRT2.1 seems to be upregulated in response to nitrate at the same time. RNA direct sequencing (RDS) with Oxford Nanopore Technologies (ONT) has revealed that nitrate nutrition has a great effect on a variety of metabolic and signaling pathways and confirms the RT-qPCR results of nitrate transporter families.

2. Results

2.1 Phylogenetic analyses.

Nitrate transporters in maritime pine were previously identified by Castro-Rodríguez et al., (2017). In the present work, 40 NPF and 8 NRT2/NRT3 transporters were identified. After sequence analysis of the maritime pine genome draft (Sterck et al., 2022), it was observed that *NRT3.5* was indeed an allelic variant of *NRT3.4*, so that *NRT3.6* has been now renamed as *NRT3.5* (Figure S3.1). A phylogenetic analysis of plant NRT3 protein sequences was

conducted to determine the evolutionary relationships of pine NRT3 transporters (Figure 3.1). The phylogenetic analysis included *Ostreococcus lucimarinus* and *Micromonas pusilla* as outer groups. The results showed that NRT3 families from angiosperms and gymnosperms seem to be quite well differentiated. Thus, the multigenic NRT3 family of conifers have no members related to NRT3 in angiosperms. Therefore, the NRT3 members of the conifers are clustered together. In conifers, NRT3 forms small multigenic families of 4-5 members, but in other gymnosperms such as ginkgo and cycads only one member was found. In angiosperms, all the analyzed species have one or two NRT3 proteins except for *P. trichocarpa* with three members of this family probably due to the recent whole-genome duplication event suffered by this species (Tuskan et al., 2006).

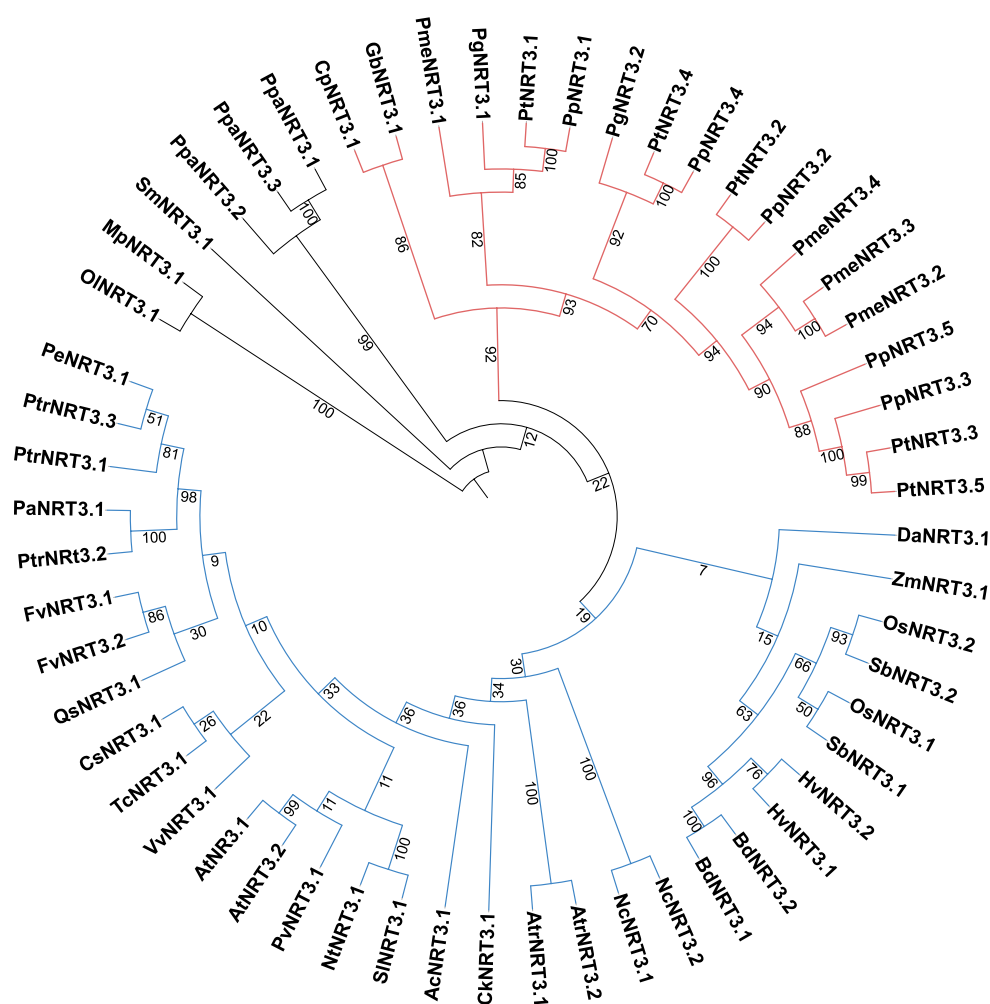


Figure 3.1. Protein phylogenetic tree of different plants' NRT3 protein sequences following a maximum-likelihood analysis. The first two letters of the sequence names correspond to the genera and species listed in Table MS2. Branch length are not presented. Numbers in the branches correspond to bootstrap values.

2.2 Gene expression analysis of NPF and NRT families.

The gene expression of *NPF*, *NRT2* and *NRT3* families of maritime pine in response to nitrate fertilization at two times (2 h and 24 h) was determined through RT-qPCR. The results are shown in a heatmap including the relative expression of family members in the presence of nitrate in comparison to control samples (Figure 3.2). The expression of the *NR* and *NiR* genes were used as controls for nitrate response. Among the nitrate transporters analyzed, only *PpNRT3.1*, *PpNRT3.3*, *PpNRT3.5*, *PpNPF1.1*, *PpNPF5.13*, *PpNPF6.1*, *PpNPF6.3* and *PpNPF8.1* were significantly upregulated but mainly in tissues treated with 10mM nitrate. The expression of the other transporters was barely affected in response to nitrate or even were downregulated in cases such as *PpNPF6.2* in cotyledons of plants treated with 0.1 mM and 10 mM nitrate after 2h. Other example is *PpNPF5.11*, which expression was downregulated in cotyledons at 0.1 mM nitrate after 2 h and in roots at 0.1 mM after 24 h. In the case of *PpNPF6.1*, the expression was upregulated in cotyledons and hypocotyls at 0.1 mM nitrate after 24 h. Finally, the expression of *PpNPF6.3* was downregulated in roots of plants treated with 10 mM nitrate at 2 h but significantly overexpressed in cotyledons of the same plants. These data were also employed to obtain a correlation map of the expression of the different studied genes that encode transporters of the NPF, NRT2 and NRT3 families of maritime pine (Figure 3.3). Among the members of the NRT2 family, only *PpNRT2.1* expression was correlated with any member of the NRT3 family, concretely with *PpNRT3.4* (0.82). Furthermore, *PpNRT3.4* expression only appeared to be associated with the gene expression of *PpNPF6.2* (0.47) and *PpNPF6.3* (-0.31). Within the NRT3 transporter, *PpNRT3.2* expression was positively correlated with a great number of NPF transporters, most of them without a significant response to nitrate application and that form a correlation cluster (*PpNPF1.3*, *PpNPF4.1*, *PpNPF4.3*, *PpNPF5.1-5.4*, *PpNPF5.8*, *PpNPF5.11*, *PpNPF5.14*, *PpNPF5.15*, *PpNPF7.1*, *PpNPF7.3*, *PpNPF7.4*, *PpNPF7.7*, *PpNPF7.8*). Another cluster, but with an opposite pattern of expression, was constituted by *PpNPF2.1*, *PpNPF2.2*, *PpNPF3.1*, *PpNPF5.5*, *PpNPF5.6*, *PpNPF5.9*, *PpNPF5.13*, *PpNPF6.3*, and *PpNPF8.3*. The expressions of *PpNRT3.1*, *PpNRT3.3* and *PpNRT3.5* were positively correlated with *NR* and *NiR* as they correspond to genes expressed in response to nitrate application. Interestingly, *PpNPF7.8* had positive correlations with all the members of *NRT3* family except for *PpNRT3.4* with a highest correlation of 0.73 for *PpNRT3.1*.

2.3 RNA direct sequencing analysis.

Nitrate nutrition triggers a great variety of responses within the plant (O'Brien et al., 2016). To determine the general transcriptome response to nitrate fertilization in the roots of maritime pine, a DRS using ONT technology was made. The samples used for this analysis were from plants irrigated with 10 mM nitrate and harvested after 2 h. Within all the samples the number of reads go from 863,733 to 2,251,158 reads with an average reading length from 1,245.01 to 668.82 bp (Tabla 3.1, Figure S3.2). The maximum reading length obtained in this experiment was 39,034 bp in the sample N2 (Table 3.1, Figure 3.2).

Table 3.1. Oxford Nanopore Direct RNA sequencing results.

Sample	Read	Mean (bp)	Max (bp)
C1	863,733	1,171.93	13,709
C2	826,899	1,068.12	12,266
C3	1,612,543	1,245.01	13,585
N1	1,335,555	668.82	6,781
N2	2,251,158	926.54	39,034
N3	2,036,890	1,018.32	11,569

The resulted data of the differential expression analysis are presented in Dataset S3.1. The analysis of the differentially expressed genes resulted in a total of 1024 upregulated genes and 966 downregulated genes when compared to control (Figure 3.4A,C). Similar to the gene expression data obtained by RT-qPCR, only the expression of NR, NiR and a few transporters were affected in response to nitrate nutrition after 2h, specifically: *NRT3.1*, *NRT3.3*, *NRT2.1* and some members of the NPF family such as *NPF7.1* (Dataset S3.1). Indeed, this data are in line with our transcriptomic analysis (Figure 3.4).

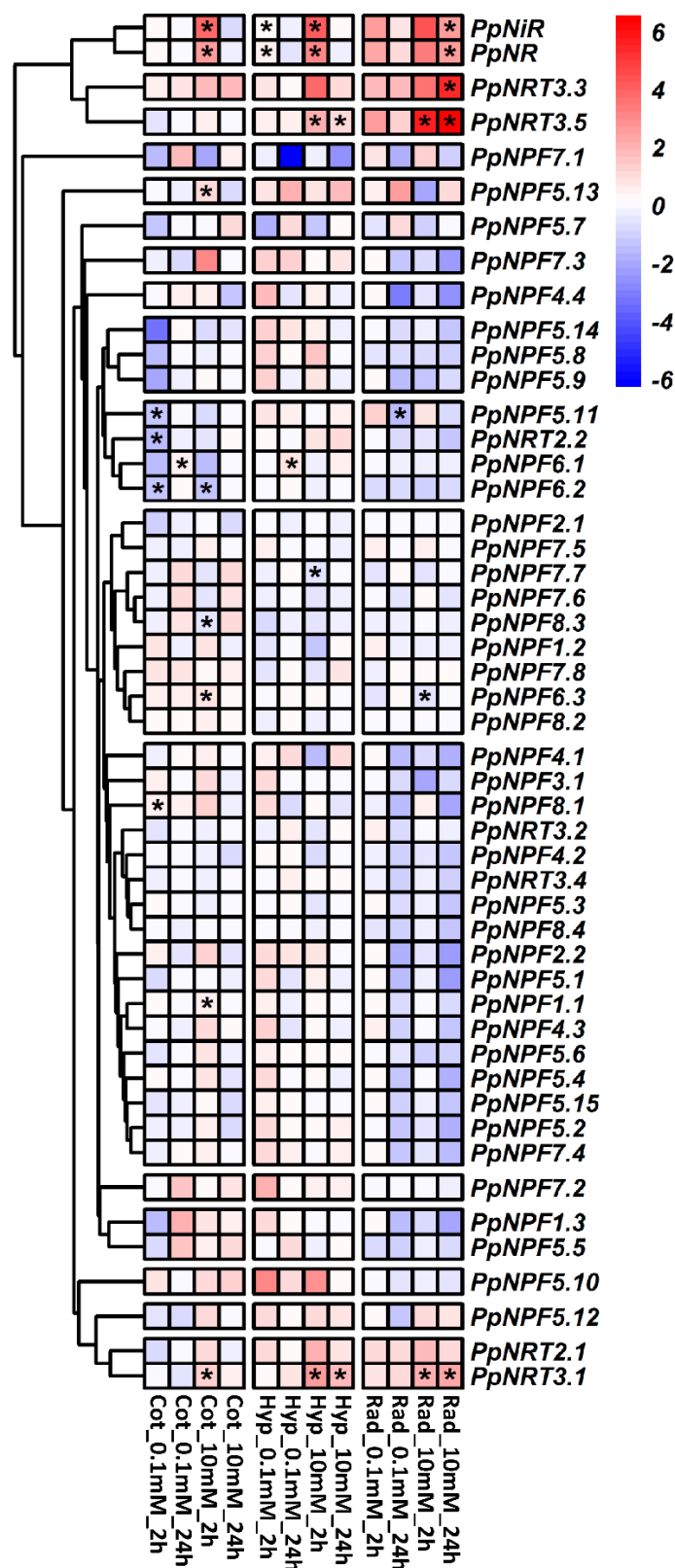


Figure 3.2. Expression heatmap of the different NPF, NRT2 and NRT3 transporters from *P. pinaster* obtained by RT-qPCR. Expression values are presented as logFC and normalized using their respective controls. Genes significantly ($p < 0.05$) upregulated or downregulated are marked with an asterisk.

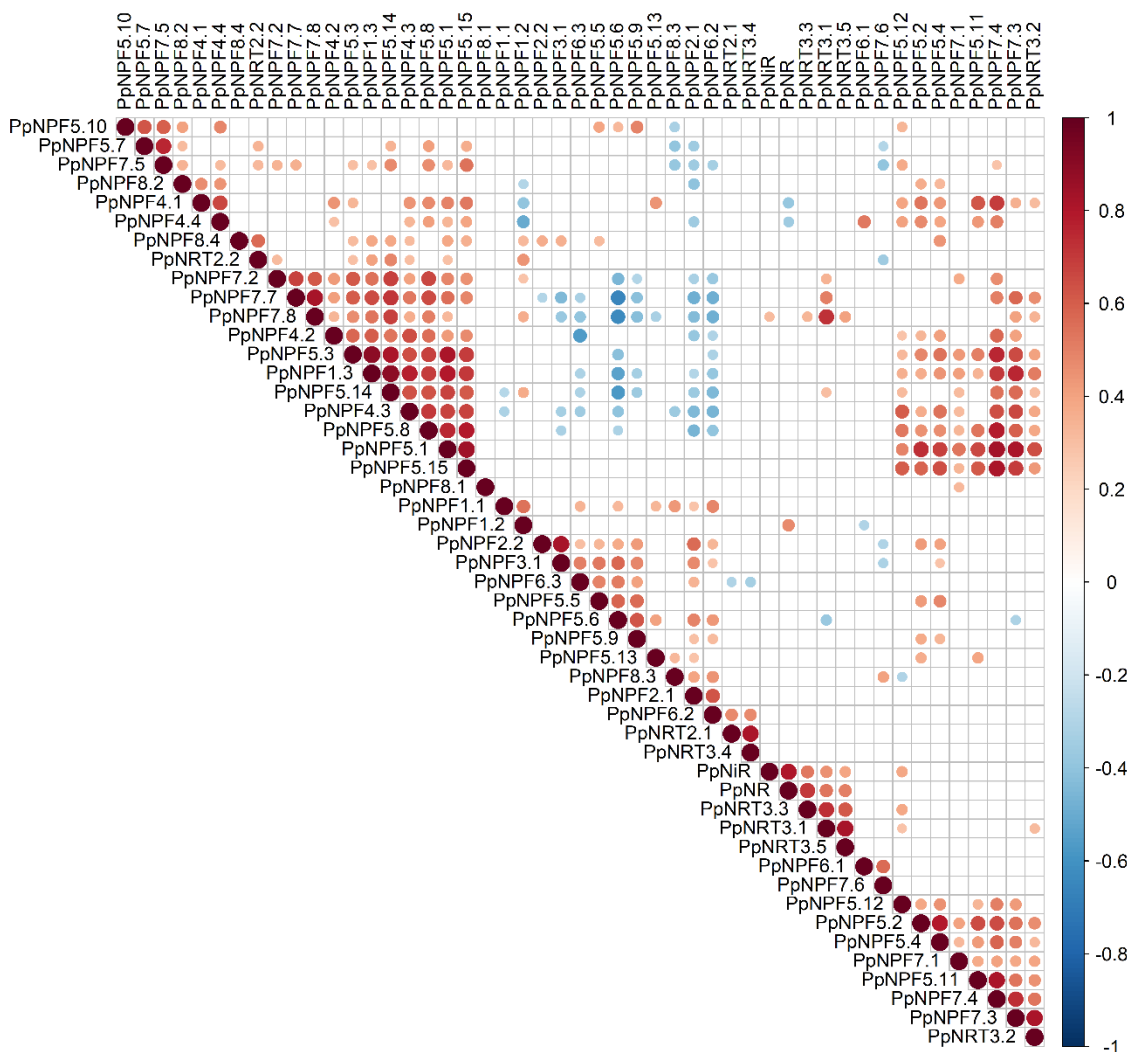


Figure 3.3. Gene expression correlation map of nitrate transporters. Only significant ($p < 0.01$) Pearson's correlations are shown with dots. The size and colour intensity of the dots indicates the correlation index values. Red dots are positive correlations. Blue dots are negative correlations. For the elaboration of this correlation plot the `corrplot` R package have been used (<https://cran.r-project.org/web/packages/corrplot/vignettes/corrplot-intro.html>)

Several biological processes have been revealed to be significantly upregulated in response to nitrate such as “negative regulation of phosphoprotein phosphatase activity” (GO:0032515), “nitrate assimilation” (GO:0042128), “gas transport” (GO:0015669), “formate catabolic process” (GO:0042183), “nitrate response” (GO:0010167) and “oxidation-reduction process” (GO:0055114) (Figure 3.4). Within the upregulated genes, Fd-NADP-reductase (FNR, EC 1.18.1.2) and formate dehydrogenase (FDH, EC 1.17.1.9), both related with redox power balance (Olson et al., 2000; Hanke et al., 2005), have been also detected (Table 3.1). Hormone metabolism were also greatly affected in pine seedlings

irrigated with nitrate. In this case, biological processes were also enriched in terms such as “response to abscisic acid” (GO:0009737) and “gibberellin mediated signaling pathway” (GO:0010476). Indeed, a considerable number of differentially expressed transcripts related to GAs such as members of the GA stimulated transcript/*Arabidopsis* (GAST/GASA) or the gibberellin 3-beta-dioxygenase 1 (GA3OX1; EC 1.14.11.15) (Table 3.2), have been found. Meanwhile, the last enzyme of the ethylene synthesis pathway the ACO (Table 3.2), was downregulated. In addition, some transcripts related to auxin response and transport have been also detected to be upregulated (Table 3.2), although any of the biological process related to this hormone were significantly upregulated. Process like “cell division” (GO:0051301) or “nuclear DNA replication” (GO:0033260), which could be related to root growth and development, were downregulated. Other biological processes that were downregulated in response to nitrate included “polysaccharide metabolic process” (GO:005976), “cellular carbohydrate metabolic process” (GO:0044262) and “cell killing” (GO:0001906).

CHAPTER 3

Table 3.2 Some of the most representative differentially expressed genes in response to nitrate.

Gene	<i>P. pinaster</i> Gene ID	<i>A. thaliana</i> Gene ID	Involved process	LogFC	References
Formate dehydrogenase	pp_243240	AT5G14780.1	Essential catalytic role in the final step of one-carbon metabolic oxidation and the generation of reducing equivalents	6	Alekseeva et al., 2011
Ferredoxin NADP reductase	pp_213314	AT4G05390.1	In non-photosynthetic tissues this enzyme oxidizes NADPH to provide reduced ferredoxin for enzymes of bioassimilation and biosynthesis.	1.45	Carrillo and Ceccarelli, 2003
SAUR-Like auxin-responsive protein family 71	pp_185097	AT1G56150.1	The SAUR family is related to auxin-induced growth. SAUR71 role remains elusive.	3.62	Stortenbeker and Bemer, 2018
SAUR-Like auxin-responsive protein family 39	pp_80840	AT3G43120.1	The SAUR family is related to auxin-induced growth. SAUR39 has been related to the negative regulation of auxin transport and synthesis in rice. A member of the AUX1 LAX family of auxin influx carriers. Lax2 have been described to present a role in vascular development, embryonic root cell organization and phyllotactic patterning.	6	Stortenbeker and Bemer, 2018
LIKE AUXIN RESISTANT 2	pp_124295	AT2G21050.1	Auxin influx carriers. Lax2 have been described to present a role in vascular development, embryonic root cell organization and phyllotactic patterning.	1.92	Bainbridge et al., 2008 Ugar-techea-Chirino et al., 2010 Péret et al., 2012
Aminocyclopropanecarboxylate oxidase	pp_148083	AT1G01480.1	Enzyme involved in the last step of ethylene biosynthesis.	-2.03	Houben and Van del Poel, 2019
Gibberelic Acid Stimulated Transcript/Arabidopsis 6	pp_212209	AT1G74670.1	Integration of GA, ABA, and glucose crosstalk. Control over seed flowering and seed germination.	-1.98	Qu et al., 2016 Zhong et al., 2016
Gibberelic Acid Stimulated Transcript/Arabidopsis 7	pp_85672	AT2G14900.1	Described to be associated with root hair and lateral root formation.	2.21	Zhang and Wang, 2008 Koskimäki et al., 2022
Gibberelic Acid Stimulated Transcript/Arabidopsis 8	pp_128453	AT2G39540.1	Remains elusive.	2.42	
Gibberelic Acid Stimulated Transcript/Arabidopsis 10	pp_85674	AT5G59845.1	Proposed to regulate cellulose synthesis by Indol-3-acetic acid (IAA)	1.36	Chen et al., 2021
gibberellin 3-beta-dioxygenase 1	pp_172169	AT1G15550.1	Involved in gibberellin biosynthesis pathway	-2.44	Mitchum et al., 2006

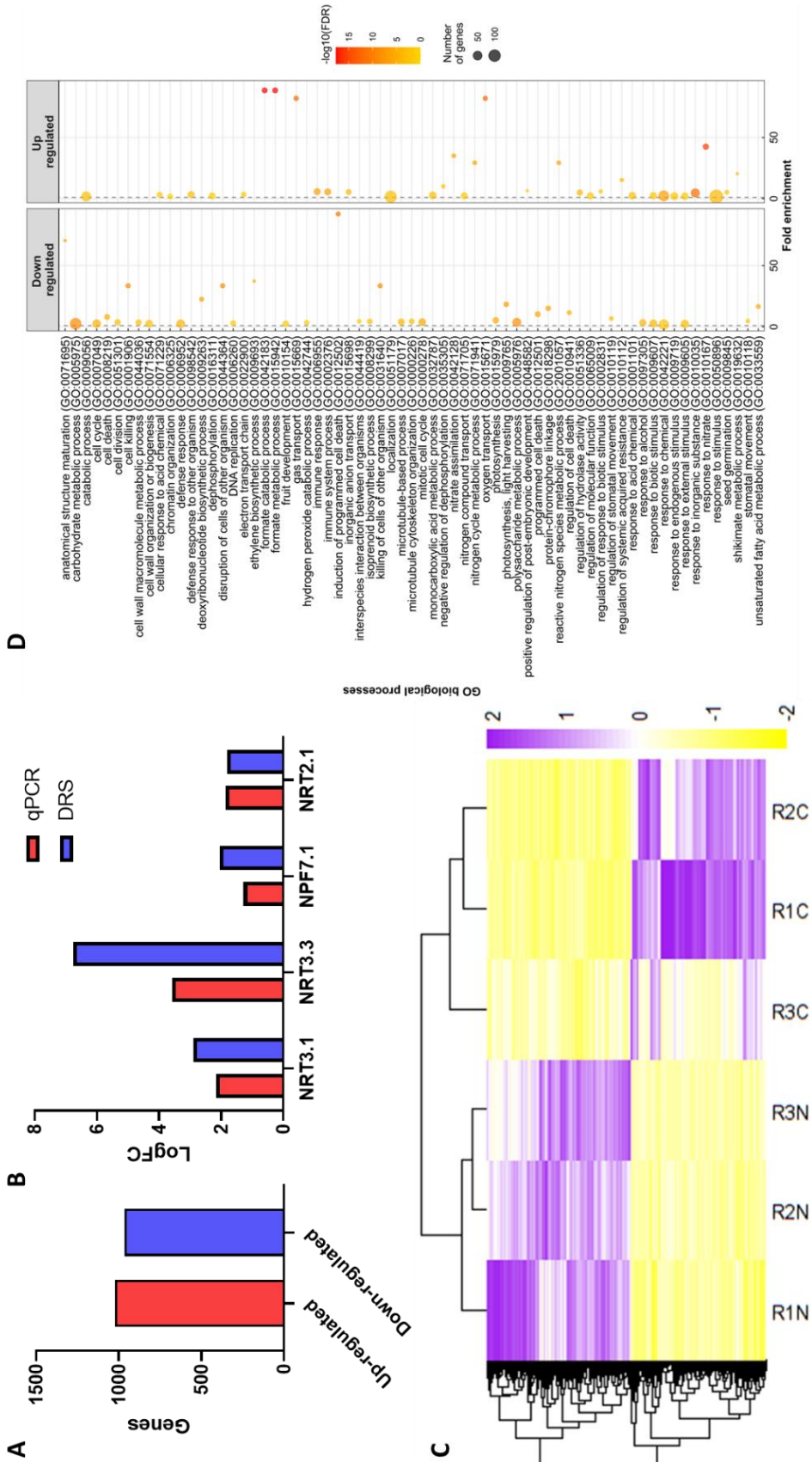


Figure 3.4 . Differential gene expression analysis. Genes upregulated and downregulated in response to 10 mM nitrate treatment after 2 hours (A). Comparison of the expression of NRT3.1, NRT3.3, NPF7.1 and NRT2.1

obtained by qPCR and by direct RNA sequencing (DRS) (B). Heatmap and clustering of the differentially expressed transcripts. Expression values correspond to counts per million (CPM) (Counts Per Million) of each transcript. For the analysis the “pheatmap” R package was employed (C). Significant GO terms from Biological Processes category after a gene enrichment analysis (D).

3. Discussion

Due to the presence of five *NRT3* genes in pine, phylogenetic analyses have been carried out in order to understand the evolution of this protein family in plants (Figure 3.1). Phylogenetic analysis conducted in this work suggests that the *NRT3* family in seed plants, both gymnosperms and angiosperms, have evolved from a common ancestor that probably presented a single *NRT3* gene. Curiously, within the gymnosperms only the group of conifers have experienced a gene expansion in the *NRT3* family (up to five members), since other gymnosperms, such as ginkgo or cycads, present only one gene. These results suggest that the expansion of the *NRT3* family was independent from the gene duplications that took place in some angiosperms species. Expansion of the gene family by gene duplication is a common phenomenon in plants (De Smet and Van de Peer, 2012) that could help to fulfill different plant needs and enable adaptation to new environmental niches. Interestingly, this gene expansion is not accompanied by a gene expansion of the *NRT2* family, which resulted to present a similar number of members to angiosperms, even though the *NRT3* family has been described to modulate *NRT2* activity (Feng et al., 2011; Kotur et al., 2012; Wang et al., 2018). This is a very interesting finding since many conifers prefer ammonium to nitrate nutrition (McFee and Stone, 1968; Van den Driessche, 1971; Kronzucker et al., 1997; Marschner et al., 1991; Lavoie et al., 1992; Warren et al., 2002; Boczulak et al., 2014) and many angiosperm species have only one or two *NRT3* genes with very more expanded *NRT2* families (Zoghbi-Rodríguez et al., 2021), even though most of them show a strong preference for nitrate as a nitrogen source.

Expression data analyses with RT-qPCR has revealed a specific effect of nitrate nutrition over the gene expression of different transporters from the *NPF*, *NRT2* and *NRT3* families (Figure 3.2). Significantly upregulated genes in response to nitrate belong mostly to the *NRT3* family. In concordance with phylogenetic analyses, this data could suggest a gene expansion within this family in order to meet different plant needs by differentially modulating the activity of different transporters. Although *NRT2* members specifically transport nitrate (O’Brien et al., 2016), only *NRT2.1* seems to be slightly upregulated but not statistically significant. This may indicate that nitrate transport by *NRT2.1* is mainly regulated through the interaction with *NRT3* rather than at the transcriptional level.

Previous experiments carried out by Ortigosa et al. (2020) in maritime pine showed a tight regulation over nitrate uptake only after 30 minutes from the start of the experiment. The rate of nitrate incorporation peaks at 15 minutes but decreases drastically after 30 minutes to almost zero. Nitrate transporters belonging to the *NRT2* family have not been affected at great scale in the RT-qPCR analyses but *NRT2.1* was up-regulated in DRS analyses. In this sense, it is tempting to consider the possibility that some of the *NRT3* proteins from pine may be able to negatively modulate the activity of different nitrate transporters. This hypothesis needs to be experimentally validated since it is opposite to the known results in other plants (Feng et al., 2011; Kotur et al., 2012; Wang et al., 2018).

In a similar way, transporters from the NPF family were barely affected in response to nitrate. Nitrate can be stored for long-term in vacuoles (Krouk et al., 2010a), therefore, this molecule can be relocated or remobilized throughout the plant after uptake, probably due to the action of several constitutively expressed nitrate transporters such as the one described for *AtNPF2.3* that plays an important role in the transport of nitrate from root to shoot (Wang et al., 2018). As explained before, some transporters from the NPF family are involved in nitrate uptake and nitrate transport within the plant, however, not all NPF transporter have been described to transport nitrate (Corratgé-Faillie and Lacombe, 2017), which could also explain this lack of transcriptional response to nitrate or its constitutive expression. In contrast, the expression of several nitrate transporters from the NPF family were even significantly downregulated, which indicate that nitrate did has an effect (direct or indirectly) over the expression of these proteins. This would be in agreement with the role of nitrate in the signaling of several processes (O'Brien et al., 2016), thus suggesting that nitrate fulfills this role also by repressing the expression of several nitrate transporters. However, it would not be prudent to rule out that the regulation of some of these transporters may also occur at the post-transcriptional level, perhaps by phosphorylation processes. Thus, it is well known that this posttranslational modification is involved in the regulation of NR enzyme activity during nitrate assimilation (Athwal et al., 1998), and nitrate signaling (Sueyoshi et al., 1999; Kaiser et al., 2002; Liu and Tsay, 2003; Engelsberger and Schulze, 2012; Migocka et al., 2013). On the other hand, the expansion of the *NRT3* family could have led to a process of neofunctionalization causing that an *NRT3* protein could now modulate the activity of one or several nitrate transporters of the NPF family independently of their transcriptions rate. Perhaps, what may be occurring is actually a combination of all of the above possibilities. However, all these points need experimental validation in the case of the NPF family in conifers.

To go further in these hypotheses, DRS with ONT has been carried out in this work using roots irrigated with 10 mM of nitrate and harvested after 2 h. Nitrate triggered the regulation of a considerable number of genes, probably as a result of its aforementioned signaling role in plants (O'Brien et al., 2016). At the same time, some of the TF families associated to nitrogen signaling, such as the bZIP family (Obertello et al., 2010; Para et al., 2014), exhibited a limited number of differentially expressed genes. This deficiency could be due to the low expression of these TFs, thus making impossible to detect them without a more sensitive technique. In fact, previous works in pine have shown that techniques such as laser capture microdissection (LCM) allow to fill this potential gap (Cañas et al., 2017; Ortigosa et al., 2022). In addition, other TFs with a key role in the nitrate signaling, such as NLP7, have been reported to be affected at the protein level but not at the transcriptional level. Nitrate triggers the phosphorylation of NLP7 through CPK and its translocation to the nucleus, where it modulates the expression of a large number of genes (Marchive et al., 2013, Liu et al., 2018).

Nitrate affected the transcription rates of some nitrate transporters from the NRT3, NRT2 and NPF family in a manner similar to the expression data obtained by RT-qPCR (Figure 3.4). Within the regulated genes, NR and NiR were also significantly overexpressed as they are the first two enzymes involved in “nitrate assimilation” (GO:0042128). Nitrate assimilation also requires great amounts of redox power to reduce nitrate to nitrite by the NR, and the nitrite to ammonium by the NiR. Because of this, nitrate is mainly assimilated in photosynthetic tissues where light-dependent reaction can supply this high requirement of reductants (Bloom, 2015). Nevertheless, this redox power can be also provided in roots allowing nitrate assimilation in this tissue. This is in agreement with the upregulated expression of genes such as FDH or FNR (Table 3.1), and biological processes such as “formate catabolic process” (GO:0042183) or “oxidation-reduction process” (GO:0055114) that could be supplying the redox power necessary for the conversion of nitrate to ammonium in roots (Hanke et al., 2005; Yoneyama and Suzuki 2019).

A previous study has shown a great effect of ammonium nutrition over hormone distribution and potential signaling in pine seedlings (Ortigosa et al., 2022). Nitrate also had an effect on the metabolic pathways of different hormones. In this case, genes related to auxin homeostasis, response and transport have been detected such as members of the small auxin upregulated RNA (SAUR) and LIKE-AUXIN RESISTANT (LAX) families (Table 3.2). Although the function of SAURs remains elusive, these auxin-responsive elements have been associated with the control of several processes such as cell expansion (Ren and Gray,

2015; Du et al., 2020; Qiu, T., et al., 2020;). Similarly, a considerable number of transcripts were related to “gibberellin mediated signaling pathway” (GO:0010476) and “response to abscisic acid” (GO:0009737), (O’Brien et al., 2016) (Figure 3.4). Nevertheless, in contrast to what has been described before (Tian et al., 2009; Zheng et al., 2013), ethylene biosynthesis is downregulated at its last biosynthetic step, the ACO (Table 3.2), and CKs do not seem to be affected. NPF transporters that have been described to be involved in phytohormone transport and signaling has not been detected either, thus supporting the hypothesis of a strong regulation over nitrate uptake and signaling in pine.

These data could also suggest a control over the hormonal levels in order to promote root growth via auxin action, thus modulating pine root architecture as it has been proposed for ammonium (Ortigosa et al., 2022). The lack of response of the CKs metabolism under nitrate nutrition could explain the ethylene biosynthesis repression, since CKs have been reported to stimulate ethylene biosynthesis (Chae et al., 2003). Interestingly, this is the opposite effect to that observed in the roots of *P. pinaster* seedlings irrigated with ammonium. In response to ammonium, ACO was significantly upregulated, and genes related to CKs were the second most representative among the differentially expressed phytohormone-related genes (Ortigosa et al., 2022), thus suggesting different effects of both nitrogen sources over pine root architecture. Ethylene have been described to mediate overall root growth inhibition by CKs, although this phytohormone is not involved in CKs effects over the root meristem (Růžička et al., 2009). On their part, CKs have been described to present an antagonist effect to auxins which has a central role in the establishment and maintenance of root cell proliferation and elongation (Petricka et al., 2012). Nitrate have been previously associated with auxin biosynthesis by upregulation of TAR2 expression under low N conditions (Zhao, 2012). Auxin biosynthesis genes are specifically expressed within the root in the niche of the stem cells (Stepanova et al., 2005; Stepanova et al., 2008). In this case, the absence of auxin biosynthesis up-regulation could be due to a non-detection of those transcripts by a dilution effect. On the other hand, auxin accumulation in the root tips is mainly due to a shoot-to-root polar transport (Blilou et al., 2005; Grieneisen et al., 2007) which would also explain the absence of transcripts related to auxin biosynthesis and the presence of transcripts related to auxins transport. This auxin-CK antagonism has been also described to be integrated by GA which promotes cell division in the meristem downstream of the auxin signal (Fu and Harberd, 2003; Úbeda-Tomás et al., 2008; Achard et al., 2009; Úbeda-Tomás et al., 2009), and repress root growth inhibition by CK (Greenboim-Wainberg et al., 2005; Moubayidin et al., 2010). Accordingly, the response to GA was upregulated in response to nitrate. This crosstalk between phytohormones and nitrate signaling could be

modulating root architecture. Indeed, Ortigosa et al. (2022) have previously reported that roots of pine seedlings irrigated with nitrate and ammonium presented statistically higher root length than those irrigated with water. Furthermore, no statistical differences were found between the primary root length of pine seedlings irrigated with nitrate or ammonium. However, nitrate was not able to promote lateral root growth unlike ammonium. In concordance with these results, nitrate probably stimulates auxin polar transport in pine, promoting this way primary root growth and avoiding lateral root formation and development. This would be totally opposite to what happens in *Arabidopsis* where nitrate promotes lateral root formation and growth and inhibits primary root elongation by stimulating auxin shootward transport and avoiding its accumulation in pericycle cells (Hu et al., 2021). In this sense, the hormone control over root architecture may have evolved differently among different groups of plants or could be related to an adaptation process to different ecological niches, which will be interesting from an evolutionary point of view.

On its part, the up-regulation of the ABA response observed in this work could be related to the stress responses (Verma et al., 2016) also upregulated in response to nitrate. Interestingly, abscisic acid has been also related to auxin transport in the tip to mediate root growth under water stress conditions as an adaptive response to low water potentials (Xu et al., 2013).

These results show that, although nitrate nutrition had little effect over the expression of the NPF transporters, this nutrient produces a great transcriptome response within the plant that shows how nitrate is able to modulate different processes. Indeed, nitrate seems to modulate the biosynthesis, transport and signaling of different phytohormones that could be responsible for the root architecture of these plants, which possible opposite effects to those described in *Arabidopsis*. Nevertheless, to confirm these hypotheses additional experiments are required.

General Discussion

GENERAL DISCUSSION

Most crop plants have evolved or have been selected upon nitrate nutrition (Cassman et al., 2002). Thus, nitrate is one of the main fertilizers used in agriculture together with urea. Nitrate also presented a great signaling potential, thus modulating several plant processes. In angiosperms, nitrate uptake, transport and signaling have been greatly studied, but little is known on this processes gymnosperms. After its uptake, nitrate will be reduced to ammonium and this ammonium will be assimilated by the GS/GOGAT cycle. GS is a key gene in N metabolism of most organisms, which can be inferred by its wide distribution in all kingdoms (Ghoshroy et al., 2010). It is also one of the oldest known genes (Kumada et al., 1993), which is why some authors have described it as a molecular clock with excellent potential for phylogenetic analyses (Pesole et al., 1991). In this work, we have presented new insights into nitrate uptake, transport and signaling in maritime pine together with a better understanding of plant GS evolution and the functional study of a new GS1b isogene in conifers.

Numerous reports have been made about the evolution of glutamine synthetase, not only in plants but also regarding the evolution of this gene family within eukaryotes (Ghoshroy et al., 2010). In this thesis, the phylogenetic analyses of different protein and nucleic acid sequences has allowed a better understating of the evolution of this family of genes in seed plants. The results of these analyses clearly suggest the occurrence of three well differentiated GS families within seed plants: GS1a, GS1b, and GS2 (Chapter 1). This hypothesis is also supported by phylogenetic analyses carried out in Chapter 2 including GS1b.2 sequences. In this context, GS2 and GS1a must be the main isoforms involved in the reassimilation of ammonium resulting from photorespiration and the primary assimilation of ammonium from nitrate reduction (Wallsgrove *et al.*, 1987; Blackwell *et al.*, 1987; Tegeder and Masclaux-Daubresse, 2017). On the other hand, enzymes in GS1b group includes the rest of cytosolic isoforms with a role in primary assimilation, reassimilation an remobilization of N, as well as in developmental processes, amino acid catabolism, senescence and stress response (Habash et al., 2001; Tabuchi et al., 2005; Martin et al., 2006; Bernard and Habash, 2009; Lothier et al., 2011; Funayama et al., 2013; Goodall et al., 2013; Bao et al., 2014; Thomsen et al. 2014 Guan et al., 2015; Urriola and Rathore, 2015; Gao et al., 2019; Ji et al., 2019; Wei et al., 2021; Fujita et al., 2022).

In recent works, the groups of *Cycadopsida* and *Ginkgoopsida* are considered gymnosperms that form a monophyletic clade (Wu et al., 2013; Li et al., 2017; One Thousand Plant Transcriptomes Initiative, 2019). In this line, our results support this assumption but, in addition, this data could indicate that the monophyletic clade conformed by *Cycadopsida*

and *Ginkgoopsida* may be more related to angiosperms than it was thought. This is also supported by our findings about GS2 gene evolution (Chapter 1). The most parsimonious hypothesis resulting from phylogenetic analyses indicates that *GS2* gene must have been absent in a common ancestor of gymnosperms and angiosperms and, probably as a result of a duplication of the *GS1a* gene, arose in a common ancestor of *Cycadopsida*/*Ginkgoopsida* and angiosperms. This also fits with the overlapping roles proposed for *GS1a* and *GS2* (Cantón et al., 1999).

The presence of this enzyme in the chloroplast confers additional advantages to the plant since a more efficient nitrate assimilation likely allowed angiosperms to colonize new ecological niches rich in nitrate, different of those ecosystems populated by gymnosperms in which ammonium was the major N source. In concordance, although conifers are widely distributed throughout the world, this group of plants is mostly present in boreal zones where temperature hinders nitrification. Moreover, several works have previously reported a preference of these species for ammonium (McFee and Stone, 1968; Van den Driessche, 1971; Kronzucker et al., 1997; Marschner et al., 1991; Lavoie et al., 1992; Warren et al., 2002; Boczulak et al., 2014; Ortigosa, Valderrama-Martín et al., 2020). However, recent studies have shown that the concentration of both nitrate and ammonium is equalized with soil depth, and that adult trees of these species can utilize both nitrate and ammonium (Zhou et al., 2021). In addition, there are gymnosperms species such as *P. pinaster*, the model of study of the present work, that are autochthonous from warm places where nitrification can take place and soils are probably richer in nitrate (Figure D1). Indeed, previous works have shown a strict regulation over nitrate uptake (Ortigosa, Valderrama-Martín et al., 2020), which is interesting considering that the NRT3 family has been expanded in this conifer and that this phenomenon has not taken place in angiosperms.

Independently of whether the presence of a plastid GS is an evolutionary advantage or better fits its function, it is a fact that conifers and gnetales conserve *GS1a* and do not have a plastidial GS isoform. Indeed, it has been reported toxicity phenotypes related to GS activity in the chloroplast. Studies carried out by Hachiya et al. (2021) in *Arabidopsis* suggested a toxic effect resulting from excessive ammonium assimilation in the chloroplast by *GS2*, probably linked to the acidification effect related to the activity of this enzyme. The homeostasis of the pH in the chloroplast is essential and excessive acidification of the stroma could lead to problems in the photosynthetic apparatus (Kuvykin et al., 2009; Tikhonov, 2013), which is necessary to produce the reducing power required for nitrogen reduction and C assimilation.

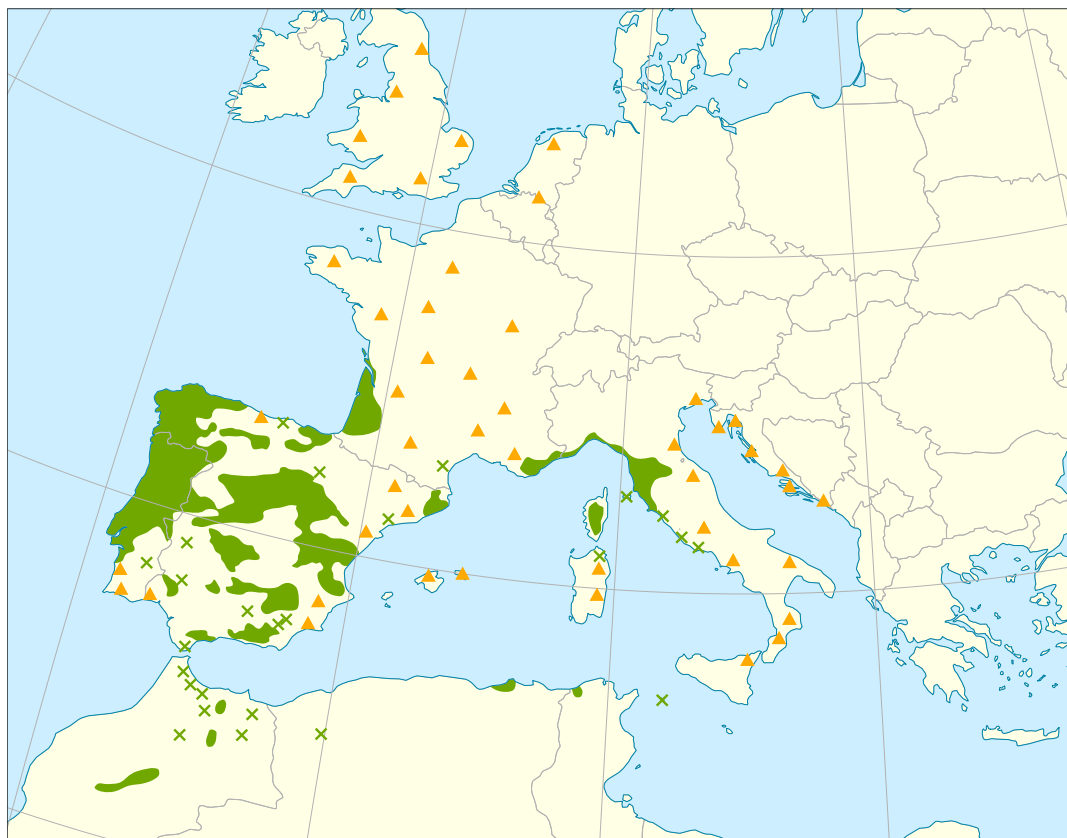


Figure D1. Distribution map of *Pinus pinaster* in the Western Mediterranean region. Green crosses indicate isolated populations; Orange triangles indicate introduced and naturalized populations. Map obtained from <http://www.euforgen.org/>

In this line, a conflict between nitrate assimilation and CO₂ fixation has been previously discussed in other works (Bloom, 2015). Rubisco is the enzyme responsible for catalyzing CO₂ fixation by carboxylation of ribulose-1,5-bisphosphate (RuBP) to produce two molecules of 3-phosphoglycerate (3-PGA), which be further used for the biosynthesis of larger molecules such as glucose or the regeneration of RuBP. However, this enzyme also catalyzes a second reaction in which O₂ is used instead of CO₂, producing one molecule of 3-PGA and a molecule of 2-phosphoglycolate (2-PG), thus leading to the restoration of RuBP from 2-PG in a process considered to be energy-wasting: photorespiration (Eisenhut et al., 2019) (Figure D2). Although the increase of CO₂ concentration in the atmosphere produces a subsequent decrease in photorespiration, which would be considered favorable, several works have reported that C₃ plants are impaired in their ability to assimilate nitrate (Bloom et al., 2012). Different hypotheses try to resolve this contradictory fact, nevertheless, the hypothesis that suggests a competence for redox power between the NR and NiR enzymes and the enzymes from the Calvin-Benson cycle (Bloom, 2015) is in concordance with sugar decrease in pine seedlings upon a nitrate bases nutrition as showed in previous works (Ortigosa et al., 2020). Thus, the photorespiration process acts as a regulator of the redox

GENERAL DISCUSSION

homeostasis allowing nitrate assimilation to happen. This phenomenon takes place both in gymnosperm and angiosperm. In gymnosperms, ammonium released during photorespiration is assimilated via GS1a in the cytosol, meanwhile, in angiosperms this ammonium is assimilated in the chloroplast via GS2. Therefore, this suggests that the localization of this enzyme, one of the main links between C and N metabolism, may not be relevant for this issue. Bloom (2015) also showed that those plants irrigated with ammonium do not present any growth problems in high CO₂ or low O₂ conditions when compared with controls, thus supporting a conflict with nitrate assimilation.

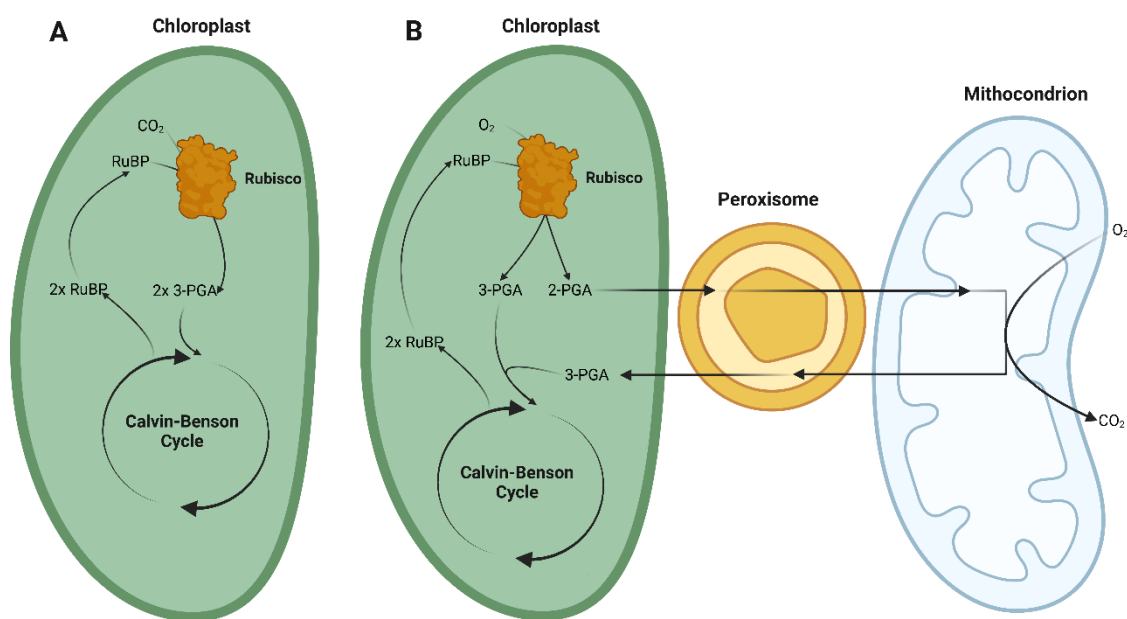


Figure D2. Overview of the carboxylase (A) and oxygenase activity of the rubisco enzyme and the photorespiration processes through the chloroplast, peroxisome and mitochondria (B). RuBP, ribulose-1,5-bisphosphate; 3-PGA, 3-phosphoglycerate; 2-PG, 2-phosphoglycolate.

The high amounts of reducing power required in nitrate assimilation would also explain differences in biomass of ammonium- and nitrate- irrigated pine seedlings. Ortigosa et al, (2020) showed a higher biomass accumulation in plants irrigated with ammonium than in those irrigated with nitrate. This would possibly explain the negative regulation of biological processes associated with polysaccharide and carbohydrate metabolisms (Chapter 3) that are in concordance with previous nutrition studies in pine. Metabolite analyses by Ortigosa et al. (2020) showed a decrease in the amount of carbohydrates in plants irrigated with nitrate compared to those irrigated with ammonium, which could be associated with a limited availability of C for such metabolic processes due to the higher requirement of reducing power by nitrate reduction. In contrast, pine seedlings irrigated with ammonium presented considerably higher concentrations of sugars such as sucrose,

D-fructose, and D-glucose. Free sugars are required for nitrogen assimilation by providing C skeletons, which explains the occurrence of high levels of these monosaccharides and disaccharides when ammonium is the main source of N, as it is assimilated directly in the roots. Nitrate is mainly long-term stored in the vacuoles and photoassimilated in smaller amounts at a timethus avoiding excessive reducing power consumption, which will then require lower levels of C skeletons. In this sense, the preference of conifers for ammonium over nitrate may be due to a more efficient assimilation of ammonium itself.

GS1b in angiosperms is encoded by a multigene family, meanwhile, GS1b in conifers is usually encoded by only one gene (James et al., 2018). In some angiosperms, the expansion of this family has led to different isoforms with overlapping functions within the plant (Castro-Rodríguez et al., 2015). In pine, *PpGS1b.2* arose probably via gene duplication of the already existent *PpGS1b.1* gene. Based on *PpGS1b.2* localized expression, a role of this enzyme in developing tissues, similar to that of some GS1b isoforms in other plants, has been proposed (Habash et al., 2001; Tabuchi et al., 2005; Martin et al., 2006; Funayama et al., 2013; Lothier et al., 2011; Goodall et al., 2013; Bao et al., 2014; Guan et al., 2015; Urriola and Rathore, 2015; Gao et al., 2019; Ji et al., 2019; Wei et al., 2021; Fujita et al., 2022) (Chapter 2). Therefore, this would imply an evolutionary convergence in which a new GS1b isoform has emerged and undergone a process of neofunctionalization to meet the different needs of the plant

Interestingly, even though these two isoforms are very similar in protein sequence, both have differences in their molecular characteristics. These enzymes have been shown to exhibit differences in their thermostability, in which GS1b.1 showed to be more thermostable than GS1b.2. Although these isoforms showed optimal activity at 42 °C, both reached their maximum activity at different pH levels (6.5 and 6 for GS1b.1 and GS1b.2, respectively). Moreover, regarding the behavior toward substrates and the kinetic properties, they exhibited several differences. Considering these results between both GS1b isoforms, two hypotheses have been suggested: a) GS1b.2 could support GS1b.1 activity in developing tissues with a high demand for glutamine or assimilated N; b) GS1b.2 could play a specific role in certain developing tissues. *In silico* studies over the promoter have also revealed differences in the regulatory region of *PpGS1b.1* and *PpGS1b.2* also supporting this idea. Nevertheless, further studies over the promoter of both isogenes will be required to bring light to this topic.

It is well known that nitrate is able to alter the expression of a large number of genes including those related with nitrate and N assimilation (O'Brien et al., 2016). However,

although *GS2* has been previously reported to be upregulated in response to nitrate nutrition (Sakakibara et al., 1997) the expression of the *GS* isogenes remains invariable in the transcriptome analyses carried out in Chapter 3. In this sense, nitrate photoassimilation could explain the absence of *GS* up-regulation in response to nitrate, since we have only analyzed root tissues and *GS1a*, the *GS2* counterpart in gymnosperms, is expressed in photosynthetic tissues as shown in Chapter 1. Nevertheless, nitrate assimilation can occur in this organ too (Yoneyama and Suzuki, 2019). The upregulation of genes coding for enzymes such as NR, NiR, FDH or FNR, and processes such as “nitrate assimilation” (GO:0042128), “oxidation-reduction process” (GO:0055114), “formate catabolic process” (GO:0042183) suggests that nitrate is probably being reduced in roots to ammonium. Since *GS1b.1* is the main *GS* isoform associated with ammonium assimilation in roots (Thomsen et al., 2014), and its expression has been showed to be upregulated in response to ammonium and nitrate nutrition in root of pine seedlings (Ortigosa et al., 2020; Ortigosa et al., 2022), is interesting that a differential expression of this gene has not been detected in this experiment. Nevertheless, the experiments performed by Ortigosa, Valderrama-Martín et al. (2020) were prolonged for 3 months, the result may be different compared to short-term experiments.

The lack of response of these *GS1b* isoforms towards nitrate nutrition rules out a possible association between nitrate-stimulated root growth and *GS1b.1* or *GS1b.2*, however, other explanations for these results should be considered. Previous work has reported that NR undergoes reversible phosphorylation, which causes this protein to degrade (Finnemann and Schjoerring 2000; Man and Kaiser, 2001). NR degradation would then prevent the release of ammonium that could regulate the expression of the *GS1b* family, although this would not agree with ammonium levels detected in the roots of pine seedlings fed only with nitrate (Ortigosa et al., 2020). On the other hand, perhaps the effects of nitrate nutrition on the expression of these genes cannot be observed at 2 h. It has been reported that the accumulation of *GS* transcripts is regulated by N metabolites and also by the C:N ratios within the cell through the 3'UTR (Ortega et al., 2006; Simon and Sengupta-Gopalan, 2010), which could have led to a posttranscriptional regulation causing their lack of detection in the DRS analysis. Moreover, in the case of *PpGS1b.2*, the localized expression of this gene could also be responsible for its lack of detection with this technique due to a dilution effect. Moreover, since transcripts level may not be in concordance with proteins levels further testing would be necessary to advance in these hypotheses.

General Conclussion



GENERAL CONCLUSIONS

1. There are three different GS genes lineages in seed plants: GS1a, GS1b, and GS2.
2. The *GS2* gene evolved in a common ancestor of *Cycadopsida*, *Ginkgoopsida*, and angiosperms clades through gene duplication of a *GS1a* and a neofunctionalization process including the acquisition of a signal peptide for plastid targeting.
3. GS1b.2 is a newly identified gene in the genera *Picea* and *Pinus* that recently evolved by duplication of an ancestral conifer GS1b gene.
4. GS1b.2 expression pattern and enzyme characteristics may associate this gene to plant organ development as occurs with different GS1b genes in angiosperms, thus implying a gene convergence evolution.
5. Minor changes in GS1b.1 and GS1b.2 amino acid sequences are responsible for the increased thermal stability of GS1b.1 and the kinetics differences between both enzymes.
6. Residues at the 264 and 267 positions of pine GS1b enzymes are involved in the affinity for ammonium.
7. NPF families and NRT2 families from *P. pinaster* present a similar number of members to those from angiosperms, meanwhile, the NRT3 family of transporters is expanded.
8. Three genes of the NRT3 transporters family are highly up-regulated by nitrate in all organs of pine seedlings when nitrate uptake is extremely reduced.
9. Nitrate nutrition triggered a considerable transcriptome response in pine roots after a short-term treatment. This transcriptome response includes the up-regulation of genes involved in nitrate reduction, oxidation status of the roots, and hormone metabolism, transport, and signaling.

Material and Methods

1. Glutamine synthetase sequence retrieve and phylogenetic analyses.

Nucleotide sequences of the genes encoding plant glutamine synthetase type II (GSII) were obtained from different public databases or assembled from transcriptomic NGS data from the SRA database at the National Center for Biotechnology Information (NCBI, <https://www.ncbi.nlm.nih.gov>) and at the European Nucleotide Archive (ENA, <https://www.ebi.ac.uk/ena>). GS sequences from *P. pinaster* were obtained by cloning and sequencing of the product. The tool employed for sequence search was BLAST (Altschul et al., 1990) using mainly the *tblastn* mode with the sequence of GS1b.1 from *Pinus taeda* as the query. For the assembly of sequences from NGS data, the raw files were uploaded to the web platform Galaxy (<https://usegalaxy.org>), which was used to make the transcriptome assemblies (Afgan et al., 2018). The raw reads were quality trimmed using TRIMMOMATIC (Bolger et al., 2014). The transcriptome assemblies were conducted with the TRINITY assembler (Grabherr et al., 2011) and the GS sequences were identified using BLAST, as described above. Database identifiers, names and species for the different GS sequences are presented in Table MS1. The subcellular localization prediction for GS proteins in Chapter 1 was determined with TARGETP (Almagro Armenteros et al., 2019) and LOCALIZER (Sperschneider et al., 2017).

For Bayesian phylogenetic analysis of the evolutionary study in Chapter 1, a data set of 169 nucleotide sequences encoding GSII from 45 different *Viridiplantae* species (Dataset MS1) and *glnA* from *E. coli* were aligned with MUSCLE (Edgar, 2004). Positions with gaps were deleted, and MRMODELTEST 2.4 was used to find the best-fitting model among the 24 models used to study molecular evolution (Nylander, 2004). The Akaike information criterion suggested the use of the model GTR + I + G. The Bayesian phylogenetic analysis was performed using MRBAYES 3.2.7 (Huelsenbeck and Ronquist, 2001) with two simultaneous runs of 77 million generations for each run, with one cold and three heated chains for each run in which the temperature parameter was set to 0.1. Trees were sampled once every 10,000 generations. The average standard deviation of split frequencies at the end of each run was <0.01, and the first 25% of the trees were discarded as burn-in samples. The consensus tree was visualized with the interactive TREE OF LIFE (ITOL) web tool (Letunic and Bork, 2019). Detailed results of the Bayesian analysis are available in Dataset MS2.

For maximum-likelihood analysis in Chapter 1, the data set was composed of 169 GS protein sequences obtained from the corresponding nucleotide sequences used for the Bayesian analyses (Dataset MS3). The alignment and phylogenetic analysis were conducted using MEGA 7 (Kumar et al., 2016). The sequences were aligned with MUSCLE (Edgar, 2004). Maximum-likelihood analyses were carried out using the complete deletion of gaps, the missing data, and the Jones–Taylor–Thornton (JTT) amino acid substitution model (Jones et al., 1992). Nearest-neighbor interchange (NNI) was used for tree inference. The initial tree was constructed using the NJ/ BioNJ method. The phylogeny test was performed using the bootstrap method with 1000 replications. Detailed results of the maximum-likelihood analysis are available in Dataset MS4. In Chapter 2, the phylogenetic analysis of GS including GS1b.2 were carried out in the same way with a data set composed by 96 GS protein sequences (Dataset MS5). Detailed results of phylogenetic analysis including GS1b.2 sequences can be found in Dataset MS6.

Sequences of the NRT3 members of several species have been used in phylogenetic analyses in Chapter 3. Nucleotide and protein sequences employed in these analyses have been retrieved from Phytozome (Goodstein et al., 2012) and PLAZA (Proost et al., 2014) with *blastp* using NRT3 sequences from *P. pinaster* as query. Database identifiers, names, and species for the different NRT3 sequences are presented in Table MS2. The data set was composed of 56 NRT3 proteins (Dataset MS7). The alignment and phylogenetic analysis were conducted using MEGA version 11 (Tamura et al., 2021) and MUSCLE for the sequence alignment (Edgar, 2004). Phylogenetic analyses were carried out with maximum-likelihood analyses as explained above. Database identifiers, names, and species for the different NRT3 sequences are presented in Table MS2. Detailed results of the maximum-likelihood analysis are available in Dataset MS8

2. Promoter analysis.

For promoter comparison, 1916 and 2408 nucleotides upstream from the translation start codon of *PpGS1b.1* and *PpGS1b.2* respectively (Dataset MS9), were retrieved from genomic data (Sterck et al., 2022). Promoters were first compared by sequence alignment (Figure S2A) with MultAlin using the Identity 1-0 algorithm (Corpet, 1988). Posterior identification of putative TF binding sites has been carried out using the binding site prediction tool of PlantRegMap (Tian et al., 2020).

3. Protein structure prediction and modeling

For the 3D modeling and structure predictions of *P. pinaster* GS1b.1 and GS1b.2 individual subunits, AlphaFold (Jumper et al., 2021; Varadi et al., 2022) through ColabFold (Mirdita et al., 2022) has been used. ColabFold allows faster protein structure prediction by integrating MMseqs2 for multiple sequence alignments and AlphaFold2, but it does not allow the structure prediction of large protein subunits or complexes. The quaternary structure prediction has been achieved using AlphaFold's models as input for the Galaxy Package, a combination of several programs that have been designed based on sequence and structure information together with physical chemistry principles (Shin et al., 2014). The models obtained from ColabFold were employed for the comparison and graphic representation of the protein structure in PyMOL (Schrödinger and DeLano, 2020) and in Jmol (<http://www.jmol.org/>). Jmol was also used for the calculation of the hydrogen bonds. Quaternary structure models obtained with AlphaFold and the Galaxy Package has been used in PyMol for the structure analysis and comparison of the models. The thermodynamic stability of the monomers has been determined using models obtained in AlphaFold together with the "foldx.mut()" function of the "ptm" R package (Aledo, 2021).

4. Plant material

Chapter 1

G. biloba seeds were obtained from several botanic gardens: *Botanische Gärten der Universität Bonn* (Bonn, Germany), *Botanischer Gärten der Universität Bern* (Bern, Switzerland), *Plantentuin Universteit Gent* (Ghent, Belgium) and *Arboretum Wespelaar* (Wespelaar, Belgium). Ginkgo seeds were stratified for 3 months in vermiculite at 4 °C. *P. pinaster* seeds from Sierra Bermeja (Estepona, Spain) (ES20, ident. 11/12) were obtained from the *Red de Centros Nacionales de Recursos Genéticos Forestales* of the Spanish *Ministerio para la Transición Ecológica y el Reto Demográfico* with authorization number ESNC87. Pine seeds were imbibed for 72 h under continuous aeration with an air pump. *M. grandiflora* seeds were obtained from the *Parque de la Alameda* garden in Málaga (Spain) and from private suppliers. Magnolia seeds were stratified in vermiculite at 4 °C for 4 months. All seeds were growth on vermiculite in order to prevent any nutritional effect of the substrate.

Ginkgo, pine, and magnolia seedlings were germinated and grown at 23 °C with a 16-h light/8-h dark photoperiod at a light intensity of 125 $\mu\text{mol m}^{-2} \text{s}^{-1}$, and watered once every 3 days with distilled water, or under continuous darkness, and watered once a week. For

light/dark transition experiments, seedlings grown in complete darkness were transferred to a 16-h light/8-h dark photoperiod for 24 h and seedlings grown with a 16-h light/8-h dark photoperiod were transferred to complete darkness for 24 h. The leaves, stems and roots of the seedlings were harvested separately. For ginkgo seedlings grown in complete darkness the primary and secondary leaves did not develop, and thus only stems and roots were harvested. To study the impact of a light–dark transition on the expression of the different genes encoding GS in ginkgo leaves, one-year-old plants with fully developed leaves were used. These plants were first exposed to a 16-h light /8-h dark photoperiod, then to complete darkness for 24 h and then back to a 16-h light/8-h dark photoperiod. The different plant samples were immediately frozen in liquid N and stored at 80°C. For the cloning of *Cycas revoluta* GS2, leaves from one-year-old plants grown under a 16-h light/8-h dark photoperiod were harvested. Leaf tissues were frozen immediately in liquid N and stored at 80°C until further use for RNA extraction.

Chapter 2

For *PpGS1a*, *PpGS1b.1* and *PpGS1b.2* expression analysis embryo and seedling samples were harvested at different stages: dry, post-imbibition and germinated (0.5 cm of emerged radicle) embryos; and one-week-old from emergence (Stage 1) and one-month-old from emergence seedlings (Stage 2). Pines were germinated and growth as explained above in 16-h light/8-h dark photoperiod. At the harvest, seedlings were divided into their different organs. For the measure of GS gene expression in different sections of roots, 2 months-old seedlings were used. The samples were immediately frozen in liquid N and stored at -80°C until powdering with a mixer mill MM400 (Retsh, Haan, Germany) and further analyses were conducted. Plant material and cDNA to analyze GS gene expression levels in maritime pine tissues from one-month-old seedlings were previously obtained by Cañas et al. (2017). RNA samples from 14 tissues isolated through laser capture microdissection were employed. The cDNA was synthesized and amplified as described by Cañas et al. (2014).

Samples from Cañas et al. (2015) were used to analyze *GS* gene expression in needles of adult trees. Briefly, needle whorls corresponding to the annual growth of a single year were harvested from different 25 years old *P. pinaster* specimens at *Los Reales de Sierra Bermeja* (Estepona, Spain). Whorls were named from 0 to 3 referring to the year of appearance of that whorl. Whorl 0 was first collected in May when they were completely formed. Samples were collected each month throughout 2012, were immediately frozen in liquid nitrogen and stored at -80°C until their utilization for RNA extraction. Buds and nascent needles

were collected from the same adult specimens once a week during April of 2013. For gene expression analyses three different trees were employed.

Juvenile and mature phloem, together with male and female strobili were harvested from 25 to 35-year-old maritime pines located at *Los Reales de Sierra Bermeja* (Estepona, Spain). Juvenile xylems were collected from the last 5 internodes in the crown and mature xylem from the base of the trunk of 28 to 31-year-old maritime pines from *Los Reales de Sierra Bermeja* by removing bark and phloem and scraping with a sterile blade. (Villalobos, 2008). All the tissues were frozen immediately using liquid nitrogen and storage at -80°C until use.

Zygotic embryos from *P. pinaster* were obtained from a single maritime pine seed orchard (PP-VG-014, Picard, Saint-Laurent-Médoc, France) and collected at different developmental stages (Avila et al., 2022). All samples were frozen in liquid nitrogen and stored at -80°C until use.

Chapter 3

For nitrate response analyses, pine seedlings were germinated as explained above with a 16-h light/8-h dark photoperiod. Pine seedlings were irrigated twice a week with water for 1 month. Afterwards, pine seedlings were randomly selected, subdivided in three groups, transplanted into forestall seedbeds and irrigated with a macro and micronutrients solution without any N source (1.16 mM KCl; 0.63 mM KH_2PO_4 ; 0.35 mM $\text{MgSO}_4 \cdot 7\text{H}_2\text{O}$; 0.17 mM $\text{CaCl}_2 \cdot \text{H}_2\text{O}$; 80 μM EDTA- FeSO_4 ; 25.9 μM H_3BO_3 ; 10.2 μM $\text{MnCl}_2 \cdot 4\text{H}_2\text{O}$; 1.3 μM $\text{ZnSO}_4 \cdot 7\text{H}_2\text{O}$; 0.7 μM $\text{Cu-SO}_4 \cdot 5\text{H}_2\text{O}$; 0.1 μM $\text{Na}_2\text{MoO}_4 \cdot 2\text{H}_2\text{O}$). After the plants were acclimated for 3 days, the control group were irrigated with 80 mL of water, meanwhile both nitrate treatment groups were irrigated with 80 mL of 0.1 mM KNO_3^- and 80 mL of 10 mM KNO_3^- , respectively. Pine seedlings for RT-qPCR were harvested at 0 h (no irrigation), 2 h and 24 h and divided in three parts: cotyledons, hypocotyl, and roots. Tissues were immediately frozen in liquid nitrogen until use. This experiment was carried out three times independently.

5. Total RNA extraction.

Ginkgo and magnolia total RNAs were extracted using the Plant/Fungi Total RNA Purification Kit (Norgen Biotek Corp., Thorold, ON, Canada) according to the manufacturer's instruction. For the total RNA extraction powdered and frozen tissues were employed. Pine and *Cycas* total RNAs were extracted as described by Canales et al. (2012). In this case, a total of 100 mg of powdered and frozen tissue were used. In 1.5 mL tubes, 600 μL of

MATERIAL AND METHODS

preheated (65°C) cetyltrimethylammonium bromide (CTAB) extraction buffer (3% (w/v) cetyltrimethylammonium bromide, 100 mM Tris pH 8, 2 M NaCl, 30 mM ethylenedinitrilotetraacetic acid (EDTA), 2% (w/v) polyvinylpyrrolidone (PVP), 2% (w/v) polyvinylpolypyrrolidone PVPP, and 4% (v/v) 2-mercaptoethanol) was added. Samples were mixed and incubated at 65°C for 5 min in a water bath with and briefly mixed each 2 minutes. Afterwards, the same volume of chloroform/isoamyl alcohol (24:1) was immediately added to the tube. Samples were then briefly mixed and incubate in ice for unless 2 min, and then centrifugated for 10 minutes at 22.000 xg at 4 °C. Supernatant is transferred to a new 1.5 mL tube, and the process was repeated by adding an equal volume of chloroform/isoamyl alcohol (24:1). After the second centrifugation step, the supernatant was recovered and an equal volume of 4 M LiCl was added and mixed by inversion. The samples were incubated overnight at 4 °C and were then centrifugated for 30 min at 22,000 xg and 4 °C in order to pellet the RNA. In this case, the supernatant was discarded, and the pellet was washed with 1mL of 70% ice cold ethanol and centrifugated at 22,000 xg for 10 min at 4 °C. Finally, ethanol was discarded, and samples were air dried for 15 min at room temperature. After samples were completely dried, 50 µl of sterilized distilled water was added. To avoid any DNA contamination, samples were treated with RQ1 RNase-Free DNase (Promega, Madison, WI, USA) following the manufacturer's instructions. Total RNA concentration and purity was determined using a Nanodrop ND-1000 (ThermoFisher Scientific, Waltham, MA, USA). The purity of the RNA was determined based on the 260/280 and 260/230 absorbance ratios. The integrity of the RNA was checked by electrophoresis.

For DRS with ONT in Chapter 3, the extraction procedure was scaled to obtain large amounts of total RNA (around 1 mg). In this case, RNA was quantified using a Qubit Fluorometer (ThermoFisher Scientific, Waltham, MA, USA) and Qubit RNA BR, Broad-Range, Assay Kit (Invitrogen, Paisley, UK). Quality of the RNA was assessed in a Bioanalyzer 2100 (Agilent, Santa Clara, CA, USA). For poly(A)-RNA, Dynabeads™ mRNA Purification Kit (Invitrogen, Paisley, UK) was used following manufacturer's instructions over those samples with a RIN value > 7. To avoid any RNA contamination, the process was repeated twice. For the determination of the poly(A)-RNA quality a Bioanalyzer 2100 (Agilent, Santa Clara, CA, USA) was employed. The total concentration was determined with a Qubit 4 Fluorometer (Invitrogen, Paisley, UK) and Qubit RNA HS, High Sensitivity, Assay Kit (Invitrogen, Paisley, UK).

6. Reverse transcription quantitative polymerase chain reaction (RT-qPCR).

For the cDNA synthesis, 500 ng of total RNA was used and retro-transcribed using the iScript™ Reverse Transcription Supermix (Bio-Rad, Hercules, CA, USA). qPCR was carried out using 10 ng of cDNA and the SsoFast™ EvaGreen Supermix (Bio-Rad, Hercules, CA, USA). The reaction was carried out in a thermal cycler CFX384™ Touch Real-Time PCR (Bio-Rad, Hercules, CA, USA). The analyses were carried out as described by Cañas et al. (2014) using the MAK3 model in the R package qpcR (Ritz and Spiess, 2008). For the RT-qPCR analysis, three technical replicates of each sample and three biological replicates were performed. The results for maritime pine were normalized using the *saposin-like aspartyl protease* (unigene1135) and an *RNA binding protein* (unigene27526) as reference genes (Granados et al., 2016). Several reference genes used to study expression in maritime pine (Granados et al., 2016) were tested in ginkgo and magnolia. In ginkgo, the orthologs of maritime pine *saposin-like aspartyl protease* (unigene1135), *myosin heavy chain-related* (unigene13291) and of an *RNA binding protein* (unigene27526) were selected and used to normalize the expression of the genes encoding GS. In magnolia, the ortholog of an *RNA binding protein* (unigene27526) from maritime pine and *Actin-7* from magnolia (Lovisetto et al., 2015) were selected and used as reference genes. The different primers used for the RT-qPCR experiments are presented in Table M1.

Table M1. List of primers used in RT-qPCR

Gene	Organism	Name	Sequence (5' → 3')	Primer sense
GbGS1b.1	<i>Ginkgo biloba</i>	Gb_GS1b.1-F	GATTGTTTGGCCATGAATGAGGGT	Forward
		Gb_GS1b.1-R	ATTCACAAACAATGCAGCATC	Reverse
GbGS1b.2	<i>Ginkgo biloba</i>	Gb_GS1b.2-F	TCTCGTTGAATAAGCAGACCACA	Forward
		Gb_GS1b.2-R	ATTGTTCTCTTCTCAAACGCGC	Reverse
GbGS1b.3	<i>Ginkgo biloba</i>	Gb_GS1b.3-F	GCTTGTGGAATAATGAGGTTCTGT	Forward
		Gb_GS1b.3-R	GTCTCCGCAAACAGGCAATATC	Reverse
GbGS1a	<i>Ginkgo biloba</i>	Gb_GS1a-F	GTCGCCCTGCATCCAACATG	Forward
		Gb_GS1a-R	TGAAGCACTCACGATTATGGCT	Reverse
GbGS2	<i>Ginkgo biloba</i>	Gb_GS2-F	ACTAACTGGAAAGCAGCAGACT	Forward
		Gb_GS2-R	GCCTTTTCCTTGCTTCTCTGTT	Reverse
Saposin-like aspartyl protease	<i>Ginkgo biloba</i>	Gb_1135-F	AGTGTTCCTGTTGACATTCCA	Forward
		Gb_1135-R	GCATTTGTAGCCAGCACTTTGA	Reverse
Myosin heavy chain-related	<i>Ginkgo biloba</i>	Gb_13291-F	TGAAAGCAGAAGTCTCCACATGA	Forward
		Gb_13291-R	CAATGCTTCCTTGCCCTCAAAC	Reverse
RNA binding protein	<i>Ginkgo biloba</i>	Gb_27526-F	GAACACAAGCAAATCTCCTCTTTC	Forward
		Gb_27526-R	TGCATCTATCGTGACCCAAGAG	Reverse

MATERIAL AND METHODS

MgGS1b.1	<i>Magnolia grandiflora</i>	Mg_GS1b.1-F	GCCCACCACATTATCTTCTTCA	Forward
		Mg_GS1b.1-R	TTGCCTCACAGACCCACT AAAA	Reverse
MgGS1b.2	<i>Magnolia grandiflora</i>	Mg_GS1b.2-F	TGAAGGACTTACAAAATACACCGG	Forward
		Mg_GS1b.2-R	GCAGCCACCCAGTTTAAAAATA	Reverse
MgGS1b.3	<i>Magnolia grandiflora</i>	Mg_GS1b.3-F	GGGCCTGAATTTCCATTGGTTT	Forward
		Mg_GS1b.3-R	CCTGCCTCTCTACAACCT CAAA	Reverse
MgGS1a	<i>Magnolia grandiflora</i>	Mg_GS1a-F	TGTCAAGAGAAAAGCTTCCCTGT	Forward
		Mg_GS1a-R	CAACACTCAAGGTAAATGCCCA	Reverse
MgGS2	<i>Magnolia grandiflora</i>	Mg_GS2-F	TGACCCACCCCTTCTATATTATCA	Forward
		Mg_GS2-R	TGCCAATCAAACAAACACCCA	Reverse
Actin	<i>Magnolia grandiflora</i>	Mg_Actin-F	CCATCACCGGAATCAAGCACAATA	Forward
		Mg_Actin-R	CAAGGCCAACAGGGAGAAAATGAC	Reverse
RNA binding protein	<i>Magnolia grandiflora</i>	Mg_27526-F	TGATGGCTGATAATTGGTGGTGA	Forward
		Mg_27526-R	GGCTATGTGATGGAGTGGGTC	Reverse
PpGS1a	<i>Pinus pinaster</i>	qPp_GS1a-F	ATCGAGGAGCTTCAGTTAGAG	Forward
		qPp_GS1a-R	TGGTCGTCTCAGCAATCATAGA	Reverse
PpGS1b.1	<i>Pinus pinaster</i>	qPp_GS1b.1-F	CCCAATTGTTTGTGGGGGATA	Forward
		qPp_GS1b.1-R	CTGAATGACAACTAGACACT G	Reverse
PpGS1b.2	<i>Pinus pinaster</i>	qPp_GS1b.2-F	CCCAATCGTTTCTGTGGATTT	Forward
		qPp_GS1b.2-R	TGGCACTGACATTACCAGT	Reverse
RNA-binding protein	<i>Pinus pinaster</i>	Pp_27526-F	AAGGCTGTCAAACCTGTCCAA	Forward
		Pp_27526-R	TTTAGCTATCAGGATGCCTCTG	Reverse
Sapoin-like aspartyl protease	<i>Pinus pinaster</i>	Pp_1135-F	AGTATGCTAAGGAATCGTGCCT	Forward
		Pp_1135-R	GTCCATAATTACACACGAACAGA	Reverse
PpNR	<i>Pinus pinaster</i>	qNR-F	ATCCCCTCCCACATCCTGTTAT	Forward
		qNR-R	ACAGAGATCAGGAGTGCTCAAT	Reverse
PpNiR	<i>Pinus pinaster</i>	qNiR-F	TTCCAATTCTCATCCATCGCCA	Forward
		qNiR-R	TTTCTGAACACGTTGGACTTCG	Reverse
PpNPF.1	<i>Pinus pinaster</i>	qNPF1.1-F	AGCTGTCATGAGATGGAATGCA	Forward
		qNPF1.1-R	GGAGTAGTTACACAGCACACCA	Reverse
PpNPF1.2	<i>Pinus pinaster</i>	qNPF1.2-F	GAGGTGAGTCGAGGTGAGTTTT	Forward
		qNPF1.2-R	TTTCCGGCAGCAAAATCAGAACC	Reverse
PpNPF1.3	<i>Pinus pinaster</i>	qNPF1.3-F	AAATTGAGAGGTGCGTCAGAGT	Forward
		qNPF1.3-R	CCCGCAAAACATAGGACGATTC	Reverse
PpNPF2.1	<i>Pinus pinaster</i>	qNPF2.1-F	CCGACATTACCTCATGCATAGC	Forward
		qNPF2.1-R	ACAGGAGTGAGATGTTTTGCCA	Reverse
PpNPF2.2	<i>Pinus pinaster</i>	qNPF2.2-F	GCAGTCTCATTGTCAGCATTGT	Forward
		qNPF2.2-R	AATTGAGAGTCCCATATCCCGC	Reverse
PpNPF3.1	<i>Pinus pinaster</i>	qNPF3.1-F	TCCCCACCAACCTCAACAGAG	Forward
		qNPF3.1-R	CCACAACGAAAGGCTTGTAGGT	Reverse
PpNPF4.1	<i>Pinus pinaster</i>	qNPF4.1-F	CGAGCACTTCCCCAGATGTATT	Forward
		qNPF4.1-R	AGCTACCTAACTAGACTTGCGT	Reverse
PpNPF4.2	<i>Pinus pinaster</i>	qNPF4.2-F	GTGGGTCGTGATATGGTCTGTA	Forward
		qNPF4.2-R	TCTGCTTTGTAATCCCTATCACCA	Reverse
PpNPF4.3	<i>Pinus pinaster</i>	qNPF4.3-F	GCTTTTCTATACGCTGCTCTGC	Forward
		qNPF4.3-R	TATTTGTACCATCTCGCCAGG	Reverse
PpNPF4.4	<i>Pinus pinaster</i>	qNPF4.4-F	ACCTTTGTTTGACGTTGTAATCCC	Forward
		qNPF4.4-R	AGTACCCAACATCAACGT CACA	Reverse
PpNPF5.1	<i>Pinus pinaster</i>	qNPF5.1-F	GGAGCTTCAGTTGGCATTGGAG	Forward
		qNPF5.1-R	TTGAGACGGGCTAGAAGTGGAG	Reverse

MATERIAL AND METHODS

PpNPF5.2	<i>Pinus pinaster</i>	qNPF5.2-F	TCTCTGAGTGCAATCAACCTTTGT	Forward
		qNPF5.2-R	TGAAGCGAGGAGTGTTCCTTCC	Reverse
PpNPF5.3	<i>Pinus pinaster</i>	qNPF5.3-F	CCCTGGGTATAGCTGTGTATTTGA	Forward
		qNPF5.3-R	TTGTCAACGAACCAGCAACTCC	Reverse
PpNPF5.4	<i>Pinus pinaster</i>	qNPF5.4-F	CCTTCGTACATTGGGCACTGTA	Forward
		qNPF5.4-R	GACTTCCCGAGCAATGCATT	Reverse
PpNPF5.5	<i>Pinus pinaster</i>	qNPF5.5-F	TTCATCGGCATGTTAGTTTGGGA	Forward
		qNPF5.5-R	TTCCTCTCCATTGCTCCTTCAA	Reverse
PpNPF5.6	<i>Pinus pinaster</i>	qNPF5.6-F	TGCATACACACCAAAGGAAAGCT	Forward
		qNPF5.6-R	CAACATACTTGCCCTTGACGCA	Reverse
PpNPF5.7	<i>Pinus pinaster</i>	qNPF5.7-F	AAAAGGCGCCTGATTTTGGTTG	Forward
		qNPF5.7-R	GCAGGCTTGGTCTTCTGTTGAG	Reverse
PpNPF5.8	<i>Pinus pinaster</i>	qNPF5.8-F	GCTCATCATCACTTTTACCAGGGT	Forward
		qNPF5.8-R	AAACTAAACCTGTCTAGCCCTGA	Reverse
PpNPF5.9	<i>Pinus pinaster</i>	qNPF5.9-F	CGCAGAATAAAATGGCAGTCGT	Forward
		qNPF5.9-R	ACTGGCATTCAATTCAGGTACCT	Reverse
PpNPF5.10	<i>Pinus pinaster</i>	qNPF5.10-F	AGGCATTAACAGAGGGCAGAG	Forward
		qNPF5.10-R	ACCATCATCAAAAGCCTCTGGG	Reverse
PpNPF5.11	<i>Pinus pinaster</i>	qNPF5.11-F	TGAAATAATTGGTAAGCCCCTCCA	Forward
		qNPF5.11-R	TCGCAATACACATACCATATCCCA	Reverse
PpNPF5.12	<i>Pinus pinaster</i>	qNPF5.12-F	TGACATTCACGACCATTTTGCT	Forward
		qNPF5.12-R	ACTCCATCATGCATGTCCTGTT	Reverse
PpNPF5.13	<i>Pinus pinaster</i>	qNPF5.13-F	CATGAGCTGCCTGTGGATATCA	Forward
		qNPF5.13-R	TAGATTCCCTGCATCATCCAGCC	Reverse
PpNPF5.15	<i>Pinus pinaster</i>	qNPF5.14-F	CATTTAGCAAACACGGCCATGT	Forward
		qNPF5.14-R	TGTCATCTGTTCGGGAGTTGAG	Reverse
PpNPF5.15	<i>Pinus pinaster</i>	qNPF5.15-F	AGAGGGAAACAACCTGAGGCTTT	Forward
		qNPF5.15-R	TACTTCCCATCCTCCTCTCAG	Reverse
PpNPF6.1	<i>Pinus pinaster</i>	qNPF6.1-F	TGAGCTATGCAACCTTCAATCTTG	Forward
		qNPF6.1-R	ACGACACTGCCATTAGACTTT	Reverse
PpNPF6.2	<i>Pinus pinaster</i>	qNPF6.2-F	GGGACACCTAAATATGCAGCTT	Forward
		qNPF6.2-R	CTCTGGTCTCCTGCATGTACTC	Reverse
PpNPF6.3	<i>Pinus pinaster</i>	qNPF6.3-F	TCGTATTTTGGGTGCGAGGAAGG	Forward
		qNPF6.3-R	CCCAAAGGTATCTCGTTGCTG	Reverse
PpNPF7.1	<i>Pinus pinaster</i>	qNPF7.1-F	TCGTTGCGATGGTTCTGTGTAT	Forward
		qNPF7.1-R	GACGATTGGGTGTTCTCTCTGT	Reverse
PpNPF7.2	<i>Pinus pinaster</i>	qNPF7.2-F	TATGTGCCTGCTTTCATGAGA	Forward
		qNPF7.2-R	GCCAGCGTTGTAAAGAAGTGTT	Reverse
PpNPF7.3	<i>Pinus pinaster</i>	qNPF7.3-F	GACACACAGATTCCATGGCAAC	Forward
		qNPF7.3-R	AATCTGTGTGAACTTGAGCCA	Reverse
PpNPF7.4	<i>Pinus pinaster</i>	qNPF7.4-F	GGCATTCTTACAGCACTTGAC	Forward
		qNPF7.4-R	TTGTCCATGGAACGTGCAATTC	Reverse
PpNPF7.5	<i>Pinus pinaster</i>	qNPF7.5-F	ATGCTTATTACCACCAGAGGCG	Forward
		qNPF7.5-R	CTCAATGCAGTCCACAACCAAA	Reverse
PpNPF7.6	<i>Pinus pinaster</i>	qNPF7.6-F	TGTTTCCAAGTTTCCAGGGTTGT	Forward
		qNPF7.6-R	TCTCTACCTCACACCAAATAGGA	Reverse
PpNPF7.7	<i>Pinus pinaster</i>	qNPF7.7-F	TCTGTCCAAGTTTAGCAAAGGT	Forward
		qNPF7.7-R	TTGACATGATCCAACCATCGCC	Reverse
PpNPF7.8	<i>Pinus pinaster</i>	qNPF7.8-F	CGGTTGTCATTGCACCAAAGA	Forward
		qNPF7.8-R	CGGCCTTTTCTTATGTTATGTCAC	Reverse
PpNPF8.1	<i>Pinus pinaster</i>	qNPF8.1-F	ACACGTTTAGATTTTCCAGGAGCG	Forward

MATERIAL AND METHODS

		qNPF8.1-R	CCGAGATCAAACCTGCCTCTTCT	Reverse
PpNPF8.2	<i>Pinus pinaster</i>	qNPF8.2-F	ATGCAGCTATCGTAGTGGTCTG	Forward
		qNPF8.2-R	CCCAGTTTTTGTAAAGCTAGGCA	Reverse
		qNPF8.3-F	GTATGGATCTCAACATTGCGCC	Forward
PpNPF8.3	<i>Pinus pinaster</i>	qNPF8.3-R	CAAGCTGAAAACGCACAAGTCT	Reverse
		qNRT3.1-F	CAGTTTGCAAGTGCTAGAACGG	Forward
PpNRT3.1	<i>Pinus pinaster</i>	qNRT3.1-R	CCTGTCAAGCCCACTACAATCT	Reverse
		qNRT2.1-F	TTAGATGCAGAAGGAGCCAAA	Forward
PpNRT3.2	<i>Pinus pinaster</i>	qNRT3.2-R	AATGAGACTGGATGCGGGATAC	Reverse
		qNRT3.3-F	GCTGTCATTTCTTACCTCAACCA	Forward
PpNRT3.3	<i>Pinus pinaster</i>	qNRT3.4-R	CGGTCTTTTTCAAGATTGTCCG	Reverse
		qNRT3.4-F	AGTGAACAGGGAGAATGCAAATG	Forward
PpNRT3.4	<i>Pinus pinaster</i>	qNRT3.4-R	ATACAGGACTCCACCCCTAAGT	Reverse
		qNRT3.5-F	TTCCCTGGACATCATCACTGC	Forward
PpNRT3.5	<i>Pinus pinaster</i>	qNRT3.5-R	TTAATTCTTCTGCGATGCCCTG	Reverse
		qNRT2.1-F	AGACCAAGGAGAACGGATACAA	Forward
PpNRT2.1	<i>Pinus pinaster</i>	qNRT2.1-R	CATTGAACGCTTGCTCTGATTT	Reverse
		qNRT2.2-F	GCTAATCGTGCTAATATGCCGC	Forward
PpNRT2.2	<i>Pinus pinaster</i>	qNRT2.2-R	TTGTTGAGCCTCTTACTTGACAG	Reverse

7. Statistics

Statistical analyses not described in other subsections were performed using PRISM 8 (Graphpad, San Diego, CA, USA) and R packages. Data obtained from gene expression quantification were analyzed using a multiple comparison two-way analysis of variance (ANOVA) test. Differences between organs were not analyzed statistically. Tukey's post hoc test was used for the statistical analysis of the gene expression data. Pearson's correlation test was also used to evaluate the relationships between the gene expressions in the different experiments. Differences and correlations were considered significant when the $p < 0.05$.

For the correlation plot in Chapter 3, RT-qPCR expression data was employed for Pearson's correlation analyses and the plot was designed using the *corrplot* package for R (<https://cran.r-project.org/web/packages/corrplot/vignettes/corrplot-intro.html>). Only those Pearson's correlation values that were significant ($p < 0.05$) are represented as dots.

8. Direct RNA sequencing.

From 2.74 to 4.4 μg of poly(A)-RNA was employed for the preparation of Nanopore DRS libraries using the Nanopore Direct RNA Sequencing kit (SQK-RNA002, Oxford Nanopore Technologies, ONT, Oxford, UK) according to manufacturer's instructions. For the ligation

of the poly(T) adapter to the mRNA, the samples were incubated for 15 min with T4 DNA ligase (New England Biolabs, Ipswich, MA, USA) in the Quick Ligase reaction buffer (New England Biolabs, Ipswich, MA, United States). For the synthesis of the first-strand cDNA SuperScript III Reverse Transcriptase (ThermoFisher Scientific, Waltham, MA, USA) was used together with the oligo(dT) adapter. The purification of the RNA-cDNA hybrid was carried out using Agencourt RNAClean XP magnetic beads (Beckman Coulter, Brea, CA, USA). DRS adapter was added by using T4 DNA ligase (New England Biolabs, Ipswich, MA, United States) for 15 min in the Quick Ligase reaction buffer (New England Biolabs, Ipswich, MA, United States), followed by a second purification with Agencourt beads (Beckman Coulter, Brea, CA, USA) as explained above.

The libraries were loaded into the R9.4 SpotOn Flow Cells (Oxford Nanopore Technologies, ONT, Oxford, UK) and the sequencing were prolonged until all the active-nanopores were depleted. For the base calling ONT Guppy software was used (<https://community.nanoporetech.com>) and reads were filtered by quality ($Q > 8$). Read alignment was carried out with minimap2 software (Li, 2018) and with maritime pine root transcriptome as reference (Ortigosa et al., 2022). The alignment parameters for DRS were set as follows: -uf and -k14. The edgeR R package was employed in the identification of differentially expressed transcripts. Transcripts were normalized by count per million mapped read (cpm) and filtered (2 cpm in at least 2 samples) (Robinson et al., 2010). Transcripts with False Discovery Rate < 0.05 were considered as differentially expressed.

9. Functional annotation and enrichment analyses

AGRIGO v2.0 web tool was employed for singular enrichment analysis (SEA) of the GO terms under a playing standard parameters and using the whole assembled transcriptome annotation (Tian et al., 2017) as GO term reference. For the representative enriched GO determination REVIGO with 0.5 as dispensability cutoff value was used (Supek et al., 2011).

10. Cloning.

In Chapter 1, the CDS of *GS2* from *Cyca revoluta* was amplified by PCR from leaf cDNA samples. The amplification was carried out using iProof HF Master Mix (Bio-Rad, Hercules, CA, USA) and cloned into the pJET1.2 vector (ThermoFisher Scientific, Waltham, MA, USA) following the manufacturers' instructions. Primers used for *CrGS2* cloning are listed in Table M2 and were designed from *Cyca hawainensis GS2* genomic sequence.

MATERIAL AND METHODS

In the Chapter 2, in the search for new *GS* genes in conifers, 3 genes in *P. pinaster* have been identified in transcriptome databases that were named as *PpGS1a*, *PpGS1b.1* and *PpGS1b.2*. The cDNA of the three genes were amplified by PCR using iProof HF Master Mix (Bio-Rad, Hercules, CA, USA) and cloned into the pJET1.2 vector (ThermoFisher Scientific, Waltham, MA, USA) following the manufacturers' instructions. The used primers were designed from sequences obtained from the maritime pine transcriptome assembled in Cañas et al. (2017). Primers are shown in Table M2. *PpGS1a* was obtained from amplified cDNA of emerging needles (EN) isolated in Cañas et al. (2017). *PpGS1b.1* and *PpGS1b.2* were obtained from amplified cDNA of developing root cortex (DRC) isolated in Cañas et al. (2017).

For the protein recombinant expression, the CDS of WT *PpGS1b.1* and *PpGS1b.2* were subcloned into pET30a vector (Merck, Darmstadt, Germany) including a N-terminal 6xHis-tag by PCR. For this task, *Asel* and *XhoI* sites were added to *PpGS1b.1* 5' and 3' ends respectively while *NdeI* and *XhoI* sites were added to *PpGS1b.2* 5' and 3' ends respectively. These restriction sites along with the 6xHis-tag were introduced by PCR. Used primers are listed in Table M2. The plasmid and PCR product were then cut using the appropriate restriction enzymes and the PCR product was inserted into the plasmid using T4 DNA ligase.

Table M2. List of primer for cloning

Gene	Organism	Application	Name	Sequence (5' → 3')	Primer sense
<i>PpGS1a</i>	<i>Pinus pinaster</i>	Cloning in pJET1.2	Pp_GS1a-F	TCTCTTGAATCTTATCCCCTTCC	Forward
			Pp_GS1a-R	TACATATAGCTTATCAGTGACGC	Reverse
<i>PpGS1b.1</i>	<i>Pinus pinaster</i>	Cloning in pJET1.2	Pp_GS1b.1-F	CTTCCTCAGGTCGGGCTTG	Forward
			Pp_GS1b.1-R	CTGAATGACAAACTAGACACTG	Reverse
<i>PpGS1b.2</i>	<i>Pinus pinaster</i>	Cloning in pJET1.2	Pp_GS1b.2-F	GCTTCCCCTGCTTTAAGGG	Forward
			Pp_GS1b.2-R	TGGCACTGACATTCACCAGT	Reverse
<i>PpGS1b.1</i>	<i>Pinus pinaster</i>	His-TAF addition and subcloning in pET30a	Pp_GS1b.1-F	AGAAATTAATGCACCATCATCATCATCATT CTCTACTGACGGATTG	Forward
			Pp_GS1b.1-R	AGAACTCGAGTCACTTCAAAGGATGGTTG	Reverse
<i>PpGS1b.2</i>	<i>Pinus pinaster</i>	His-TAF addition and subcloning in pET30a.2	Pp_GS1b.2-F	AGAACATATGCACCATCATCATCATCATTC TCTGTTGACAGATTTG	Forward
			Pp_GS1b.2-R	AGAACATATGCACCATCATCATCATCATTC TCTGTTGACAGATTTG	Reverse
<i>CrGS2</i>	<i>Cyca revoluta</i>	Cloning in pJET1.2	Cr_GS2-F4	TCGGGATTGGACATTCGTAGCAAGGCTAGA	Forward
			Gr_GS2-R5	TCTCTTGAATCTTATCCCCTTCC	Reverse

11. Site-directed mutagenesis

Attending to the characteristics and properties of the amino acids that differ between *GS1b.1* and *GS1b.2*, residues at position 264 and 267 were selected to be shifted between

MATERIAL AND METHODS

both isoenzymes. Site-directed mutagenesis has been carried out following Edelheit et al. (2009). The WT CDS from those sequences included on the vector pET30a were amplified by PCR using two reverse-complementary primers (Table M3) that already include the mutation to be introduced. The primers were used separately in a PCR reaction using 50 or 500 ng of plasmid and 10 pmol of each primer. The final products of both reactions were then mixed and hybridized. The PCR products were checked out in an agarose gel and then purified using NucleoSpin® Gel and PCR Clean-up (Macherey-Nagel, Düren, Germany). Finally, the PCR product was digested with FastDigest® DpnI (ThermoFisher Scientific, Waltham, MA, USA) to degrade the vector used as template for the amplification.

12. Bacteria transformation

pET30a including GS1b.1 and GS1b.2 CDS sequences and a N-terminal 6xHis-tag were transformed in the *Escherichia coli* strain BL-21 (DE3) RIL (Agilent, Santa Clara, CA, USA). Transformation was done by thermal shock. A total of 50-100 ng of plasmid was mixed with 100 µL BL-21 (DE3) RIL competent cells and the incubated in ice for 30 min. Afterwards, cells are incubated at 42 °C for 1 min and then cooled in ice for unless 2 min, followed by the addition of 900 µL of LB and 1 h incubation at 37 °C. Finally, cells are plated in LB-agar medium with kanamycin and chloramphenicol to select cells which have introduced the plasmid.

Table M3. List of primer for site-directed mutagenesis

Gene	Mutation	Name	Sequence (5' → 3')	Primer sense
<i>PpGS1b.1</i>	264 Mutant	GS1b.1-K264E-F	AAGAAGGGGAATTGAAGTGATCAAAAAGGCC	Forward
		GS1b.1-K264E-R	GGCCTTTTTGATCACTTCAATTCCTTCTT	Reverse
<i>PpGS1b.2</i>	264 Mutant	GS1b.2-E264K-F	AAGAAGGTGGAATAAAAAGTGATCCATAAGGCC	Forward
		GS1b.2-E264K-R	GGCCTTATGGATCACTTTTATTCCACCTTCTT	Reverse
<i>PpGS1b.1</i>	267 Mutant	GS1b.1-K267H-F	GGGGGAATTAAGTGATCCATAAGGCCATT	Forward
		GS1b.1-K267H-R	AATGGCCTTATGGATCACTTTAATTCCCC	Reverse
<i>PpGS1b.2</i>	267 Mutant	GS1b.2-H267K-F	GGTGAATAGAAGTGATCAAGAAGGCCATT	Forward
		GS1b.2-H267K-R	AATGGCCTTCTTGATCACTTCTATTCCACC	Reverse
<i>PpGS1b.1</i>	Double mutant	GS1b.1-264,267-F	GGGGGAATTGAAGTGATCCATAAGGCCATT	Forward
		GS1b.1-264,267-R	AATGGCCTTATGGATCACTTCAATTCCTTCTT	Reverse
<i>PpGS1b.2</i>	Double mutant	GS1b.2-264,267-F	GGTGAATAAAAGTGATCAAGAAGGCCATT	Forward
		GS1b.2-264,267-R	AATGGCCTTCTTGATCACTTTTATTCCACC	Reverse

13. Recombinant expression of proteins

For GS1b.1 and GS1b.2 protein expression, the bacterial clones were grown at 37 °C and 180 rpm in an orbital shaker in 500 mL of Luria-Bertani medium supplemented with kanamycin (0.05 mg/mL) and chloramphenicol (0.034 mg/mL). When the optical density (OD) reached a 0.5-0.6 value at 600 nm, cultures were tempered and isopropyl- β -D-thiogalactoside was added to a final concentration of 1 mM to induce protein expression. Once the isopropyl- β -D-thiogalactoside was supplied the cultures were incubated at 25 °C and 120 rpm for 5 h, after that, cells were collected by centrifugation and stored at -80 °C until use.

14. Protein purification

The bacterial pellet was resuspended in 5 mL of buffer A (Tris 50 mM pH 8; NaCl 300 mM; imidazole 250 mM) with 4 mg of lysozyme and incubated for 30 min in ice, bacteria were then lysed by ultrasonication with 20 pulses of 5 seconds at 20% amplitude with 5 seconds rest between pulses in a Branson Sonifier® Digital SFX 550 (Branson Ultrasonics, CT, USA). The soluble fraction was clarified by centrifugation (1,620 xg at 4 °C for 30 min). Proteins from soluble fraction were purified by affinity chromatography with Protino Ni-TED Packed Columns 2000 (Macherey-Nagel, Düren, Germany) based on the His-tag tail. The soluble fraction from bacterial lysate was loaded in a column previously equilibrated with buffer A. Protein elution was performed by adding buffer B (Tris 50 mM pH8; NaCl 300 mM; imidazole 250 mM) and a total of 9 mL of eluate was recovered in 1 mL fractions. Collected fractions were quantified by Bradford (Bradford, 1976) and analyzed on SDS-page and western-blot using GS-specific antibodies obtained from rabbit (Figure M1; Figure M2) (Cantón et al., 1996). The fractions containing the proteins were concentrated with Amicon® Ultra-15 Centrifugal Filters Ultracel®-100K (Merck-Millipore, Burlington, Massachusetts, State of Virginia) with 100 kDa pores and the resulting concentrate was stored in 50% (v/v) glycerol at -20 °C for posterior kinetic measurements and physicochemical analyses.

15. SDS-PAGE and Western-blot analysis.

For SDS-PAGE analysis, loading buffer (30 mM Tris-HCl, pH 6.8, 1% (w/v) sodium dodecyl sulfate (SDS), 10% (v/v) glycerol, 0.001% (w/v) bromophenol blue, 0.5 M 2-mercaptoethanol) was added to the different samples which were then boiled for 5 min at 100 °C. Samples were immediately used for electrophoresis or stored at -20 °C until use.

MATERIAL AND METHODS

Electrophoresis of the GS recombinant proteins were carried out the different elution fractions from the enzyme purification step in 12.5% (w/v) SDS-polyacrylamide gels (Laemmli, 1970) loading a total of 10 µg of protein and 5 µL of All Blue Precision Plus Protein™ Prestained Standard (Bio-Rad, Hercules, CA, USA) as marker ladder. Polyacrilamide gels containing GS proteins were stained with Coomassie blue solution (0.1% (w/v) Coomassie R-250, 10% (v/v) acetic acid, 40% (v/v) methanol) for 25 min and then destained overnight (2% (v/v) acetic acid, 40% (v/v) methanol). For the obtention of the SDS-PAGE gels images, a ChemiDoc XRS+ (Bio-Rad, Hercules, CA, USA) was employed (Figure M1). For western blotting analysis, polyacrylamide gels were equilibrated for 10 min in Towbin transfer buffer (25 mM Tris, 192 mM glycine pH 8.3, 20% methanol) (Towbin et al., 1979). Polyacrilamide gels were then electroblotted to nitrocellulose membrane (Amershan Protran Premium 0.45 NC) in a Trans-Blot® Turbo™ Transfer System (Bio-Rad) for 32 min at 18V. Nitrocellulose membranes were blocked for 1 h with 5% (w/v) of non-fat milk powder dissolved in tween-phosphate buffered saline (TPBS): 1X PBS (3 mM KCl, 140 mM NaCl, 1.47 mM KH₂PO₄, 5 mM Na₂HPO₄, pH 7.4) with 0.05% (v/v) Tween-20. For GS1b.1 and GS1b.2 protein detection, membranes were incubated at 4 °C overnight with GS-specific antibodies obtained from rabbit (Cantón et al., 1996) in a 1:5000 dilution in TPBS with 0.05% (w/v) of bovine serum albumin (BSA). Membranes were then washed 3 times in TTBS for 10 minutes and incubated for 2 h at room temperature with a goat anti-rabbit IgG-HRP antibody (Santa Cruz Biotechnologies) diluted in TPBS with 0.05% (w/v) BSA in a 1:10.000 dilution. After the incubation with the secondary antibody, membranes were washed twice with TPBS for 10 min and once with PBS for 10 min. For protein immunodetection, Supersignal West Pico Chemiluminescent Substrate (ThermoFisher Scientific, Waltham, MA, USA) was employed following manufacturer's instructions. Images were captures with a ChemiDoc XRS+ (Bio-Rad, Hercules, CA, USA) (Figure M2).

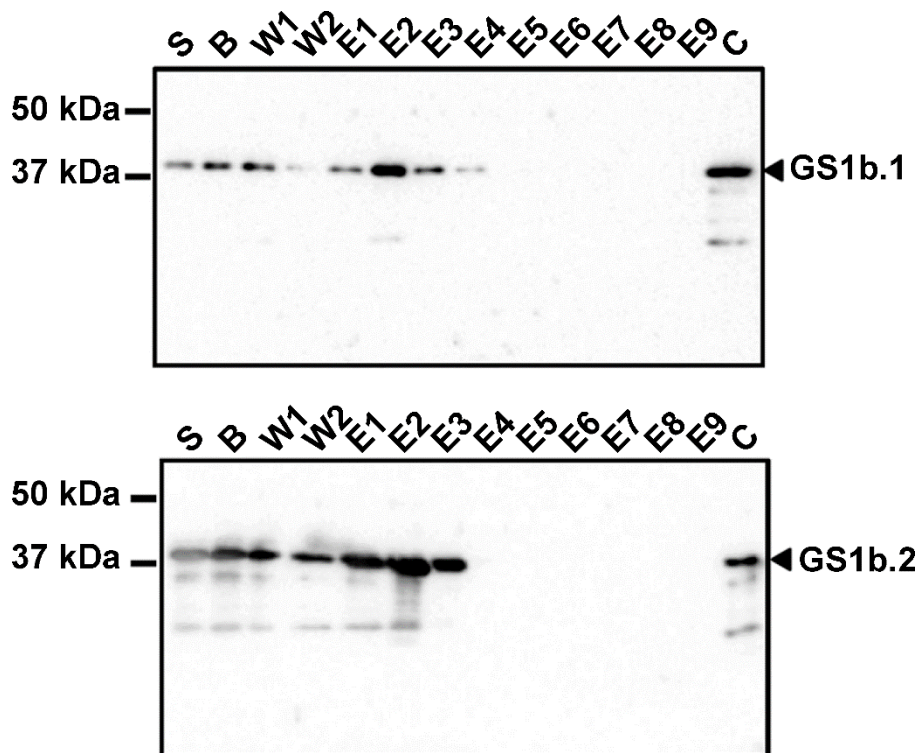


Figure M1. SDS page analysis of GS1b.1 and GS1b.2 purification and concentration processes. Sol, soluble fraction; B, binding fraction; W1, wash fraction 1; W2, wash fraction 2; EL1-9, elution fraction 1-9; C, concentrate fraction.

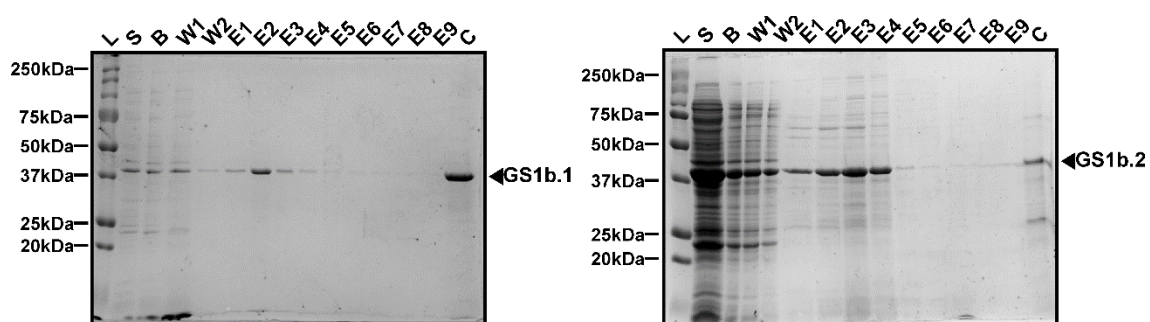


Figure M2. Western-blot page analysis of GS1b.1 and GS1b.2 purification and concentration processes. L, molecular weight ladder; S, soluble fraction; B, binding fraction; W1, wash fraction 1; W2, wash fraction 2; EL1-9, elution fraction 1-9; C, concentrate fraction.

16. GS Physicochemical assays

Physicochemical properties were determined by conducting the transferase assay as described in Cánovas et al. (1991). Reactions were carried out in 96 well microtiter plates with a final reaction volume of 150 μ L. The reaction mix contained 90.6 mM MOPS pH 7, 20 mM arsenate, 2.93 mM $MnCl_2$, 60 mM NH_2OH and 0.4 mM ADP. Different buffers were used instead when determining the optimal pH level for the activity of the different isoforms: acetate (4.5-5); MES (6-6.5); HEPES (7-7.5); Tris (8-8.5); and sodium carbonate (9-10). The reaction was initiated by adding glutamine in a final concentration of 120 mM and, after 15 minutes of incubation at 37 °C, 150 μ L of STOP solution (10% $FeCl_3 \cdot 6 H_2O$ in HCl 0.2 N; 24% trichloroacetic acid and 5% HCl) was added to stop the reaction. Finally, the plate was centrifugated for 3 minutes at 3220 x g and 100 μ L of the reaction volume were withdrawn for its absorbance measurement at 540 nm in a PowerWave HY (BioTek, Winooski, VT; USA) plate lector. For thermostability characterization, proteins were preincubated at different times and temperatures before adding the reaction mix.

17. GS Kinetic assays

For the quantification of the kinetic properties, biosynthetic assays were carried out as described by Gawronski and Benson (2004) with some modifications. Reactions were conducted in 96 wells microtiter plates in a final volume of 100 μ L and GS activity was determined as a function of NADH absorbance depletion at 340 nm in a coupled reaction using lactate-dehydrogenase (LDH, EC 1.1.1.27) and pyruvate kinase (PyrK, EC 2.7.1.40). For GS activity, the following reaction mix was used: 50 mM HEPES pH 7, 10 mM $MgCl_2$, 60 mM NH_4Cl , 250 mM glutamate, 6.25 mM ATP, 1 mM phosphoenolpyruvate, 0.6 mM NADH, 1 U PyRK and 1 U LDH. Reactions were pre-incubated for 5 minutes at 37 °C and the GS activity was initiated by adding different concentrations of the substrate that is being analyzed. Reactions were developed for 40 min at 37 °C with shaking and absorbance measurement at 340 nm each minute. Analysis of the kinetic characteristics of GS1b.1 WT, GS1b.2 WT and their mutants were performed with GraphPad Prism 8.0.0 (GraphPad, San Diego, CA, USA).

References

REREFENCES

Achard, P., Gusti, A., Cheminant, S., Alioua, M., Dhondt, S., Coppens, F., Beemster, G.T.S & Genschik, P. (2009). Gibberellin signaling controls cell proliferation rate in *Arabidopsis*. *Current biology*, 19, 1188-1193.

Afgan, E., Baker, D., Batut, B., van den Beek, M., Bouvier, D., Cech, M. et al. (2018). The galaxy platform for accessible, reproducible and collaborative biomedical analyses: 2018 update. *Nucleic Acids Research*, 46, W537– W544.

Aledo, J.C. (2021). ptm: an R package for the study of methionine sulfoxidation and other post-translational modifications. *Bioinformatics*, 37, 3979–3980

Alekseeva, A.A., Savin S.S. & Tishkov, V.I. (2011). NAD⁺-dependent formate dehydrogenase from plants. *Acta Naturae*, 3, 38-54.

Almagro, A., Lin, S.H. & Tsay, Y.F. (2008). Characterization of the *Arabidopsis* nitrate transporter NRT1.6 reveals a role of nitrate in early embryo development. *The Plant Cell*, 6, 3289-3299.

Almagro, Armenteros, J.J., Salvatore, M., Emanuelsson, O., Winther, O., von Heijne, G., Elofsson, A. & Nielsen, H. (2019). Detecting sequence signals in targeting peptide using deep learning. *Life Science Alliance*, 2, e201900429.

Altschul, S.F., Gish, W., Miller, W., Myers, E.W. & Lipman, D.J. (1990). Basic local alignment search tool. *Journal of Molecular Biology*, 215, 403–410.

Alvarez, J.M., Riveras, E., Vidal, E.A., Gras, D.E., Contreras-Lopez, O., Tamayo, K.P., Aceituno, F., Gomez, I., Ruffel, S., Lejay, L., et al. (2014). Systems approach identifies TGA1 and TGA4 transcription factors as important regulatory components of the nitrate response of *Arabidopsis thaliana* roots. *The Plant journal*, 80, 1–13.

Amiour, N., Décousset, L., Rouster, J., Quenard, N., Buet, C., Dubreuil, P. et al. (2021). Impacts of environmental conditions, and allelic variation of cytosolic glutamine synthetase on maize hybrid kernel production. *Communications Biology*, 4, 1095.

Aranda, I., Alía, R., Ortega, U., Dantas, Â.K. & Majada, J. (2010). Intra-specific variability in biomass partitioning and carbon isotopic discrimination under moderate drought stress in seedlings from four *Pinus pinaster* populations. *Tree Genetics & Genomes*, 6, 169-178.

REFERENCES

- Athwal, G.S., Huber, J.L. & Huber, S.C. (1998). Phosphorylated nitrate reductase and 14-3-3 proteins. *Plant Physiology*, 118, 1041-1048.
- Avery, G.S., Burkholder, P.R., and Creighton, H.B. (1937). Nutrient deficiencies and growth hormone concentration in *Helianthus* and *Nicotiana*. *American Journal of Botany*, 24, 553–557.
- Avery, G.S., and Pottorf, L. (1945). Auxin and nitrogen relationships in green plants. *American Journal of Botany*, 32, 666–669.
- Ávila-Sáez, C., Muñoz-Chapuli, R., Plomion, C., Frigerio, J. & Cánovas, F.M. (2000). Two genes encoding distinct cytosolic glutamine synthetases are closely linked in the pine genome. *FEBS Letters*, 477, 237–243.
- Ávila, C., Suárez, M.F., Gómez-Maldonado, J. & Cánovas, F.M. (2001). Spatial and temporal expression of two cytosolic glutamine synthetase genes in scots pine: functional implications on nitrogen metabolism during early stages of conifer development. *The Plant Journal*, 25, 93–102.
- Ávila, C., Llebrés, M.T., Castro-Rodríguez, V., Lobato-Fernández, C., Reymond, I., Harvengt, L., Trontin, J.F. & Cánovas, F.M. (2022). Identification of metabolic pathways differentially regulated in somatic and zygotic embryos of maritime pine. *Frontiers in Plant Science*, 13.
- Bainbridge, K., Guyomarc'h, S., Bayer, E., Swarup, R., Bennett, M., Mandel, T. & Kuhlemeier, C. (2008). Auxin influx carriers stabilize phyllotactic patterning. *Genes & Development*, 22, 810–823.
- Bajgain, P., Russell, B. & Mohammadi, M. (2018). Phylogenetic analyses and in-seedling expression of ammonium and nitrate transporters in wheat. *Scientific Reports*, 8.
- Bao, A., Zhao, Z., Ding, G., Shi, L., Xu, F. & Cai, H. (2014). Accumulated expression level of cytosolic glutamine synthetase 1 gene (*OsGs1;1* or *OsGS1;2*) alter plant development and the carbon-nitrogen metabolic status in rice. *PLoS ONE*, 9.
- Berling, D.J. & Bermer, R.A. (2000). Impact of a Permo-carboniferous high O₂ event on the terrestrial carbon cycle. *Proceedings of the National Academy of Sciences of the United States of America*, 97, 12428–12432.

REFERENCES

- Bernard, S.M. & Habash, D.Z. (2009). The importance of cytosolic glutamine synthetase in nitrogen assimilation and recycling. *New Phytologist*, 182, 608–620.
- Biesiadka, J. & Legocki, A.B. (1997). Evolution of the glutamine synthetase gene in plants. *Plant Science*, 128, 51–58.
- Birol, I., Raymond, A., Jackman, S.D., Pleasance, S., Coope, R., Taylor, G.A. et al. (2013). Assembling the 20 Gb white spruce (*Picea glauca*) genome from whole-genome shotgun sequencing data. *Bioinformatics*, 12, 1492–1497.
- Blackwell, R.D., Murray, A.J.S. & Lea, P.J. (1987). Inhibition of photosynthesis in barley with decreased levels of chloroplastic glutamine synthetase activity. *Journal of Experimental Botany*, 196, 1799–1809.
- Blilou, I., Xu, J., Wildwater, M., Willemsen, V., Paponov, I., Friml, J., Heidstra, R., Aida, M., Palme, K. & Scheres, B. (2005). The PIN auxin efflux facilitator network controls growth and patterning in *Arabidopsis* roots. *Nature*, 443, 39–44.
- Bloom, A.J., Asensio, J.S.R., Randall, L., Rachmilevitch, S., Cousins, A.B. & Carlisle, E.A. (2012). CO₂ enrichment inhibits shoot nitrate assimilation in C₃ but not C₄ plants and slows growth under nitrate in C₃ plants. *Ecology*, 93, 355–367.
- Bloom, A.J. (2015). Photorespiration and nitrate assimilation: a major intersection between plant carbon and nitrogen. *Photosynthesis Research*, 123, 117–128.
- Boczulak, S.A., Hawkins, B.J. & Roy, R. Temperature effects on nitrogen from uptake by seedling roots of three contrasting conifers. *Tree physiology*, 34, 513–523.
- Bolger, A.M., Lohse, M. & Usadel, B. (2014). Trimmomatic: a flexible trimmer for Illumina sequence data. *Bioinformatics*, 30, 2114–2120.
- Bouguyon, E., Perrine-Walker, F., Pervent, M., Rochette, J., Cuesta, C., Benkova, E., et al. (2016). Nitrate controls root development through posttranscriptional regulation of the NRT1.1/NPF6.3 transporter/sensor. *Plant Physiology*, 172, 1237–1248.
- Bradford, M.M. (1976). A rapid and sensitive method for the quantitation of microgram quantities of protein utilizing the principle of protein-dye binding. *Analytical Biochemistry*, 72, 248–254.

REFERENCES

- Britto, D.T. & Kronzucker, H.J. (2001). Constancy of nitrogen turnover kinetics in the plant cell: insights into the integration of subcellular N fluxes. *Planta*, 213, 175-181.
- Britto, D.T. & Kronzucker, H.J. (2002). NH_4^+ toxicity in higher plants: a critical review. *Journal of Plant Physiology*, 159, 567-584.
- Britto, D.T. & Kronzucker, H.J. (2006). Futile cycling at the plasma membrane: a hallmark of low-affinity nutrient transport. *TRENDS in Plant Science*, 11, 529-534.
- Cameron, K.C., Di, H.J. & Moir, J.L. (2013). Nitrogen losses from the soil/plant system: a review. *Annals of Applied Biology*, 162, 145-173.
- Canales, J., Rueda-López, M., Craven-Bartle, B., Avila, C. & Cánovas, F.M. (2012). Novel insights into regulation of asparagine synthetase in conifers. *Frontiers in Plant Science*, 24, 3-100.
- Canfield, D.E., Glazer, A.N. & Falkowski, P.G. (2010). The evolution and future of earth's nitrogen cycle. *Science*, 8, 192-196.
- Cánovas, F.M., Cantón, F.R., Gallardo, F., García-Gutiérrez, A. & de Vicente A. 1991. Accumulation of glutamine synthetase during early development of maritime pine seedlings (*Pinus pinaster*). *Planta*, 185, 372-378.
- Cánovas, F.M., Ávila, C., Cantón, F.R., Cañas, R.A. & de la Torre, F. (2007). Ammonium assimilation and amino acid metabolism in conifers. *Journal of Experimental Botany*, 58, 2307-2318.
- Cantón, F.R., García-Gutiérrez, A., Gallardo, F., de Vicente, A. & Cánovas, F.M. (1993). Molecular characterization of a cDNA clone encoding glutamine synthetase from a gymnosperm, *Pinus sylvestris*. *Plant Molecular Biology*, 22, 819-828.
- Cantón, F.R., García-Gutiérrez, A., Crespillo, R. & Cánovas, F.M. (1996). High-level expression of *Pinus sylvestris* glutamine synthetase in *Escherichia coli*. Production of polyclonal antibodies against the recombinant protein and expression studies in pine seedlings. *FEBS Letters*, 393, 205-210.
- Cantón, F.R., Suárez, M.F., José-Estanyol, M. & Cánovas, F.M. (1999). Expression analysis of a cytosolic glutamine synthetase gene in cotyledons of scots pine seedlings: developmental,

REFERENCES

light regulation and spatial distribution of specific transcripts. *Plant Molecular Biology*, 404, 623–634.

Cantón, F.R., Suárez, M.F. & Cánovas, F.M. (2005). Molecular aspects of nitrogen mobilization and recycling in trees. *Photosynthesis Research*, 83, 265-278.

Cañas, R.A., Canales, J., Gómez-Maldonado, J., Ávila, C. & Cánovas, F.M. (2014). Transcriptome analysis in maritime pine using laser capture microdissection and 454 pyrosequencing. *Tree Physiology*, 34, 1278– 1288.

Cañas, R.A., Canales, J., Muñoz-Hernández, C., Granados, J.M., Ávila, C., García-Martín, M.L. & Cánovas, F.M. (2015). Understanding developmental and adaptive cues in pine through metabolite profiling and co-expression network analysis. *Journal of Experimental Botany*, 66, 3113-3127.

Cañas, R.A., Li, Z., Pascual, M.B., Castro-Rodríguez, V., Ávila, C., Sterck, L., Van de Peer, Y. & Cánovas, F.M. (2017). The gene expression landscape of pine seedling tissues. *The Plant Journal*, 91, 1064-1087.

Carrillo, N. & Ceccarelli E.A. (2003). Open questions in ferredoxin-NADP⁺ reductase catalytic mechanism. *European Journal of Biochemistry*, 271, 1900-1915.

Cassman, K.G., Dobermann, A., and Walters, D.T. (2002). Agroecosystems, nitrogen-use efficiency, and nitrogen management. *AMBIO: A Journal of the Human Environment*, 31, 132-141.

Castro-Rodríguez, V., García-Gutiérrez, A., Canales, J., Ávila, C., Kirby, E.G. & Cánovas, F.M. (2011). The glutamine synthetase gene family in *Populus*. *BMC Plant Biology*, 11.

Castro-Rodríguez, V., García-Gutiérrez, A., Cañas, R.A., Pascual, M.B., Ávila, C. & Cánovas, F.M. (2015). Redundancy and metabolic function of the glutamine synthetase gene family in poplar. *BMC Plant Biology*, 15, 20.

Castro-Rodríguez, V., Cañas, R.A., de la Torre, F.N., Pascual, M.B., Ávila, C. & Cánovas, F.M. (2017). Molecular fundamentals of nitrogen uptake and transport in trees. *Journal of Experimental Botany*, 68, 2489-2500.

REFERENCES

- Cerezo, M., Tillard, P., Filleur, S., Muños, S., Daniel-Vedele, F. & Gojon, A. (2001). Major alterations of the regulation of root NO₃⁻ uptake are associated with the mutation of *Nrt2.1* and *Nrt2.2* genes in *Arabidopsis*. *Plant Physiology*, 127, 262-271.
- Chae, H.S., Faure, F. & Kieber, J.J. (2003). The *eto1*, *eto2*, and *eto3* mutations and cytokinin treatment increase ethylene biosynthesis in *Arabidopsis* by increasing the stability of ACS protein. *The Plant Cell*, 15, 545-559.
- Chardon, F., Noël, V. & Masclaux-Daubresse, C. (2012). Exploring NUE in crops and in *Arabidopsis* ideotypes to improve yield and seed quality. *Journal of Experimental Botany*, 63, 3401-3412.
- Chen, B., Sun, Y., Tian, Z., Fu, G., Pei, X., Pan, Z., Nazir, M.F., Song, S., Li, H., Wang, X., et al. (2021). GhGASA10-1 promotes the cell elongation in fiber development through the phytohormones IAA-induced. *BMC Plant Biology*, 21.
- Choi, Y.A., Kim, S.G. & Kwon, Y.M. (1999). The plastidic glutamine synthetase activity is directly modulated by means of redox change at two unique cysteine residues. *Plant Science*, 149, 175-182.
- Chopin, F., Orsel, M., Dorbe, M.F., Chardon, F., Truong, H.N., Miller, A.J., Krapp, A. Daniel-Vedele, F. (2007). The *Arabidopsis ATNRT2.7* nitrate transporters control nitrate content in seed. *The Plant Cell*, 19, 1590-1602.
- Clement, C.R., Hopper, M.J. & Jones L.H.P. (1978). The uptake of nitrate by *Lolium perenne* from flowing nutrient solution: I. effect of NO₃⁻ concentration. *Journal of Experimental Botany* 29, 453-464.
- Clemente, M.T. & Márquez A.J. (2000). Site-directed mutagenesis of Cys-92 from the α -polypeptide of *Phaseolus vulgaris* glutamine synthetase reveals that this highly conserved residue is not essential for enzyme activity but it is involved in thermal stability. *Plant Science*, 154, 189-197.
- Corpet, F. (1988). Multiple sequence alignment with hierarchical clustering. *Nucleic Acids Research*, 16, 10881-10890.
- Corratgé-Faillie, C. & Lacombe, B. (2017). Substrate (un)specificity of *Arabidopsis* NRT1/PTR FAMILY (NPF) proteins. *Journal of Experimental Botany*, 68, 3107-3113.

REFERENCES

- Courty, P.E., Smith, P., Koegel, S., Redecker, D. & Wipf, D. (2016). Inorganic nitrogen uptake and transport in beneficial plant root-microbe interactions. *Critical Reviews in Plant Science*, 34, 4-16.
- de Graaf, M.C.C., Bobbink, R., Roelofs, J.G.M. & Verbeek, P.J.M. (1998). Differential effects of ammonium and nitrate on three heathland species. *Plant Ecology*, 135, 185-196.
- de la Torre, F., García-Gutiérrez, A., Crespillo, R., Cantón, F.R., Ávila, C. & Cánovas, F.M. (2002). Functional expression of two pine glutamine synthetase genes in bacteria reveals that they encode cytosolic holoenzymes with different molecular and catalytic properties. *Plant & Cell Physiology*, 437, 802–809.
- De Seoane, C.L.V., Gallego-Fernández, J., Vidal-Pascual, C. (2007). Manual of restoration of coastal dunes. Edited by the Ministry of the Environment of Spain. General Direction of Coasts.
- De Smet, R. & Van de Peer, Y. (2012). Redundancy and rewiring of genetic networks following genome-wide duplication events. *Current Opinion in Plant Biology*, 15, 168-176.
- Diaz, R.J. & Rosenberg, R. (2008). Spreading dead zones and consequences for marine ecosystems. *Science*, 321, 926-929.
- Dietrich, D., Hammes, U., Thor, K., Suter-Grotemeyer, M., Fluckiger, R., Slusarenko, A.J., Ward, J.M. & Rentsch, D. (2004). *AtPTR1*, a plasma membrane peptide transporter expressed during seed germination and in vascular tissue of *Arabidopsis*. *The Plant Journal*, 40, 488–99
- Du, M., Spalding, E.P. & Gray, W.M. (2020). Rapid auxin-mediated cell expansion. *Annual Review of Plant Biology*, 71, 379-402.
- Edelheit, O., Hanukoglu, A. & Hanukoglu, I. (2009). Simple and efficient site-directed mutagenesis using two single-primer reactions in parallel to generate mutants for protein structure-function studies. *BMC Biotechnology*, 9.
- Edgar, R.C. (2004). MUSCLE: multiple sequence alignment with high accuracy and high throughput. *Nucleic Acids Research*, 32, 1792–1797.
- Eisenberg, D., Gill, H.S., Pfluegl, G.M.U. & Rotstein, S.H. (2000). Structure-function relationships of glutamine synthetases. *Biochimica et Biophysica Acta*, 1477, 122-145.

REFERENCES

- Eisenhut, M., Roell, M.S. & Weber, A.P.M. (2019). Mechanistic understanding of photorespiration paves the way to a new green revolution. *New Phytologist*, 223, 1762-1769.
- El-Azaz, J., Cánovas, F.M., Barcelona, B., Ávila, C. & de la Torre, F. (2022). Deregulation of phenylalanine biosynthesis evolved with the emergence of vascular plants. *Plant Physiology*, 188, 134–150.
- Engelsberger, W.R. & Schulze, W.X. (2012). Nitrate and ammonium lead to distinct global dynamic phosphorylation patterns when resupplied to nitrogen-starved *Arabidopsis* seedlings. *The Plant Journal*, 69, 978–995.
- Esteban, R., Ariz, I., Cruz, C. & Moran, J.F. (2016). Review: Mechanisms of ammonium toxicity and the quest for tolerance. *Plant Science*, 248, 92-101.
- Fan, S.C., Lin, C.S., Hsu, P.K., Lin, S.H. & Tsay, Y.F. (2009). The *Arabidopsis* nitrate transporter NRT1.7, expressed in phloem, is responsible for source-to-sink remobilization of nitrate. *The Plant Cell*, 21, 2750-2761.
- Fan, X., Feng, H., Tan, Y., Xu, Y., Miao, Q. & Xu, G. (2016). A putative 6-transmembrane nitrate transporter *OsNRT1.1b* plays a key role in rice under low nitrogen. *Journal of Integrative Plant Biology*, 58, 590-599.
- Fan, X., Naz, M., Fan, X., Xuan, W., Miller, A.J. & Xu, G. (2017). Plant nitrate transporters: from gene function to application. *Journal of Experimental Botany*, 68, 2463-2475.
- Feng, H., Yan, M., Fan, X., Li, B., Shen, Q., Miller, A.J. & Xu, G. (2011). Spatial expression and regulation of rice high-affinity nitrate transporters by nitrogen and carbon status. *Journal of Experimental Botany*, 62, 2319-2332.
- Ferreira, M.J., Vale, D., Cunha, L. & Melo, P. (2017). Role of the C-terminal extension peptide of plastid located glutamine synthetase from *Medicago truncatula*: crucial for enzyme activity and needed for protein import into the plastids. *Plant Physiology and Biochemistry*, 111, 226-233.
- Ferreira, S., Moreira, E., Amorim, I., Santos, C. & Melo, P. (2019). *Arabidopsis thaliana* mutants devoid of chloroplast glutamine synthetase (GS2) have non-lethal phenotype under photorespiratory conditions. *Plant Physiology Biochemistry*, 144, 365–374.

REFERENCES

- Filleur, S., Dorbe, M.F., Cerezo, M., Orsel, M., Granier, F., Gojon, A. & Daniel-Vedele, F. (2001). An Arabidopsis T-DNA mutant affected in Nrt2 genes is impaired in nitrate uptake. *FEBS Letters*, 489, 220-224.
- Finnemann, J. & Schjoerring, J.K. (2000). Post-translational regulation of cytosolic glutamine synthetase by reversible phosphorylation and 14-3-3 protein interaction. *The Plant Journal*, 24, 171-181.
- Fontaine, J.X., Ravel, C., Pegeau, K., Heumez, E., Dubois, F., Hirel, B. & Le Gouis, J. (2009). A quantitative genetic study for elucidating the contribution of glutamine synthetase, glutamate dehydrogenase and other nitrogen-related physiological traits to the agronomic performance of common wheat. *Theoretical and Applied Genetics*, 119, 645-662.
- Forde, B.G. & Clarkson, D.T. (1999). Nitrate and ammonium nutrition of plants: physiological and molecular perspective. *Advances in Botanical Research*, 30, 1-90.
- Forde, B.G. & Lea, P.J. (2007). Glutamate in plants: metabolism, regulation, and signaling. *Journal of Experimental Botany*, 58, 2339-2358.
- Forde, B.G. (2014). Glutamate signalling in roots. *Journal of Experimental Botany*, 65, 779-787.
- Franklin, O., Cambui, C.A., Gruffman, L., Palmroth, S., Oren, R. & Näsholm, T. (2017). The carbon bonus of organic nitrogen enhances nitrogen use efficiency of plants. *Plant, Cell and Environment*, 40, 25-35.
- Fu, X. & Harberd, N.P. (2003). Auxin promotes Arabidopsis root growth by modulating gibberellin response. *Nature*, 421, 740-743.
- Fujita, T., Beier, M.P., Tabuchi-Kobayashi, M., Hayatsu, Y., Nakamura, H., Umetsu-Ohashi, T., et al. (2022). Cytosolic glutamine synthetase GS1;3 is involved in rice grain ripening and germination. *Frontiers in Plant Science*, 13.
- Funayama, K., Kojima, S., Tabuchi-Kobayashi, M., Sawa, Y., Nakayama, Y., Hayakawa, T. & Yamaya, T. (2013). Cytosolic glutamine synthetase 1;2 is responsible for the primary assimilation of ammonium in rice roots. *Plant and Cell Physiology*, 54, 934-943.

REFERENCES

- Gallais, A. & Hirel, B. (2004). An approach to the genetics of nitrogen use efficiency in maize. *Journal of Experimental Botany*, 55, 295-306.
- Galloway, J.N., Leach, A.M., Bleeker, A. & Erisman, J.W. (2013). A chronology of human understanding of the nitrogen cycle. *Philosophical Transactions of The Royal Society B*, 368.
- Gao, Y., de Bang, T.C. & Schjoerring, J.K. (2019). Cisgenic overexpression of cytosolic glutamine synthetase improves nitrogen utilization efficiency in barley and prevents grain protein decline under elevated CO₂. *Plant Biotechnology Journal*, 17, 1209-1221.
- García-Gutiérrez, A., Dubois, F., Cantón, F.R., Gallardo, F., Sangwan, R.S. & Cánovas, F. (1998). Two different models of early development and nitrogen assimilation in gymnosperm seedlings. *The Plant Journal*, 132, 187-199.
- Gawronski, J.D. & Benson, D.R. (2004). Microtiter assay for glutamine synthetase biosynthetic activity using inorganic phosphate detection. *Analytical Biochemistry*, 327, 114-118.
- Ghoshroy, S., Binder, M., Tartar, A. & Robertson, D.L. (2010). Molecular evolution of glutamine synthetase II: phylogenetic evidence of a nonendosymbiotic gene transfer event early in plant evolution. *BMC Evolution Biology*, 10, 198.
- Glass, A.D.M., Britto, D.T., Kaiser, B.N., Kinghorn, J.R., Kronzucker, H.J., Kumar, A., et al. (2002). The regulation of nitrate and ammonium transport systems in plants. *Journal of Experimental Botany*, 53, 855-864.
- Gojon, A. & Gaymard, F. (2010). Keeping nitrate in the roots: an unexpected requirement for cadmium tolerance in plants. *Journal of Molecular Cell Biology*, 2, 299-301.
- Gómez-Maldonado, J., Ávila, C., Barnestein, P., Crespillo, R. & Cánovas, F.M. (2004a) Interaction of cis-acting elements in the expression of a gene encoding cytosolic glutamine synthetase in pine seedlings. *Physiologia Plantarum*, 121, 537-545.
- Gómez-Maldonado, J., Cánovas, F.M. & Ávila, C. (2004b). Molecular analysis of the 5'-upstream of a gibberellin-inducible cytosolic glutamine synthetase gene (GS1b) expressed in pine vascular tissue. *Planta*, 218, 1036-1045.

REFERENCES

- Goodall, A.J., Kumar, P. & Tobin, A.K. (2013). Identification and expression analyses of cytosolic glutamine synthetase genes in barley (*Hordeum vulgare* L.). *Plant and Cell Physiology*, 54, 492-505.
- Goodstein, D.M., Shu, S., Howson, R., Neupane, R., Hayes, R.D., Fazo, J., et al. (2012). Phytozome: a comparative platform for green plant genomics. *Nucleic Acids Research*, 40, 1178-1186.
- Grabherr, M.G., Haas, B.J., Yassour, M., Levin, J.Z., Thompson, D.A., Amit, I. et al. (2011). Full-length transcriptome assembly from RNA-seq data without a reference genome. *Nature Biotechnology*, 29, 644–652.
- Granados, J.M., Ávila, C., Cánovas, F.M. & Cañas, R.A. (2016). Selection and testing of reference genes for accurate RT-qPCR in adult needles and seedlings of maritime pine. *Tree Genetic & Genomes*, 12, 60–75.
- Greenboim-Wainberg, Y., Maymon, I., Borochoy, R., Alvarez, J., Olszewski, N., Ori, N., Eshed, Y. & Weiss, D. (2005). Cross talk between gibberellin and cytokinin: the *Arabidopsis* GA response inhibitor SPINDLY plays a positive role in cytokinin signaling. *The Plant Cell*, 17, 92-102.
- Grieneisen, A.V., Xu, j., Marée, A.F.M., Hogeweg, P. & Scheres, B. (2007). Auxin transport is sufficient to generate a maximum and gradient guiding root growth. *Nature*, 449, 1008-1013.
- Guan, M., Moller, I.S. & Schjoerring, J.K. (2015). Two cytosolic glutamine synthetase isoforms play specific roles for seed germination and seed yield structure in *Arabidopsis*. *Journal of Experimental Botany*, 66, 203-212.
- Guan, R., Zhao, Y., Zhang, H., Fan, G., Liu, X., Zhou, W. et al. (2016). Draft genome of the living fossil *Ginkgo biloba*. *Gigascience*, 5, 49.
- Guo, F.Q., Young, J. & Crawford, N.M. (2003). The nitrate transporter *AtNRT1.1* (CHL1) functions in stomatal opening and contributes to drought susceptibility in *Arabidopsis*. *The Plant Cell*, 15, 107-117.
- Gutierrez, R.A., Lejay, L.V., Dean, A., Chiaromonte, F., Shasha, D., and Coruzzi, G.M. (2007). Qualitative network models and genome wide expression data define carbon/nitrogen-responsive molecular machines in *Arabidopsis*. *Genome Biology*, 8.

REFERENCES

- Gutiérrez, R.A. (2012). Systems biology for enhanced plant nitrogen nutrition. *Science*, 336, 1673-1675.
- Habash, D.Z., Massiah, A.J., Rong, H.L., Wallsgrave, R.M. & Leigh, R.A. (2001). The role of cytosolic glutamine synthetase in wheat. *Annals of Applied Biology*, 138, 83-89.
- Habash, D.Z., Bernard, S., Schondelmaire, J., Weyen, J. & Quarrie, S.A. (2007). The genetics of nitrogen use in hexaploidy wheat: N utilization, development and yield. *Theoretical and Applied Genetics*, 114, 403-419.
- Hachiya, T., Inaba, J., Wakazaki, M., Sato, M., Toyooka, K., Miyagi, A. et al. (2021). Excessive ammonium assimilation by plastidic glutamine synthetase causes ammonium toxicity in *Arabidopsis thaliana*. *Nature Communications*, 12, 4944.
- Hanke, G.T., Okutani, S., Satomi, Y., Takao, T., Suzuki, A. & Hase, T. (2005). Multiple iso-proteins of FNR in *Arabidopsis*: evidence for different contributions to chloroplast function and nitrogen assimilation. *Plant, Cell and Environment*, 28, 1146-1157.
- Havé, M., Marmagne, A., Chardon, F. & Masclaux-Daubresse, C. (2017). Nitrogen remobilization during leaf senescence: lessons from *Arabidopsis* to crops. *Journal of Experimental Botany*, 68, 2513–2529.
- He, Y.X., Gui, L., Liu, Y.Z., Du, Y., Zhou, Y., Li, P. & Zhou, C.Z. (2009). Crystal structure of *Saccharomyces cerevisiae* glutamine synthetase Gln1 suggests a nanotube-like supramolecular assembly. *Proteins*, 76, 249-254.
- He, Y.N., Peng, J.S., Cai, Y., Liu, D.F., Guan, Y., Yi, H.Y. & Gong, J.M. (2017). Tonoplast-localized nitrate uptake transporters involved in vacuolar nitrate efflux and reallocation in *Arabidopsis*. *Scientific Reports*, 7.
- Heldt, H. & Piechulla, B. (2011) *Plant Biochemistry*, fourth edition. San Diego: Academic Press, Elsevier.
- Hirel, B., Bertin, P., Quilleré, I., Bourdoncle, W., Attagnant, C., Dellay, C., et al. (2001). Towards a better understanding of the genetic and physiological basis for nitrogen use efficiency in maize. *Plant Physiology*, 125, 1258-1270.

REFERENCES

- Hirel, B., Tétu, T., Lea, P.J. & Dubois, F. (2011). Improving nitrogen use efficiency in crops for sustainable agriculture. *Sustainability*, 3, 1452-1485.
- Hirel, B. & Krapp, A. (2021). Nitrogen utilization in plants I biological and agronomic importance. In: Jez, J. (Ed.) *Encyclopedia of biological chemistry III*, Third edition. Amsterdam: Elsevier, pp. 127–140.
- Ho, C.H., Lin, S.H., Hu, H.C. & Tsay, Y.F. (2009). CHL1 functions as a nitrate sensor in plants. *Cell*, 138, 1184-1194.
- Houben, M. & Van de Poel, B. (2019). 1-aminocyclopropane-1-carboxylic acid oxidase (aco): the enzyme that makes the plant hormone ethylene. *Frontier in Plant Science*, 10.
- Hsu, P.K. & Tsay, Y.F. (2013). Are important for redistributin xylem-borne nitrate to enhance plant growth. *Plat Physiology*, 163, 844-856.
- Hu, H.C., Wang, Y.Y., and Tsay, Y.F. (2009). AtCIPK8, a CBL-interacting protein kinase, regulates the low-affinity phase of the primary nitrate response. *The Plant Journal*, 57,264–278.
- Hu, L., Xu, Z., Wang, M., Fan, R., Yuan, D., Wu, B. et al. (2019). The chromosome-scale reference genome of black pepper provides insight into piperine biosynthesis. *Nature Communications*, 10, 4702.
- Hu, Q.Q., Shu, J.Q., Li, W.M. & Wang, G.Z. (2021). Role of auxin and nitrate signaling in the development of root system architecture. *Frontiers in Plant Science*, 12.
- Huelsenbeck, J.P. & Ronquist, F. (2001). MRBAYES: Bayesian inference of phylogeny. *Bioinformatics*, 17, 754–755.
- Huérffano, X., Fuertes-Mendizábal, T., Duñabeitia, M.K., González-Murua, C., Estavillo, J.M., and Menéndez, S. (2015). Splitting the application of 3, 4-dimethylpyrazole phosphate (DMPP): Influence on greenhouse gases emissions and wheat yield and quality under humid Mediterranean conditions. *European Journal of Agronomy*, 64, 47-57.
- Ishiyama, K., Inoue, E., Tabuchi, M., Yamaya, T. & Takahashi, H. (2004a). Biochemical background and compartmentalized functions of cytosolic glutamine synthetase for active ammonium assimilation in rice roots. *Plant and Cell Physiology*, 45, 1640-1647.

REFERENCES

- Ishiyama, K., Inoue, E., Watanabe-Takahashi, A., Obara, M., Yamaya, T. & Takahashi, H. (2004b). Kinetic properties and ammonium-dependent regulation of cytosolic isoenzymes of glutamine synthetase in *Arabidopsis*. *The Journal of Biological Chemistry*, 279, 16598-16605.
- Ishiyama, K., Inoue, E., Yamaya, T. & Takahashi, H. (2006). Gln49 and Ser174 residues play critical roles in determining the catalytic efficiencies of plant glutamine synthetase. *Plant and Cell Physiology*, 47, 299-303.
- Jackson, R.B. & Caldwell, M.M. (1993). The scale of nutrient heterogeneity around individual plants and its quantification with geostatistics. *Ecology*, 74, 612-614.
- James, D., Borphukan, B., Fartyal, D., Achary, V.M.M. & Reddy, M.K. (2018). Transgenic manipulation of glutamine synthetase: a target with untapped potential in various aspects of crop improvement. In: Gosal, S.S. & Wani, S.H. (Eds.) *Biotechnology of Crop Improvement*. Cham: Springer International Publishing AG, pp. 367-416.
- Ji, Y., Li, Q., Liu, G., Selvaraj, G., Zheng, Z. & Wei, Y. (2019). Roles of cytosolic glutamine synthetase in *Arabidopsis* development and stress responses. *Plant and Cell Physiology* 60, 657-671.
- Jmol. An open-source Java viewer for chemical structures in 3D. <http://www.jmol.org/>. Accessed August 2022.
- Jones, D.T., Taylor, W.R. & Thornton, J.M. (1992). The rapid generation of mutation data matrices from protein sequences. *Computer Applications in the Biosciences*, 8, 275-282.
- Jumper, J., Evans, R., Pritzel, A., Green, T., Figurnov, M., Ronneberger, O., et al. (2021). Highly accurate protein structure prediction with AlphaFold. *Nature*, 596, 583-589.
- Kaiser, W.M., Weiner, H., Kandlbinder, A., Tsai, C.B., Rockel, P., Sonoda, M. & Planchet, E. (2002). Modulation of nitrate reductase: some new insights, an unusual case and a potentially important side reaction. *Journal of Experimental Botany*, 53, 875-882.
- Kaminski, K.P., Kørup, K., Andersen, M.N., Sønderkær, M., Andersen, M.S., Kirk, H.G. & Nielsen, K.L. (2015). Cytosolic glutamine synthetase is important for photosynthetic efficiency and water use efficiency in potato as revealed by high-throughput sequencing QTL analysis. *Theoretical and Applied Genetics*, 128, 2143-2153.

REFERENCES

Kanno, Y., Hanada, A., Chiba, Y., Ichikawa, T., Nakazawa, M., Matsui, M., Koshiba, T., Kamiya, Y. & Seo, M. (2012). Identification of an abscisic acid transporter by functional screening using the receptor complex as a sensor. *Proceedings of the National Academy of Sciences of the United States of America*, 109, 9653-9658.

Kanno, Y., Kamiya, Y. & Seo, M. (2013). Nitrate does not compete with abscisic acid as a substrate of *AtNPF4.6/NRT1.2/AIT1* in *Arabidopsis*. *Plant signaling & Behavior*, 8.

Kiba, T., Feria-Bourrellier, A.B., Lafouge, F., Lezhneva, L., Boutet-Mercery, S., Orsel, M., Bréhaut, V., Miller, A., Daniel-Vedele, F., Sakakibara, H. & Krapp, A. (2012). The *Arabidopsis* nitrate transporter NRT2.4 plays a double role in roots and shoots of nitrogen-starved plants. *The Plant Cell*, 24, 245-258.

Kishorekumar, R., Bulle, M., Wany, A. & Gupta, K.J. (2020). An overview of Important Enzymes Involved in Nitrogen Assimilation of Plants. In: Gupta, K.J., editor. *Nitrogen Metabolism in Plants: Methods and Protocols*. New York: Springer, pp. 1-13.

Komarova, N.Y., Thor, K., Gubler, A., Meier, S., Dietrich, D., Weichert A., Grotemeyer, M.S., Tegeder, M. & Rentsch, D. (2008). AtPTR1 and AtPTR5 transport dipeptides in *Planta*. *Plant Physiology*, 148, 856-869.

Kong, D., Ju, C., Parihar, A., Kim, S., Cho, D. & Kwak, J.M. (2015). *Arabidopsis* glutamate receptor homolog3.5 modulates cytosolic Ca²⁺ level to continue effect of abscisic acid in seed germination. *Plant Physiology*, 167, 1630-1642.

Koskimäki, J.J., Pohjanen, J., Kvist, J., Fester, T., Härtig, C., Podolich, O., Fluch, S., Edesi, J., Häggman, H. & Pirttilä, A.M. (2022). The meristem-associated endosymbiont *Methylobacterium extorquens* DSM13060 reprograms development and stress responses of pine seedlings. *Tree Physiology*, 42, 391-410.

Kotur, Z., Mackenzie, N., Ramesh, S., Tyerman, S.D., Kaiser, B.N. & Glass, A.D.M. (2012). Nitrate transport capacity of the *Arabidopsis thaliana* NRT2 family members and their interactions with AtNAR2.1. *New Phytologist*, 194, 724-731.

Krajewski, W.W., Collins, R., Holmberg-Schiavone, L., Jones, T.A., Karlberg, T. & Mowbray, L. (2008). Crystal structures of mammalian glutamine synthetases illustrate substrate-induced conformational changes and provide opportunities for drug and herbicide design. *Journal of Molecular Biology*, 375, 217-228.

REFERENCES

- Krapp, A. (2015). Plant nitrogen assimilation and its regulation: a complex puzzle with missing pieces. *Current Opinion in Plant Biology*, 25, 115–122.
- Kronzucker, H.J., Siddiqi, M.Y. & Glass, A.D.M. (1997). Conifer root discrimination against soil nitrate and the ecology of forest succession. *Nature*, 385, 59-61.
- Krouk, G., Lacombe, B., Bielach, A., Perrine-Walker, F., Malinska, K., Mounier, E., et al. (2010a). Nitrate-regulated auxin transport by NRT1.1 defines a mechanism for nutrient sensing in plants. *Developmental Cell*, 18, 927-937.
- Kumada, Y., Benson, D.R., Hillemann, D., Hosted, T.J., Rochefort, D.A., Thompson, C.J. et al. (1993). Evolution of the glutamine synthetase gene, one of the oldest existing and functioning genes. *Proceedings of the National Academy of Sciences of the United States of America*, 90, 3009–3013.
- Kumar, S., Stecher, G. & Tamura, K. (2016). MEGA7: molecular evolutionary genetics analysis version 7.0 for bigger datasets. *Molecular Biology and Evolution*, 33, 1870–1874.
- Kumar, V., Yadav, S., Soumya, N., Kumar, R., Babu, N.K. & Singh, S. (2017). Biochemical and inhibition studies of glutamine synthetase from *leishmania donovani*. *Microbial Pathogenesis*, 107, 164–174.
- Kuvykin, I.V., Vershubskii, A.V., Priklonskii, V.I. & Tikhonov, A.N. (2009). Computer simulation study of pH-dependent regulation of electron transport in chloroplasts. *Biophysics*, 54, 455-464.
- Kuzmin, D.A., Ferachuk, S.I., Sharov, V.V., Cybin, A.N., Makolov, S.V., Putintseva, A. et al. (2019). Stepwise large genome assembly approach: a case of Siberian larch (*Larix sibirica* Ledeb). *BMC Bioinformatics*, 20, 37.
- Laemmli, U.K. (1970). Cleavage of structural proteins during the assembly of the head of bacteriophage T4. *Nature*, 227, 680-685.
- Lavoie, N., Vézina, L.P. & Margolis, H.A. (1992). Absorption and assimilation of nitrate and ammonium ions by jack pine seedlings. *Tree Physiology*, 11, 171-183.
- Lea, P.J. & Ireland, R.J. (1999). Nitrogen metabolism in higher Plants. In: Singh, B.K., editor. *Plant Amino Acids*. New York: Marcel Dekker Inc, pp. 1-47.

REFERENCES

- Lea, P.J. & Miflin, B.J. (2018). Nitrogen assimilation and its relevance to crop improvement. In: Foyer, C.H. & Zhang, H., editors. Annual Plant Reviews. Volume 42. Nitrogen Metabolism In Plants in the Post-Genomic Era. Chichester: Wiley-Blackwell, pp. 1–40.
- Léran, S., Varala, K., Boyer, J.C., Chiurazzi, M., Crawford, N., Daniel-Vedele, F., et al. (2014). A unified nomenclature of NITRATE TRANSPORTER 1/PEPTIDE TRANSPORTER family members in plants. Trends in Plant Science, 19, 5-9.
- Letunic, I. & Bork, P. (2019). Interactive tree of life (iTOL) v4: recent updates and new developments. Nucleic Acids Research, 47, W256–W259.
- Levitzki, A. & Koshland, Jr D.E. (1976). The role of negative cooperativity and half-of-the-sites reactivity in enzyme regulation. Current Topics in Cellular Regulation, 10, 1-40.
- Lezhneva, L., Kiba, T., Feria-Bourrellier, A.B., Lafouge, F., Boutet-Mercey, S., Zoufan, P., Sakakibara, H., Daniel-Vedele, F. & Krapp, A. (2014). The *Arabidopsis* nitrate transporter NRT2.5 plays a role in nitrate acquisition and remobilization in nitrogen-starved plants. The Plant Journal, 80, 230-241
- Li, H., Yu, M., Du, X.Q., Wang, Z.F., Wu, W.H., Quintero, F.J., Jin, X.H., Li, H.D. & Wang, Y. (2017). NRT1.5/NPF7.3 functions as a proton-coupled H⁺/K⁻ antiporter for K⁺ loading into the xylem in *Arabidopsis*. The Plant Cell, 29, 2016-2026.
- Li, J.Y., Fu, Y.L., Pike, S.M., Bao, J., Tian, W., Zhang, Y., et al. (2010). The *Arabidopsis* nitrate transporter NRT1.8 functions in nitrate removal from the xylem sap and mediates cadmium tolerance. The Plant Cell, 22, 1633-1646.
- Li, Y., Ouyang, J., Wang, Y.Y., Hu, R., Xia, K., Duan, J., Wang, Y., Tsay, Y.F. & Zhang, M. (2015). Disruption of the rice nitrate transporter *OsNPF2.2* hinders root-to-shoot nitrate transport and vascular development. Scientific Reports, 5.
- Li, Z., De La Torre, A.R., Sterck, L., Cánovas, F.M., Ávila, C., Merino, I. et al. (2017). Single-copy genes as molecular markers for phylogenomic studies in seed plants. Genome Biology & Evolution, 9, 1130–1147.
- Li, H. (2018). Minimap2: pairwise alignment for nucleotide sequences. Bioinformatics, 34, 3094-3100.

REFERENCES

- Lima, L., Seabra, A., Melo, P., Cullimore, J. & Carvalho, H. (2006a). Phosphorylation and subsequent interaction with a 14-3-3 proteins regulate plastid glutamine synthetase in *Medicago truncatula*. *Planta*, 223, 558-567.
- Lima, L., Seabra, A., Melo, P., Cullimore, J. & Carvalho, H. (2006b). Post-translational regulation of cytosolic glutamine synthetase of *Medicago truncatula*. *Journal of Experimental Botany*, 57, 2751-2761.
- Little, D.Y., Rao, H., Oliva, S., Daniel-Vedele, F., Krapp, A. & Malamy, J.E. (2005). The putative high-affinity nitrate transporter NRT2.1 represses lateral root initiation in response to nutritional cues. *Proceedings of the National Academy of Sciences of the United States of America*, 102, 13693-13698.
- Liu, K.H., Huang, C.Y. & Tsay, Y.F. (1999). CHL1 is a dual-affinity nitrate transporter of *Arabidopsis* involved in multiple phases of nitrate uptake. *The Plant Cell*, 11, 865-874.
- Liu, K.H. & Tsay, Y.F. (2003). Switching between the two action modes of the dual-affinity nitrate transporter CHL1 by phosphorylation. *The EMBO Journal*, 22, 1005-1013.
- Liu, K.H., Niu, Y., Konishi, M., Wu, Y., Du, H., Chung, H.S., et al. (2018). Discovery of nitrate-CPK-NLP signalling in central nutrient-growth networks. *Nature*, 545, 311-316.
- Llorca, O., Betti, M., González, J.M., Valencia, A., Márquez, A.J. & Valpuesta, J.M. (2006). The three-dimensional structure of an eukaryotic glutamine synthetase: Functional implications of its oligomeric structure. *Journal of Structural Biology*, 156, 469-479.
- Llorca, O., Betti, M., González, J.M., Valencia, A., Márquez, A.J., López-Bucio, J.S., de la Cruz, H.R., & Guevara-García, A.A. (2019). Glutamate sensing in plants. In: Ramakrishna, A., Roshchina, V.V., editors. *Neurotransmitters in plants: perspectives and applications*. Raton: CRC Press, pp. 231-140.
- Lothier, J., Gaufichon, L., Sormani, R., Lemaître, T., Azzopardi, M., Morin, H., Chardon, F., Reisdorf-Cren, M., Avice, J.C. & Masclaux-Daubresse, C. (2011). The cytosolic glutamine synthetase GLN1;2 plays a role in the control of plant growth and ammonium homeostasis in *Arabidopsis* rosettes when nitrate supply is not limiting. *Journal of Experimental Botany*, 62, 1375-1390.

REFERENCES

- Lovisetto, A., Masiero, S., Rahim, M.A., Mendes, M.A. & Casadoro, G. (2015). Fleshy seeds form in the basal angiosperm *Magnolia grandiflora* and several MADS-box genes are expressed as fleshy seed tissues develop. *Evolution & Development*, 1, 82–91.
- Lozano-Juste, J., Colom-Moreno, R. & León, J. (2011). In vivo protein tyrosine nitration in *Arabidopsis thaliana*. *Journal of Experimental Botany*, 62, 3501-3517.
- Man, H.M. & Kaiser, W.M. (2001). Increased glutamine synthetase activity and changes in amino acids pools in leaves treated with 5-aminoimidazole-4-carboxamide ribonucleoside (AICAR). *Physiologia plantarum*, 111, 291-296.
- Marchive, C., Roudier, F., Castaings, L., Bréhaut, V., Blondet, E., Colot, V., Meyer, C. & Krapp, A. (2013). Nuclear retention of the transcription factor NLP7 orchestrates the early response to nitrate in plants. *Nature Communications*, 4.
- Marschner, H., Häussling, M. & George, E. (1991). Ammonium and nitrate uptake rates and rhizosphere pH in non-mycorrhizal roots of Norway spruce [*Picea abies* (L.) Karst.]. *Trees*, 5, 14-21.
- Martin, A., Lee, J., Kichey, T., Gerentes, D., Zivy, M., Tatout, C., Dubois, F., et al. (2006). Two cytosolic glutamine synthetase isoforms of maize are specifically involved in the control of grain production. *The Plant Cell*, 18, 3252-3274.
- Masclaux-Daubresse, C., Carrayol, E. & Valadier, M.H. (2005). The two nitrogen mobilisation- and senescence-associated GS1 and GDH genes are controlled by C and N metabolites. *Planta*, 221, 580-588.
- Matakiadis, T., Alboresi, A., Jikumaru, Y., Tatematsu, K., Pichon, O., Renou, J.P., Kamiya, Y., Nambara, E., and Truong, H.N. (2009). The *Arabidopsis* abscisic acid catabolic gene CYP707A2 plays a key role in nitrate control of seed dormancy. *Plant Physiology*, 149, 949–960.
- Mathis, R., Gamas, P., Meyer, Y. & Cullimore, J.V. (2000). The presence of GSI-like genes in higher plants: support for the paralogous evolution of GSI and GSII. *Journal of Molecular Evolution*, 50, 116–122.
- McFee, W.W., & Stone, E.L. (1968). Ammonium and nitrate as nitrogen sources for *Pinus radiata* and *Picea glauca*. *Soil Science Society of America Journal*, 32, 879–884.

REFERENCES

- McKenzie, F.C. & Williams, J. (2015). Sustainable food production: constraints, challenges and choices by 2050. *Food Security*, 7, 221-233.
- Medici, A. & Krouk, G. (2014). The primary nitrate response: a multifaceted signalling pathway. *Journal of Experimental Botany*,
- Melo, P.M., Silva, L.S., Ribeiro, I., Seabra, A.R. & Carvalho, H.G. (2011). Glutamine synthetase is a molecular target of nitric oxide in root nodules of *Medicago truncatula* and is regulated by tyrosine nitration. *Plant Physiology*, 157, 1505-1517.
- Michard, E., Lima, P.T., Borges, F., Silva, A.C., Portes, M.T., Carvalho, J.E., Gilliam, M., Liu, L.H., Obermeyer, G. & Feijó, J.A. (2011). Glutamate receptor-like genes form Ca²⁺ channels in pollen tubes and are regulated by pistil D-serine. *Science* 332, 434-437.
- Migocka, M., Warzybok, A., Papierniak, A. & Klobus, G. (2013). NO₃⁽⁻⁾/H⁽⁺⁾ antiport in the tonoplast of cucumber root cells is stimulated by nitrate supply: evidence for a reversible nitrate-induced phosphorylation of vacuolar NO₃⁽⁻⁾/H⁽⁺⁾ antiport. *PLoS One* 8.
- Miller, A.J., and Cramer, M.D. (2005). Root nitrogen acquisition and assimilation. In: Lambers, H. & Colmer, T.D., editors. *Root Physiology: from Gene to Function*. Dordrecht: Springer, pp. 1-36.
- Mirdita, M., Schütze, K., Moriwaki, Y., Heo, L., Ovchinnikov, S. & Steinegger, M. (2022). ColabFold: making protein folding accessible to all. *Nature Methods*, 19, 679-682.
- Mitchum, M.G., Yamaguchi, S., Hanada, A., Kuwahara, A., Yoshioka, Y., Kato, T., Tabata, S., Kamiya, Y. & Sun, T.P. (2006). Distinct and overlapping roles of two gibberellin 3-oxidases in *Arabidopsis* development. *The Plant Journal*, 45, 804-818.
- Miyazawa, S.I., Nishiguchi, M., Futamura, N., Yukawa, T., Miyao, M., Maruyama, T.E. et al. (2018). Low assimilation efficiency of photorespiratory ammonia in conifer leaves. *Journal of Plant Research*, 131, 789-802.
- Mondal, R., Kumar, A. & Chattopadhyay, S.K. (2021). Structural property, molecular regulation and functional diversity of glutamine synthetase in higher plants: a data-mining bioinformatics approach. *The Plant Journal*, 108, 1565-1584.

REFERENCES

- Moran-Zuloaga, D., Dippold, M., Glaser, B. & Kuzyakov, Y. (2015). Organic nitrogen uptake by plants: reevaluation by position-specific labeling of amino acids. *Biogeochemistry*, 125, 359-374.
- Moreira, E., Coimbra, S. & Melo, P. (2022). Glutamine synthetase: an unlikely case of functional redundancy in *Arabidopsis thaliana*. *Plant Biology*, 24, 713-720.
- Mosca, E., Cruz, F., Gómez-Garrido, J., Bianco, L., Rellstab, C., Brodbeck, S. et al. (2019). A reference genome sequence for the European silver fir (*Abies alba* mill.): a community-generated genomic resource. *G3 (Bethesda)*, 9, 2039–2049.
- Moubayidin, L., Perilli, S., Ioio, D., Di Mambro, R. Costatino, P. & Sabatini, S. (2010). The rate of cell differentiation control the *Arabidopsis* root meristem growth phase. *Current Biology*, 20, 1138-1143.
- Muños, S., Cazettes, C., Fizames, C., Gaymard, F., Tillard, P., Lepetit, M., Lejay, L. & Gojon, A. (2004). Transcript profiling in the *chl1-5* mutant of *Arabidopsis* reveals a role of the nitrate transporter NRT1.1 in the regulation of another nitrate transporter, NRT2.1. *The Plant Cell*, 16, 2433-2447.
- Nacry, P., Bouguyon E. & Gojon A. (2013). Nitrogen acquisition by roots: physiological and developmental mechanisms ensuring plant adaptation to a fluctuating resource. *Plant Soil*, 370, 1-29.
- Näsholm, T., Kielland, K. & Ganeteg, U. (2009). Uptake of organic nitrogen by plants. *New Phytologist*, 182, 31-48.
- Neale, D.B., Wegrzyn, J.L., Stevens, K.A., Zimin, A.V., Puiu, D., Crepeau, M.W. et al. (2014). Decoding the massive genome of loblolly pine using haploid DNA and novel assembly strategies. *Genome Biology*, 15, R59.
- Neale, D.B., McGuire, P.E., Wheeler, N.C., Stevens, K.A., Crepeau, M.W., Careno, C. et al. (2017). The Douglas-Fir genome sequence reveals specialization of the photosynthetic apparatus in Pinaceae. *G3 (Bethesda)*, 7, 3157–3167.
- Nogueira, E.D., Olivares, F.L., Japiassu, J.C., Vilar, C., Vinagre, F., Baldani, J.I. et al. (2005). Characterization of glutamine synthetase genes in sugar cane genotypes with different rates of biological nitrogen fixation. *Plant Science*, 169, 819–832.

REFERENCES

- Nylander, J.A.A. (2004). MrModeltest v2. Program distributed by the author. Evolutionary Biology Centre, Uppsala University. <https://github.com/nylander/MrModeltest2>
- Nystedt, B., Street, N.R., Wetterbom, A., Zuccolo, A., Lin, Y.C., Scofield, D.G. et al. (2013). The norway spruce genome sequence and conifer genome evolution. *Nature*, 497, 579–584.
- Obara, M., Kajiura, M., Fukuta, Y., Yano, M., Hayashi, M., Yamaya, T. & Sato, T. (2001). Mapping of QTLs associated with cytosolic glutamine synthetase and NADH-glutamate synthase in rice (*Oryza sativa* L.) *Journal of Experimental Botany*, 52, 1209-1217.
- Obara, M., Sato, T., Sasaki, S., Kashiba, K., Nagano, A., Nakamura, I., Ebitani, T., Yano M. & Yamaya, T. (2004). Identification and characterization of a QTL on chromosome 2 for cytosolic glutamine synthetase content and panicle number in rice. *Theoretical and Applied Genetics*, 110, 1-11.
- Obertello, M., Krouk, G., Katari, M.S., Runko, S.J. & Coruzzi, G.M. (2010). Modeling the global effect of the basic-leucine zipper transcription factor 1 (bZIP1) on nitrogen and light regulation in *Arabidopsis*. *BMC, Systems Biology*, 4.
- O'Brien, J.A., Vega, A., Bouguyon, E., Krouk, G., Gojon, A., Coruzzi, G. & Gutiérrez, A. (2016). Nitrate transport, sensing, and responses in plants. *Molecular Plant*, 9, 837-856.
- Oliveira, I.C. & Coruzzi, G.M. (1999). Carbon and amino acids reciprocally modulate the expression of glutamine synthetase in *Arabidopsis*. *Plant Physiology*, 121, 301-309.
- One Thousand Plant Transcriptomes Initiative. (2019). One thousand plant transcriptomes and the phylogenomics of green plants. *Nature*, 574, 679–685.
- Ortega, J.L. Roche, D. & Sengupta-Gopalan, C. (1999). Oxidative turnover of soybean root glutamine synthetase. *In vitro* and *in vivo* studies. *Plant Physiology*, 119, 1483-1495.
- Ortega, J.L., Temple, S.J. & Sengupta-Gopalan, C. (2001). Constitutive overexpression of cytosolic glutamine synthetase (GS1) gene in transgenic alfalfa demonstrates that GS1 may be regulated at the level of RNA stability and protein turnover. *Plant Physiology*, 126, 109-121.
- Ortega, J.L., Moguel-Esponda, S., Potenza, C., Conklin, C.F., Quintana, A. & Sengupta-Gopalan, C. (2006). The 3' untranslated region of a soybean cytosolic glutamine synthetase (GS1)

REFERENCES

affects transcript stability and protein accumulation in transgenic alfalfa. *The Plant Journal*, 45, 832-846.

Ortega, J.L., Wilson, O.L. & Sengupta-Gopalan, C. (2012). The 5' untranslated region of the soybean cytosolic glutamine synthetase β_1 gene contains prokaryotic translation initiation signals and acts as a translational enhancer in plants. *Molecular Genetics and Genomics*, 287, 881-893.

Ortigosa, F., Valderrama-Martín, J.M., Urbano-Gámez, J.A., García-Martín, M.L., Ávila, C., Cánovas, F.M. & Cañas, R.A. (2020). Inorganic nitrogen form determines nutrient allocation and metabolic responses in maritime pine seedlings. *Plants*, 9.

Ortigosa, F., Lobato-Fernández, C., Shikano, H., Ávila, C., Taira, S., Cánovas, F.M. & Cañas, R.A. (2022). Ammonium regulates the development of pine roots through hormonal crosstalk and differential expression of transcription factors in the apex. *Plant, Cell and Environment*, 45, 915-935.

Para, A., Li, Y., Marshall-Colon, A., Varala, K., Francoeur, N.J., Moran, T.M., et al. (2014). Hit-and-run transcriptional control by bZIP1 mediates rapid nutrient signaling in *Arabidopsis*. *Proceedings of the National Academy of Sciences of the United States of America*, 111, 10371-10376.

Pascual, M.B., El-Azaz, J., de la Torre, F.N., Cañas, R.A., Ávila, C. & Cánovas, F.M. (2016). Biosynthesis and metabolic fate of phenylalanine in conifers. *Frontiers in Plant Science*, 7.

Péret, B., Swarup, K., Ferguson, A., Seth, M., Yang, Y., Dhondt, S., James, N., Casimiro, I., Perry, P., Syed, A., et al. (2012). AUX/LAX genes encode a family of auxin influx transporters that perform distinct functions during *Arabidopsis* development. *The Plant Cell*, 24, 2874-85.

Pérez-Delgado, C.M., García-Calderón, M., Márquez, A.J. & Betti, M. (2015). Reassimilation of photorespiratory ammonium in *Lotus japonicus* plants deficient in Plastidic glutamine synthetase. *PLoS One*, 10, e0130438.

Pérez-Rodríguez, M.J., Suárez, M.F., Heredia, R., Ávila, C., Breton, D., Trontin, F., et al. (2005). Expression patterns of two glutamine synthetase genes in zygotic and somatic pine embryos support specific roles in nitrogen metabolism during embryogenesis. *New Phytologist*, 169, 35-44.

REFERENCES

- Pesole, G., Bozzetti, M.P., Lanave, C., Preparata, G. & Saccone, C. (1991). Glutamine synthetase gene evolution: a good molecular clock. *Proceedings of the National Academy of Sciences of the United States of America*, 88, 522–526.
- Petricka, J.J., Winter, C.M. & Benfey, P.N. (2012). Control of *Arabidopsis* root development. *Annual Review of Plant Biology*, 63, 563-590.
- Plett, D., Garnett, T. & Okamoto, M. (2017). Molecular genetics to discover and improve nitrogen use efficiency in crop plants. In: Hossain, M.A., Kamiya, T., Burritt, D.J., Tran, L.S.P. & Fujiwara, T., editors. *Plant macronutrient use efficiency*. London: Academic Press, pp. 93-122.
- Proost, S., Van Bel, M., Vaneechoutte, D., Van de Peer, Y., Inzé, D., Mueller-Roeber, B. & Vandepoele, K. (2015). PLAZA 3.0: an Access point for plant comparative genomics. *Nucleic Acids Research*, 43, 974-981.
- Qiu, T., Qi, M., Ding, X., Zheng, Y., Zhou, T., Chen, Y., Han, N., Zhu, M., Bian, H. & Wang, J. (2020). The SAUR41 subfamily of SMALL AUXIN UP RNA genes is abscisic acid inducible to modulate cell expansion and salt tolerance in *Arabidopsis thaliana* seedlings. *Annals of Botany*, 125, 805-819.
- Qiu, X.M., Sun, Y.Y., Ye, X.Y. & Li, Z.G. (2020). Signaling role of glutamate in plants. *Frontiers in Plant Science*, 13.
- Qu J, Kang SG, Hah C, Jang JC. Molecular and cellular characterization of GA-stimulated transcripts GASA4 and GASA6 in *Arabidopsis thaliana*. *Plant Sci*. 2016 May;246:1-10.
- Raven, J.A. (2018). Evolution and palaeophysiology of the vascular system and other means of long-distance transport. *Philosophical Transactions of the Royal Society B*, 373, 20160497.
- Remans, T., Nacry, P., Pervent, M., Filleur, S., Diatloff, E., Mounier, E., Tillard, P., Forde, B.G. & Gojon A. (2006a). The *Arabidopsis* NRT1.1 transporter participates in the signaling pathway triggering root colonization of nitrate-rich patches. *Proceedings of the National Academy of Sciences of the United States of America*, 103, 19206-19211.
- Remans, T., Nacry, P., Pervent, M., Girin, T., Tillard, P., Lepetit, M. Gojon, A. (2006b). A central role for the nitrate transporter NRT2.1 in the integrated morphological and physiological responses of the root system to nitrogen limitation in *Arabidopsis*. *Plant Physiology*, 140, 909-921.

REFERENCES

- Ren, H. & Gray, W.M. (2015). SAUR proteins as effectors of hormonal and environmental signals in plant growth. *Molecular Plant*, 8, 1153-1164.
- Renault, H., Werck-Reichhart, D. & Weng, J.K. (2019). Harnessing lignin evolution for biotechnological applications. *Current Opinion in Biotechnology*, 56, 105–111.
- Rensch, D., Laloi, M., Rouhara, I., Schmelzer, E., Delrot, S. & Frommer, W.B. (1995). NTR1 encodes a high affinity oligopeptide transporter in *Arabidopsis*. *FEBS Letters*, 370, 264-268.
- Ritz, C. & Spiess, A.N. (2008). qpcR: an R package for sigmoidal model selection in quantitative real-time polymerase chain reaction analysis. *Bioinformatics*, 24, 1549–1551.
- Riveras, E., Alvarez, J.M., Vidal, E.A., Oses, C., Vega, A. & Guíérrez, A. (2015). The calcium ion is a second messenger in the nitrate signaling pathway of *Arabidopsis*. *Plant Physiology*, 169, 1397-1404.
- Robertson, D.L. & Tartar, A. (2006). Evolution of glutamine synthetase in heterokonts: evidence for endosymbiotic gene transfer and the early evolution of photosynthesis. *Molecular Biology and Evolution*, 23, 1048–1055.
- Robinson, M.D., McCarthy, D.J., and Smyth, G.K. (2010). edgeR: a Bioconductor package for differential expression analysis of digital gene expression data. *Bioinformatics*, 26, 139-140.
- Rosenblueth, M., Ormeño-Orrillo, E., López-López, A., Rogel, M.A., Reyes-Hernández, B.J., Martínez-Romero, J.C., Reddy, P.M. & Martínez-Romero E. (2018). Nitrogen fixation in cereals. *Frontiers in Microbiology*, 9.
- Ruffel, S., Krouk, G., Ristova, D., Shasha, D., Birnbaum, K.D., and Coruzzi, G.M. (2011). Nitrogen economics of root foraging: transitive closure of the nitrate-cytokinin relay and distinct systemic signaling for N supply vs. demand. *Proceedings of the National Academy of Sciences of the United States of America*, 108, 18524–18529.
- Ruffel, S., Poitout, A., Krouk, G., Coruzzi, G.M., and Lacombe, B. (2016). Long-distance nitrate signaling displays cytokinin dependent and independent branches. *Journal of Integrative Plant Biology*, 58, 226–229.

REFERENCES

- Růžička, K., Šimášková, M., Duclercq, J., Petrášek, J., Zažímalová, E., Simon, S., Friml, J., Van Montagu, M.C.E. & Benková, E. (2009). Cytokinin regulated root meristem activity via modulation of the polar auxin transport. *Proceedings of the National Academy of Sciences of the United States of America*, 106, 4284-4289.
- Sakakibara, H., Shimizu, H., Hase, T., Yamazaki, Y., Takao, T., Shimonishi, Y. & Sugiyama, T. (1996). Molecular identification and characterization of cytosolic isoforms of glutamine synthetase in maize roots. *The Journal of Biological Chemistry*, 271, 29561-29568.
- Sakakibara, H., Kobayashi, K., Deji, A. Sugiyama, T. (1997). Partial characterization of the signaling pathway for the nitrate-dependent expression of genes for nitrogen-assimilatory enzymes using detached maize leaves. *Plant and Cell Physiology*, 38, 837-847.
- Schneider, W.L. & Gifford, D.J. (1994). Loblolly pine seed dormancy. I. The relationship between protein synthesis and the loss of dormancy. *Physiologia Plantarum*, 90, 246-252.
- Schrödinger and DeLano. 2020. PyMol. <http://www.pymol.org/pymol>. Accessed August 2022.
- Scott, A.D., Zimin, A.V., Puiu, D., Workman, R., Britton, M., Zaman, S. et al. (2020). A reference genome sequence for giant Sequoia. *G3 (Bethesda)*, 10, 3907–3919.
- Seabra, A.R., Vieira, C.P., Cullimore, J.V. & Carvalho, H.G. (2010). *Medicago truncatula* contains a second gene encoding a plastid located glutamine synthetase exclusively expressed in developing seeds. *BMC Plant Biology*, 10.
- Sharma, N., Sinha, V.B., Kumar, N.A.P., Subrahmanyam, D., Neeraja, C.N., Kuchi, S., Jha, A., Parsad, R., Sitaraman, V. & Raghuram, N. (2021). Nitrogen use efficiency phenotype and associated genes: roles of germination, flowering, root growth, crop duration and yield at low N. *Frontier in Plant Science*, 11:587464
- Shatters, R.G. & Kahn, M.L. (1989). Glutamine synthetase II in rhizobium: reexamination of the proposed horizontal transfer of DNA from eukaryotes to prokaryotes. *Journal of Molecular Evolution*, 29, 422–428.
- Shin, W.H., Lee, G.R., Heo, L., Lee, H. & Seok, C. 2014. Prediction of protein structure and interaction by GALAXY protein modelin programs. *Bio Design*, 2, 1-11.

REFERENCES

- Simon, B. & Sengupta-Gopalan, C. (2010). The 3' untranslated region of the two cytosolic glutamine synthetase (GS1) genes in alfalfa (*Medicago sativa*) regulated transcript stability in response to glutamine. *Planta*, 232, 1151-1162.
- Singh, R.P. (2021). Nitrogen Nutrition in Higher Plants. Astral International Pvt. Ltd. New Delhi, India.
- Song, W., Koh, S., Czako, M., Marton, L., Drenkard, E., Becker, J.M. & Stacey, G. (1997). Antisense expression of the peptide transport gene *AtPTR2-B* delays flowering and arrests seed development in transgenic *Arabidopsis* plants. *Plant Physiology*, 114, 927-935.
- Sperschneider, J., Catanzariti, A.M., DeBoer, K., Petre, B., Gardiner, D.M., Singh, K.B. et al. (2017). LOCALIZER: subcellular localization prediction of both plant and effector proteins in the plant cell. *Scientific Reports*, 16, 44598.
- Sponseller, R.A., Gundale, M.J., Fitter, M., Ring, E., Nordin, A., Näsholm, T. Laudon, H. (2016). Nitrogen dynamics in managed boreal forests: Recent advances and future research directions. *AMBIO: a Journal of the Human Environment*, 45, 175-187.
- Stepanova, A.N., Hoyt, J.M., Hamilton, A.A. & Alonso, J.M. (2005). A link between ethylene and auxin uncovered by the characterization of two root-specific ethylene-insensitive mutants in *Arabidopsis*. *The Plant Cell*, 17, 2230-2242.
- Stepanova, A.N., Robertson-Hoyt, J., Yun, J., Benavente, L.M., Xie, D.Y., Doležal, K., Schlereth, A., Jürgens, G. & Alonso, J.M. (2008). TAA1-mediated auxin biosynthesis is essential for hormone crosstalk and plant development. *Cell*, 133, 177-191.
- Sterck, L., de María, N., Cañas, R.A., de Miguel, M., Perdiguero, P., Raffin, A., et al. (2022). Maritime Pine Genomics in Focus. In: De La Torre, A.R., editor. *The Pine Genomes. Compendium of Plant Genomes*. Springer, Cham, 67-123.
- Stevens, K.A., Wegrzyn, J.L., Zimin, A., Puiu, D., Crepeau, M., Cardeno, C. et al. (2016). Sequence of the sugar pine Megagenome. *Genetics*, 204, 1613–1626.
- Stortenbeker, N. & Bemer, M. (2019). The SAUR gene family: the plant's toolbox for adaptation of growth and development. *Journal of Experimental Botany*, 70, 17-27.

REFERENCES

- Suárez, M.F., Ávila, C., Gallardo, F., Cantón, F.R., García-Gutiérrez, A.G., Claros, M.G. & Cánovas, F.M. (2002). Molecular and enzymatic analysis of ammonium assimilation in woody plants. *Journal of experimental Botany*, 53, 891-904.
- Sueyoshi, K., Mitsuyama, T., Sugimoto, T., Kleinhofs, A., Warner, R.L. & Oji, Y. (1999). Effects of inhibitors for signaling components on the expression of the genes for nitrate reductase and nitrite reductase in excised barley leaves. *Soil Science and Plant Nutrition*, 45, 1015–1019.
- Supek, F., Bošnjak, M., Škunca, N., and Šmuc, T. (2011). REVIGO summarizes and visualizes long lists of gene ontology terms. *PloS One*, 6.
- Tabuchi, M., Sugiyama, K., Ishiyama, K., Inoue, E., Sato, T., Takahashi, H. & Yamaya, T. (2005). Severe reduction in growth rate and grain filling of rice mutants lacking OsGS1;1 a cytosolic glutamine synthetase1;1. *The Plant Journal*, 42, 641-651.
- Tal, I., Zhang, Y., Jørgensen, M.E., Pisanty, O., Barbosa, I.C.R., Zourelidou, M., et al. (2016). The *Arabidopsis* NPF3 protein is a GA transporter. *Nature Communications*, 7.
- Tamura, K., Stecher, G. & Kumar, S. (2021). MEGA11: molecular evolutionary genetics analysis version 11. *Molecular Biology and Evolution*, 38, 3022-3027.
- Taochy, C., Gaillard, I., Ipotesi, E., Oomen, R., Leonhardt, N., Zimmermann, S., et al. (2015). The *Arabidopsis* root stele transporter NPF2.3 contributes to nitrate translocation to shoots under salt stress. *The Plant Journal*, 83, 466-479.
- Tateno, Y. (1994). Evolution of glutamine synthetase genes is in accordance with the neutral theory of molecular evolution. *The Japanese Journal of Genetics*, 69, 489–502.
- Tegeder, M. & Masclaux-Daubresse, C. (2017). Source and sink mechanisms of nitrogen transport and use. *New Phytologist*, 217, 35–53.
- Thomsen, H.C., Erikson, D., Møller, I.S. & Schjoerring, J.K. (2014). Cytosolic glutamine synthetase: a target for improvement of crop nitrogen use efficiency? *Trends in Plant Science*, 19, 656–663.
- Tian, F., Yang, D.C., Meng, Y.Q., Jin, J. & Gao, G. (2020). PlantRegMap: charting functional regulatory maps in plants. *Nucleic Acids Research*, 48, D1104-D1113.

REFERENCES

- Tian, Q.Y., Sun, P., and Zhang, W.H. (2009). Ethylene is involved in nitrate-dependent root growth and branching in *Arabidopsis thaliana*. *New Phytologist*, 184, 918–931.
- Tikhonov, A. (2013). pH-dependent regulation of electron transport and ATP synthesis in chloroplast. *Photosynthesis Research*, 116, 511-534.
- Tian, T., Yue, L., Hengyu, Y., Qi, Y., Xin, Y., Zhou, D., Wenying, X., and Zhen, S. (2017). agriGO v2.0: a GO analysis toolkit for the agricultural community. *Nucleic Acids Research* 45, 122-129.
- Towbin, H., Staehelin, T. & Gordon, J. (1979). Electrophoretic transfer of proteins from polyacrylamide gels to nitrocellulose sheets: procedure and some applications. *Proceedings of the National Academy of Sciences*, 76, 4350-4354.
- Úbeda-Tomás, S., Swarup, R., Coates, J., Swarup, K., Laplaze, L., Beemster, G.T.S., Hedden, P., Bhalerao, R. & Bennet, M.J. (2008). Root growth in *Arabidopsis* requires gibberellin/DELLA signalling in the endodermis. *Nature Cell Biology*, 10, 625-628.
- Úbeda-Tomás, S., Federici, F., Casimiro, I., Beemster, G.T.S., Bhalerao, R., Swarup, r., Doerner, P., Haseloff, J. & Bennet, M.J. (2009). Gibberellin signaling in the endodermis control *Arabidopsis* root meristem size. *Current Biology*, 19, 1194-1199.
- Ugartechea-Chirino, Y., Swarup, R., Swarup, K., Péret, B., Whitworth, M., Bennett, M. & Bougourd, S. (2010). The AUX1 LAX family of auxin influx carriers is required for the establishment of embryonic root cell organization in *Arabidopsis thaliana*. *Annals of Botany*, 105, 277-89.
- Undurraga, S.F., Ibarra-Henríquez, C., Fredes, I., Álvarez, J.M. & Gutiérrez, R.A. (2017). Nitrate signaling and early responses in *Arabidopsis* roots. *Journal of Experimental Botany*, 68, 2541-2551.
- Unno, H., Uchida, T., Sugawara, H., Kurisu, G., Sugiyama, T., Yamaya, T., Sakakibara, H., Hase, T. & Kusunoki, M. (2006). Atomic structure of plant glutamine synthetase a key enzyme for plant productivity. *Journal of Biological Chemistry*, 281, 29287-29296.
- Urriola, J. & Rathore, K.S. (2015). Overexpression of a glutamine synthetase gene affects growth and development in sorghum. *Transgenic Research*, 24, 397-407.

REFERENCES

- Valderrama-Martín, J.M., Ortigosa, F., Ávila, C., Cánovas, F.M., Hirel, B., Cantón, F.R. & Cañas, R.A. (2022). A revised view on the evolution of glutamine synthetase isoenzymes in plants. *The Plant Journal*, 110, 946-960.
- Valpuesta, J.M. (2006). The three-dimensional structure of an eukaryotic glutamine synthetase: Functional implications of its oligomeric structure. *Journal of Structural Biology*, 156, 469-479.
- Van den Driessche R. (1971). Response of conifer seedlings to nitrate and ammonium sources of nitrogen. *Plant and Soil*, 34, 421-439.
- Varadi, M., Anyango, S., Deshpande, M., Nair, S., Natassia, C., Yordanova, G., et al. (2022). AlphaFold protein structure database: massively expanding the structure coverage of protein-sequence space with high-accuracy models. *Nucleic Acids Research*, 50, D439-D444.
- Verma, V., Ravindran, P. & Kumar, P.P. (2016). Plant hormone-mediated regulation of stress responses. *BMC Plant Biology*, 14, 16-86.
- Verzeaux, J., Hirel, B., Dubois, F., Lea, P.J. & Tétu T. (2017). Agricultural practices to improve nitrogen use efficiency through the use of arbuscular mycorrhizae: Basic and agronomic aspects. *Plant Science*, 264, 48-56.
- Villalobos, D.P. (2008). Aproximación genómica al estudio de la formación de la madera en los pinos. Universidad de Málaga, Málaga (Spain). Doctoral dissertation.
- von Wirén, N., Gazzarrini, S., Gojon, A. & Frommer, W.B. (2000). The molecular physiology of ammonium uptake and retrieval. *Current Opinion in Plant Biology*, 3, 254-261.
- von Wittgenstein, N.J.J.B., Le, C.H., Hawkins, B.J. & Ehrling, J. (2014). Evolutionary classification of ammonium, nitrate, and peptide transporters in land plants. *BMC Evolutionary Biology*, 14.
- Wallsgrave, R.M., Turner, J.C., Hall, N.P., Kendall, A.C. & Bright, S.W. (1987). Barley mutants lacking chloroplast glutamine synthetase-biochemical and genetic analysis. *Plant Physiology*, 83, 155-158.
- Wan, T., Liu, Z.M., Li, L.F., Leitch, A.R., Leitch, I.L., Lohaus, R. et al. (2018). A genome for gnetophytes and early evolution of seed plants. *Nature Plants*, 4, 82-89.

REFERENCES

- Wang, H., Wan, Y., Buchner, P., King, R., Ma, H. & Hawkesford, M.J. (2020). Phylogeny and gene expression of the complete NITRATE TRANSPORTERS 1/PEPTIDE TRANSPORTERS FAMILY in *Triticum aestivum*. *Journal of Experimental Botany*, 71, 4531-4546.
- Wang, R., Tischner, R., Gutierrez, R.A., Hoffman, M., Xing, X., Chen, M., Coruzzi, G., and Crawford, N.M. (2004). Genomic analysis of the nitrate response using a nitrate reductase-null mutant of *Arabidopsis*. *Plant Physiology*, 136, 2512–2522.
- Wang, Y.Y., Hsu, P.K. & Tsay, Y.F. (2012). Uptake, allocation and signaling of nitrate. *Trends in Plant Science*, 17, 458-467.
- Wang, Y.Y., Cheng, Y.H., Chen, K.E. & Tsay, Y.F. (2018). Nitrate transport, signaling and use efficiency. *Annual Review of Plant Biology*, 68, 85-122.
- Ward, B.B. (2008). Nitrification. In: Jørgensen, S.E. & Fath, B.D., editors. *Encyclopedia of Ecology*. Amsterdam: Elsevier Science, pp. 2511–2518.
- Warren, C.R. & Adams, M.A. (2002). Possible causes of slow growth of nitrate-supplied *Pinus pinaster*. *Canadian Journal of Forest Research*, 35, 569-580.
- Watanabe, A., Takagi, N., Hayashi, H., Chino, M. & Watanabe, A. (1997). Internal Gln/Glu ratio as a potential regulatory parameter for the expression of a cytosolic glutamine synthetase gene of radish in cultured cells. *Plant and Cell Physiology*, 38, 1000-1006.
- Wedler, F.C. & Horn, B.R. (1976). Catalytic mechanisms of glutamine synthetase enzymes. Studies with analogs of possible intermediates and transition states. *Journal of Biological Chemistry*, 251, 7530-7538.
- Wei, Y., Xiong, S., Zhang, Z., Meng, X., Wang, L., Zhang, X., Yu, M., Yu, H., Wang, X. & Ma, X. (2021). Localization, gene expression, and functions of glutamine synthetase isoenzymes in wheat grain (*Triticum aestivum* L.). *Frontiers in Plant Science*, 12.
- Wu, C.S., Chaw, S.W. & Huang, Y.Y. (2013). Chloroplast Phylogenomics indicates that *Ginkgo biloba* is sister to cycads. *Genome Biology & Evolution*, 5, 243–254.
- Wudick, M.M., Portes, M.T., Michard, E., Rosas-Santiago, P., Lizzio, M.A., Nunes, C.O., et al. (2018). CORNICHON sorting and regulation of GLR channels underlie pollen tube Ca²⁺ homeostasis. *Plant Science*, 360, 533-536.

REFERENCES

- Xu, G., Fan, X. & Miller, A.J. (2012). Plant nitrogen assimilation and use efficiency. *Annual Review of Plant Biology*, 63, 153–182.
- Xu, W., Jia, L., Shi, W., Liang, J., Zhou, F., Li, Q. & Zhang, J. (2013). Abscisic acid accumulation modulated auxin transport in the root tip to enhance proton secretion for maintaining root growth under moderate water stress.
- Xuan, W., Beeckman, T. & Xu, Guohua. Plant nitrogen nutrition: sensing and signaling. *Current Opinion in Plant Biology*, 39, 57-65.
- Yadav, S.K. (2009). Computational structural analysis and kinetic studies of a cytosolic glutamine synthetase from *Camellia sinensis* (L.) O. Kuntze. *Protein Journal*, 28, 428-434.
- Yamaya, T. & Kusano, M. (2014). Evidence supporting distinct functions of three cytosolic glutamine synthetases and two NADH-glutamate synthases in rice. *Journal of Experimental Botany*, 65, 5519-5525.
- Yoneyama, T. & Suzuki, A. (2019). Exploration of nitrate-to-glutamate assimilation in non-photosynthetic roots of higher plants by studies of ¹⁵N-tracing, enzymes involved, reductant supply, and nitrate signalin: a review and synthesis. *Plant Physiology and Biochemistry*, 136, 245-254.
- Zhang, S.C. & Wang, X.J. (2008). Expression pattern of GASA, downstream genes of DELLA, in *Arabidopsis*. *Plant Development Biology*, 53, 3839-3846.
- Zhang, G.B., Yi, H.Y. & Gong, J.M. (2014). The Arabidopsis ethylene/jasmonic acid-NRT signaling module coordinates nitrate reallocation and the trade-off between growth and environmental adaptation. *The Plant Cell*, 26, 3984-3998.
- Zhao, W., Yang, J., Tian, Y., Fu, X., Zhu, B., Xue, Y., Gao, J., Han, H.J., Peng, R. & Yao, Q.H. (2014). Expression, purification, and characterization of recombinant mangrove glutamine synthetase. *Molecular Biology Reports*, 41, 7575-7583.
- Zhao, Y. (2012). Auxin biosynthesis: a simple two-step pathway converts tryptophan to indole-3-acetic acid in plants. *Molecular Plant*, 5, 334–338.

REFERENCES

Zheng, D., Han, X., An, Y.I., Guo, H., Xia, X. & Yin, W. (2013). The nitrate transporter NRT2.1 functions in the ethylene response to nitrate deficiency in *Arabidopsis*. *Plant, Cell and Environment*, 36, 1328–1337.

Zhong, C., Xu, H., Ye, S., Wang, S., Li, L., Zhang, S. & Wang, X. (2015). Gibberellic acid-stimulated *Arabidopsis* serves as an integrator of gibberellin, abscisic acid, and glucose signaling during seed germination in *Arabidopsis*. *Plant Physiology*, 2015, 3, 2288-2303.

Zhou, J.Y., Hao, D.L. & Yang, G.Z. (2021). Regulation of cytosolic pH: the contributions of plant plasma membrane H⁺-ATPases and multiple transporters. *International Journal of Molecular Sciences*, 22.

Zimin, A., Stevens, K.A., Crepeau, M.W., Holtz-Morris, A., Koriabine, M., Marçais, G. et al. (2014). Sequencing and assembly of the 22-gb loblolly pine genome. *Genetics*, 196, 875–890.

Zoghbi-Rodríguez, N.M., Gamboa-Tuz, S.D., Pereira-Santana, A., Rodríguez-Zapata, L.C., Sánchez-Teyer, L.F. & Echevarría-Machado, I. (2021). Phylogenomic and microsynteny analysis provides evidence of genome arrangements of high-affinity nitrate transporter gene families of plants. *International Journal of molecular Sciences*, 22.

Appendix

Appendix 1

Inorganic Nitrogen Form Determines Nutrient Allocation and Metabolic Responses in Maritime Pine Seedlings

Francisco Ortigosa 1,† , José Miguel Valderrama-Martín 1,† , José Alberto Urbano-Gámez 1, María Luisa García-Martín 2, Concepción Ávila 1 , Francisco M. Cánovas 1 and Rafael A. Cañas 1,*

1 Grupo de Biología Molecular y Biotecnología, Departamento de Biología Molecular y Bioquímica, Universidad de Málaga, Campus Universitario de Teatinos, 29071 Málaga, Spain; fortigosa@uma.es (F.O.); jmvalderrama@uma.es (J.M.V.-M.); alburb@uma.es (J.A.U.-G.); cavila@uma.es (C.Á.); canovas@uma.es (F.M.C.)

2 BIONAND, Centro Andaluz de Nanomedicina y Biotecnología, Junta de Andalucía, Universidad de Málaga, 29590 Málaga, Spain; mlgarcia@bionand.es

* Correspondence: rcanas@uma.es; Tel.: +34-952-13-4272

† These authors contributed equally to this work.

Abstract: Nitrate and ammonium are the main forms of inorganic nitrogen available to plants. The present study aimed to investigate the metabolic changes caused by ammonium and nitrate nutrition in maritime pine (*Pinus pinaster* Ait.). Seedlings were grown with five solutions containing different proportions of nitrate and ammonium. Their nitrogen status was characterized through analyses of their biomass, different biochemical and molecular markers as well as a metabolite profile using ¹H-NMR. Ammonium-fed seedlings exhibited higher biomass than nitrate-fed seedlings. Nitrate mainly accumulated in the stem and ammonium in the roots. Needles of ammonium-fed seedlings had higher nitrogen and amino acid contents but lower levels of enzyme activities related to nitrogen metabolism. Higher amounts of soluble sugars and L-arginine were found in the roots of ammonium-fed seedlings. In contrast, L-asparagine accumulated in the roots of nitrate-fed seedlings. The differences in the allocation of nitrate and ammonium may function as metabolic buffers to prevent interference with the metabolism of photosynthetic organs. The metabolite profiles observed in the roots suggest problems with carbon and nitrogen assimilation in nitrate-supplied seedlings. Taken together, this new knowledge contributes not only to a better understanding of nitrogen metabolism but also to improving aspects of applied mineral nutrition for conifers.

Keywords: *Pinus pinaster*; nutrition; nitrate; ammonium; nitrogen use efficiency (NUE)

1. Introduction

Nitrogen (N) is an essential element for life because it is a main constituent of biomolecules such as nucleic acids, proteins, chlorophylls, and hormones [1]. For plants, N is the main limiting nutrient due to the high amount that is needed to maintain sustained growth and its low availability in soil [2]. Although molecular dinitrogen is highly abundant in the atmosphere, it is not directly available to plants because it can only be assimilated by plant species in symbiosis with diazotrophic bacteria [2]. In the soil, there are different organic and inorganic forms of N that can be incorporated by plants. Nevertheless, the amount and proportions of these N molecules change depending on the climate and soil conditions as well as biological competition such as the decrease of soil nitrification caused by secondary metabolites from plant root exudates that inhibit the growth of nitrifying microorganisms [3].

The main forms of inorganic N that are available to plants in soil are ammonium and nitrate [4]. Their relative abundances in the soil have an important relationship because of the nitrification performed by microorganisms in the rhizosphere [5]. Ammonium is the initial substrate of the nitrification process, which is carried out under aerobic conditions and depends on temperature and pH [6]. Overall, plants tolerate or prefer different inorganic N forms depending on the soil in which they are grown. Most crops are adapted to temperate climates, so they grow well with N in the form of nitrate. Due to the economic importance of this fact, nitrate plant nutrition has been widely studied and is quite well understood [7–9]. The strong dependence of crop yield on N supply causes large amounts of N fertilizers to be applied to agricultural soils. This is economically and environmentally costly because it increases production costs and promotes environmental problems [8]. However, plants that are adapted to soils with low nitrification rates, such as rice or conifers, prefer or tolerate ammonium nutrition [10].

The assimilation of N into organic molecules always requires that N be in the form of ammonium. Thus, nitrate is reduced by nitrate reductase (NR, EC 1.7.1.1) using reduced nicotinamide adenine dinucleotide (NADH) and producing nitrite in the cytosol. Nitrite is toxic and quickly reduced in plastids by nitrite reductase (NiR, EC 1.7.2.1) using six molecules of reduced ferredoxin to produce ammonium. Nitrate reduction is a highly energy-consuming process that, depending on the plant species, takes place in the shoots or in the roots. The energy for the process comes from photosynthesis and is mainly expended in the NiR reaction. NiR employs ferredoxin that is directly reduced by the photosynthetic electron transport chain in photosynthetic tissues or is indirectly reduced by NADPH

(reduced nicotinamide adenine dinucleotide phosphate): ferredoxin oxidoreductase (EC 1.18.1.2) in the amyloplasts of non-photosynthetic tissues using NADPH obtained from the photoassimilates that are transported from shoots to roots [1]. Ammonium is assimilated by the glutamine synthetase (GS, EC 6.3.1.2) /glutamate synthase (GOGAT, NADH-dependent EC 1.4.1.14; ferredoxin-dependent EC 1.4.7.1) cycle. GS produces glutamine from glutamate and ammonium expending one molecule of adenosine triphosphate (ATP). Glutamine is used by GOGAT with 2-oxoglutarate to produce two molecules of glutamate using the reduction power of NADH or ferredoxin depending on the enzyme isoform. One glutamate molecule feeds the cycle and the other is the net product of the cycle. ferredoxin-GOGAT is mainly expressed in photosynthetic tissues, while NADH-GOGAT is more highly expressed in non-photosynthetic tissues [11]. In angiosperms and ginkgo, there is usually one gene encoding GS localized in the chloroplasts, GS2, and several genes encoding cytosolic isoforms, called GS1 [12]. GS2 and ferredoxin-GOGAT act in the photosynthetic tissues and have important roles in the re-assimilation of ammonium released during photorespiration and the assimilation of ammonium from nitrate reduction [13]. GS1 and NADH-GOGAT manage the assimilation of N in roots and the reallocation of N in different metabolic and physiological processes such as senescence, fruit filling or stress responses [12,14,15]. All N compounds in plants are derived from the glutamine and glutamate produced in this cycle mainly through aminotransferase reactions [1].

Nitrate can be stored in plant vacuoles until its use without causing problems [16]. Nitrate is preferentially accumulated in different organs depending on the species and is remobilized from vacuoles to be reduced under adequate light conditions when photosynthesis is active because nitrate reduction is coupled to photosynthetic energy production [17]. However, excessive amounts of ammonium are toxic for most plant species even if large amounts of ammonium can be stored in the vacuoles [18]. Among the symptoms caused by ammonium excess there are chlorosis, growth suppression, yield depression, declines in cations such as potassium, calcium, and magnesium, increases in amino acids, and decreases in dicarboxylic acids such as malic acid, etc. [10].

Conifers are trees with long lifespans and life cycles, most of which have perennial leaves. Conifers cover vast areas of planet Earth. This confers extraordinary ecological importance to these plants because their forests are widely extended ecosystems, mainly located in the Northern Hemisphere [19]. Additionally, they represent a remarkable source of raw materials, such as wood or resin, for human use. Sustainable forest management is essential for obtaining adequate yields of these biomaterials

while also conserving these ecosystems. As for all other plants, N is essential for conifer growth [20]. Most conifers prefer ammonium as the main inorganic N form for their growth [10,21,22]. This preference could be linked to the photorespiration process. It has been observed that pine saplings fed with nitrate as their sole N source grew slowly under high atmospheric CO₂ concentrations and showed low photorespiration rates under normal or low atmospheric CO₂ concentrations [23]. Interestingly, conifers have no GS2; rather, they have a cytosolic isoform, GS1a, in their photosynthetic tissues that has roles similar to those of GS2, including re-assimilation of ammonium released from photorespiration [14,24].

Maritime pine (*Pinus pinaster* Ait.) is a conifer tree from the southwestern Mediterranean region with great environmental and economic importance in France, Portugal, and Spain. However, it is also cultured and utilized in other regions. In some cases, it has become an invasive species, particularly in South Africa [25]. This species grows better with ammonium than with nitrate nutrition [20]. Despite its high phenotypic plasticity and high tolerance to abiotic stresses [26,27], this tree is adapted to live in temperate regions where conditions favor soil nitrification, at least during the warm seasons. Additionally, maritime pine has a complete set of transporters related to nitrate transport, including at least 40 members of the Nitrate Transporter 1/Peptide Transporter family (NPF) and 2 members of the Nitrate Transporter 2 family (NRT2), and an expanded family of nitrate transport regulators, 6 NRT3 [28]. The characterization of the response to inorganic nitrogen nutrition is of paramount importance to understand the development of plants, including trees, which have long life cycles. The aim of the present work is to determine the metabolic changes that the inorganic N form, nitrate or ammonium, causes in maritime pine seedlings. The main goals are to determine the differences in the incorporation rates of two inorganic nitrogen forms (nitrate/ammonium) and to analyze the effects that both nitrogen forms have on the growth and metabolism of pine seedlings, providing information that may serve as a precedent for future works on nitrogen nutrition in maritime pine and conifers.

2. Results

2.1. Biomass Accumulation and Seedling N Content in Response to Ammonium and Nitrate Supply

The main goal of the present work was to evaluate the effect of the inorganic N form on maritime pine seedlings. Five different nutritional conditions were tested (Figure 1), all with a total N concentration of 8 mM but with different proportions of ammonium and nitrate (8/0 mM; 6/2 mM; 4/4 mM; 2/6 mM; and 0/8 mM, respectively). The first and most obvious effect of the different N sources was the differential biomass accumulation among

seedlings (Figure 1a,b). Biomass decreased with the increase in nitrate content in the supplied solution, which was statistically significant in the case of seedlings fed with 8 mM nitrate. However, this effect was mainly caused by the root biomass where there were significant differences among seedlings. No differences among treatments were found in needle and stem biomass. This caused the root:shoot ratios to be significant higher in the seedlings supplied with more ammonium (Figure 1c). The water content was clearly higher in the roots than in the rest of the organs (Figure 1d). There were some differences in the water content between treatments in stem and roots with a slight tendency of a lower water content in the seedlings supplied only with nitrate.

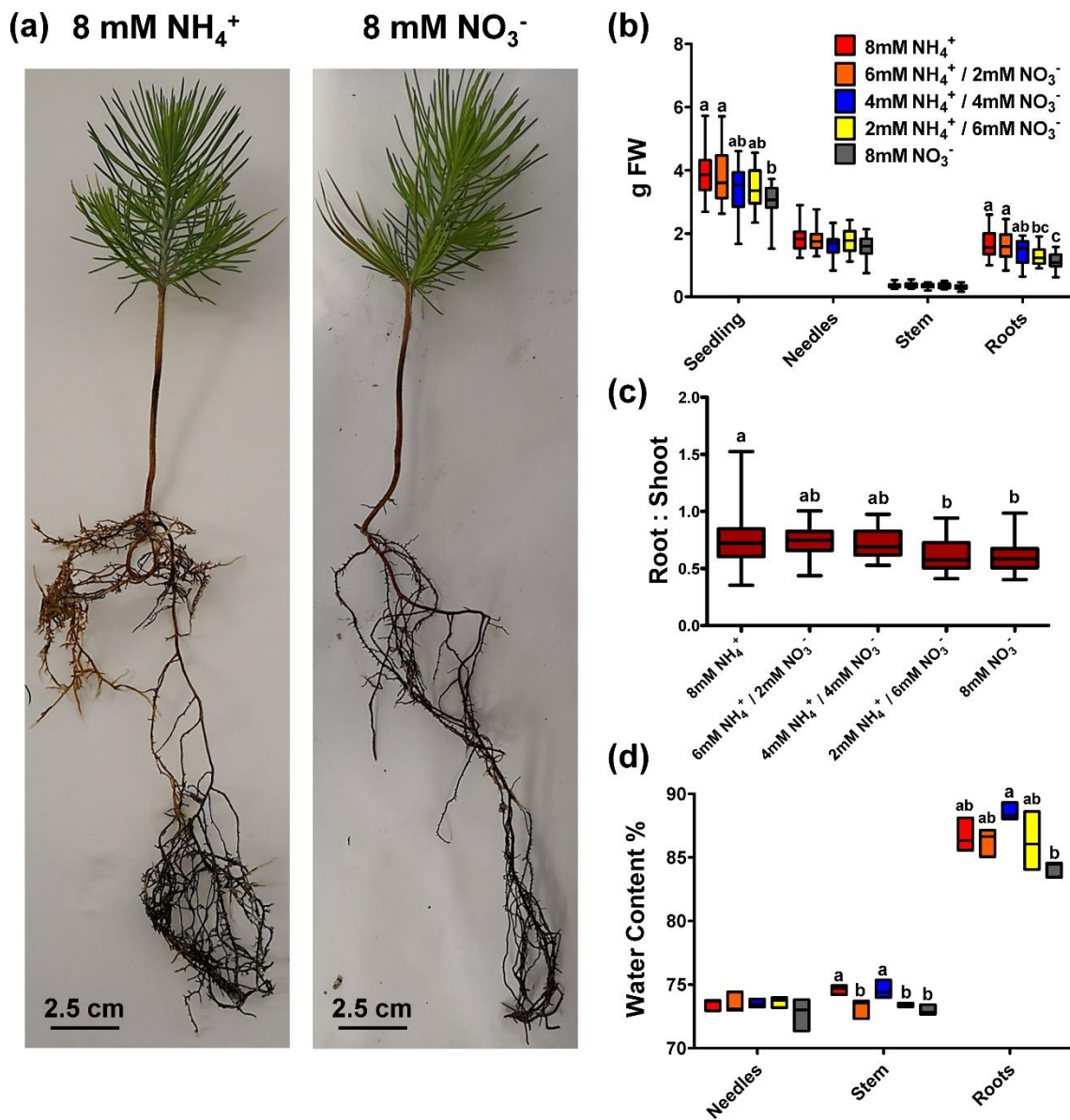


Figure 1. Biomass accumulation, root:shoot ratio, and water content in the different organs (needles, stem, and roots) of pine seedlings under the nutrient treatments. (a) Photographs of two seedlings (stem, and roots) of pine seedlings under the nutrient treatments. (a) Photographs of two seedlings after treatment with 8 mM ammonium and 8 mM nitrate; (b) Biomass accumulation in the whole after treatment with 8 mM ammonium

APPENDIX

and 8 mM nitrate; (b) Biomass accumulation in the whole seedling and the different organs (needles, stem, and roots); (c) Root:shoot ratio; (d) Water content. seedling and the different organs (needles, stem, and roots); (c) Root:shoot ratio; (d) Water content. Red columns correspond to 8 mM+NH₄⁺ supply; orange columns correspond to 6 mM+ NH₄⁺/2 mM⁻ columns correspond to 8 mM NH₄ supply; orange columns correspond to 6 mM NH₄ /2 mM NO₃ NO₃⁻ supply; blue columns correspond to 4 mM N+H₄⁺/4 mM NO₃⁻ supply; yellow columns correspond supply; blue columns correspond to 4 mM NH₄ /4 mM NO₃ supply; yellow columns correspond to 2 mM NH₄⁺/6 mM NO₃⁻ supply; grey columns correspond to 8 mM NO₃⁻ supply. Significant to 2 mM NH + /6 mM NO - supply; grey columns correspond to 8 mM NO - supply. Significant differences were determined with a one-way ANOVA for each organ or entire seedling. Letters above differences were determined with a one-way ANOVA for each organ or entire seedling. Letters above the columns show significant differences based on a Newman-Keuls post-hoc test ($p < 0.05$). Boxplots the columns show significant differences based on a Newman-Keuls post-hoc test ($p < 0.05$). Boxplots show minimum, maximum, and median values with $n = 6$ for biomass and root:shoot ratio. Error bars show minimum, maximum, and median values with $n = 6$ for biomass and root:shoot ratio. Error bars show SE with $n = 3$. FW corresponds to fresh weight.

Ammonium mainly accumulated in the roots of the pine seedlings (Figure 2a). There were significant differences between ammonium-fed and nitrate-fed seedlings in every organ; these differences were most evident in the roots where there was 3 times more ammonium in the seedlings fed only ammonium than in those fed only nitrate. When the ammonium and nitrate contents were compared, the ammonium levels were higher in almost every case except in the stems of plants supplied with more nitrate (Figure 2a,b). The differences were more evident in the roots where the ammonium content was between 30-10 $\mu\text{mol g}^{-1}$ dry weight (DW) and the nitrate content was approximately 1-2 $\mu\text{mol g}^{-1}$ DW. There were no significant differences in the nitrate content among treatments, although there was a tendency for seedlings supplied with higher amounts of nitrate to accumulate nitrate in their stems (Figure 2b). However, there was an evident partitioning of nitrate accumulation between organs, with nitrate accumulation being higher in stems than in roots (nearly four times higher) and not being detected in needles. The form of inorganic N did not have an evident effect on the N content in the different organs (Figure 2c). The only significant differences were that the N content in the needles was higher in the seedlings supplied with higher amounts of ammonium (Figure 2c). In the rest of the organs, no significant differences were observed, though the N content was generally lower in the seedlings fed only nitrate. The patterns above resulted in significant differences in the carbon:nitrogen (C:N) ratios in the needles, which were higher in the seedlings supplied with more nitrate. There were no significant differences in the C:N ratios in the rest of the organs, although the ratio was slightly higher in the seedlings fed only nitrate (Figure 2d). This is the ratio was slightly higher in the seedlings fed only

nitrate (Figure 2d). This is because there were no significant differences in the carbon (C) content among the seedlings. The no significant differences in the carbon (C) content among the seedlings. The nitrogen use efficiency (NUE) reflects differences among treatments in N uptake (Figure 2i) but not (NUE) reflects differences among treatments in N uptake (Figure 2i) but not in N utilization (Figure 2h). in N utilization (Figure 2h). The nitrogen utilization efficiency (NUE) was slightly higher in seedlings supplied with more nitrate, while the nitrogen uptake efficiency (NUE) tended to be higher in seedlings fed with more ammonium, seedlings fed with more ammonium, with significant differences from the seedlings only supplied with nitrate.

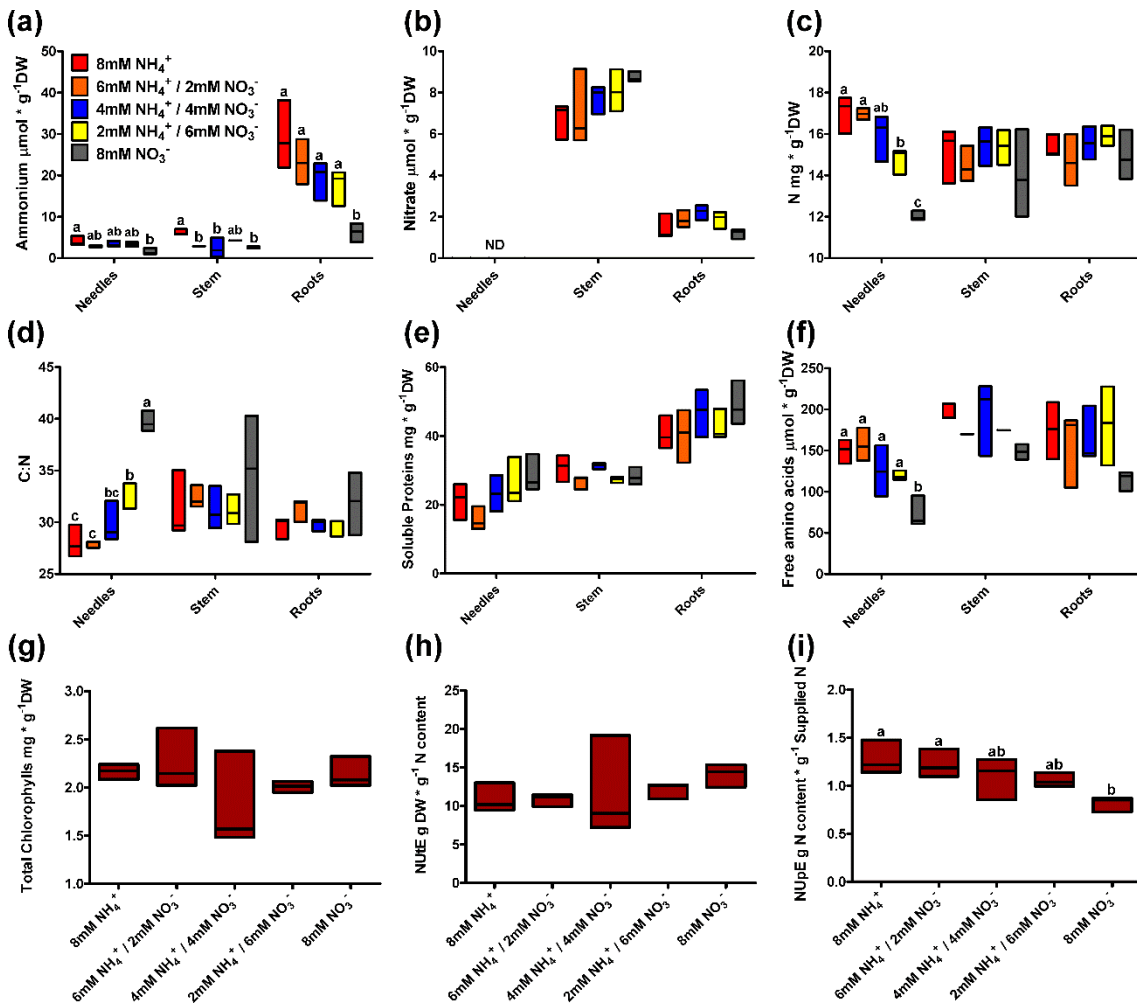


Figure 2. Profiles of plant N status markers in different organs (needles, stem, and roots) of pine seedlings under the nutrient treatments. (a) Ammonium content; (b) Nitrate content; (c) N content; (d) C:N ratio; (e) seedlings under the nutrient treatments. (a) Ammonium content; (b) Nitrate content; (c) N content; Soluble protein content; (f) Total

free amino acid content; (g) Total chlorophyll content in pine seedling (d) C:N ratio; (e) Soluble protein content; (f) Total free amino acid content; (g) Total chlorophyll content needles; (h) Nitrogen utilization efficiency (NUtE) in the seedlings under the different treatments; (i) in pine seedling needles; (h) Nitrogen utilization efficiency (NUtE) in the seedlings under the different Nitrogen uptake efficiency (NUpE) in the seedlings under the different treatments. Red columns correspond to 8 mM NH₄ supply; orange columns correspond to 6 mM NH₄ /2 mM NO₃ supply; blue columns correspond to 8 mM NH₄ supply; orange columns correspond to 6 mM NH₄ /2 mM NO₃ supply; blue columns correspond to 4 mM NH₄ /4 mM NO₃ supply; yellow columns correspond to 2 mM NH₄ /6 mM supply; blue columns correspond to 4 mM NH₄ /4 mM NO₃ supply; yellow columns correspond 2 mM NH₄ /6 mM NO₃ supply; grey columns correspond to 8 mM NO₃ supply. Significant differences were determined with a one-way ANOVA for each organ or entire seedling. Letter above the columns show significant differences based on a Newman-Keuls post-hoc test ($p < 0.05$). Error bars show SE with $n = 3$.

Additionally, different indicators of the N status that are usually considered N sinks were measured. Soluble proteins and total chlorophylls are two good markers of the N content [2]. In the present work, there were no significant differences in these two parameters among the nutrient treatments (Figure 2g,e). However, soluble proteins tended to accumulate more in needle and root samples from seedlings fed with higher amounts of nitrate (Figure 2e). An additional analyzed N marker was the free amino acid content (Figure 2f). In the needles, significantly lower levels of amino acids were detected when the plants were supplied only with nitrate than when the plants were grown under the other conditions. No significant differences were observed in the amino acid levels of the stems and roots among the different treatments, although there was a tendency for plants supplied only with nitrate to accumulate lower levels of amino acids.

2.2. ¹⁵N-labeled Ammonium and Nitrate Uptake

Considering the results for NU_pE, the N uptake was analyzed with ¹⁵N-labeled ammonium and nitrate (Figure 3). One-month-old seedlings were fed with 7.5 mM of ¹⁵N-labeled ammonium or nitrate. The N incorporation was determined through the measurement of the ¹⁵N content in the different organs. As expected, ¹⁵N accumulation was much higher in the roots than in the other organs (Figure 3a–c). In every organ, the ¹⁵N incorporation during the first 30 min was higher in nitrate-fed seedlings than in ammonium-fed seedlings. From the first hour, there was an inversion of this trend, with higher ¹⁵N incorporation in the ammonium seedlings. This was due to an increase in ¹⁵N accumulation from 30 min to 2 h, although the amount in stems and roots was stable from 2 h to the end of the experiment in the ammonium-fed seedlings, and the ¹⁵N content stabilized in seedlings fed with nitrate (Figure 3a–c,g). This was statistically significant in roots and in whole seedlings, although the profiles were similar for every organ. The ¹⁵N incorporation rate was very high for the

first 15 min in nitrate-fed seedlings, followed by an extreme decrease in the ^{15}N incorporation until the end of the experiment (Figure 3h). For the ammonium condition, the incorporation rate increased from 15 min to one hour, maintaining its value until 2 h and decreasing to minimum levels at the end of the assay (Figure 3h). The distribution of ^{15}N was analyzed using the percentage of ^{15}N in each organ with respect to the total ^{15}N in the seedlings (Figure 3d–f). In the needles and stems, the percentages of ^{15}N were higher in nitrate seedlings than in ammonium seedlings from 15 and 30 min to the final point, although the difference was only significant in needles. However, these percentages were inverse in the roots, being higher in ammonium-fed seedlings than in nitrate-fed seedlings at every time point.

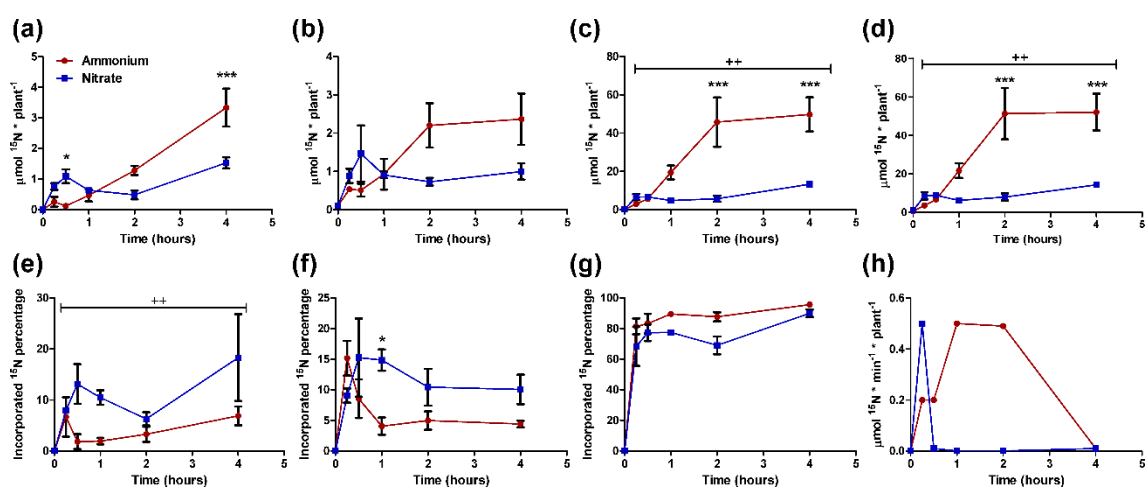


Figure 3. ^{15}N incorporation in different organs (needles, stem, and roots) of pine seedlings under the two nutrient treatments. The red line corresponds to 7.5 mM ^{15}N -labeled ammonium. The blue line corresponds to 7.5 mM ^{15}N -labeled nitrate. ^{15}N amount in needles (a); stems (b); roots (c); and the whole seedling (g). Percentage of ^{15}N contained in needles (d); stems (e); and roots (f) with respect to whole seedling. ^{15}N Incorporation rate in the seedling (h). Differences between treatments were determined with a two-way ANOVA. Significant differences are indicated with crosses crosses (++ at $p < 0.01$). Differences between treatments in each individual time point were determined with a Bonferroni post-hoc test. Significant differences are indicated with asterisks on top of the columns: * at columns: * at $p < 0.05$; ** at $p < 0.01$, *** at $p < 0.001$. Error bars show SE with $n = 3$.

2.3. Enzyme Activity and Gene Expression Profiles

Some of the enzymatic activities and the expression levels of genes coding for the main actors in N metabolism were measured in the present work (Figure 4). GS activity was higher in needles than in stems and roots (by 2–3 times) (Figure 4a). In needles, GS activity was significantly higher only in the nitrate-fed seedlings and tended to increase with the

nitrate supply. The opposite effect was observed in the stem, with a significant decrease in GS activity in the 8 mM nitrate treatment and a tendency to decrease with the nitrate supply. The different treatments did not have a clear effect on glutamate dehydrogenase (GDH) activity, although in the stems, there were significant differences (Figure 4b). The GDH activity increased from the top to the bottom of the seedlings. There was a slight and not statistically significant increase in GDH activity in the needles in parallel to the increase in the nitrate supply. Alanine and aspartate aminotransferase (AspAT and AlaAT, respectively) activities increased from the needles to the roots and were, in general, significantly higher under the conditions with more nitrate, except for the AspAT activity in the roots where no significant differences were observed (Figure 4c,d).

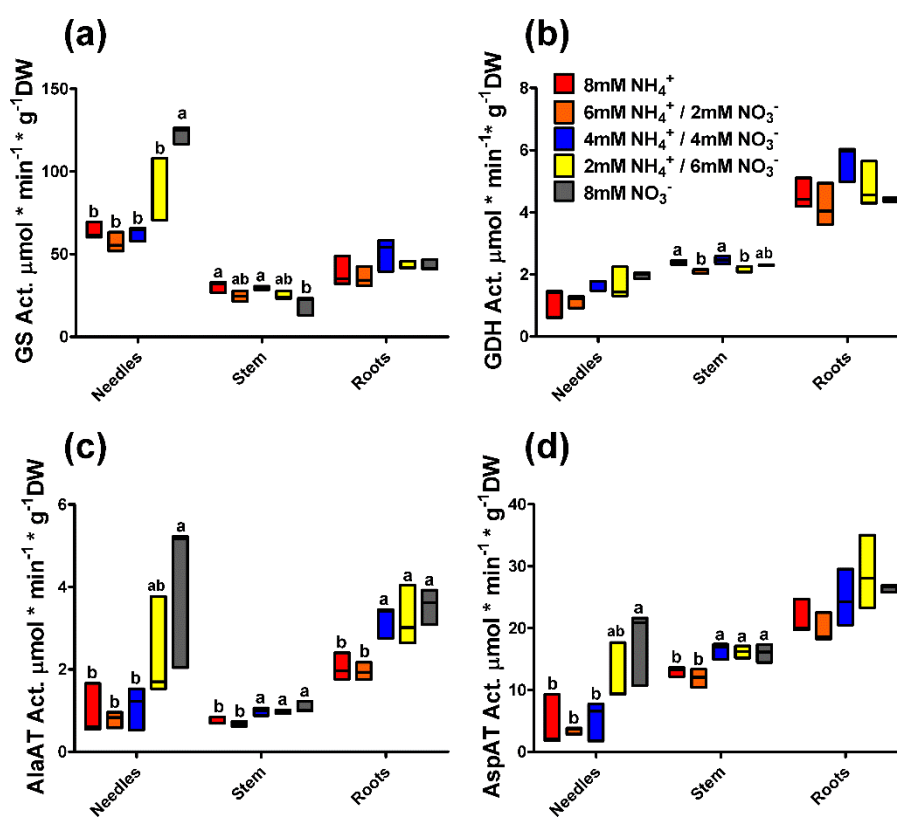


Figure 4. Enzyme activity in the different organs (needles, stem, and roots) of pine seedlings under the nutrient treatments. (a) glutamine synthetase (GS, EC 6.3.1.2) activity; (b) Glutamate dehydrogenase (GDH, EC 1.3.1.3) activity; (c) Alanine aminotransferase (AlaAT, EC 2.6.1.2) activity; (d) Aspartate aminotransferase (AspAT, EC 2.6.1.1) activity. Red columns correspond to 8 mM NH₄⁺ supply; orange columns correspond to 6 mM NH₄⁺/2 mM NO₃⁻ supply; blue columns correspond to 4 mM NH₄⁺/4 mM NO₃⁻ supply; yellow columns correspond to 2mM NH₄⁺/6 mM NO₃⁻ supply; grey columns correspond to 8 mM NO₃⁻ supply. Significant differences were determined with one-way ANOVA for each organ or entire seedling. Letters above the columns show significant differences based on Newman-Keuls post-hoc test ($p < 0.05$). Error bars show SE with $n = 3$.

The expression of the gene encoding nitrate reductase (PpNR) was mainly observed in the needles and roots and was very low in the stems (Figure 5a). In roots, PpNR expression was significantly lower in plants under 8mM nitrate supply, with the highest expression in the roots of seedlings under 8mM ammonium. The expression profile of the gene encoding nitrite reductase (PpNiR) was similar to that of PpNR, with two exceptions, the expression in needles was low in comparison to that in roots, and the differences in the roots between treatments were not significant, although the profile was the same as that for PpNR expression (Figure 5b). The expression of both GS genes, PpGS1a and PpGS1b, had no significant differences among treatments (Figure 5c,d). PpGS1a was mainly expressed in the needles, while PpGS1b was expressed in all the organs, especially in the roots, where the levels were twice those in the needles and stems. The expression profile of the gene encoding ferredoxin-dependent glutamate synthase (PpNADH-GOGAT) among organs were similar to those observed for PpGS1b, with higher levels in the roots than in the other organs (Figure 5f). Additionally, the expression of PpNADH-GOGAT in the stems changed significantly among the treatments; the highest expression was observed in the seedlings with 6 mM ammonium/2 mM nitrate. Lower expression was observed in the seedlings with 8 mM ammonium and 8 mM nitrate with a tendency to diminish its expression with the increase in the nitrate supply. Furthermore, the expression levels of genes encoding enzymes involved in the first use of assimilated N in the form of glutamate were analyzed, i.e., aspartate aminotransferase (PpAspAT), alanine aminotransferase (PpAlaAT), and glyoxylate-glutamate aminotransferase (PpGGT). For all three pine PpAspAT genes, there was no clear expression profile related to the nutritional treatments, although in most of the cases, the expression level in 8 mM ammonium-fed seedlings was the lowest (Figure 5g-i). Only PpAspAT1 expression in the roots exhibited some significant differences, being higher in the 8 mM nitrate treatment than in the 6 mM ammonium/2 mM nitrate and 2 mM ammonium/6 mM nitrate treatments. PpAspAT1 encodes a cytosolic protein, and the expression levels among organs were similar. However, the product of PpAspAT2 has a predicted mitochondrial location, while that of PpAspAT3 has a putative chloroplastic location. PpAspAT2 was most highly expressed in roots (Figure 5h), and PpAspAT3 was most highly expressed in needles (Figure 5i). PpAlaAT1, which produces a mitochondrial localized protein, had a moderate expression that was higher in the roots (Figure 5j). Nevertheless, PpAlaAT2 expression was extremely low and almost residual (Figure 5k). As expected, the expression of the PpGGT gene was very high in the needles and did not show significant differences among treatments despite its lower expression in the 8 mM ammonium and 8 mM nitrate seedlings in comparison to that for the rest of the conditions, especially in the 6 mM ammonium/2 mM nitrate treatment (Figure 5l).

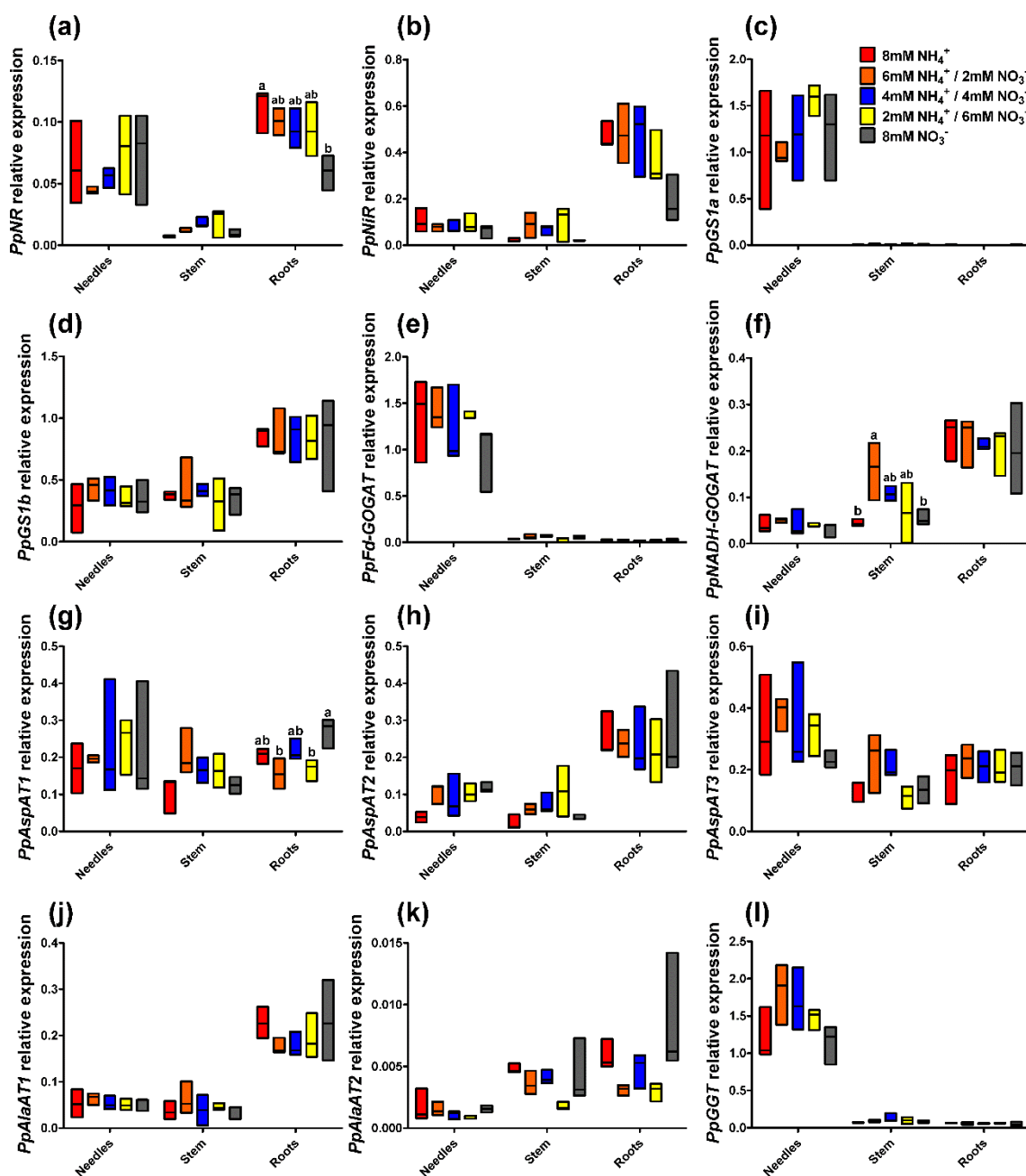


Figure 5. Gene expression profiles in the different organs (needles, stem, and roots) of pine seedlings under the nutrient treatments. (a) Nitrate reductase (*PpNRT*); (b) Nitrite reductase (*PpNiR*); (c) Glutamine synthetase 1a (*PpGS1a*); (d) Glutamine synthetase 1b (*PpGS1b*); (e) Ferredoxin dependent glutamate synthase (*PpFd-GOGAT*); (f) NADH-dependent glutamate synthase (*PpNADH-GOGAT*); (g) Aspartate aminotransferase 1 (*PpAspAT1*); (h) Aspartate aminotransferase 2 (*PpAspAT2*); (i) Aspartate aminotransferase 3 (*PpAspAT3*); (j) Alanine aminotransferase 1 (*PpAlaAT1*); (k) Alanine aminotransferase 2 (*PpAlaAT2*); (l) Glyoxylate-glutamate aminotransferase (*PpGGT*). Red columns correspond to 8 mM NH₄⁺ supply; orange columns correspond to 6 mM NH₄⁺/2 mM NO₃⁻ supply; blue columns correspond to 4 mM NH₄⁺/4 mM NO₃⁻ supply; yellow columns correspond to 2mM NH₄⁺/6 mM NO₃⁻ supply; grey columns correspond to 8 mM NO₃⁻

supply. Significant differences were determined with one-way ANOVA for each organ or entire seedling. Letters above the columns show significant differences based on Newman-Keuls post-hoc test ($p < 0.05$). Error bars show SE with $n = 3$.

3. Discussion

The preference of conifers for different inorganic N forms has been previously discussed in different works [21,22,29]. Depending on the species habitat, including climatic and soil conditions, conifers show preferences for the uptake and utilization of ammonium or nitrate [22]. Most of the conifers are tolerant to ammonium [20,30]. In the case of *P. pinaster*, its growth is higher with ammonium than with nitrate [21], although it is a conifer species with extensive families of nitrate transporters (NPF and NRT2) and transport regulators (NRT3) [28] and also lives in the Western Mediterranean region where climate conditions can promote high nitrification rates in the soil. In this context, the goal of the present work was to identify the main changes caused at the metabolic level by ammonium or nitrate supply in maritime pine seedlings.

The results included in this study considerably expand the knowledge of N nutrition in maritime pine provided by previous reports. The seedlings with a higher ammonium supply grew better (Figure 1), but the whole plants also accumulated more N through higher N uptake efficiency (NUpE) (Figure 2). In fact, the ^{15}N labeling experiment supported this observation; the ammonium uptake in seedlings was higher, and there was a high incorporation rate (at the μmolar level) during most part of the experiment (Figure 3). Interestingly, the differential biomass accumulation took place mainly in the roots, causing an increase in the root:shoot ratio in ammonium-fed seedlings. The application of high amounts of ammonium usually inhibits root growth and decreases the root:shoot ratio in plants [10]. In maritime pine seedlings, it seems that root growth increases following ammonium application, or at least, the growth inhibition is lower than that in seedlings fed with nitrate (Figure 1). In conifers, the root growth and the root:shoot ratio vary depending on the N source, which can include organic compounds such as L-arginine, which favors root development and a high root:shoot ratio [31]. In fact, this is considered a good trait for the field establishment of conifer seedlings [31,32]. Thus, the above results support the preference of maritime pine for ammonium as an inorganic N form over nitrate and suggest that the ammonium preference promotes beneficial root development. In this context, roots were the only organ with significant differences in metabolite content among treatments in the present study (Figure 6, Table S1). This is significant considering that roots seem to be

the organ where primary N assimilation occurs in pine (Figure 5), despite the resolution of the analytical procedure being only in the mM range (400 MHz NMR spectrometer).

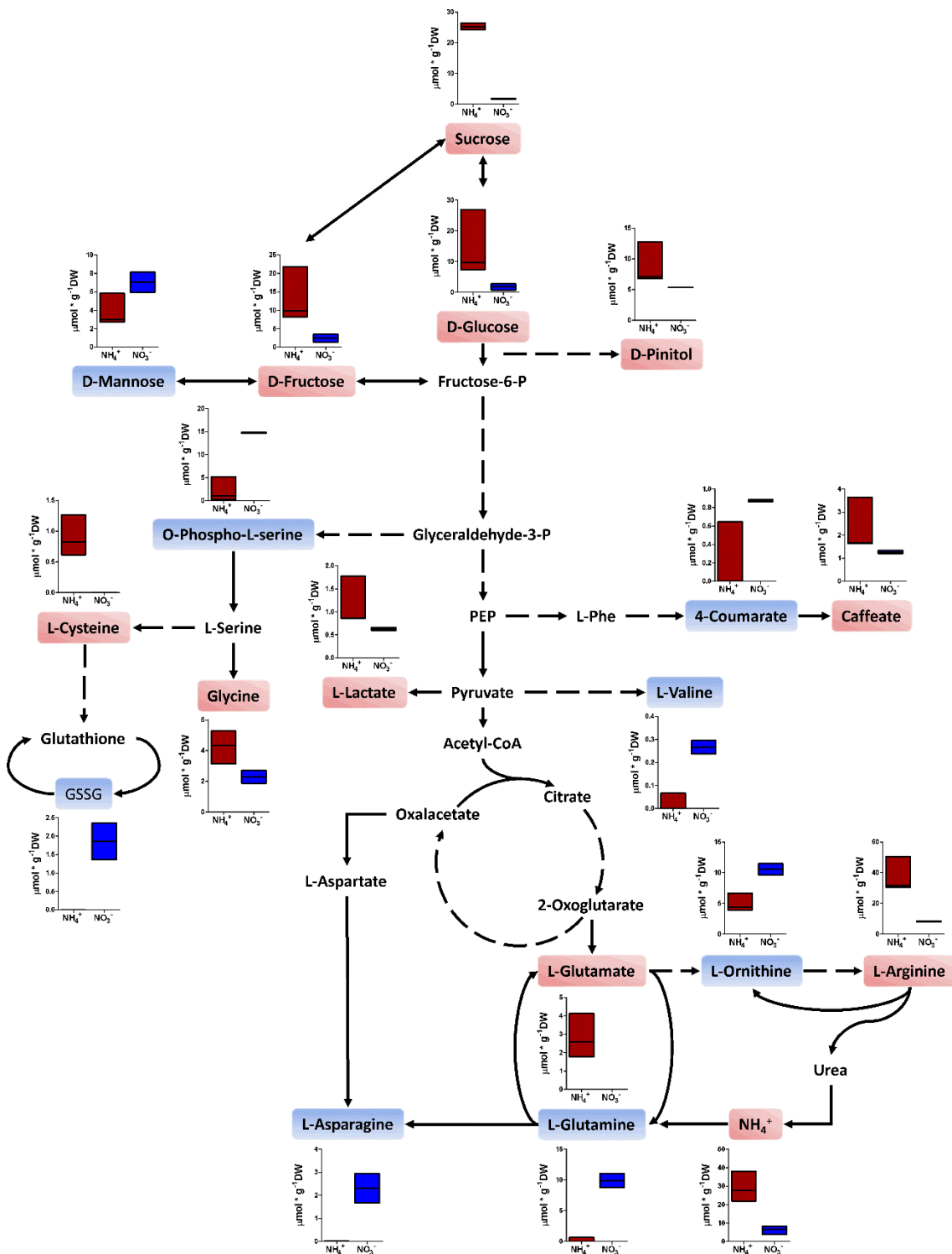


Figure 6. Main significant metabolites in the roots of seedlings fed 8 mM ammonium or 8 mM nitrate. Red columns correspond to 8 mM NH₄⁺ supply; blue columns correspond to 8 mM NO₃⁻ supply. Metabolites highlighted in red were significantly more accumulated in the roots of seedlings fed 8 mM ammonium. Metabolites highlighted in blue were significantly more accumulated in the roots of seedlings fed 8 mM nitrate.

APPENDIX

GSSG: Oxidized glutathione; PEP: Phosphoenolpyruvate; L-Phe: L-Phenylalanine. Significant differences were determined with a t-test (FDR < 0.05). Error bars show SE with n = 3.

The N content clearly increased in the seedlings supplied with ammonium that had higher N uptake efficiency (NUpE) (Figure 2). However, changes in the N content occurred mainly in the needles. Considering the N partitioning, the free amino acid content seems to be the main factor responsible for this effect, with slight participation from the ammonium content (Figure 2). The metabolite profile in roots also suggests that ammonium-fed plants had a better N status (Figure 6, Table S1). Certain amino acids are good markers of a healthy N status, such as L-glutamate, L-cysteine, and L-arginine. L-glutamate is the net product of the GS/GOGAT cycle, which is the pathway mainly responsible for N assimilation [14]. L-cysteine is the final product in the sulfur assimilation pathway, but its biosynthesis depends on the availability of assimilated N [33]. Furthermore, L-cysteine acts as a precursor for antioxidants and defense compounds [34] and is related to the transcriptional response of ammonium nutrition in plants that have a greater tolerance for ammonium [35]. L-arginine is synthesized from L-glutamate and is an amino acid with an important role as an N reserve in pine. This amino acid is very abundant in storage proteins and is an important sink for assimilated N surplus [20,36]. Additionally, the metabolite profile in the roots indicates that the availability of C for metabolic processes was reduced in nitrate-fed seedlings (Figure 6, Table S1). The levels of the main soluble sugars, such as sucrose, D-fructose, and D-glucose, were extremely low in nitrate-fed seedlings in comparison to those in ammonium-fed seedlings. In fact, some C sinks such as D-pinitol or caffeic acid were also more accumulated in the ammonium-feed seedlings. This correlates well with the accumulation of L-asparagine, L-glutamine, and L-ornithine in the nitrate-fed plants. L-asparagine is an amino acid that is synthesized from L-glutamine and L-aspartate and is employed as a temporal N reserve when C is depleted [37]. Similarly, the accumulation of L-ornithine could suggest the active catabolism of L-arginine to mobilize the stored N and produce L-glutamate [38]. Interestingly, in the roots of the ammonium-fed seedlings, a greater amount of choline (4 times) was observed than in the roots of nitrate-fed plants (Table S1). Choline is the precursor of glycinebetaine in most living organisms and it is well known to play a role in osmotic stress [39], which could be related to ammonium levels since a higher water content was observed in the ammonium-fed seedlings compared to nitrate-fed plants (Figure 1d). Furthermore, glycinebetaine plays a role in oxidative stress responses by enhancing antioxidative responses [39,40] which could be linked to the transcriptomic response to ammonium [41].

Interestingly, the main accumulation of nitrate and ammonium was not in needles. This suggests that the changes in N content in the needles were related to metabolic processes associated with N management (assimilation and recycling). Additionally, the partitioning of ammonium and nitrate within the seedlings was different. The seedlings accumulated the most ammonium in the roots, avoiding major increases in its concentration in aerial organs. In plants, primary ammonium assimilation generally occurs in the roots [42]. Pine plants may subtly regulate and buffer the ammonium content in their organs via primary assimilation in the roots and the accumulation of the ammonium excess in the same organ, probably in the vacuoles [18,43]. This regulatory mechanism can prevent problems derived from the high levels of ammonium released during photorespiration in the photosynthetic tissues or during lignification that occurs mainly in the stem [14]. Additionally, free ammonium levels were higher in seedlings fed ammonium, mainly in the roots. However, the differences in nitrate content between the different treatments were not very large (not statistically significant), and the levels of nitrate accumulation were several times lower than the ammonium accumulation in the same organs. This fact and the total N content of the seedlings suggest that ammonium uptake is less restricted than nitrate uptake in maritime pine. The nitrate incorporation rate was only higher than the ammonium incorporation rate during the first 15 min, suggesting precise regulation by nitrate transporters (Figure 3). This low nitrate uptake rate has also been observed in white spruce, and the authors proposed that nitrate uptake systems are atrophied in plants that prefer ammonium [4,44]. However, maritime pine possesses a complete set of nitrate transporters and even an expanded gene family that encodes nitrate transport regulators (NRT3). In this context, it is tempting to speculate that maritime pine senses nitrate to be a toxic molecule.

Although it is well known that plants prefer to accumulate nitrate over ammonium, which can produce cellular toxicity in several ways [10,42], pine is able to store more ammonium than nitrate at similar supply levels. Curiously, excess nitrate is mainly stored in the stem, an organ with a less important N assimilatory role than needles and roots, as suggested by the PpNR and PpNiR expression levels (Figure 5). This observation, along with the observed content of L-arginine in the stem (Figure S2) and the accumulation of L-asparagine in the seedling hypocotyl during the postgermination phase [38,45], suggests that the pine stem has a role as a store of N that accumulates not only vegetative storage proteins (VSPs) in the bark [46], but also free metabolites such as nitrate, L-arginine or L-asparagine. It is known that trees are able to transiently accumulate N in free amino acids [47]; in the future, it will be interesting to analyze the role of adult pine stems in the storage of N through the accumulation of small metabolites such as nitrate or free amino acids.

Interestingly, nitrate did not accumulate in the needles (Figure 2), and the activity of enzymes involved in basal N metabolism increased in the needles with the nitrate supply (Figure 4). These results suggest a limited ability for nitrate assimilation in maritime pine, which may be related to the photorespiration pathway. Conifers lack a chloroplastic GS isoform (GS2) that is involved in the photoassimilation of nitrate and the reassimilation of ammonium released during photorespiration in angiosperm plants [14]. This could explain the increase in GS activity in the needles of nitrate-fed seedlings (Figure 4). In fact, a strong relationship between nitrate assimilation and photorespiration in pine has been observed in *Pinus taeda* saplings, which grew better with nitrate under low CO₂ concentrations than under elevated CO₂ concentrations; in contrast, CO₂ concentration had no effect in the growth rate of ammonium-fed saplings [23]. However, it seems that needle metabolism is influenced by the form of available inorganic N. In this context, these effects appear to be regulated through the allocation of the inorganic N forms to the different organs and through their assimilation in the roots, as indicated by the expression levels of PpNR and PpNiR genes (Figure 5). Despite the expression of these genes, the ¹⁵N incorporation assay indicated that nitrate was relatively better transported from roots to stem and needles than ammonium (Figure 3d–f), at least when the nitrate incorporation rate was high. It is possible that nitrate assimilation into the needles negatively affects photosynthetic/photorespiration metabolism, inducing a negative feedback with nitrate transport in the roots. Nitrate uptake inhibition has been previously observed in different plants when enough nitrate is assimilated, but not in such a drastic manner [48].

Another interesting finding is the lack of correlation between enzyme activity (GS, AspAT, and AlaAT) and the expression of the genes coding for the enzymes that catalyze these reactions (Figures 3 and 4). These findings suggest that the response to the N form must be regulated through a post-transcriptional (translational or post-translational) mechanism. This could involve changes in translation or in the proteolysis rates. A second mechanism has been proposed for the GS enzyme in mammals, wherein the increase in glutamine levels drives ubiquitination and proteasome degradation of the protein [49,50]. In plants, ubiquitination-dependent proteolysis also plays a role in N metabolism during plant adaptation to N starvation [51,52].

4. Materials and Methods

4.1. Plant Material

Maritime pine seeds (*Pinus pinaster* Ait.) from Sierra Bermeja (Estepona, Spain) (ES20, Ident. - 11/12) were obtained from the Área de Recursos Genéticos Forestales of the Spanish Ministerio de Agricultura, Pesca y Alimentación. Pine seeds were imbibed in distilled water for 48 h under continuous aeration and germinated with vermiculite as an inert substrate. Pine seedlings were cultivated in a growth chamber with a 16/8 h light/dark photoperiod, light intensity of 125 $\mu\text{mol m}^{-2} \text{s}^{-1}$, constant temperature of 26–27 °C, and 75%–80% relative humidity. Forty seedlings aged one month were randomly transplanted into forestall seedbeds for each experimental condition. The seedlings were grown in a greenhouse from February to April of 2019 at a mean temperature of 25 °C and 50/70%

relative humidity with a 16/8-h photoperiod (Instituto de Hortifruticultura Subtropical y Mediterránea, IHSM La Mayora UMA-CSIC). Each group was irrigated twice per week with 40 mL of the corresponding N solution or 40 mL of distilled water. Five experimental conditions were tested: 8 mM NH_4Cl ; 6 mM NH_4Cl –2 mM KNO_3 ; 4 mM NH_4Cl –4 mM KNO_3 ; 2 mM NH_4Cl –6 mM KNO_3 ; 8 mM KNO_3 . After 60 days of treatment, seedlings were subdivided and harvested in three random groups. The seedlings were divided into three different sections (cotyledon, hypocotyl, and roots). Each section was weighed and immediately frozen in liquid N_2 . For the N uptake analyses, one-month-old seedlings grown in vermiculite and only irrigated with distilled water were used. They were separated into two groups. One group was fed with 7.5 mM of ^{15}N -labelled ammonium and the second one with 7.5 mM of ^{15}N -labelled nitrate. The plants were harvested at different times after nutrient application: 0, 15, 30, 60, 120, and 240 min. Each organ was isolated, weighed, and immediately frozen in liquid N_2 . Three biological replicates were taken. Each replicate consisted of a pool of five seedlings. All samples were stored at –80 °C until powdering with a mixer mill MM400 (Retsh, Haan, Germany) and further analyses were conducted.

4.2. Elemental Analysis and NUE Component Estimation

Ground powder (100 mg) of cotyledons, hypocotyls, and roots was dried at 70 °C for 48 h in an oven. Total C and N contents in different sections of pine seedlings were determined in triplicate by an elemental macro-analyzer Leco truSpec CHNS (Leco Corporation, St. Joseph, MI) at the Atomic Spectrometry Unit, University of Málaga. ^{15}N determinations were performed by mass spectrometry using a Flash IRMS Elemental Analyzer (EA-IRMS), Delta V IRMS, Conflo IV Universal Interface (Thermo Scientific, MA, USA). The N content and

biomass of the samples were used to calculate the nitrogen utilization efficiency (NUtE) and nitrogen uptake efficiency (NUpE) [53].

4.3. Free Amino Acids, Ammonium, Nitrate, and Nitrite Contents

Free amino acids and ammonium were extracted with 2% 5-sulfosalicylic acid (100 mg FW mL⁻¹) [54]. Soluble amino acids were determined using the procedure described by Sun et al. [55]. Free ammonium was measured using the Berthelot reaction (phenol hypochlorite assay) [56]. Nitrate and nitrite measures were performed as described by García-Robledo et al. [57]. Nitrite was determined spectrophotometrically at 540 nm after a colorimetric reaction using Griess' reagent (equal volumes of 60 mM sulfanilamide in 1.2 N HCl and 4 mM N-(1-naphthyl) ethylenediamine dihydrochloride) after 20 min incubation at room temperature. Nitrate was reduced to nitrite with 2% vanadium (III) chloride (VCl₃) in 6N HCl, and the produced nitrite was measured as described above. Nitrite was measured prior the nitrate reduction with the aim of determining the basal nitrite present in the samples. Nitrite and nitrate contents were calculated based on a standard curve using commercial sodium nitrite from Sigma-Aldrich (MO, USA).

4.4. Soluble Protein, Enzyme Activity, and Chlorophylls Determinations

Soluble proteins were extracted using 100 mg of sample ground powder for stem and roots and 50 mg in the case of needles. The extraction was performed by adding 1 mL of extraction buffer (50 mM Tris-HCl pH 8, 1 mM EDTA, 10 mM MgCl₂, 0.5 mM dithiothreitol (DTT), 20% (w/v) glycerol, 0.1% (v/v) Triton X-100, 1% (w/v) polyvinylpyrrolidone (PVP), and 1% (w/v) polyvinyl(poly)pyrrolidone (PVPP)) and 30 mg of fine sea sand. The resulting extract was centrifuged at 12,000 g for 30 min at 4 °C. The obtained supernatants were recovered and used for soluble protein determination through Bradford's procedure using a commercial reagent (Protein Assay Dye Reagent; Bio-Rad, CA, USA) and bovine serum albumin as a standard [58].

Glutamine synthetase (GS, EC 6.3.1.2) activity was determined by the transferase assay following Cánovas et al. [59]. The final reaction volume was 150 µL. Reactions were incubated for 15 min at 37 °C with 10 s of agitation every minute; the reactions were stopped with 150 µL of STOP solution (10% FeCl₃·6H₂O in 0.2 N HCl, 24% trichloroacetic acid and 50% HCl) and centrifuged for 3 min at 3220 g. After centrifugation, 200 µL of the supernatant was recovered, and absorbance was measured at 540 nm in a microplate reader. For estimation of glutamate dehydrogenase (GDH, EC 1.4.1.2) activity, the NADH-GDH assay was used [60]. The reaction was developed in a final volume of 100 µL. Aspartate

aminotransferase (AspAT, EC 2.6.1.1) and alanine aminotransferase (AlaAT, EC 2.6.1.2) activities were measured following Gibon et al. [61] in a final reaction volume of 100 μ L.

Chlorophyll extraction was performed using 50 μ L of protein extract mixed with 950 μ L of 80% (v/v) acetone. Samples were incubated at 4 °C overnight. Resulting extracts were centrifuged at 13,500 g at 4 °C for 10 min, and the absorbance was measured at 664 and 647 nm. The chlorophyll content was calculated according to Lichtenthaler and Buschmann [62].

4.5. Metabolite Profiling

The metabolites for ¹H-NMR analysis were extracted following the protocol previously described by Kruger et al. [63]. Two hundred milligrams of frozen powder were used for extractions. The ¹H-NMR analyses were performed on a Bruker ASCEND™ 400 MHz NMR Spectrometer (Bionand, Centro Andaluz de Nanomedicina y Biotecnología, Málaga, Spain). The 1D-¹H-NMR spectrum for each sample was obtained as previously described by Cañas et al. [64]. Quantitative analysis of the NMR spectra was performed using LCModel software (Linear Combination of Model Spectra) [65] and a previously generated reference metabolite spectral library [64]. The internal reference was an electronically generated signal, ERETIC (electronic reference to access in vivo concentrations) [66]. The metabolite amounts were determined at millimolar concentrations.

The metabolite contents were analyzed with MetaboAnalyst 4.0 [67]. Data were normalized using the quantile method, then log transformation and mean centered. MetaboAnalyst 4.0 was used to construct a Heatmap and perform a t-test with the metabolite data.

4.6. RNA Extraction and Reverse-Transcription Quantitative PCR (RT-qPCR)

RNA was extracted as described by Canales et al. [68] from ground powder stored at -80 °C. A treatment with RQ1 RNase-Free DNase (Promega, Wis, USA) was applied to remove genomic DNA from the RNA samples. Total RNA quantification and purity were estimated using a NanoDrop ND-1000 spectrophotometer (Thermo Scientific, MA, USA), and RNA integrity was checked by agarose gel. Reverse transcription reactions were performed using iScript™ Reverse Transcription Supermix (Bio-Rad, CA, USA) using 1 μ g of total RNA. The qPCR reactions were carried out using 5 ng of cDNA and SsoFast™ EvaGreen® Supermix (Bio-Rad, CA, USA) in a final volume of 10 μ L. The reactions were developed on a C1000™ Thermal Cycler with a CFX384™ Touch Real-Time PCR Detection System (Bio-Rad, CA, USA) under the following conditions: 3 min at 95 °C (1 cycle), 1 s at 95 °C, and 5 s at 60 °C

(50 cycles), with a melting curve from 60 °C to 95 °C. The raw fluorescence data from each reaction were fitted to the MAK2 model [69]. The initial target concentration (D0 parameter) was determined using the R package qpcR [70]. Expression data were normalized to two reference genes, SKP1/ASK1 and SLAP, that were previously tested for RT-qPCR experiments in maritime pine [71]. For the qPCR analysis, three biological replicates and three technical replicates per sample were used. Primers used for qPCR are presented in Table S2.

4.7. Statistics

Biomass and root:shoot ratio results are presented in boxplots including minimum, maximum, and median values. For the rest of experiments, the mean values for three pools of plants with standard errors ($SE = SD/\sqrt{(n-1)}$) are presented. Statistical analyses were performed using Prism 5 (Graphpad, CA, USA) except for metabolite data that were analyzed using MetaboAnalyst 4.0 [67]. Differences among organs were not statistically analyzed. For each organ and whole seedling, nutritional differences were statistically analyzed to reduce problems with distribution and variance of data. In this line, one-way ANOVA was used for the analyses of all data except for 15N incorporation and metabolite profile assuming that data met ANOVA conditions. When one-way ANOVA was significant, a Newman-Keuls multiple comparison test was carried out. The 15N incorporation time experiment was analyzed using two-way ANOVA (mixed model) with a Bonferroni post-test determining significant differences in nutrition conditions between the global time experiment and each individual time point. Root metabolite profiles were analyzed using t-tests. In every case, significant differences were considered when $p < 0.05$ except for t-test analyses, where $FDR < 0.05$ was assumed.

5. Conclusions

The results of the present work demonstrate that ammonium and nitrate nutrients behave differently from each other in pine, although their assimilation into organic molecules occurs through the same pathway, the GS/GOGAT cycle. Their chemical characteristics and the reduction of nitrate to ammonium before its assimilation are crucial differences that affect plant metabolism and growth. Ammonium promotes better root growth than nitrate, which could be used to increase the performance during the field establishment of conifer seedlings. Additionally, other differences were found in the photosynthetic organs, where nitrate induced important changes correlated with the decreased growth of pine seedlings. A differential accumulation of nitrate and ammonium occurred in the pine organs and buffered the individual effects induced by each molecule. The role of pine stems in the

storage of N compounds, such as nitrate and L-asparagine, and the interaction between photosynthetic metabolism and nitrate will require further research efforts in the near future.

Supplementary Materials: The following are available online at <http://www.mdpi.com/2223-7747/9/4/481/s1>, Figure S1: Heatmap of the metabolite profile data, Figure S2: L-Arginine amounts, Table S1: Metabolite profile results, Table S2: qPCR primer list.

Author Contributions: Conceptualization, F.O. and R.A.C.; methodology, R.A.C.; validation, R.A.C.; formal analysis, F.O., J.M.V.-M., and R.A.C.; investigation, F.O., J.M.V.-M., J.A.U.-G., and M.L.G.-M.; resources, R.A.C., C.Á., and F.M.C.; data curation, F.O. and J.M.V.-M.; writing—original draft preparation, R.A.C.; writing—review and editing, C.Á. and F.M.C.; funding acquisition, R.A.C., C.Á., and F.M.C. All authors have read and agreed to the published version of the manuscript.

Funding: This research was funded by Spanish *Ministerio de Economía y Competitividad*, grant numbers BIO2015-73512-JIN MINECO/AEI/FEDER, UE, RTI2018-094041-B-I00, and EQC2018-004346-P. FO and JAUG were supported by grants from the *Universidad de Málaga* (UMAJI11 and UMAJI21, respectively, *Programa Operativo de Empleo Juvenil vía SNJG, FEDER, FSE, Junta de Andalucía*). JMVM was supported by a grant from the Spanish *Ministerio de Educación y Formación Profesional* (FPU17/03517).

Acknowledgments: We are grateful to Lucía Cruzado for her technical support in the greenhouse. **Conflicts of Interest:** The authors declare no conflict of interest.

References

1. Buchanan, B.B.; Gruissem, W.; Jones, R.L. *Biochemistry and Molecular Biology of Plants*, 2nd ed.; John Wiley & Sons: Chichester, West Sussex, UK, 2015.
2. Marschner, P. *Marschner's Mineral Nutrition of Higher Plants*, 3rd ed.; Academic Press: London, UK, 2012.
3. Moreau, D.; Bardgett, R.D.; Finlay, R.D.; Jones, D.L.; Philippot, L. A plant perspective on nitrogen cycling in the rhizosphere. *Funct. Ecol.* **2019**, *33*, 540–552. [[CrossRef](#)]
4. Britto, D.T.; Kronzucker, H.J. Ecological significance and complexity of N-source preference in plants. *Ann. Bot.* **2013**, *112*, 957–963. [[CrossRef](#)] [[PubMed](#)]
5. Wendeborn, S. The Chemistry, Biology, and Modulation of Ammonium Nitrification in Soil. *Angew. Chem. Int. Ed. Engl.* **2020**, *59*, 2182–2202. [[CrossRef](#)] [[PubMed](#)]
6. Norton, J.; Ouyang, Y. Controls and Adaptive Management of Nitrification in Agricultural Soils. *Front. Microbiol.* **2019**, *10*, 1931. [[CrossRef](#)] [[PubMed](#)]
7. Xu, G.; Fan, X.; Miller, A.J. Plant nitrogen assimilation and use efficiency. *Annu. Rev. Plant Biol.* **2012**, *63*, 153–182. [[CrossRef](#)] [[PubMed](#)]
8. Li, H.; Hu, B.; Chu, C. Nitrogen use efficiency in crops: Lessons from *Arabidopsis* and rice. *J. Exp. Bot.* **2017**, *68*, 2477–2488. [[CrossRef](#)]
9. Iqbal, A.; Qiang, D.; Alamzeb, M.; Xiangru, W.; Huiping, G.; Hengheng, Z.; Nianchang, P.; Xiling, Z.; Meizhen, S. Untangling the molecular mechanisms and functions of nitrate to improve nitrogen use efficiency. *J. Sci. Food Agric.* **2020**, *100*, 904–914. [[CrossRef](#)]
10. Britto, D.T.; Kronzucker, H.J. NH_4^+ toxicity in higher plants: A critical review. *J. Plant Physiol.* **2002**, *159*, 567–584. [[CrossRef](#)]
11. Suzuki, A.; Knaff, D.B. Glutamate synthase: Structural, mechanistic and regulatory properties, and role in the amino acid metabolism. *Photosynth. Res.* **2005**, *83*, 191–217. [[CrossRef](#)]

12. Bernard, S.M.; Habash, D.Z. The importance of cytosolic glutamine synthetase in nitrogen assimilation and recycling. *New Phytol.* **2009**, *182*, 608–620. [[CrossRef](#)]
13. Mifflin, B.J.; Habash, D.Z. The role of glutamine synthetase and glutamate dehydrogenase in nitrogen assimilation and possibilities for improvement in the nitrogen utilization of crops. *J. Exp. Bot.* **2002**, *53*, 979–987. [[CrossRef](#)] [[PubMed](#)]
14. Cánovas, F.M.; Ávila, C.; Cantón, F.R.; Cañas, R.A.; de la Torre, F. Ammonium assimilation and amino acid metabolism in conifers. *J. Exp. Bot.* **2007**, *58*, 2307–2318. [[CrossRef](#)] [[PubMed](#)]
15. Thomsen, H.C.; Eriksson, D.; Møller, I.S.; Schjoerring, J.K. Cytosolic glutamine synthetase: A target for improvement of crop nitrogen use efficiency? *Trends Plant Sci.* **2014**, *19*, 656–663. [[CrossRef](#)] [[PubMed](#)]

16. Granstedt, R.C.; Huffaker, R.C. Identification of the leaf vacuole as a major nitrate storage pool. *Plant Physiol.* **1982**, *70*, 410–413. [[CrossRef](#)]
17. Liu, X.Y.; Koba, K.; Makabe, A.; Liu, C.Q. Nitrate dynamics in natural plants: Insights based on the concentration and natural isotope abundances of tissue nitrate. *Front Plant Sci.* **2014**, *5*, 355. [[CrossRef](#)]
18. Wood, C.C.; Porée, F.; Dreyer, I.; Koehler, G.J.; Udvardi, M.K. Mechanisms of ammonium transport, accumulation, and retention in oocytes and yeast cells expressing Arabidopsis AtAMT1;1. *FEBS Lett.* **2006**, *580*, 3931–3936. [[CrossRef](#)]
19. Farjon, A. *A Handbook of the World's Conifers*, 1st ed.; Brill Academic Pub.: Leiden, The Netherlands, 2010.
20. Cañas, R.A.; de la Torre, F.; Pascual, B.; Avila, C.; Cánovas, F.M. Nitrogen economy and nitrogen environmental interactions in conifers. *Agronomy* **2016**, *6*, 26. [[CrossRef](#)]
21. Warren, C.R.; Adams, M.A. Possible causes of slow growth of nitrate-supplied *Pinus pinaster*. *Can. J. Forest Res.* **2002**, *32*, 569–580. [[CrossRef](#)]
22. Boczulak, S.A.; Hawkins, B.J.; Roy, R. Temperature effects on nitrogen form uptake by seedling roots of three contrasting conifers. *Tree Physiol.* **2014**, *34*, 513–523. [[CrossRef](#)]
23. Bloom, A.J.; Rubio-Asensio, J.S.; Randall, L.; Rachmilevitch, S.; Cousins, A.B.; Carlisle, E.A. CO₂ enrichment inhibits shoot nitrate assimilation in C3 but not C4 plants and slows growth under nitrate in C3 plants. *Ecology* **2012**, *93*, 355–367. [[CrossRef](#)]
24. Cantón, F.R.; Suárez, M.F.; Cánovas, F.M. Molecular aspects of nitrogen mobilization and recycling in trees. *Photosynth. Res.* **2005**, *83*, 265–278. [[CrossRef](#)] [[PubMed](#)]
25. Gaertner, M.; Breeyen, A.D.; Hui, C.; Richardson, D.M. Impacts of alien plant invasions on species richness in Mediterranean-type ecosystems: A meta-analysis. *Prog. Phys. Geogr.* **2009**, *33*, 319. [[CrossRef](#)]
26. Aranda, I.; Alía, R.; Ortega, U.; Dantas, A.K.; Majada, J. Intra-specific variability in biomass partitioning and carbon isotopic discrimination under moderate drought stress in seedlings from four *Pinus pinaster* populations. *Tree Genet. Genomes* **2010**, *6*, 169–178. [[CrossRef](#)]
27. Gaspar, M.J.; Velasco, T.; Feito, I.; Alía, R.; Majada, J. Genetic variation of drought tolerance in *Pinus pinaster* at three hierarchical levels: A comparison of induced osmotic stress and field testing. *PLoS ONE* **2013**, *8*, e79094. [[CrossRef](#)]

28. Castro-Rodríguez, V.; Cañas, R.A.; de la Torre, F.N.; Pascual, M.B.; Ávila, C.; Cánovas, F.M. Molecular fundamentals of nitrogen uptake and transport in trees. *J. Exp. Bot* **2017**, *68*, 2489–2500. [[CrossRef](#)]
29. Koyama, L.A.; Kielland, K. Black spruce assimilates nitrate in boreal winter. *Tree Physiol.* **2019**, *39*, 536–543. [[CrossRef](#)]
30. Kronzucker, H.J.; Siddiqi, M.Y.; Glass, A. Kinetics of NH_4^+ Influx in Spruce. *Plant Physiol.* **1996**, *110*, 773–779. [[CrossRef](#)]
31. Gruffman, L.; Ishida, T.; Nordin, A.; Näsholm, T. Cultivation of Norway spruce and Scots pine on organic nitrogen improves seedling morphology and field performance. *Forest Ecol. Manag.* **2012**, *276*, 118–124. [[CrossRef](#)]
32. Davis, A.S.; Jacobs, D.F. Quantifying root system quality of nursery seedlings and relationship to outplanting performance. *New Forest* **2005**, *30*, 295–311. [[CrossRef](#)]
33. Koprivova, A.; Kopriva, S. Molecular mechanisms of regulation of sulfate assimilation: First steps on a long road. *Front Plant Sci.* **2014**, *5*, 589. [[CrossRef](#)]
34. Álvarez, C.; Bermúdez, M.Á.; Romero, L.C.; Gotor, C.; García, I. Cysteine homeostasis plays an essential role in plant immunity. *New Phytol.* **2012**, *193*, 165–177. [[CrossRef](#)] [[PubMed](#)]
35. Sun, L.; Di, D.; Li, G.; Kronzucker, H.J.; Shi, W. Spatio-temporal dynamics in global rice gene expression (*Oryza sativa* L.) in response to high ammonium stress. *J. Plant Physiol.* **2017**, *212*, 94–104. [[CrossRef](#)] [[PubMed](#)]
36. Llebrés, M.T.; Pascual, M.B.; Debille, S.; Trontin, J.F.; Harvengt, L.; Ávila, C.; Cánovas, F.M. The role of arginine metabolic pathway during embryogenesis and germination in maritime pine (*Pinus pinaster* Ait.). *Tree Physiol.* **2018**, *38*, 471–484. [[CrossRef](#)] [[PubMed](#)]
37. Gaufichon, L.; Rothstein, S.J.; Suzuki, A. Asparagine Metabolic Pathways in *Arabidopsis*. *Plant Cell Physiol.* **2016**, *57*, 675–689. [[CrossRef](#)]
38. Cañas, R.A.; Villalobos, D.P.; Díaz-Moreno, S.M.; Cánovas, F.M.; Cantón, F.R. Molecular and functional analyses support a role of Ornithine- δ -aminotransferase in the provision of glutamate for glutamine biosynthesis during pine germination. *Plant Physiol.* **2008**, *148*, 77–88. [[CrossRef](#)] [[PubMed](#)]
39. Chen, T.H.; Murata, N. Glycinebetaine protects plants against abiotic stress: Mechanisms and biotechnological applications. *Plant Cell Environ.* **2011**, *34*, 1–20. [[CrossRef](#)]
40. Sakamoto, A.; Murata, A.; Murata, N. Metabolic engineering of rice leading to biosynthesis of glycinebetaine and tolerance to salt and cold. *Plant Mol. Biol.* **1998**, *38*, 1011–1019. [[CrossRef](#)]
41. Patterson, K.; Cakmak, T.; Cooper, A.; Lager, I.; Rasmusson, A.G.; Escobar, M.A. Distinct signalling pathways and transcriptome response signatures differentiate ammonium- and nitrate-supplied plants. *Plant Cell Environ.* **2010**, *33*, 1486–1501. [[CrossRef](#)]
42. Hachiya, T.; Sakakibara, H. Interactions between nitrate and ammonium in their uptake, allocation, assimilation, and signalling in plants. *J. Exp. Bot.* **2017**, *68*, 2501–2512. [[CrossRef](#)]

43. Bai, L.; Ma, X.; Zhang, G.; Song, S.; Zhou, Y.; Gao, L.; Miao, Y.; Song, C.P. A Receptor-Like Kinase Mediates Ammonium Homeostasis and Is Important for the Polar Growth of Root Hairs in Arabidopsis. *Plant Cell* 2014, 26, 1497–1511. [CrossRef]
44. Kronzucker, H.J.; Siddiqi, M.Y.; Glass, A.D.M. Conifer root discrimination against soil nitrate and the ecology of forest succession. *Nature* 1997, 385, 59–61. [CrossRef]
45. Cañas, R.A.; de la Torre, F.; Cánovas, F.M.; Cantón, F.R. High levels of asparagine synthetase in hypocotyls of pine seedlings suggest a role of the enzyme in re-allocation of seed-stored nitrogen. *Planta* 2006, 224, 83–95. [CrossRef]
46. Li, G.; Coleman, G.D. Nitrogen storage and cycling in trees. In *Advances in Botanical Research. Molecular Physiology and Biotechnology of Trees*, 1st ed.; Cánovas, F.M., Jacquot, J.P., Eds.; Academic Press: London, UK, 2019; Volume 89, pp. 127–155. [CrossRef]
47. Rennenberg, H.; Wildhagen, H.; Ehling, B. Nitrogen nutrition of poplar trees. *Plant Biol.* 2010, 12, 275–291. [CrossRef] [PubMed]
48. Tischner, R. Nitrate uptake and reduction in higher and lower plants. *Plant Cell Environ.* 2000, 23, 1005–1024. [CrossRef]
49. Nguyen, T.V.; Lee, J.E.; Sweredoski, M.J.; Yang, S.J.; Jeon, S.J.; Harrison, J.S.; Yim, J.H.; Lee, S.G.; Handa, H.; Kuhlman, B.; et al. Glutamine Triggers Acetylation-Dependent Degradation of Glutamine Synthetase via the Thalidomide Receptor Cereblon. *Mol. Cell* 2016, 61, 809–820. [CrossRef]
50. Nguyen, T.V.; Li, J.; Lu, C.J.; Mamrosh, J.L.; Lu, G.; Cathers, B.E.; Deshaies, R.J. p97/VCP promotes degradation of CRBN substrate glutamine synthetase and neosubstrates. *Proc. Natl. Acad. Sci. USA* 2017, 114, 3565–3571. [CrossRef]
51. Peng, M.; Hannam, C.; Gu, H.; Bi, Y.M.; Rothstein, S.J. A mutation in NLA, which encodes a RING-type ubiquitin ligase, disrupts the adaptability of Arabidopsis to nitrogen limitation. *Plant J.* 2007, 50, 320–337. [CrossRef]
52. Park, B.S.; Yao, T.; Seo, J.S.; Wong, E.C.C.; Mitsuda, N.; Huang, C.H.; Chua, N.H. Arabidopsis NITROGEN LIMITATION ADAPTATION regulates ORE1 homeostasis during senescence induced by nitrogen deficiency. *Nat. Plants* 2018, 4, 898–903. [CrossRef]
53. Good, A.G.; Shrawat, A.K.; Muench, D.G. Can less yield more? Is reducing nutrient input into the environment compatible with maintaining crop production? *Trends Plant Sci.* 2004, 9, 597–605. [CrossRef]
54. Ferrario-Méry, S.; Valadier, M.H.; Foyer, C. Overexpression of nitrate reductase in tobacco delays drought-induced decreases in nitrate reductase activity and mRNA. *Plant Physiol.* 1998, 117, 293–302. [CrossRef]
55. Sun, S.W.; Lin, Y.C.; Weng, Y.M.; Chen, M.J. Efficiency improvements on ninhydrin method for amino acid quantification. *J. Food Compos. Anal.* 2006, 19, 112–117. [CrossRef]
56. Husted, S.; Hebborn, C.A.; Mattson, M.; Schjoerring, J.K. A critical experimental evaluation of methods for determination of in plant tissue, xylem sap and apoplastic fluid. *Physiol. Plant.* 2000, 109, 167–179. [CrossRef]
57. García-Robledo, E.; Corzo, A.; Pappaspyrou, S. A fast and direct spectrophotometric method for the sequential determination of nitrate and nitrite at low concentrations in small volumes. *Mar. Chem.* 2014, 162, 30–36. [CrossRef]

58. Bradford, M.M. A rapid and sensitive method for the quantitation of microgram quantities of protein utilizing the principle of protein-dye binding. *Anal. Biochem.* 1976, 72, 248–254. [[CrossRef](#)]
59. Cánovas, F.; Valpuesta, V.; Núñez de Castro, I. Characterization of glutamine synthetase from tomato leaves. *Plant Sci. Lett.* 1984, 37, 79–85. [[CrossRef](#)]
60. Turano, F.J.; Dashner, R.; Upadhyaya, A.; Caldwell, C.R. Purification of mitochondrial glutamate dehydrogenase from darkgrown soybean seedlings. *Plant Physiol.* 1996, 112, 1357–1364. [[CrossRef](#)]
61. Gibon, Y.; Blaesing, O.E.; Hannemann, J.; Carillo, P.; Höhne, M.; Hendriks, J.H.; Palacios, N.; Cross, J.; Selbig, J.; Stitt, M. A Robot-based platform to measure multiple enzyme activities in Arabidopsis using a set of cycling assays: Comparison of changes of enzyme activities and transcript levels during diurnal cycles and in prolonged darkness. *Plant Cell.* 2004, 16, 3304–3325. [[CrossRef](#)]
62. Lichtenthaler, H.K.; Buschmann, C. Chlorophylls and carotenoids: Measurement and characterization by UV-VIS spectroscopy. In *Current Protocols in Food Analytical Chemistry*; Wrolstad, R.E., Ed.; John Wiley & Sons Inc.: Hoboken, NJ, USA, 2001; pp. F4.3.1–F4.3.8. [[CrossRef](#)]
63. Kruger, N.J.; Troncoso-Ponce, M.A.; Ratcliffe, R.G. ¹H NMR metabolite fingerprinting and metabolomic analysis of perchloric acid extracts from plant tissues. *Nat. Protoc.* 2008, 3, 1001–1012. [[CrossRef](#)]
64. Cañas, R.A.; Canales, J.; Muñoz-Hernández, C.; Granados, J.M.; Ávila, C.; García-Martín, M.L.; Cánovas, F.M. Understanding developmental and adaptive cues in pine through metabolite profiling and co-expression network analysis. *J. Exp. Bot.* 2015, 66, 3113–3127. [[CrossRef](#)]
65. Provencher, S.W. Estimation of metabolite concentrations from localized in vivo proton NMR spectra. *Magn. Reson. Med.* 1993, 30, 672–679. [[CrossRef](#)]
66. Akoka, S.; Barantin, L.; Trierweiler, M. Concentration measurement by proton NMR using the ERETIC method. *Anal. Chem.* 1999, 71, 2554–2557. [[CrossRef](#)] [[PubMed](#)]
67. Chong, J.; Soufan, O.; Li, C.; Caraus, I.; Li, S.; Bourque, G.; Wishart, D.S.; Xia, J. MetaboAnalyst 4.0: Towards more transparent and integrative metabolomics analysis. *Nucleic Acids Res.* 2018, 46, 486–494. [[CrossRef](#)] [[PubMed](#)]
68. Canales, J.; Rueda-López, M.; Craven-Bartle, B.; Ávila, C.; Cánovas, F.M. Novel insights into regulation of asparagine synthetase in conifers. *Front. Plant Sci.* **2012**, 3, 100. [[CrossRef](#)] [[PubMed](#)]
69. Boggy, G.J.; Woolf, P.J. A mechanistic model of PCR for accurate quantification of quantitative PCR data. *PLoS ONE* **2010**, 5, e12355. [[CrossRef](#)]
70. Ritz, C.; Spiess, A.N. qpcR: An R package for sigmoidal model selection in quantitative real-time polymerase chain reaction analysis. *Bioinformatics* **2008**, 24, 1549–1551. [[CrossRef](#)]
71. Granados, J.M.; Ávila, C.; Cánovas, F.M.; Cañas, R.A. Selection and testing of reference genes for accurate RT-qPCR in adult needles and seedlings of maritime pine. *Tree Genet. Genomes* **2016**, 12, 60. [[CrossRef](#)]